AD-A127 799 THE EFFECTS OF FREE-STREAM TURBULENCE ON THE TURBULENCE STRUCTURE AND HEA..(U) UNITED TECHNOLOGIES RESEARCH CENTER EAST HARTFORD CT M F BLAIR ET AL. NOV 82 1/2

UNCLASSIFIED UTRC/R82-915634-2 AFOSR-TR-83-0355 F/G 20/4 NL

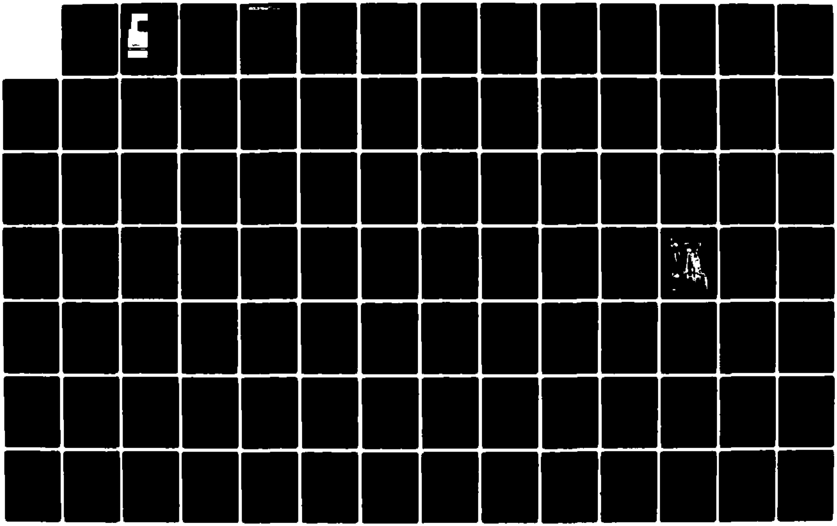

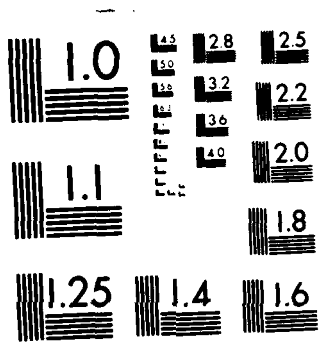
1.0
2.8
2.5
3.2
2.2
3.6
2.0
4.0
1.1
1.8
1.25
1.4
1.6

AFOSR-TR- 83-0355

(11)

AD A127799

UNITED TECHNOLOGIES

Copy available to DTIC does not permit fully legible reproduction

UNITED TECHNOLOGIES RESEARCH CENTER

East Hartford, Connecticut 06108

83 05 06-157

[illegible] for public release; [illegible]tion unlimited.

DISCLAIMER NOTICE

THIS DOCUMENT IS BEST QUALITY PRACTICABLE. THE COPY FURNISHED TO DTIC CONTAINED A SIGNIFICANT NUMBER OF PAGES WHICH DO NOT REPRODUCE LEGIBLY.

UNITED TECHNOLOGIES RESEARCH CENTER

UNITED TECHNOLOGIES

East Hartford, Connecticut 06108

(11)

R82-915634-2

The Effects of Free-Stream Turbulence on the Turbulence Structure and Heat Transfer in Zero Pressure Gradient Boundary Layers

Contract No. F49620-81-C-0053

REPORTED BY M. F. Blair

M. F. Blair

D. E. Edwards

D. E. Edwards

APPROVED BY R P Dring

R. P. Dring

DATE November 1982

NO. OF PAGES ________ COPY NO. ________

UNCLASSIFIED

SECURITY CLASSIFICATION OF THIS PAGE (When Data Entered)

REPORT DOCUMENTATION PAGE

READ INSTRUCTIONS BEFORE COMPLETING FORM

1. REPORT NUMBER AFOSR-TR- 83-0355	2. GOVT ACCESSION NO. AD-A127797	3. RECIPIENT'S CATALOG NUMBER
4. TITLE (and Subtitle) THE EFFECTS OF FREE-STREAM TURBULENCE ON THE TURBULENCE STRUCTURE AND HEAT TRANSFER IN ZERO PRESSURE GRADIENT BOUNDARY LAYERS		5. TYPE OF REPORT & PERIOD COVERED INTERIM
		6. PERFORMING ORG. REPORT NUMBER
7. AUTHOR(s) M F BLAIR D E EDWARD R P DRING		8. CONTRACT OR GRANT NUMBER(s) F49620-81-C-0053
9. PERFORMING ORGANIZATION NAME AND ADDRESS UNITED TECHNOLOGIES RESEARCH CENTER EAST HARTFORD, CT 06108		10. PROGRAM ELEMENT, PROJECT, TASK AREA & WORK UNIT NUMBERS 61102F 2307/A4
11. CONTROLLING OFFICE NAME AND ADDRESS AIR FORCE OFFICE OF SCIENTIFIC RESEARCH/NA BOLLING AFB, DC 20332		12. REPORT DATE November 1982
		13. NUMBER OF PAGES 186
14. MONITORING AGENCY NAME & ADDRESS(if different from Controlling Office)		15. SECURITY CLASS. (of this report) Unclassified
		15a. DECLASSIFICATION DOWNGRADING SCHEDULE

16. DISTRIBUTION STATEMENT (of this Report)

Approved for Public Release; Distribution Unlimited.

17. DISTRIBUTION STATEMENT (of the abstract entered in Block 20, if different from Report)

18. SUPPLEMENTARY NOTES

19. KEY WORDS (Continue on reverse side if necessary and identify by block number)

FREE STREAM TURBULENCE
HEAT TRANSFER
BOUNDARY LAYER
TURBULENCE MEASUREMENTS

20. ABSTRACT (Continue on reverse side if necessary and identify by block number)

In an earlier AFOSR funded investigation, experimental research was conducted to determine the influence of free-stream turbulence boundary layer heat transfer and mean profile development. The data obtained under this earlier contract indicated that both the skin friction and the heat transfer increased significantly with increased free-stream turbulence level. Under the present investigation detailed boundary layer turbulence structural data and turbulent heat transfer data were obtained for experimental test conditions and profile locations selected from the earlier test matrix.

DD FORM 1473 1 JAN 73 EDITION OF 1 NOV 65 IS OBSOLETE

UNCLASSIFIED

83 05 06-152

SECURITY CLASSIFICATION OF THIS PAGE (When Data Entered)

Numerous measurements assured that the present test conditions (boundary layer development and free-stream turbulence distributions) duplicated those of the earlier AFOSR contract. The purposes for making these present detailed boundary layer turbulence measurements were: (1) to provide data to which current finite-difference boundary layer turbulence models could be compared, and (2) to generate a data base for the development of new analytical models for boundary layer heat transfer prediction. The results from the present program have shown that the distributions of both the turbulence kinetic energy and the turbulence structural coefficients were affected by increased levels of free-stream turbulence. Local profile measurements indicated that the effect of increased free-stream turbulence was to decrease the near-wall turbulent Prandtl number relative to values expected for low free-stream turbulence. Turbulent Prandtl numbers in the outer region of the boundary layer were slightly increased for higher free-stream turbulence. A turbulence dependent correlation for the measured distribution of turbulent Prandtl number is given. With the completion of the experimental portion of this investigation, a theoretical effort was made to assess the capability of a finite difference boundary layer computer program, ABLE (Analysis of the Boundary Layer Equations) for predicting the effect of free-stream turbulence on momentum and thermal boundary layers. Comparisons with experimental data of mean flow velocity, mean flow temperature, Reynolds shear stress, turbulent heat transport, and turbulence kinematic energy were made in this investigation. In addition, the turbulent Prandtl number correlation deduced from the experimental measurements was used in the boundary layer analysis and its effect on surface heating evaluated. The results indicated that this boundary layer analysis, which uses a one equation eddy viscosity turbulence model, can provide adequate predictions of zero pressure gradient flows with high free-stream turbulence and wall heating.

R82-915634-2

The Effects of Free-Stream Turbulence on the Turbulence Structure and Heat Transfer in Zero Pressure Gradient Boundary Layers

TABLE OF CONTENTS

TABLE OF CONTENTS

(Continued)

ABSTRACT

In an earlier AFOSR funded investigation, experimental research was conducted to determine the influence of free-stream turbulence on turbulent boundary layer heat transfer and mean profile development. The data obtained under this earlier contract indicated that both the skin friction and the heat transfer increased significantly with increased free-stream turbulence level. Under the present investigation, detailed boundary layer turbulence structural data and turbulent heat transfer data were obtained for experimental test conditions and profile locations selected from the earlier test matrix. Numerous measurements assured that the present test conditions (boundary layer development and free-stream turbulence distributions) duplicated those of the earlier AFOSR contract. The purposes for making these present detailed boundary layer turbulence measurements were: (1) to provide data to which current finite-difference boundary layer turbulence models could be compared, and (2) to generate a data base for the development of new analytical models for boundary layer heat transfer prediction. The results from the present program have shown that the distributions of both the turbulence kinetic energy and the turbulence structural coefficients were affected by increased levels of free-stream turbulence. Local profile measurements indicated that the effect of increased free-stream turbulence was to decrease the near-wall turbulent Prandtl number relative to values expected for low free-stream turbulence. Turbulent Prandtl numbers in the outer region of the boundary layer were slightly increased for higher free-stream turbulence. A turbulence dependent correlation for the measured distribution of turbulent Prandtl number is given.

With the completion of the experimental portion of this investigation, a theoretical effort was made to assess the capability of a finite difference boundary layer computer program, ABLE (Analysis of the Boundary Layer Equations) for predicting the effect of free-stream turbulence on momentum and thermal boundary layers. Comparisons with experimental data of mean flow velocity, mean flow temperature, Reynolds shear stress, turbulent heat transport, and turbulence kinetic energy were made in this investigation. In addition, the turbulent Prandtl number correlation deduced from the experimental measurements was used in the boundary layer analysis and its effect on surface heating evaluated. The results indicated that this boundary layer analysis, which uses a one equation eddy viscosity turbulence model, can provide adequate predictions of zero pressure gradient flows with high free-stream turbulence and wall heating.

INTRODUCTION

The search for improved gas turbine performance has led steadily in the direction of higher turbine inlet temperatures. The last twenty years have seen an increase in turbine inlet temperatures of roughly 1400°F but an increase in allowable blade metal temperature of only roughly 200°F. The difference between these two increases in temperature can be related directly to improved cooling technology. As an integral part of this advancing cooling technology, engine manufacturers are continually seeking improved techniques for calculating heat transfer coefficient distributions on gas turbine airfoils. As the level of cooling technology has been driven upward, and with it turbine inlet temperature, it is not surprising that the result is a design methodology which is extremely unforgiving of even small errors. The temptation is always present to overcool the airfoils but this is unacceptable due to the powerful negative impact of cooling air on the cycle and on turbine efficiency. It is this dilemma which has often led to extremely long and expensive developmental testing of advanced technology turbines.

Gas turbine thermal design systems are typically not based on fundamental fluid mechanics and heat transfer data and analysis alone but rather they are calibrated, or adjusted, to provide agreement with engine experience. Without the benefit of a first-principles understanding of the effects involved there is the likelihood that a designer will unknowingly either overcool the component or go beyond the range of validity of the design system calibration. There is, then, a clear requirement for the development of airfoil heat transfer distribution prediction procedures which are based on fundamental fluid mechanics and heat transfer data. The great emphasis placed on the development of accurate boundary layer calculation techniques over the past few years reflects the recognition of these needs.

One particularly important topic in the general context of turbine airfoil convective heat transfer is the influence of the free-stream turbulence on fully turbulent boundary layer development. It has, of course, long been recognized that increasing the free-stream turbulence level can cause a forward shift of the laminar to turbulent transition region. This particular phenomenon, the reduction of the boundary layer transition Reynolds number with increased free-stream turbulence level, is well documented in the open literature for zero pressure gradient flows and can be adequately predicted with currently available boundary layer prediction schemes. In addition, a number of investigators have studied the effects of free-stream turbulence level on turbulent boundary layer growth, profile structure, skin friction distribution and heat transfer. The consensus of these studies, is that free-stream turbulence has a very large and important influence on both the heat transfer and the boundary layer characteristics. As an example, it has been shown in a recently completed AFOSR funded contract at UTRC that a free-stream turbulence intensity of 5 percent produces an increase in Stanton number of approximately 15 percent over the value expected for a low turbulence freestream. While a number of existing boundary layer analysis procedures (including the UTRC ABLE code) account reasonably well for the influence of free-stream turbulence on mean velocity profile development and skin friction, no currently available analysis satisfactorily predicts the observed increased heat transfer rates.

The present program was designed to provide detailed boundary layer turbulence and turbulent heat flux distribution data for a range of free-stream turbulence levels. As part of this program these experimental data were employed to evaluate the analytical turbulence models currently incorporated in the UTRC ABLE code. It is anticipated that in the future these experimental data will be used by both UTRC and other workers in the field of boundary layer computation for development of new analytical turbulence models.

The contract effort consisted of acquiring, documenting and analyzing experimental flat wall boundary layer mean and fluctuating profile data to determine the influence of free-stream turbulence on fully turbulent boundary layer flows. For fully turbulent, zero pressure gradient flows, the following profile data were obtained for a range of free-stream turbulence intensities; boundary layer mean and fluctuating velocities and temperatures, turbulent shear stresses, and turbulent Prandtl numbers. In addition, in order to improve the ability of the UTRC boundary layer deck to predict the effects of free-stream turbulence on heat transfer rates, a turbulent Prandtl number distribution model was incorporated into the UTRC boundary layer code. Calculations were carried out employing the measured turbulent Prandtl number distributions and comparisons made between the predicted and measured heat transfer distributions.

DESCRIPTION OF TEST EQUIPMENT

1. Wind Tunnel and Heat Transfer Test Surface

All experimental data for the present investigation were obtained in the United Technologies Research Center (UTRC) Boundary Layer Wind Tunnel (Fig. 1). This tunnel was designed specifically to generate large-scale, two-dimensional, incompressible boundary layers with Reynolds numbers and free-stream turbulence levels typical of turbomachinery airfoils. Complete descriptions of this facility including measurements documenting the tunnel flow uniformity and two-dimensionality of the test boundary layers are given in Refs. 1 and 2. The tunnel test section consisted of a flat upper wall instrumented for heat transfer measurements which served as the boundary layer test surface, plexiglass vertical sidewalls and a flexible lower wall. The test section was 34-in. wide, 96-in. long and 8-in. high at the entrance. For all test flows in this study the lower flexible test section wall was adjusted to produce a constant velocity along the test section.

A photograph of the Boundary Layer Wind Tunnel is presented in Fig. 2. Also shown in Fig. 2 are both the telescope used to position probes relative to the test wall and the computer controlled probe traverse mechanism.

The boundary layer test surface (upper wall of test section) consisted of a uniform heat flux electrically heated plate instrumented for the measurement of local convective coefficients (Fig. 3). The heated flat plate was constructed from a block of rigid urethane foam 34-in. wide by 96-in. long by 4-in. thick mounted in a plexiglass frame with 6-in. wide strips of 316 stainless steel foil cemented to the test surface. Details of the flat plate model and its instrumentation are presented in Refs. 1 and 2. Rigid foam was employed for the substrate of the heated flat plate model because of its extremely low thermal conductivity (0.025 Btu/hr ft°F). Less than 1/2 percent of the heat generated on the surface of the plate was conducted away from the test surface. Electric current passing through the metal foil strips cemented to the test surface produced the surface heating. The metal foil strips were wired in series and were powered by a single low-ripple, regulated dc power supply. The foil test surface was instrumented with an array of 203 Cr-Al 0.13 mm diameter bead welded thermocouples. Each thermocouple was welded to the back surface of the foil through a hole in the rigid foam plate. Forty-eight surface static pressure taps were also installed along the test surface.

The dc power current passing through the surface strips was measured using two precision shunt resistors and a digital voltmeter. The temperatures of the test surface thermocouples were measured relative to a single test section free-stream reference junction using a digital voltmeter.

In order to insure a known, constant test surface emissivity and hence a known radiation loss, the completed foil test surface was coated with 3M C-101 high emissivity flat black paint (ϵ = 0.99). Test results indicated that this surface was aerodynamically smooth, producing no premature boundary layer transition.

Local convective coefficients were determined by ignoring the negligible conduction losses, subtracting power lost through thermal radiation and dividing by the temperature difference from the wall (T_w) to the freestream (T_e). To illustrate the magnitude of the radiation losses from the test surface, for U_e = 100 ft/sec, for turbulent boundary layer flow with $T_w - T_e$ = 25°F, the radiation loss was approximately 4 percent of the total surface power.

As shown in Fig. 1, at the test section entrance a bleed scoop formed the leading edge of the heated boundary layer test surface. The scoop, which was mounted smoothly on the front edge of the heated test wall, provided a very short unheated starting length (ξ = 1.7 in.) upstream of the heated test surface. The leading edge of the scoop was a 4 x 1 ellipse in order to prevent a local separation bubble and premature transition of the test surface boundary layer. Details of the scoop including its instrumentation and adjustment are given in Refs. 1 and 2.

2. Turbulence Generating Grids

As described in Ref. 1, this wind tunnel has a relatively low residual test section turbulence level (< 1/4%). Higher turbulence levels required for this study were generated by inserting various square array biplane grids constructed from rectangular bars at the entrance to the main tunnel contraction (see Fig. 1). Four turbulence generating grids were designed using the correlations of Ref. 3. The grids will be referred to as Grids 1, 2, 3 and 4 corresponding to mesh widths, M, of 7/8, 2 9/16, 7 and 9 in. The minimum turbulence configuration (no grid) will be referred to as Grid 0. Details of the grid configuration are given in Ref. 1. This present arrangement differs from that used for nearly all the earlier investigations of this subject in which the turbulence grids were located in the test section just upstream of the boundary layer test surface. The benefits derived from locating the grids at the contraction entrance were that the generated turbulence was more homogeneous and had a lower decay rate along the test section. Since grid generated turbulence decays approximately as $u'/U \propto (x/b)^{-5/7}$ (Ref. 3), the change in turbulence level with distance along the test section was reduced by increasing the distance from the grid to the test section entrance. In addition, the results of Ref. 3 indicate that approximately 10 grid mesh lengths are required to establish a uniform turbulent flow. Locating the grid a distance upstream of the test section requires, of course, a more coarse grid to achieve a given test section turbulence intensity.

Another effect considered was the expected influence of the contraction of the components of the grid generated turbulence. It was recognized that rearrangement of the relative magnitudes of the turbulence components would occur due to the contraction. However, since the contraction ratio was small (2.8), it was concluded that any effects of induced anisotropy would be small in comparison to the advantages gained in homogeneity and reduced decay rate. To determine the validity of the assumption, all three components of the test section turbulence were documented for all test cases.

3. Boundary Layer Total Pressure and Thermocouple Probes and Traverse Control

Boundary layer mean velocity profile data were measured using United Sensor Model Ba-0.020 impact probes with flattened tips. The probes used in the program were inspected for defects using both a Nikon Model II toolmakers microscope and a Jones and Lamson Model PC14 Shadowgraph. Mean temperature data were measured with miniature thermocouple probes designed using the results of Ref. 4. The thermocouple sensing elements for these probes were constructed from 0.001 in. dia. Chromel-Alumel bead welded wires. The thermocouple bead (≈ 0.003 in. dia.) was located at the center of the probe support prongs which were fabricated of heavier Chromel and Alumel wire. The results of Ref. 4 indicate that a probe of this design was virtually free of wire conduction errors and was capable of measuring boundary layer mean temperature profile data into the viscous sublayer region.

Movement of the boundary layer probes was achieved using and L.C. Smith ball/screw traverse drive with an optical shaft encoder capable of resolving relative probe location to within 0.0005 in. The traverse mechanism was suspended on a linear ball bearing track beneath the test section. The traverse could be located anywhere in the center 75 percent of the test section width from the leading to trailing edges of the test wall. A telescope sighted through the tunnel sidewall was used to accurately position probes relative to the test wall. Estimated absolute accuracy of measured probe distance from the test surface was 0.002 in. for any location in the test boundary layers.

HOT WIRE DATA ACQUISITION AND ANALYSIS TECHNIQUES

1. General

Measurements of fluctuating velocities and temperatures in the test boundary layers were obtained using multi-element hot wire anemometry techniques. For a large number of the test cases the wind tunnel was operated without wall heating, the resulting boundary layers being isothermal. Both vertical and horizontal x-type 2 wire probes were employed for these isothermal test cases. For cases with wall heating the velocity and temperature fluctuations in the flows were determined by using specially designed 3 wire probes, one wire of which was operated at a lower overheat than the other two. Detailed descriptions of both the 2 and 3 wire probes are given below in section 2. The voltage signals from the various hot wire probes were digitized, recorded and subsequently reduced to fluctuating velocity and temperature records using a minicomputer. A detailed description of the data system is provided in section 4. An analysis of the uncertainties of the various hot wire measurements is given in Appendix A.

2. Description of the Hot Wire Probes

2.1 Probe Design

The present study involved the measurement, using arrays of inclined hot wires, of fluctuating velocities and temperatures within boundary layer flows. In order to minimize potential errors for these measurements (errors largely arising from the inherent mean velocity and temperature gradients in the flows and the finite probe size) the hot wire probes were custom-designed and fabricated specifically for this program. The results from a large number of previous boundary layer turbulence and general hot wire studies were incorporated into the probe designs (Refs. 5-14). For the 2 wire x-type probes used in the isothermal tests three important design principles were adopted from these earlier studies. (1) To reduce the effects of the mean gradients in the flows the active length (or the size of the array of wires in the direction of the gradients) of the wires should be minimized. (2) To reduce end effects (nonuniform temperature along the active length) and to insure that a "Champagne k^2" (Ref. 7) form of angular sensitivity could be employed, an active length/diameter ratio of 200 was chosen. (3) To maximize the spatial correlation coefficient (maximum accuracy of cross-products such as Reynolds stress) without introducing wire cross-talk effects a transverse wire spacing of $3\ell/4$ was chosen.

Considerations (1) and (2) required that the diameter (d) be as small as possible--the limitation being practical considerations of probe fabrication and sensor survivability. A probe development program (UTC funded) conducted jointly with DISA, Inc. resulted in the conclusion that the minimum practical wire diameter for these probes was 2.5 μm (0.0001 in.) for platinum plated tungsten wires. From consideration (2) the active length of the wires was chosen as .50 mm (0.020 in.) and from (3) the transverse spacing was selected as 0.015 in. These wire arrays were employed

for x-type configurations oriented in both the vertical and horizontal planes. As will be discussed in the results section, cross-checks indicate that the fluctuating data measured with probes of this design are consistent and accurate.

The special 3 wire probes consisted of vertical x-type wire arrays with a third wire mounted equidistant between the wires of the x. This third wire was parallel to one of the wires of the x array. All three wires were constructed from the same material (platinum plated tunsten) and had the same diameter (0.0001 in.) and active length (0.020 in.). The transverse separation between adjacent wires of the 3 wire array was 0.015 in. With this wire arrangement the two parallel wires of the array were exposed to equal effective velocities during any given data sample period. Details of the techniques used to determine instantaneous velocities and temperatures with the 3 wire probes are given in section 4.

2.2 Probe Calibration

Prior to calibration all probe sensors were operated for approximately two hours in the 100 ft/sec mainstream of the wind tunnel. During this "wire curing" step the sensors were set to operate at overheat ratios slightly higher than those used during actual testing. These "curing" steps (1) provided some assurance that the sensors on a given probe would be likely to survive the calibration and testing environments, and (2) improved the stability of the calibration constants of a given sensor. Each probe was calibrated for temperature-resistance characteristics in a low temperature recirculating oven. Typically five temperature vs. resistance points were measured for each sensor. A least-squares data reduction program was used to find a best temperature-resistance coefficient.

$$R_w = R_{32}\left[1 + \alpha(T_w - 32)\right] \tag{1}$$

where R_w = resistance of the active sensor
R_{32} = sensor resistance at 32°F
T_w = sensor temperature
α = temperature-resistance coefficient

Following the preliminary "burn-in" and the resistance temperature calibration each sensor was calibrated for velocity and angular sensitivity in a low-turbulence 1½-in. dia. jet flow. The sensors of the 2 wire probes were calibrated to an overheat ($R_{w\text{-}hot}/R_{adiabatic}$) of 1.5. For the 3 sensor probes the outside two sensors were calibrated at an overheat of 1.5 while the center sensor was calibrated at an overheat of 1.2. With the main probe support stem oriented perpendicular to the jet axis (wires ± 45° to the jet axis) mean velocity and bridge output voltage were recorded for approximately 20 jet speeds ranging from 7 to 130 ft/sec. The mean response equation of each sensor was assumed to be of the form

$$N_u = A_1 + B_1 R_e^{0.45} \tag{2}$$

which can be algebraically manipulated to

$$E_w^2 = \frac{A_2(R_s+R_w)^2}{R_w} T^{0.76} (T_w-T) + \frac{B_2(R_s+R_w)^2}{R_w} (T_w-T) U_E^{0.45} \tag{3}$$

where E_W = wire voltage
R_S = probe body, cable and internal anemometer resistance
R_W = sensor resistance
T = air temperature
T_W = sensor temperature
U_E = effective velocity
A_2, B_2 = empirical constants

The constants A_2 and B_2 were determined for each sensor from a least-squares fit of the data to Equation (3). Next, using a pitching fixture, pitch angle versus voltage data were obtained with the probes rotated from +20° to -20° in steps of 5°. The center of pitch coincided with the intersection of the wires of the x. Pitch sensitivity data were obtained for three jet velocities, 50, 80 and 100 ft/sec. The angular sensitivity of the wires was assumed to conform to Champagne's k^2 law (Ref. 7),

$$U_E^2(\phi) = U^2(\phi=0)(\cos^2\phi + k^2\sin^2\phi) \tag{4}$$

where ϕ = angle between wire and direction normal to the flow ($\phi \approx 45°$ with wall probe stem normal to the flow)
U_E = effective velocity

Using a least-squares routine to find a best fit of the pitch-voltage data to Champagne's equation, optimum values of k were determined for each sensor.

In summary, the temperature-resistance, mean velocity and pitch calibrations were used to determine the following calibration constants.

(1) R_{32} - sensor resistance at 32°F
(2) α - temperature-resistance coefficient
(3) A_2 and B_2 - empirical constants (Eq. 3)
(4) k - empirical constant (Eq. 4).

3. Description of the Data System

For all test cases, both for isothermal flows and for flows with wall heating, the multi-element hot-wires were driven by Thermo Systems, Inc. (TSI) Model 1050 constant temperature anemometers. Signals from the anemometers were first passed through a wide band amplifier (Preston Model 8300 XWB) and then digitized using a TSI Model 1075 Multichannel Digitizer. A feature of this particular analog-to-digital converter which is important to this application is that the various

channels are sampled and held simultaneously. This simultaneous sample-hold feature permits cross-products of the various fluctuating quantities to be computed. Storage restrictions of the main memory of the minicomputer limited the total number of samples taken in a continuous stream to 18,432. The anemometer signals were sampled at 3906 Hz (6144 total samples) per channel or 2604 Hz (9216 total samples) per channel for 2 or 3 wire applications, respectively. The sampling rates resulted in total continuous sample periods of 2.36 sec for both 2 and 3 wire applications. The digitized voltage samples were stored on magnetic disks using a DEC Model RX02 floppy disk recorder.

The RX02 is a "double density" system and can record up to 512 K bytes of information on a single floppy disk. Reduction of the voltage-time records to either velocity-time records (isothermal flow - 2 wires) or velocity-temperature-time records (flows with wall heating - 3 wires) was accomplished off-line using an LSI 11-03 minicomputer. The reduced temperature-velocity-time or velocity-time results were written onto double-density magnetic disks and copied onto magnetic tape for purposes of plotting and tabulation.

4. Data Analysis Techniques

The digitized voltage vs. time records from the multi-wire probes were reduced to turbulence quantities using an LSI 11-03 minicomputer. For this reduction step the digitized data were read into the computer from the RX02 unit while the following constants for each sensor were input through a terminal.

R_{32} - sensor resistance at 32°F
$R_{adiabatic}$ - sensor resistance in flow with no overheat
R_{hot} - sensor resistance at operating temperature
R_s - probe, cable and anemometer (40 Ω for TSI-1050 sets) series resistance
α - temperature-resistance coefficient
A_2, B_2 - calibration constants from Eq. 3
k - calibration constant from Eq. 4

4.1 Isothermal Flows (2 Wire Probes)

Solution for the velocity components (u and v for the vertical wire arrays, u and w for the horizontal arrays) for each time step proceeded as follows. First, using the adiabatic resistances (no sensor overheat) measured for the sensors in the test flow and Eq. 1, the temperature (T) of the flow was computed. The hot sensor temperatures (T_w) were then computed from R_{hot} and Eq. 1. For each time step the voltages for each of the sensors were input to Eq. 3 to determine the sensor effective velocity (U_E). Next, assuming that the wires of the x array were perpendicular to each other and at ± 45° to the mainstream flow direction, the simultaneously measured effective sensor velocities were combined using Eq. 4 to find either u and v (vertical array) or u and w (horizontal arrays). As a check on the accuracy of the assumption that the wires were at exactly ± 45° to the mainstream one of the probes was also calibrated using the "wire effective angle" method of Refs. 14 and 15.

Voltage vs. time records were reduced to fluctuating velocity components using these two different calibration-reduction techniques and the results were in very close agreement. Once the velocity component vs. time record was generated it remained a straightforward matter to compute any desired statistical quantities for the entire time record. The following turbulence quantities were computed for the u-v (vertical array) components. Similar quantities with the transverse velocity component (w) substituted for the vertical component (v) were computed for the horizontal probe arrays.

$\overline{u}$, $\overline{u'^2}$, $\overline{u'^3}$, $\overline{u'^4}$	- first through the fourth moments of the streamwise fluctuating velocity
$\overline{v}$, $\overline{v'^2}$, $\overline{v'^3}$, $\overline{v'^4}$	- first through the fourth moments of the normal fluctuating velocity
$\overline{u'v'}$, $\overline{u'^2v'}$, $\overline{u'v'^2}$	- double and triple cross-products (and their correlation coefficients
Su, Sv, Fu, Fv	- skewness and flatness of both velocity components

4.2 Flows with Wall Heating (3 Wire Probes)

For the 3 wire probes employed for these measurements the two parallel wires of the array were operated at different overheats ($R_{w\text{-}hot}/R_{adiabatic}$ = 1.5 and 1.2). The data reduction technique used for these measurements was based upon the assumption that during any time step the effective velocities over the two parallel wires were equal (for velocity scales equal to or larger than the separation distance between the wires). The solution technique proceeded by first finding the fluid temperature (T) for a given time step. Using the voltages (E_w) from the two parallel sensors and assuming that U_e was equal for both wires, Eq. 3 was iteratively solved for T. Once T was known the solution for the velocity components (u and v) for each step proceeded as in 4.1. In addition to computing the turbulence quantities listed in section 4.1, the following items were determined for the cases with wall heating.

$\overline{t}$, $\overline{t'^2}$, $\overline{t'^3}$, $\overline{t'^4}$	- first through the fourth moments of the fluctuating temperature
$\overline{v't'}$, $\overline{v't'^2}$	- velocity-temperature cross-products (and their correlation coefficients)
S_T, F_T	- skewness and flatness of temperature

4.3 Reynolds Stress and Turbulent Heat Flux Corrections for Sensor Separation

The accuracy of cross-products of correlated turbulent quantities is directly influenced by the spacing between the sensors used to measure these quantities (Ref. 13). The contributions of the smallest scales of the turbulence (smaller than the transverse sensor spacing) are excluded from the correlated products. As examples of the impact of this effect Refs. 9, 10, 11, 12 and 14 all present Reynolds stress measurements ($-\overline{u'v'}$) which are about 30 percent lower than expected. Unfortunately this effect cannot be eliminated completely because a minimum limit for sensor separation is reached when sensor "cross-talk" errors become significant. As discussed in Section 2.1, the probes used for the present program were specifically designed to minimize these effects.

Correction factors for the cross-product terms measured in this program were determined by the following technique. Using the parallel wires of the 3 wire probes, the transverse spatial correlation coefficient (ψ parallel) was determined as a function of position (y/δ) in the test boundary layers. Wire separation distances (r) for each of the probes were accurately measured using a Nikon Model II toolmaker's microscope. By assuming that the correlation coefficient fell with the square of the separation distance (r^2) (Ref. 16) an appropriate spatial correlation coefficient could then be calculated for any x-type probe/boundary layer location combination. Next, assuming that the contributions to the cross-products were directly proportional to the spatial correlation coefficient, a correction factor for the probe/location combination was determined:

$$\beta = (1 - \Psi_{parallel}) \left[\frac{r\,(x\ \text{probe})}{r\,(\text{parallel})} \right]^2 \qquad (5)$$

As an example the correction procedure for a measured Reynolds stress was as follows:

$$(\overline{u'v'})_{corrected} = \frac{(\overline{u'v'})_{measured}}{1-\beta} \qquad (6)$$

Typical correction factors (β) for the various probes, quantities and locations ranged from 0.12 to 0.2. A journal article documenting the development of this correction technique is currently in preparation.

EXPERIMENTAL DATA

1. Experimental Test Program

Measurements were obtained for three test flow conditions of incompressible, zero pressure gradient flow along a flat, uniform heat flux, test wall. The three test cases of this program reproduced conditions employed for an earlier AFOSR Contract (Ref. 2). For all test cases the free-stream velocity was 100 ft/sec and the test surface boundary layer passed through natural transition, i.e., no artificial trips were employed to promote boundary layer transition. Data were obtained for three levels of free-stream turbulence, (1) at the tunnel minimum turbulence level and (2) and (3) at higher levels of free-stream turbulence generated with bi-plane grids. Using the nomenclature of Refs. 1 and 2, the free-stream turbulence levels of this program are designated as follows

(1) No grid-low free-stream turbulence (Grid 0) - $T_e \approx \frac{1}{4}$ percent
(2) Grid number 2 ($\frac{1}{2}$ in. bars) - $T_{e_{nom}} = 2$ percent
(3) Grid number 4 (2 in. bars) - $T_{e_{nom}} = 6$ percent

A complete documentation of the multi-component turbulence decay, integral length scale growth and spectral distributions generated by these particular test grids is available in Refs. 1 and 2.

For each of these flow conditions experimental boundary layer profile data were obtained at three streamwise locations (x = 52, 68 and 84 inches) for both an adiabatic test surface (no wall heating) and with a uniform surface heat flux condition. With no wall heating the following data were measured:

Type of Data	Instrumentation	Measurement Stations Per Profile
Profiles of streamwise velocity (mean and fluctuating)	Single, horizontal, linearized hot wire	30
Profiles of streamwise and normal velocities	Vertical x-type wires with analog-digital data system	17
Profiles of streamwise and transverse velocities (mean and fluctuating)	Horizontal x-type wires with analog-digital data system	17

With the uniform wall heat flux conditions the following data were measured:

Type of Data	Instrumentation	Measurement Stations Per Profile
Surface Stanton Number distribution	Thermocouple instrumentation incorporated into uniform heat flux test surface	210 surface locations
Profiles of streamwise mean velocity	Miniature boundary layer pitot probes	90
Profiles of mean temperature	Miniature boundary layer thermocouple probes	90
Profiles of temperatures and streamwise and normal velocities (mean and fluctuating)	3-Wire probes with analog-digital data system	17

In summary, for each of the three flow conditions surface heat transfer distributions and three stations of profile data were measured. In total (3 conditions) x (3 profiles) x (6 types of profile data) = 54 profile surveys were documented.

2. Boundary Layer Profile Data Format

The mean and fluctuating quantities measured for the various flow conditions and profile locations have been assembled in both graphical and tabular form. Comparisons of these results for the various flow conditions and with similar results from other experiments will be presented in the Analysis of Results section below. The compiled data for all the measurements stations are given in Appendix B - Experimental Data. As a guide to the format of the presentation and results, the data for a single sample profile are given in Figs. 4 through 5E and in Tables 1 through 3B. These particular sample profile data were obtained at the "middle" free-stream turbulence level (Grid 2, Te = 1.6%) at X = 68 in. The mean profile (total pressure and thermocouple probe) data for the sample set are presented in graphical form in Fig. 4 and in tabular form in Table 1. Table 2 presents a compilation of the test flow conditions and values computed from the mean profile data. These mean profile data are presented both in the form of velocity and temperature ratios versus y/δ and in the coordinates of the universal velocity and temperature "laws of the wall". As discussed in the Data Analysis Techniques section, the digitized data reduction system made possible the computation of any desired moments and cross-products of the various measured fluctuating quantities. A total of 38 quantities were selected for presentation on the grounds that they met either or both of the following criterion: (1) the quantity is employed in some existing boundary layer turbulence modeling method or (2) the quantity serves as a diagnostic of the characteristics of the turbulence, e.g.,

intermittency. These various quantities were both plotted and tabulated for each profile station (see Appendix B). The results for the sample profile are presented in Figs. 5A through E and in Table 3A and B. The distribution of a series of turbulence quantities computed from the fluctuating velocity data are presented in Fig. 5A. Starting in the upper left-hand corner of the figure, the distributions of the individual components of the turbulence are compared with the results of Klebanoff (obtained for near-zero free-stream turbulence). Moving clockwise, the next figure presents the measured distributions of the Reynolds stress nondimensionalized by the friction velocity (U_τ was determined independently from the mean profile data) and the distribution of the shear stress correlation coefficient. Also included in this plot is the distribution of shear stress computed from the mean profile data using the technique of Ref. 17. The lower right-hand corner plot of Fig. 5A presents the transport velocities of turbulent shear stress and kinetic energy defined as follows

$$V_\tau = \frac{\overline{u'v'^2}}{\overline{u'v'}} \tag{7}$$

$$V_q = \frac{\overline{v'(u'^2 + v'^2)}}{\overline{u'^2} + \overline{v'^2}} \tag{8}$$

See Ref. 14, pp. 220-239, and Ref. 18 for the development of these terms. (Due to a software error V_τ was not computed for the data of Grid 2 and does not appear for this sample plot.) The remaining plot of Fig. 5A presents the structural coefficient (as defined in Ref. 19) distributions for this case.

Turbulence quantities computed from the fluctuating velocities and temperatures are presented in Fig. 5B. Distributions of the turbulent heat flux and its correlation coefficient are given for the plot in the upper left-hand corner. The turbulent heat flux distribution is shown nondimensionalized by the independently measured wall heat flux. Also shown in this plot is the distribution of heat flux through the boundary layer as computed from the mean velocity and temperature profile data (see Ref. 17). The upper right-hand corner plot of Fig. 5B presents the fluctuating temperature distribuitons in two forms: (1) nondimensionalized by the friction temperature and (2) nondimensionalized by the temperature difference between the wall and free-stream. The lower two plots of Fig. 5B give the distributions of the turbulent Prandtl number, Pr_t, and two structural coefficients, $a_{1,\theta}$ and $G_{1,\theta}$ (see Ref. 19).

$$Pr_t = \frac{\overline{-u'v'}\ \dfrac{\partial T}{\partial y}}{\overline{v't'}\ \dfrac{\partial U}{\partial y}} \tag{9}$$

$$a_{1,\theta} = \frac{\overline{v't'}}{t'\sqrt{\overline{-u'v'}}} \tag{10}$$

$$G_{1,\theta} = \frac{\overline{v' t'^2}}{2 \overline{t'^2} U_\tau} \qquad (11)$$

Triple product distributions of the fluctuating velocity components are given in Fig. 5C. Streamwise-transverse (u'w') products are grouped on the left-hand plot while streamwise-normal (u'v') products appear in the right.

For Fig. 5D the left-hand figure presents the skewness factor distributions for the fluctuating temperatures and velocities. Note that skewness factor distributions of the streamwise component (u') were determined both from the data from the vertical x probes (S_{uv}) and the horizontal x probes (S_{uh}). The correlation coefficients for the triple products of Fig. 5C are given in the right-hand plot of Fig. 5D.

Flatness factor distributions for the fluctuating temperatures and velocities are given in Fig. 5E. As with the skewness factors of Fig. 5D flatness factor distributions of the streamwise component are given for both the data for the vertical x (F_{u_v}) and horizontal x (F_{u_h}) probes. To avoid crowding on the figure the flatness of the temperature fluctuations was plotted after dividing by 2.

Tabulated values of these fluctuating quantities are given in Table 3A and 3B.

ANALYSIS AND DISCUSSION OF EXPERIMENTAL RESULTS

The present experimental test program was designed to examine, in detail, the effects of free-stream turbulence on the heat transfer through turbulent boundary layers. The test conditions for the present program were intended to reproduce cases for which other experimental data had been obtained previously under an earlier AFOSR contract (Ref. 2).

1. Comparisons of Present Results with Results of Ref. 2

A number of the measurements reported in Ref. 2 were repeated during the present program providing a measure of consistency for the two sets of data. Note that these various measurements were obtained in the same test facility and on the same test surface but about three years apart.

1.1 Free-Stream Turbulence Data

Measurements of the components of the free-stream turbulence (outside the boundary layer) were generally in excellent agreement (absolute levels of individual components agreed within 0.3 percent) with the measurements of Ref. 2. The exceptions to this rule were the transverse (w') fluctuation levels measured for Grid 4. These data were consistently higher (relatively 15% higher) than those measured for the same flow condition of Ref. 2. This discrepancy will be discussed in more detail in a following section.

1.2 Heat Transfer Distributions

For all three test conditions the agreement between the Stanton numbers measured for the present program and for Ref. 2 was excellent (±1%). The heat transfer distributions for the no grid (Grid 0), Grid 2 and Grid 4 cases were virtually identical with those presented in Ref. 2 in Figs. 41, 49 and 57, respectively and are not repeated here.

1.3 Boundary Layer Transition Location

For the Grid 2 and 4 test cases the agreement between the present transition location data and the similar data of Ref. 2 was within ± 3 percent. For the no-grid case, however, the transition Reynolds number increased from $Re_x = 1.2 \times 10^6$ to $Re_x = 1.35 \times 10^6$. This change in observed transition location was related to the three dimensional character of the transition process for the no-grid case. As discussed in Refs. 1 and 2, test section corner flows contaminate the flat test wall laminar boundary layer for the low free-stream turbulence case and produce premature transition along the tunnel centerline. This sidewall contamination was not important for the higher levels of free-stream turbulence because two-dimensional natural transition resulted well upstream of these effects. For the present no-grid test conditions the leading edge scoop adjustment was improved over the setting of the

tests of Ref. 2 producing reduced secondary corner flows and an increased transition Reynolds number. The transition Reynolds number (Re_θ) for the present tests was in excellent agreement with classic two-dimensional transition vs. turbulence correlations. The turbulent boundary layers which developed downstream of transition for both the present test and the test of Ref. 2 both exhibited the classic characteristics for zero-pressure gradient, low free-stream turbulence, two-dimensional flow.

1.4 Mean Profile Data

Integral thicknesses (δ^* and θ) computed from the prifle data for the Grid 2 and 4 cases agreed within 2 percent with the results from Ref. 2 at the respective locations. For the no-grid case the integral thicknesses were about 12 percent reduced from those computed for Ref. 2 at similar stations. This reduction in boundary layer thickness resulted from the increased length of laminar flow upstream of transition for the present no-grid data.

If comparisons are made only for profiles with equal Re_θ the results for all the grids (0, 2 and 4) are practically identical to the respective cases in Ref. 2. When plotted in U^+ or T^+ vs. Y^+ coordinates the mean velocity and temperature profiles exhibit significant regions ($30 < Y^+ < 300$) of logarithmic behavior. Both the velocity and temperature wakes showed significant reduction with increasing free-stream turbulence as did the similar data of Ref. 2. Skin friction coefficients computed from fits of the mean velocity data to the "law-of-the-wall" were in excellent agreement with the results of Ref. 2.

1.5 Comparison with Earlier Data - Conclusion

The conclusion reached from the free-stream turbulence, heat transfer and mean profile data was that the test conditions of Ref. 2 were closely duplicated for the present series of measurements. In effect these present measurements can be considered as an additional set of data for the same test conditions as Ref. 2.

2. Profile Data with Low Free-Stream Turbulence

A number of comparisons have been made between the data obtained for the present no-grid (low free-stream turbulence) profiles and measurements from other experiments. These comparisons are intended to provide a measure of the accuracy and consistency of the present boundary layer turbulence data.

The distributions of the u' and v' components of the turbulence profiles were in very good agreement with the classic results of Klebanoff (Ref. 20), see for example Appendix B—Fig. B-4A. The transverse component (w') measurements, however, were typically about 15 percent reduced from Klebanoff's results with w' only slightly greater than v'. These present w' distributions are thought to be accurate as they are in close agreement (as were the u' and v' distributions) with the recent results of Ref. 14. The turbulent shear stress distributions measured for these low free-stream turbulence cases were in excellent agreement with the shear stress

distributions computed from the mean profiles, Fig. B-4A. The accuracy of these particular measurements is also supported by the fact that for all cases the u'v' correlation coefficient was near the widely accepted value of 0.44 (Ref. 21) across most of the boundary layer. The measured distributions of the "structural" coefficients were in good agreement with the widely accepted constants, $a_1 = \overline{u'v'}/\overline{q^2} = 0.15$, $a_2 = \overline{u'^2}/\overline{q^2} = 0.5$, $a_3 = \overline{v'^2}/\overline{q^2} = 0.2$.

A number of the turbulence quantities computed from the present data were also determined for a similar zero-pressure gradient, low free-stream turbulence flow in the work of Ref. 14. The present distributions of transport velocity of turbulent shear stress (V_τ), transport velocity of turbulent kinetic energy (V_q) (Fig. B-4A), u'v' and u'w' triple products (Fig. B-4C), skewness factors (Fig. B-4D) and flatness factors (Fig. B-4E) were all in good agreement with the respective data of Ref. 14.

The turbulent heat flux distribution measurements were in reasonably close agreement with the distributions inferred from the mean profiles (Fig. B-4B). The accuracy of these mean profile distributions is unclear because of extreme sensitivity to uncertainties in the mean temperature profiles. The fluctuating temperature distributions agreed very closely with the distributions measured in Ref. 21 (Fig. B-4B). The values of the thermal coefficient a_{1_θ} were about 30 percent greater than those determined in Ref. 21 with the cause of the difference uncertain. The authors were unaware of any other measurements of G_{1_θ} to which the present data could be compared. Finally the turbulent Prandtl number distributions measured for the low free-stream turbulence cases were in excellent agreement with the proposed distribution of Rotta (Ref. 22).

There were, then, a large number of experimentally determined turbulence quantities in the present program which agreed very closely with the results of other studies. The conclusions reached from this result are that one can have a high level of confidence in the present data acquisition and reduction technique and that the turbulence quantities reported here can be expected to be both accurate and self-consistent.

3. Effects of High Free-Stream Turbulence on the Fluctuating Velocities

The impact of increased free-stream turbulence on the boundary layer turbulence kinetic energy distribution is shown in Fig. 6. Presented in this figure are experimental data from the present program obtained at stations with nearly equal momentum thickness Reynolds numbers ($Re_\theta \approx 5500 \pm 100$) for Grids 0, 2 and 4. Also given in Fig. 6 are turbulence kinetic energy distributions measured for similar zero pressure gradient, low speed flows by other investigators (Refs. 12 and 21). Integral thicknesses were not computed for these other data but based upon the stated values of δ it is estimated that for Ref. 12 Re_θ was about 3500 while for Ref. 21 $Re_\theta \approx 700$. Agreement between the present low free-stream turbulence profile case (Grid 0) and the similar data of Ref. 21 is reasonably good except very close to the wall. As discussed earlier this near-wall discrepancy resulted from the

relatively higher values of w' determined in the study of Ref. 21. For the profiles with higher free-stream turbulence there were no cases where the present flow conditions (Re_θ and T_e) were identical with those of Ref. 12. Despite this a comparison of these results shows reasonably good agreement for both the trends and absolute magnitudes of the kinetic energy distributions. Both the present data and the independent results from Refs. 12 and 21 indicate a progressive increase in boundary layer turbulence kinetic energy with increasing free-stream turbulence. Increased levels of turbulence kinetic energy were measured across the entire thickness of the boundary layer.

The effects of the free-stream turbulence level on the indivdiual components of the boundary layer turbulence for these same three profiles are shown in Fig. 7. The streamwise (u') component followed the same trends as the turbulence kinetic energy, increasing with free-stream turbulence level over the entire thickness of the boundary layer. The normal component (v'), however, was damped by the presence of the solid wall and showed virtually no change over the lower half of the boundary layer. See Ref. 23 for an in-depth study of the interaction of solid surfaces with turbulent fluctuations. The distribution of w' for Te = 4.2 percent showed a large increase over the distributions for the lower turbulence levels. Outside the boundary layer w' was also measured to be about 20 percent higher than u' or v'. On the grounds that earlier independent measurements of the free-stream turbulence for this grid showed the turbulence to be isotropic at this station (Ref. 1) and the unreasonably large "jump" in the w' distribution across the entire boundary layer it has been concluded that these w' measurements are in error. It is thought that there was an error in the calibration for the horizontal x wire probe used for the Grid 4 test cases. The Grid 4 w' data are reported here as measured, that is uncorrected for this probable error. It is estimated that by reducing the measured w' data by 20 percent a reasonably accurate set of distributions of the transverse component for this Grid 4 case would result.

With the Grid 4 w' data reduced by 20 percent the conclusion that can be reached from Fig. 7 is that the u' and w' component of turbulence increased progressively with increasing free-stream turbulence level. Both components increased at all locations in the boundary layer. The vertical component v', however, was essentially constant and independent of free-stream turbulence level for the lower half of the boundary layer.

Distributions of the boundary layer turbulence structural coefficients (Bradshaw, et al., Ref. 19) are given in Figs. 8A and 8B. As can be seen from an inspection of Fig. 8A the ratio of shear stress to turbulence kinetic energy (a_1) decreased across the entire boundary layer with increasing free-stream turbulence. The observed decrease was most extreme over the outer 60 percent of the boundary layer. Also shown with the present a_1 distribtuion data are similar results from Refs. 14 and 21. Agreement between these similar (not identical, Re_θ and Te were slightly different) sets of data was very good.

The ratios of the direct stress components to the turbulent kinetic energy (a_2, a_3 and a_4) are given in the remaining plots of Figs. 8A and 8B. Employing the

previously described 20 percent reduction to the w' component for Te = 4.2 percent (this also reduces $\overline{q^2}$ for T_e = 4.2 percent), fairings of the corrected structural coefficient distributions for the highest turbulence level are given in the figures. Using the measured results for T_e = 0.2 percent and 1.5 percent and the corrected fairings for Te = 4.2 percent the following conclusions were reached. As the free-stream turbulence stress level was increased a_2 $(\overline{u'^2}/\overline{q^2})$ increased slightly above 0.5, the value widely used for low free-stream turbulence boundary layers. The greatest percentage change was observed for the lower half of the boundary layer for a_3 ($a_3 = \overline{v'^2}/\overline{q^2}$). This ratio decreased progressively with increasing T_e dropping to about 0.12 (40% reduction from classic value of 0.2) for Te = 4.2 percent. Only very small changes were observed for a_4 ($a_4 = \overline{w'^2}/\overline{q^2}$) with the measured values grouping around 0.3 for the lower half of the boundary layer.

A number of previous studies of free-stream turbulence effects on turbulent boundary layers (Refs. 8, 10, 11, 14 and 234) have reported finite turbulent shear stress levels beyond the edge of the velocity boundary layer. This effect was also observed for the present program. A comparison between the present results and those of the previous investigations is given in Fig. 9 where the turbulent shear level at the edge of the boundary layer (δ 0.995) is given as a function of T_e. The data from the present study and the results reported for most of the other experiments are tightly grouped. Taken together, these data indicate an increase of turbulent shear at the boundary edge directly proportional to the free-stream turbulence level. Huffman's results, which are believed (Ref. 2) to contain significant errors due to anistropy, show much larger levels of turbulent shear than the other studies.

Additional evidence of the impact of free-stream turbulence on the characteristics of the turbulence near the boundary layer edge is provided by the measurements of flatness factor. The flatness factor $\overline{u'^4}/(\overline{u'^2})^2$ is an indication of the distribution of velocity fluctuations in a set of samples. For a normal Gaussian distribution the flatness factor is equal to 3 with larger values indicating contributions from intermittent turbulent fluctuations. Flatness factor distributions of the streamwise fluctuating velocity component are given in Fig. 10 as a function of position in the boundary layer. An examination of Fig. 10 shows that the intermittent character of the turbulence near the edge of the boundary layer was greatly reduced by increased free-stream turbulence. For a boundary layer beneath a low turbulence mainstream a relatively sharp irregular "edge" of turbulent boundary layer flow results adjacent to the non-turbulent freestream. With higher levels of free-stream turbulence this distinct border appears to have disappeared.

4. Effects of High Free-Stream Turbulence on the Turbulent Prandtl Number

The measured distributions of turbulent shear stress ($\overline{u'v'}$), the turbulent heat flux ($\overline{v't'}$) and the normal derivatives of the mean velocity and temperature were combined to form local turbulent Prandtl numbers.

$$Pr_t = \frac{\epsilon_m}{\epsilon_h} \tag{12}$$

where ϵ_m = eddy diffusivity of mass

ϵ_h = eddy diffusivity of heat

$$Pr_t = \frac{\overline{-u'v'}\ \frac{\partial T}{\partial y}}{\overline{v't'}\ \frac{\partial U}{\partial y}} \tag{9}$$

The distributions of turbulent Prandtl number measured for the various test cases are presented in Fig. 11. The results from all three profile locations (x = 52, 68 and 84 inches) for all three free-stream turbulence levels are included in Fig. 11 with an average free-stream turbulence level assigned to each set. For all points above the wall the turbulent Prandtl numbers were determined from the turbulent heat flux and shear stresses measured with the hot wire probes and from the derivatives of the mean profiles measured with the total pressure and thermocouple probes. At the wall the turbulent Prandtl numbers were determined from the mean temperature and velocity profile data by assuming that for at least some small distance the ratio of shear stress to heat flux remains at the wall value.

$$\frac{\tau}{\mathring{q}} \approx \frac{\tau_{wall}}{\mathring{q}_{wall}} = \frac{\rho_w \overline{u'v'}}{\rho_w c_p \overline{v't'}} \tag{13}$$

$$\frac{\overline{u'v'}}{\overline{v't'}} = \frac{\rho_w c_p U_\tau^2}{\mathring{q}_{wall}} \tag{14}$$

$$Pr_t\,(wall) = \frac{\rho_w c_p U_\tau^2}{\mathring{q}_{wall}} \frac{\partial T}{\partial U} \tag{15}$$

Near-wall values of the turbulent Prandtl number were evaluated from Eq. 15 using friction velocities (U_τ) determined from the mean velocity profile fits to the "law-of-the-wall". Values of $\partial T/\partial U$ were determined graphically from the near-wall velocity and temperature profile data.

Errors in the four measured terms of Eq. 9 combined to produce considerable scatter in the data of Fig. 11. This scatter, however, is much less than reported for the similar measurements of Refs. 21 and 25. It is expected that the consistency and absolute accuracy of such local turbulent Prandtl number measurements could be further improved by employing larger samples of the turbulent data.

The turbulent Prandtl number distributions measured for the low free-stream turbulence profiles were in good agreement with the similar data of Ref. 17. (Ref. 17 employed mean profile data only.) In addition, Rotta's (Ref. 22) suggested Pr_t distribution for low free-stream turbulence boundary layers appears to represent the present low turbulence data well.

$$Pr_t = 0.95 - 0.45\,(y/\delta)^2 \qquad (16)$$

An examination of Fig. 11 indicates that as the free-stream turbulence level was raised the turbulent Prandtl number increased over nearly the entire boundary layer. Values of Pr_t over unity were recorded at $y/\delta \approx 0.3$ for the highest free-stream turbulence level. These increased outer region turbulent Prandtl numbers for high free-stream turbulence levels had not been expected. At the outset of the program the turbulence characteristics of the outer portion of the boundary layer were known to be altered considerably by increased levels of free-stream turbulence. It was also known from the measurements of Ref. 1 that the free-stream turbulence had a large impact on the turbulent heat transfer with the Reynolds analogy factor increasing with increasing turbulence level. It was speculated that the increased Reynolds analogy factor might result from lowered Pr_t levels (relatively greater increase in $\overline{v't'}$ as comapred to $\overline{u'v'}$) in the outer portions of the boundary layer. The experimental results of Fig. 11 indicate just the opposite effect. As the free-stream turbulence level was increased the outer region Pr_t levels increased while the near-wall values (determined from the mean profile data) indicate a small but progressive decrease. The following expression, a modification of Rotta's (Eq. 16) low free-stream turbulence equation, represents the measured results reasonably well.

$$Pr_t = \left[\left[0.95 - 0.45\,(y/\delta)^2\right](1+2T)^2\right] - \frac{5T}{\cosh^{10y/\delta}} \qquad (17)$$

Equation 17 is shown in Fig. 11 for the three turbulence levels for which the experimental data were obtained. At T_e = 0.2 percent, Eq. 17 is practically identical to Rotta's (Eq. 16) expression.

The mean velocity and temperature profile data from both the present program and from Ref. 1 provide additional evidence that the near-wall turbulent Prandtl number decreased with increased free-stream turbulence level. (The arguments for this conclusion will be presented here in a highly abbreviated form. A more in-depth examination of these effects will be conducted during the preparation of a technical journal article on this contract work.) The effects of the free-stream turbulence on the similarity between the mean velocity and temperature profiles was examined by plotting the velocity ratio (U/U_e) versus the temperature ratio (T_w-T/T_w-T_e) across the boundary layers. Plots of these ratios for all profile locations and free-stream turbulence levels are given in Fig. 12. Also given in Fig. 12 are the similar data from the same stations and turbulence levels obtained in Ref. 1. An examination of Fig. 12 indicates that for all cases, independent of the free-stream turbulence level, the mean velocity and temperature profiles remained highly similar. This similarity between the velocity and temperature profiles extends across at least the outer 90 percent of the boundary layer thickness including all the wake and at least some of the logarithmic zone. It follows that the shapes of the velocity and temperature profiles should also be similar when plotted in universal (U^+ or T^+ vs. Y^+) coordinates. It has been observed in virtually every study of free-stream turbulence effects on turbulent boundary layers that the wake strength of the velocity boundary layer was progressively reduced with increasing free-stream turbulence. It was also

observed in Refs. 2 and 26 that for a given turbulence level the temperature wake was reduced by a larger amount than was the velocity wake. Implicit in the formulation of the temperature law-of-the-wall is the assumption that the turbulent Prandtl number is constant across the entire boundary layer. The large thermal wake depressions reported in Refs. 2 and 26 followed from the use of an average boundary layer turbulent Prandtl number for all the profiles. The following interpretation, however, is more consistent with the conclusion from Fig. 12, that the shapes of the outer region velocity and temperature profiles remained similar for all turbulence levels and streamwise locations. If the near-wall turbulent Prandtl numbers were assumed to be reduced with increased T_e (as Fig. 11 indicates) the slope of the temperature law-of-the-wall ($1/\kappa_\theta = Pr_t/\kappa$) would be reduced. With a reduced logarithmic region slope the apparent temperature wake strength, which is the maximum deviation from the log-law, would increase. An examination of the temperature profiles of Ref. 2 (in T^+ vs. Y^+ coordinates) indicated that good fits to the temperature law-of-the-wall could be achieved from $Y^+ \approx 30$ to $Y/\delta = 0.1$ if Π_θ was set equal to Π. For the present data, very good agreement between the thermal and velocity wake strengths resulted from the use of the near-wall turbulent Prandtl numbers of Fig. 11 for the respective profiles.

Finally, with regard to a potential physical mechanism producing the reduced near-wall Pr_t, the diffusion terms of the turbulence kinetic energy transport equation for velocity and temperature (Ref. 19) differ by the contribution of the pressure-velocity fluctuation product. Blom (Ref. 27) has pointed out that the pressure fluctuations serve to transfer energy from the relatively higher u' component of turbulence to the relatively smaller v' and w' components. Blom also argued that the absence of the p'v' term in the temperature diffusion term could explain the reduction of Pr_t below unity. Since the effect of increased T_e was to increase the difference between the u' and v' components of turbulence near the wall the importance of the p'v' term may grow with T_e. In other words, with increasing difference between u' and v' the effect of the $\overline{p'v'}$ term may be to progressively decrease Pr_t.

The overall impact of free-stream turbulence on boundary layer heat transfer rates is, then, to depress the near-wall turbulent Prandtl number. Since the heat and momentum transport in turbulent boundary layers are dominated by the turbulent eddy contributions the result is that the Reynolds analogy factor rises with increasing free-stream turbulence level. It should be pointed out, however, that the results of Refs. 2 and 14 clearly show that the effects of free-stream turbulence on turbulent boundary layers are not dependent on turbulence intensity alone. For a fixed free-stream intensity the largest impact on a turbulent boundary layer results if the integral scale of the turbulence is about equal to the boundary layer thickness. Turbulence with integral scales significantly smaller or larger than the boundary layer thickness will produce reduced effects.

THEORETICAL ANALYSIS

The experimental data discussed previously in this report was used to assess the capability of a boundary layer analysis for predicting the effect of free-stream turbulence on momentum and thermal boundary layers. Previously, Blair and Werle (Ref. 2) examined the effects of free-stream turbulence on zero pressure gradient flows. They also evaluated the ability of a finite difference code (Ref. 28), which used a turbulence model of McDonald et al. (Refs. 29 and 30), to predict surface heating and skin friction. The present analytical investigation, which is a continuation of the work initiated by Blair and Werle, makes use of a boundary layer analysis (ABLE - Analysis of the Boundary Layer Equations) recently developed by Edwards, Carter and Werle (Ref. 31). This new boundary layer analysis contains the McDonald et al. turbulence model (Refs. 29 and 30) utilized by Blair and Werle's (Ref. 2) previous work. In addition, it was demonstrated in Ref. 31 that results obtained from the ABLE analysis and the boundry layer procedure employed by Blair and Werle were in excellent agreement for zero pressure gradient flows. In the present study, the capability of the ABLE code to accurately predict mean flow velocity, mean flow temperature, Reynolds shear stress and turbulent heat transport profiles is determined. In addition, the turbulent Prandtl number distribution deduced from the experimental measurements discussed earlier in this report is used in the boundary layer analysis and its effect on surface heating is evaluated.

1. Prediction Method

The ABLE boundary-layer code provides a rapid computation of two dimensional or axisymmetric boundary-layer flows subject to a prescribed distribution of edge Mach number, streamwise velocity, or static pressure. At the surface a distribtuion of either wall temperature or heat flux may be imposed. This analysis is applicable to attached flows which are laminar, transitional, or turbulent. A detailed description of the theory used in the ABLE code is given in Ref. 31 and a flow chart of the code is shown in Fig. 13. An implicit finite-difference technique is used in the ABLE code to solve the boundary-layer equations which are written in nondimensional form for two dimensional flow as follows.

continuity

$$\frac{\partial \rho u}{\partial s} + \frac{\partial \rho v}{\partial n} = 0 \qquad (18)$$

momentum

$$\rho u \frac{\partial u}{\partial s} + \rho v \frac{\partial u}{\partial n} = -\frac{\partial p}{\partial s} + \frac{\partial}{\partial n}\left(\mu \frac{\partial u}{\partial n} - \rho \overline{u'v'}\right) \qquad (19)$$

energy

$$\rho u \frac{\partial H}{\partial s} + \rho v \frac{\partial H}{\partial n} = \frac{\partial}{\partial n}\left[\mu\left(1-\frac{1}{Pr}\right)u\frac{\partial u}{\partial n} + \frac{\mu}{Pr}\frac{\partial H}{\partial n} - \rho\overline{h'v'} - \rho u\,\overline{u'v'}\right] \tag{20}$$

In the above equations, s is the coordinate along the surface, n is the coordinate normal to the surface, u is the streamwise velocity, v is the normal velocity, ρ is the static density, P is the static pressure, h is the static enthalpy and H is the total enthalpy where (in non-dimensional form)

$$H = T + \frac{1}{2}u^2 = h + \frac{1}{2}u^2$$

The placement of a bar over several terms is used to denote the time average of various turbulent fluctuating quantities which are generally considered to represent the dominant Reynolds stress terms in the turbulent boundary layer equations.

The ABLE code currently contains two turbulence models, the Cebeci-Smith algebraic model (Ref. 32) and the McDonald et al., one equation turbulence model (Refs. 29 and 30). Both models are based on an eddy viscosity concept in which the Reynolds shear stress is related to the mean flow velocity gradient by

$$-\rho\overline{u'v'} = \mu_T \frac{\partial u}{\partial n} \tag{21}$$

In addition, the turbulent heat transport is related to the Reynolds shear stress and mean flow quantities through a Reynolds analogy type of argument

$$-\rho\overline{h'v'} = \frac{-\rho\overline{u'v'}}{Pr_t}\,\frac{\frac{\partial h}{\partial n}}{\frac{\partial u}{\partial n}} = \frac{\mu_T}{Pr_t}\,\frac{\partial h}{\partial n} \tag{22}$$

where Pr_t is the turbulent Prandtl number. This code presently contains two transition models, the first of which is the Dhawan and Narasimha (Ref. 33) forced transition model which requires the specification of the start and length of transition. The second model is a natural transition model developed by McDonald and Fish (Ref. 29) where the prediction of transition is controlled by the integrated form of the turbulence kinetic energy equation. In the present investigation the ABLE code is applied to the experimental flows discussed previously using the one equation turbulence model of McDonald and Kreskovsky (Ref. 30), the details of which are given in the next section.

2. Turbulence Model

The one equation turbulence model of McDonald and Kreskovsky (Ref. 30) permits the effect of free-stream turbulence to be included in the computed boundary layer

analysis. This turbulence model, which accounts for the proper approach of the turbulence le·e· in the outer region of the boundary layer to the local edge value, is based on the integral form of the turbulence kinetic energy equation. This model is an extension of a turbulence model developed earlier by McDonald and Fish (Ref. 29). The eddy viscosity coefficient is expressed in nondimensional form as

$$\left(\frac{\mu_T}{\mu}\right) = \frac{\rho}{\mu} \ell^2 \frac{\partial u}{\partial n} Re^{1/2} \tag{23}$$

where Re is a reference Reynolds number, and ℓ, the local mixing length, is expressed as a function of the mixing length ℓ_e at the boundary layer edge through the relation

$$\ell = \mathcal{D} \ell_e \left\{ \tanh\left(\frac{\kappa n}{\ell_e}\right) + \frac{1}{2}\left(1 - \tanh\left(\frac{\kappa \delta}{\ell_e}\right)\right)\left[1 - \cos\left(\frac{n\Pi}{\delta_\tau}\right)\right]\right\} \tag{24}$$

and

$$\mathcal{D} = \sqrt{\frac{1}{2}\left[1 + \operatorname{erf}\left(\frac{n^+ - 23}{8}\right)\right]} \tag{25}$$

where κ is the von Karman constant, δ is the boundary-layer thickness, and δ_τ is the "shear stress" thickness which is defined as the first location from the outer edge of the boundary layer where

$$\frac{\tau}{\tau_{max}} \geq 0.02 \tag{26}$$

and τ_{max} is the maximum shear stress at each streamwise location.

The local value of ℓ_e is obtained through the solution of the integral form of the turbulence kinetic energy equation which is expressed in nondimensional form as

$$\frac{d}{d_s}\left[\frac{\rho_e u_e^3}{2a_1} \phi_1\right] = \rho_e u_e^3 \left(\phi_2 - \phi_3\right) + E \tag{27}$$

where

$$E = \frac{q_e^2}{2}\left[\rho_e u_e \frac{d\delta_\tau}{ds} - (\rho v)_e \sqrt{Re}\right] \tag{28}$$

$$\phi_1 = \int_0^{\delta_\tau} \frac{\rho u}{\rho_e u_e}\left[\ell \frac{\partial}{\partial n}\left(\frac{u}{u_e}\right) + a_1 f\,(n/\delta_\tau)\,\frac{q_e^2}{u_e^2}\right]^2 dn \tag{29}$$

$$\phi_2 = \sqrt{Re} \int_0^{\delta_T} \frac{\rho}{\rho_e} \ell^2 \left[\frac{\partial}{\partial n}\left(\frac{u}{u_e}\right)\right]^3 (1-\ell/L)\ dn \tag{30}$$

$$\phi_3 = \int_0^{\delta_T} \frac{\rho}{\rho_e} \left(\frac{a_2-a_3}{a_1}\right)\left\{\left[\ell \ \frac{\partial}{\partial n}\left(\frac{u}{u_e}\right)\right]^2 + a_1 f\left(\frac{n}{\delta_T}\right)\frac{q_e^2}{u_e^2}\right\} \frac{1}{u_e}\ \frac{du}{ds}\ dn \tag{31}$$

and

$$L = .118\ \mathcal{D}\ \tanh\left[\frac{\kappa n}{.118}\right] \tag{32}$$

$$q_e = \sqrt{(\overline{u'u'} + \overline{v'v'} + \overline{w'w'})_e} \tag{33}$$

$$f\left(\frac{n}{\delta_T}\right) = \frac{1}{2}\left[1 - \cos\left(\frac{n\Pi}{\delta_T}\right)\right] \tag{34}$$

where the subscript e denotes the flow quantities at the boundary-layer edge. The influence of the free-stream turbulence in the one equation model comes through the term, q_e^2, which acts as a source term in Eq. 27. In the above relation, L is a dissipation length and a_1, a_2, and a_3 are structural coefficients that relate the Reynolds shear stress and turbulence intensity components to the turbulent kinetic energy as suggested by Townsend (Ref. 34) and Bradshaw and Ferris (Ref. 19). These coefficients are given by

$$-\overline{u'\ v'} = a_1 \left\{\overline{q^2} - f\left(\frac{y}{\delta_T}\right)\ \overline{q_e^2}\right\} \tag{35}$$

$$\overline{u'\ u'} = a_2\ \overline{q^2} \tag{36}$$

$$\overline{v'\ v'} = a_3\ \overline{q^2} \tag{37}$$

$$\overline{w'\ w'} = (1 - a_2 - a_3)\ \overline{q^2} \tag{38}$$

where McDonald and Fish (Ref. 29) suggest the values a_2 = .5 and a_3 = .2 and that a_1 be expressed as follows

$$a_1 = \frac{a_0\left(\frac{\tilde{R}_\theta}{100}\right)}{1+6.666\, a_0\left(\frac{\tilde{R}_\theta}{100}-1\right)} \tag{39}$$

where

$$a_0 = 0.0115$$

and $\tilde{R}_\theta$, which is referred to as the Reynolds number based on momentum thickness by Shamroth and McDonald (Ref. 35) but is in fact a correlation given in terms of an integrated turbulent Reynolds number R_T.

$$\tilde{R}_\theta = \begin{cases} 100\, R_T^{0.22} & R_T \le 1 \\ 0.0098215\,(R_T-1)^3 + 1.165\,(R_T-1)^2 + 22\,(R_T-1) + 100 & 1 < R_T < 40 \\ 68.26\, R_T - 614.33 & R_T \ge 40 \end{cases} \tag{40}$$

and

$$R_T = \frac{\frac{1}{\delta}\int_0^{\delta_T} \nu_T\, dn}{\frac{1}{\delta_s}\int_0^{\delta_s} \nu\, dn} \tag{41}$$

where δ_s is an estimate of the inner wall layer. The computational transition process is controlled by the structural coefficient a_1 as it varies from zero in laminar flow to .15 in in fully turbulent flow. For the present analysis, the structural coefficients a_1, a_2 and a_3 are constant over the boundary layer using the values suggested by McDonald and Fish (Ref. 29). However the experimental structural coefficients were observed to vary across the boundary layer (Figs. 8(a) and 8(b) and the effect of varying the structural coefficients in the analysis should be assessed in the future. A detailed description of the one equation turbulence model is given in Ref. 36.

3. Turbulent Prandtl Number Model

In the present investigation an evaluation is made of the effect of a variable turbulent Prandtl number, Pr_t, across the boundary layer on the ABLE code prediction of the turbulent heat transport and surface heating. Three different functional forms of Pr_t have been applied in this investigation. They are given by

1) McDonald (Ref. 28)

$$Pr_t = .9\, P\left(\frac{n^+-23}{8}\right) / P\left(\frac{n^+-23.6}{10}\right) \tag{42}$$

where

$$P(x) = \frac{1}{2}\left[1 + \mathrm{erf}\left(\frac{x}{\sqrt{2}}\right)\right]$$

2) Rotta (Ref. 22)

$$Pr_t = .95 - .45(n/\delta)^2 \tag{43}$$

3) Present experimental investigation

$$Pr_t = \left[.95 - .45(n/\delta)^2\right]\left[1 + 2\,Tu\right]^2 - 5\,Tu/\cosh\left[10\,n/\delta\right] \tag{44}$$

where

$$Tu = 1/3\,\overline{qe^2}$$

A comparison of these three turbulent Prandtl number distributions are shown in Fig. 14. McDonald's function (Eq. 42) has a maximum value of 1.7 at the wall and decreases rapidly in the laminar sublayer of the turbulent boundary layer but is nearly constant and equal to .9 for $\eta^+ > 50$. Rotta's function (Eq. 43) has a maximum value of Pr_t of .95 at the wall and decreases linearly with respect of $(\eta/\delta)^2$ to the edge of the boundary layer to a value of .5. The Pr_t distribution obtained in the experimental portion of the present investigation (Eq. 44) is essentially a modification of Rotta's distribution to account for the effects of free-stream turbulence. An assessment of the accuracy of each of these turbulent Prandtl number formulations is made in the next section using the ABLE code and the experimental results presented above. However, since the turbulent heat transport $\overline{h'v'}$ is modeled in terms of $u'v'$, the turbulent Prandtl number and the normal derivatives of u and h as given in Eq. 22, then all of these quantities are compared with the experimental data before an assessment is made of the effect of Pr_t on the calculation of the turbulent heat transport.

DISCUSSION OF ANALYTICAL RESULTS

A series of calculations have been made with the ABLE code for the flow over a heated flat plate for each of the nominal inlet free-stream turbulence levels of 1%, 2%, 4% and 6% generated by the use of inlet turbulence Grids 1, 2, 3 and 4, respectively. A calculation was not performed for the case of the flow with .25 percent inlet turbulence since it was concluded by Blair and Werle (Ref. 2) that the transition process of this flow is three dimensional and thus the turbulence model of McDonald et al. (Refs. 29 and 30) cannot accurately predict the location and length of the transition region. For each case, a calculation is made with the ABLE code for each of the turbulent Prandtl number formulations discussed in the previous section. The mean flow quantities, Reynolds shear stress and turbulence kinetic energy predicted from the ABLE code were found to be insensitive to the different turbulent Prandtl number formulations; hence, these quantities are presently for only the present Pr_t formulation given in Eq. 44. This result was expected since the experimental flows are low speed and thus the momentum equation (Eq. 19) is essentially uncoupled from the energy equation (Eq. 20).

For all of the test cases analyzed in this investigation with the ABLE code, the gas is assumed to be air with a constant ratio of specific heats, γ, equal to 1.4 and a constant Prandtl number equal to .72. The von Karman constant for turbulent flow is set to .43 as suggested by McDonald and Kreskovsky (Ref. 30). The following flow conditions were used in all test cases

$$U_e = 100 \text{ ft/sec}$$
$$P_{T_e} = 14.78 \text{ lb/in}^2$$

and the streamwise variation of the free-stream turbulence for each flow with a specified inlet grid is obtained from the following expression

$$Tu = .78 \left(\frac{2.54x + 132}{b}\right)^{-5/7} \qquad (45)$$

where b (grid bar width) = .48, 1.27, 3.81, and 5.08 for Grids 1, 2, 3, and 4, respectively. This relation was shown to be accurate in earlier testing reported in Ref. 2. The measured wall temperature levels are tabulated in Table I of Ref. 2, with the free-stream static temperature set to 530°R ($^{T}T_e$ = 530.83°R) for all calculations. The temperature distributions were numerically smoothed to eliminate spurious variations in the computed wall results due to minor experimental error. The smoothed temperature distribtuions were used as input to the ABLE code. Comparison of the measured and smoothed temperature distributions for each of the flow cases are shown in Fig. 15. The smoothing procedure is a least squares polynomial curve fit described in Ref. 37.

A computational mesh consisting of 101 grid points in the normal direction and 100 points in the streamwise direction was used in each of the calcualtions. A grid stretching based on a geometric progression was applied in each direction to insure

that a fine grid distribution was placed in the high gradient regions. The initial profile for the boundary layer calculation is the Blasius profile (Ref. 38) which was imposed at the flat plate leading edge. In addition, two iterations per streamwise station are applied in the computational procedure due to large streamwise temperature gradients which are encountered in the transition region of the flow. The current calculations required approximately 1 minute of CPU time on a UNIVAC 1180 operating system to compute the flow over the 8 foot length of the test section.

In this section comparisons are presented in Figs. 16-27 between the results obtained from the ABLE code with those measured experimentally both in the present investigation and in the previous investigation by Blair and Werle (Ref. 2). These comparisons are made for zero pressure gradient flows for the two cases with inlet turbulence levels of 2 percent and 6 percent. The following quantities are compared:

1. skin friction
2. displacement thickness
3. momentum thickness
4. mean velocity profile
5. mean temperature profile
6. Reynolds shear stress profile
7. turbulent kinetic energy profile
8. profiles of the components of turbulence intensity
9. turbulent Prandtl number profile
10. turbulent heat transport profile

The profile comparisons are shown only at $X = 68$ inches from the leading edge of the test section; similar comparisons were obtained at the other measuring stations.

Figure 16 is a comparison of the computed skin friction coefficient distribution with that obtained experimentally along the flat plate surface for inlet turbulence levels of 2 percent and 6 percent. The theoretical distribution is slightly higher (approximately 5%) than the experimental distribution for the flow with an inlet turbulence of 2 percent while the result obtained for the flow with an inlet turbulence of 6 percent is in excellent agreement with the experimental result. A comparison of the theoretical and experimental displacement and momentum thickness distributions are shown in Figs. 17 and 18, respectively. It is apparent from these figures that the computed integral quantities are in good agreement with the experiment over most of the test section. Figures 19 and 20 are comparisons of the computed mean velocity and temperature profiles with the experimental measurements for inlet turbulence levels of 2 percent and 6 percent. In all profile comparisons, the theoretical boundary layer thickness, δ, was used to nondimensionalize the normal coordinate. It is observed from Figs. 19 and 20 that the computed results are in excellent agreement with the experimental results for both flows. From Figs. 16-20 it is concluded that the ABLE boundary layer analysis with the McDonald and Kreskovsky turbulence model (Ref. 30) produces good agreement with the mean flow quantities of zero pressure gradient flows with various levels of inlet turbulence.

In order to determine how well the boundary layer analysis will predict turbulent fluctuating quantities, comparisons of computed profiles with experimental data

were made of the flows with inlet turbulence levels of 2 percent and 6 percent. Figure 21 is a comparison of the computed Reynolds shear stress profile with that obtained experimentally. Several interesting features are noted in this figure. By using the turbulence modeling(Eqs. 28-32) developed by McDonald and Kreskovsky in the computational procedure, the predicted Reynolds shear stress in the inner layer of the turbulent boundary layer is in excellent agreement with the experimental measurements. The theoretical results exhibit the same shape and level as the experimental results. However, in the outer layer, as the free-stream turbulence increases, the deviation between the computed and experimental results grows significantly as it is observed that the computed $\overline{u'v'} \rightarrow 0$ whereas the experimental $\overline{u'v'}$ approaches a finite value. Figure 22 is a comparison of the measured and computed turbulence kinetic energy distribtuions. It is observed that the computed results are in good agreement with the experimental data for both levels of free-stream turbulence. This result indicates that McDonald and Kreskovsky's modeling of free-stream turbulence in the turbulence kinetic energy equation (Eq. 27) captures the correct shape of the turbulence kinetic energy across the boundary layer for zero pressure gradient flows with different levels of free-stream turbulence. Figures 23-25 are comparisons of the measured and computed components of turbulence intensity, $\overline{u'u'}$, $\overline{v'v'}$, $\overline{w'w'}$. From these figures it is observed that the predicted results are in fair agreement with the experimental data across the boundary layer.

An anomaly appears in the results shown in Figs. 19-25. First, from Figs. 22-25, the computed turbulence kinetic energy and its various components are in realtively good agreement with the experimental results. Secondly, the computed mean velocity (Fig. 19) is in excellent agreement with the experiment. However, the computed Reynolds shear stress (Figs. 21) has a significant deviation from the experimental results in the outer region of the boundary layer as the inlet turbulence level increases. This difference tends to suggest that the eddy viscosity modeling of turbulence (Eq. 21) does not properly model flows with significant levels of free-stream turbulence since by applying this model, the computed Reynolds shear stress is forced to zero at the edge of the boundary layer. The inability of the turbulence model to predict accurate Reynolds shear stress distributions over the entire boundary layer will affect the transition model (Eq. 39) since the transition process is controlled by an integrated form of the turbulent Reynolds number R_T (Eq. 41). An investigation is needed to determine an analytical turbulence model that will properly represent the Reynolds shear stress in the outer region of the turbulent boundary layer for flows with significant levels of free-stream turbulence.

A comparison of McDonald's, Rotta's, and the present turbulent Prandtl number formulation with the experimentally determined distribution is shown in Fig. 26(a) and Fig. 26(b) for flows with 2 percent and 6 percent turbulence levels, respectively. In Fig. 26(a) it is observed that McDonald's distribution, which is essentially constant over the boundary-layer overpredicts the experimental results over most of the boundary layer while Rotta's and the present distribtuion exhibit the same general shape and level as the experiment distributions. For the high inlet turbulent flow (Fig. 26(b)), the present Pr_t distribution exhibits the same shape and level as the experimental distribution while the relatively constant McDonald distribtuion does not have the same shape or level as the experimental results.

Also, Rotta's distribution exhibits the best shape of the experimental data but is not at the same level. Figures 27(a) and 26(b) are comparisons of the measured and computed turbulent heat flux distributions for the flows with turublence levels of 2 percent and 6 percent, respectively. From these figures, it is noted that except near the wall, the computed turbulent heat flux distribution across the boundary layer is essentially the same for each of the three different Pr_t formulations which are used. Figures 27(a) and 27(b) show that the computed results are in reasonable agreement with the experimental results except at the edge of the boundary layer where the theoretical results go to zero and the experimental data does not. Since the turbulent heat flux is determined from Eq. (22) and all the computed quantities in that equation are in reasonable agreement with experimental data except the Reynolds shear stress, this suggests that the inaccuracy of predicting the turbuent heat flux in the outer portion of the boundary layer is due to the modeling of the Reynolds shear stress in the outer region of a turbulent boundary layer with significant levels of free-stream turbulence. Further investigation of this feature of the flow is needed.

In Figure 28, comparisons are presented between measured and computed Stanton number distributions for the flows with inlet turbulence levels of 1, 2, 4 and 6 percent. The following observations about the Stanton number prediction in the fully turbulent region of the flows are made. The predicted Stanton number using McDonald's formulation is in good agreement with the experiment for the flow with an inlet turbulence level of 1 percent; however, as the inlet turbulence level increases, the computational procedure using McDonald's formulation underpredicts the measured Stanton number distribution. The computational procedure using Rotta's formulation overpredicts the Stanton number for the flow with the 1 percent inlet turbulence level. However, as the inlet turbulence level increases the computed results tend to slightly overpredict the measured Stanton number distribution. The present turbulent Prandtl number formulation yields essentially the same results as the computed with Rotta's formulation since the present formulation is a perturbation of Rotta's Pr_t formulation. The results shown in Fig. 28 indicate that the computation using the present distribution shows no marked improvement over the computation using Rotta's distribution. However, for the flows with inlet turbulence of 2 percent or larger, computations using either Rotta's or the present formulation result in predicted Stanton number distributions which are in better agreement with the experimental results than that obtained using McDonald's formulation. A further indication of the advantage of Rotta's or the present formulation is shown in Fig. 29 where the predicted Reynolds analogy factor, $2\ S_t/C_f$, from calculations using the present and McDonald's turbulent Prandtl number distributions are compared to the experimentally deduced Reynolds analogy. In this figure it is observed that the calculation using the present (or Rotta's) formulation predicted Reynolds analogy factors that are in better agreement with the experiment than the computation which uses McDonald's formulation. The overall implication of these results is that the analysis using the McDonald and Kreskovsky turbulence model (Ref. 30) with either Rotta's or the present turbulent Prandtl number formulation can accurately represent the momentum and energy transport mechanisms for zero pressure gradient flows in the wall region of the boundary layer but that there is a severe weakness in its

ability to represent the momentum and energy transport mechanisms in the region near the edge of the boundary layer for flows with significant levels of free-stream turbulence.

CONCLUSIONS

The present program was designed to examine, both experimentally and analytically, the effect of free-stream turbulence on the heat transfer through turbulent boundary layers. The experimental test conditions for the present program were intended to reproduce cases for which numerous other experimental data had been obtained under an earlier AFOSR contract (Ref. 2). Measurements of multi-component free-stream turbulence intensities, test surface Stanton number distributions, transition Reynolds numbers and boundary layer integral thicknesses were in excellent agreement with the respective quantities of the earlier contract. It has been concluded that these present measurements can be viewed as additional data for the same test conditions as were previously studied. A number of comparisons were made between low free-stream turbulence boundary layer turbulence data obtained in the present study and similar results from other investigations. These comparisons showed excellent agreement indicating that the present boundary layer turbulence data are of high quality.

The conclusions reached from the experimental measurements obtained for higher levels of free-stream turbulence were as follows:

1. The present data indicate a progressive increase of boundary layer turbulence kinetic energy with increasing free-stream turbulence. Increased levels of turbulence kinetic energy were measured across the entire thickness of the boundary layer. These results are in agreement with data from other independent studies.

2. Both the u' and w' components of turbulence increased progressively with increasing free-stream turbulence level. The u' component increased more than the w' component. The vertical component (v'), however, was essentially constant and independent of free-stream turbulence level for the inner half of the boundary layer.

3. The ratio of shear stress to turbulence kinetic energy decreased across the entire boundary layer with increasing free-stream turbulence level. The decrease was most extreme over the outer 60 percent of the boundary layer.

4. The effects of free-stream turbulence level on the ratios of the direct stress components to the turbulence kinetic energy were to a) increase $\overline{u'u'}/\overline{q^2}$, b) decrease $\overline{v'v'}/\overline{q^2}$ and c) leave $\overline{w'w'}/\overline{q^2}$ nearly constant.

5. Reynolds stress distribution measurements indicated that at high levels of free-stream turbulence the turbulent shear stresses extend beyond the mean velocity boundary layer. The present data and results from other sources indicate an increase in turbulent shear at the boundary layer edge directly proportional to the free-stream

turbulence level. Flatness factor measurements indicated that as the free-stream turbulence level was increased the "border" between the fluid in the boundary layer and the free-stream fluid became less distinct.

6. Measurements of the boundary layer turbulent Prandtl number distribution for the case of the low free-stream turbulence were in good agreement with a model suggested by Rotta. The present data indicate that as the free-stream turbulence level was increased, the near-wall Pr_t decreased while Pr_t over the outer region of the boundary layer slightly increased. A correlation, Pr_t (y/δ, Te), which fit the observed data reasonably well was suggested.

The experimental data was used to assess the capability of a boundary-layer computer program, ABLE (Analysis of the Boundary Layer Equations) for predicting the effect of free-stream turbulence on momentum and thermal boundary layers. In addition the turbulent Prandtl number formulation deduced from the experimental measurements was used in the boundary layer analysis and its effect on surface heating was determined. The following conclusions were reached from the theoretical portion of this investigation:

1. The modeling of free-stream turbulence in the one equation turbulence model of McDonald and Kreskovsky captures the correct shape and level of the turbulence kinetic energy.

2. For increased levels of free-stream turbulence, the Reynolds shear stress and turbulent heat flux determined from the turbulence model is significantly smaller than that observed experimentally in the wake region of the turbulent boundary layer. This discrepancy could be due to the eddy viscosity concept used in McDonald and Kreskovsy's model and further investigation of turbulence models is needed.

3. Analytical calculations using either Rotta's turbulent Prandtl number correlation or the correlation of the present investigation predicted Reynolds analogy factors ($2S_t/C_f$) that are in reasonable agreement with experimental measurements and accurately predict the increase in surface heat transfer due to increased free-stream turbulence.

LIST OF SYMBOLS

a_1, a_2, a_3, a_4, $a_{1,\theta}$	Turbulence structural coefficients
c_p	Specific heat at constant pressure
d	Hot wire sensor diameter
$\mathcal{D}$	Wall damping function in turbulence
Fu_v	Flatness factor (vertical x probe) = $\overline{u'^4}/(\overline{u'^2})^2$
Fu_h	Flatness factor (horizontal x probe) = $\overline{u'^4}/(\overline{u'^2})^2$
Fv_v	Flatness factor (vertical x probe) = $\overline{v'^4}/(\overline{v'^2})^2$
Fw_h	Flatness factor (horizontal x probe) = $\overline{w'^4}/(\overline{w'^2})^2$
F_T	Flatness factor (tri-x probe) = $\overline{t'^4}/(\overline{t'^2})^2$
$G_{1,\theta}$	Turbulence structural coefficient (Eq. 11)
h	Height of hot wire sensor array
h	Static enthalpy
$\overline{h'v'}$	Reynolds thermal flux
H	Total enthalpy
ℓ	Active length of hot wire sensor
ℓ	Mixing length function in turbulence model
ℓ_e	Free-stream mixing length
L	Dissipation length scale
n	Distance normal to surface
n^+	Dimensionless normal distance to surface,
Nu	Nusselt number of hot wire sensor
p	Static pressure
Pr_t	Turbulent Prandtl number (Eq. 9)
$\underset{\rightarrow}{\dot{q}}$	Heat flux
$\overline{q^2}$	Turbulence kinetic energy
r	Separation distance between hot wire sensors
Re	Reynolds number
Re_θ	Reynolds number based on momentum thickness
R_T	Turbulent Reynolds number
$\tilde{R}_\theta$	McDonald's correlation of Re_θ

s	Coordinate along wall surface
Su_v	Skewness factor (vertical x probe) = $\overline{u'^3}/(\overline{u'^2})^{3/2}$
Su_h	Skewness factor (horizontal x probe) = $\overline{u'^3}/(\overline{u'^2})^{3/2}$
Sv_v	Skewness factor (vertical x probe) = $\overline{v'^3}/(\overline{v'^2})^{3/2}$
Sw_h	Skewness factor (horizontal x probe) = $\overline{w'^3}/(\overline{w'^2})^{3/2}$
S_T	Skewness factor (tri-x probe) = $\overline{t'^3}/(\overline{t'^2})^{3/2}$
T	Mean static temperature
Te	Free-stream turbulence level
T_T	Total temperature
T_τ	Friction temperature = $q_W/\rho_W c_p U_\tau$
T^+	Dimensionless temperature = T_W-T/T_τ
t'	Fluctuating temperature
u	Streamwise velocity
U	Mean streamwise velocity
U_τ	Friction velocity
U^+	Dimensionless velocity - U/U_τ
$\overline{u'u'}$, $\overline{v'v'}$, $\overline{w'w'}$	Components of turbulent intensity
u', v', w'	Streamwise normal and transverse fluctuating velocities
$-\overline{u'v'}$	Reynolds shear stress
v	Normal velocity
V_q	Transport velocity of turbulence kinetic energy (Eq. 8)
V_τ	Transport velocity of turbulent shear stress (Eq. 7)
x	Distance from plate leading edge
y	Distance from wall
y^+	Dimensionless distance from wall = yU_τ/ν
δ	Boundary layer thickness
δ_τ	Thermal boundary layer thickness
δ_s	Thickness of inner wall region of boundary layer
δ^*	Boundary layer displacement thickness
θ	Boundary layer momentum thickness
κ	von Karman constant for velocity of law-of-the-wall
κ_θ	von Karman constant for temperature law-of-the-wall

μ	Molecular viscosity
μ_T	Eddy viscosity
ν	Kinematic viscosity
Π	Wake strength for velocity boundary layer
Π_θ	Wake strength for temperature boundary layer
ρ	Density
τ	Shear stress
ΨB_v	Correlation coefficient = $\overline{u'^2v'}/\overline{u'^2}\sqrt{\overline{v'^2}}$
ΨB_w	Correlation coefficient = $\overline{u'^2w'}/\overline{u'^2}\sqrt{\overline{w'^2}}$
ΨC_v	Correlation coefficient = $\overline{u'v'^2}/\overline{u'^2}\sqrt{\overline{v'^2}}$
ΨC_w	Correlation coefficient = $\overline{u'w'^2}/\overline{u'^2}\sqrt{\overline{w'^2}}$

Subscripts

e	Freestream
w	Wall
0.995	where U = 0.995 Ue

REFERENC'S

1. Blair, M. F., D. A. Bailey and R. H. Schlinker: Development of a Large-Scale Wind Tunnel for the Simulation of Turbomachinery Airfoil Boundary Layers, ASME Paper 81-GT-6 presented at ASME Gas Turbine Conference, March 1981, ASME Journal of Engineering for Power, Vol. 103, pp. 678-687, 1981.

2. Blair, M. F. and M. J. Werle: The Influence of Freestream Turbulence on the Zero Pressure Gradient Fully Turbulent Boundary Layer, UTRC Report R80-915388-12, September 1980.

3. Baines, W. D. and E. G. Peterson: An Investigation of Flow Through Screens, Trans. of ASME, Vol. 73, pp. 467-480, July 1951.

4. Blackwell, B. F. and R. J. Moffat: Design and Construction of a Low Velocity Boundary-Layer Temperature Probe, AIAA Paper No. 74-709, ASME Paper No. 74-HT-29, July 1974.

5. Guitton, D. E. and R. P. Patel: An Experimental Study of the Thermal Wake Interference Between Closely Spaced Wires of a X-Type Hot-Wire Probe. McGill University Report 69-7, June 1969.

6. Guitton, D. E.: Correction of Hot Wire Data for High Intensity Turbulence, Longitudinal Cooling and Probe Interference. McGill University Report 68-6, 1968.

7. Champagne, F. H., C. A. Sleicher and O. H. Wehrmann: Turbulence Measurements with Inclined Hot-Wires Part I - Heat Transfer Experiments with Inclined Hot Wires, Part II Hot Wire Response Equations, JFM, Vol. 28, 1967, pp. 153-182.

8. Charnay, G., J. P. Schon and M. Sunyach: Isolation and Sampling of Random Signals Transmitted by Several Hot Wire Anemometers. Entropie No. 50, March-April 1973 (in French).

9. Johnson, D. S.: Velocity and Temperature Fluctuation Measurements in a Turbulent Boundary Layer Downstream of a Stepwise Discontinuity in Wall Temperature, Journal of Applied Mechanics, Vol. 26, 1959.

10. Charnay, G., G. Comte-Bellot and J. Mathieu: Development of a Turbulent Boundary Layer on a Flat Plate in an External Turbulent Flow. AGARD, CP 93, paper No. 27, 1971.

11. Huffman, F. D., D. R. Zimmerman and W. A. Bennet: The Effect of Free-Stream Turbulence Level in Turbulent Boundary Layer Behavior. AGARD AG164, pp. 91-115, 1972.

12. Charnay, G., J. Mathieu and G. Comte-Bellot: Response of a Turbulent Boundary Layer to Random Fluctuations in the External Stream, Physics of Fluids, Vol. 19, No. 9, September 1976.

13. Sandborn: Resistance Temperature Transducers, Metrology Press, Fort Collins, CO, 1972, pp. 205-209.

14. Hancock, P. D.: Effect of Free-Stream Turbulence in Turbulent Boundary Layers, Ph.D. thesis, Imperial College, London University, 1980.

15. Bradshaw, P.: An Introduction to Turbulence and Its Measurement, Pergammon Press, 1971, pp. 121-126.

16. Batchelor, G. K.: The Theory of Homogeneous Turbulence, Cambridge University Press, 1967, pp. 46-47.

17. Simpson, R. L., D. G. Whitten and R. J. Moffat: An Experimental Study of the Turbulent Prandtl Number of Air with Injection and Suction. Int. J. Heat and Mass Transfer, Vol. 13, 1970, pp. 124-143.

18. Bradshaw, P.: The Turbulence Structure of Equilibrium Boundary Layers, JFM, Vol. 29, Part 4, pp. 624-645, 1967.

19. Bradshaw, P., D. H. Ferriss, and N. P. Atwell: Calculation of Boundary Layer Development Using the Turbulent Energy Equation, JFM, Vol. 28, pp. 593-616, 1967.

20. Klebanoff, P. S.: Characteristics of Turbulence in a Boundary Layer with Zero Pressure Gradient, NACA Report 1247 (1955).

21. Subramanian, C. S. and R. A. Antonia: Effect of Reynolds Number on a Slightly Heated Turbulent Boundary Layer, Int. J. of Heat and Mass Transfer, Vol. 25, No. 11, pp. 1833-1846, 1981.

22. Rotta, J. C.: Temperaturverteilungen in der Turbulenten Grezschicht an der Ebenen Platte, Int. J. of Heat and Mass Transfer 7, 1964, pp. 215-228.

23. Thomas, N. H. and P. E. Hancock: Grid Turbulence Near a Moving Wall, JFM, Vol. 82, Part 3, 1977, pp. 481-496.

24. Evans, R. L.: Free-Stream Turbulence Effects on the Turbulent Boundary Layer, A.R.C. C.P. 1282, 1974.

25. Senda, M., K. Suzuki and T. Sato: Turbulence Structure Related to the Heat Transfer in a Turbulent Boundary Layer with Injection, Turbulent Shear Flows, Vol. 2, Selected Papers from the 2nd Int. Symposium on Turbulent Shear Flows, Springer-Verlag, 1980.

26. Simonich, J. C. and P. Bradshaw: Effect of Free-Stream Turbulence on Heat Transfer through a Turbulent Boundary Layer, ASME Journal of Heat Transfer, Vol. 100, No. 4, 1978.

27. Blom, J.: An Experimental Determination of the Turbulent Prandtl Number in a Developing Temperature Boundary Layer, Ph.D. Thesis, Technological University, Eindhoven, The Netherlands, 1970.

28. McDonald, H.: User's Manual for the Finite-Difference Boundary Layer Prediction Deck (M093). United Aircraft Research Laboratories Report UAR-J228, 1970.

29. McDonald, H. and R. W. Fish: Practical Calculations of Transitional Boundary Layers. Int. J. Heat Mass Transfer, Vol. 16, pp. 1729-1744, 1973.

30. McDonald, H. and J. P. Kreskovsky: Effect of Free Stream Turbulence on the Turbulent Boundary Layer. Int. J. Heat Mass Transfer, Vol. 17, pp. 705-716, 1974.

31. Edwards, D. E., J. E. Carter and M. J. Werle: Analysis of Boundary Layer Equations Including a New Composite Coordinate Transformation, UTRC Report No. UTRC81-30, May 1982.

32. Cebeci, T. and A. M. O. Smith: Analysis of Turbulent Boundary Layers, Academic Press, New York, 1974.

33. Dhawan, S. and R. Narasimha: Some Properties of Boundary Layer Flow During the Transition from Laminar to Turbulent Motion, J. Fluid Mech., Vol. 3, 1958.

34. Townsend, A. A.: The Structure of Turbulent Shear Flow. Cambridge University Press, 1956.

35. Shamroth, S. J. and H. McDonald: Assessment of a Transitional Boundary Lyaer Theory at Low Hypersonic Mach Numbers. NASA CR-2131, November 1972.

36. Walker, J. D. and M. J. Werle: Summary and Critique of a Turbulence Model for Free-Stream Turbulence Effects on Boundary Layer Characteristics, UTRC Report UTRC82-18.

37. IMSL Library 2 Reference Manual, Edition 66, International Mathematical and Statistics Libraries, Inc., 1977.

38. Schlichting, H.: Boundary Layer Theory, 6th Ed., McGraw-Hill Co., Inc., New York, 1978.

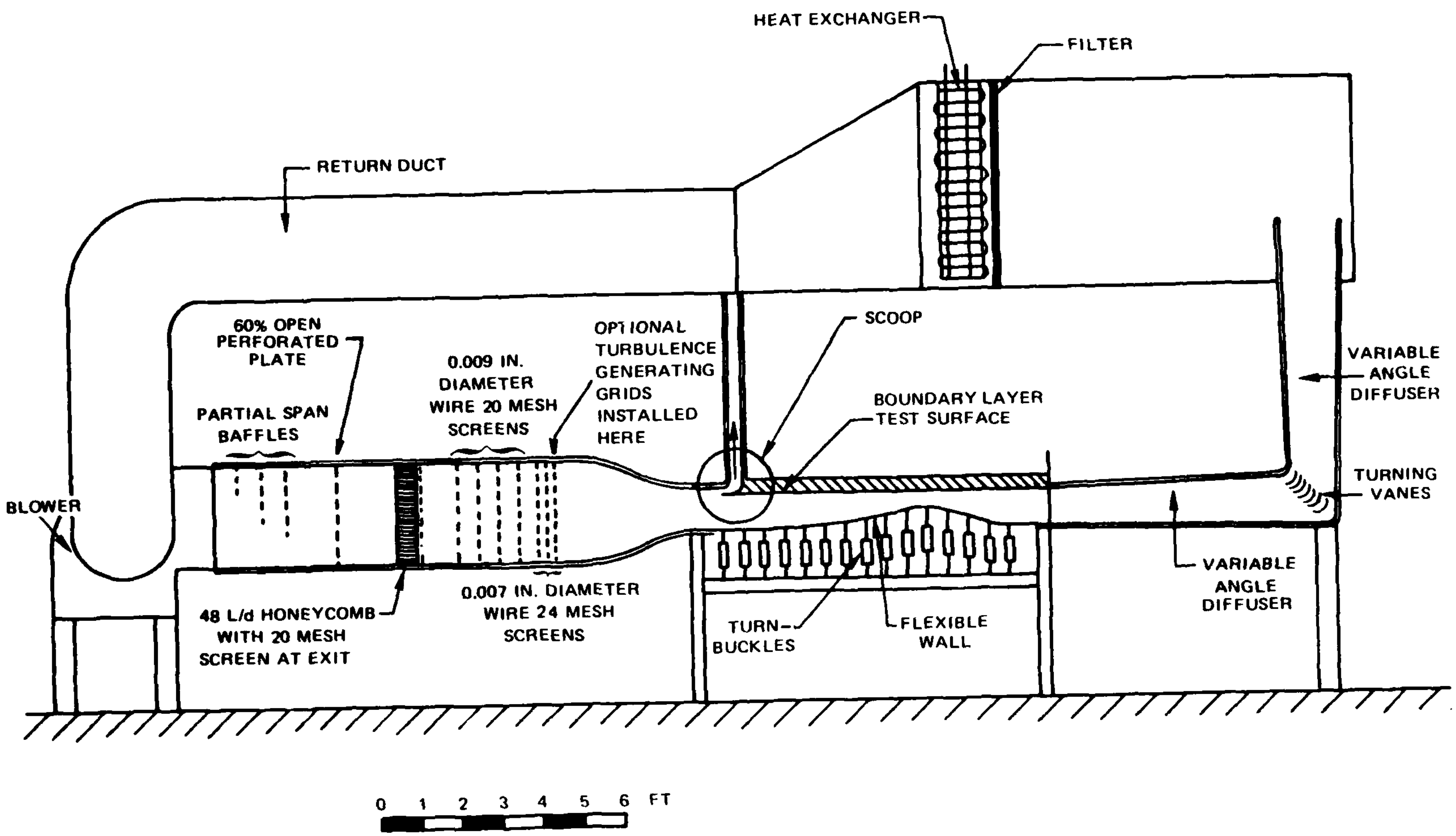

Figure 1. United Technologies Research Center Boundary Layer Wind Tunnel

80-8-95-6

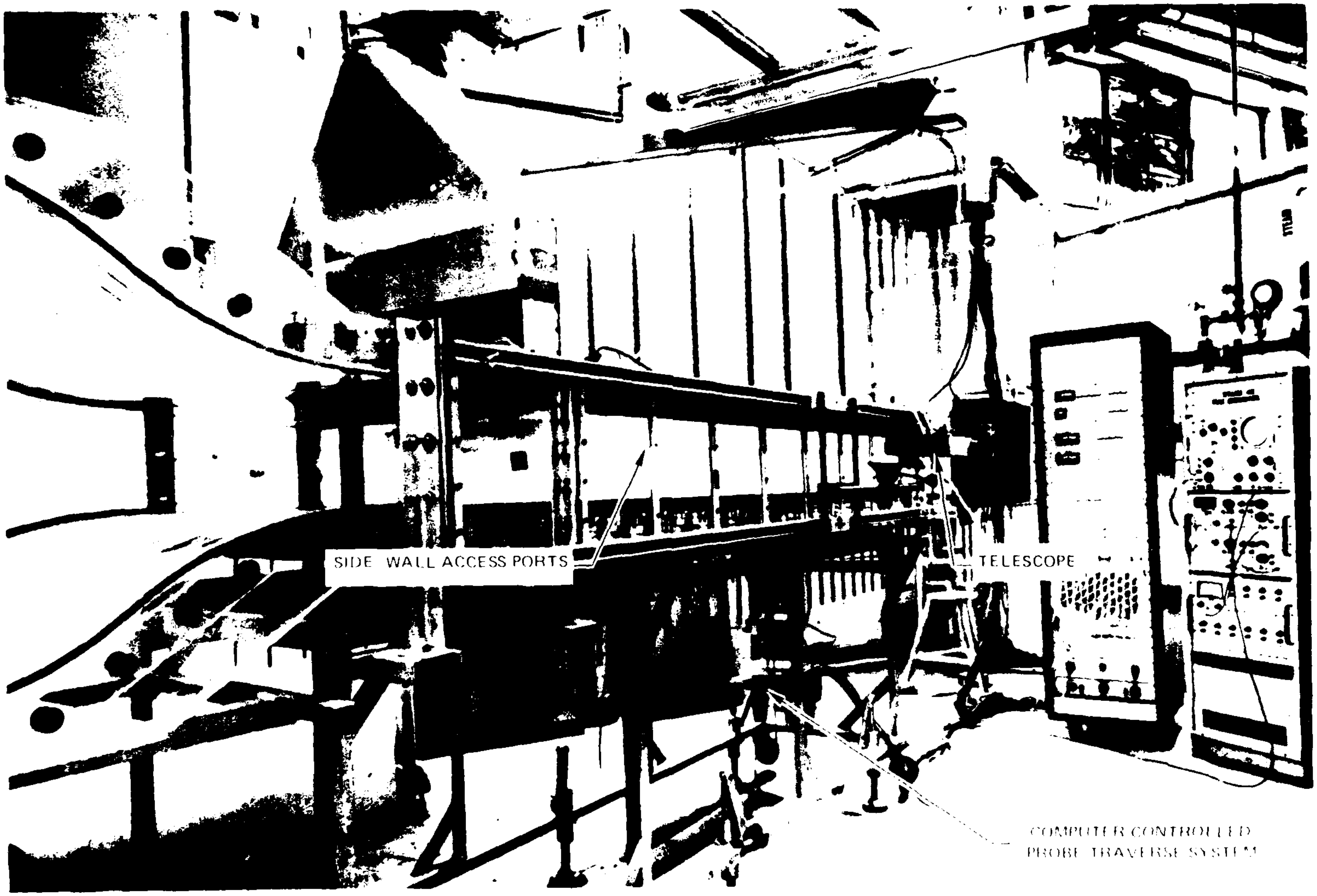

Figure 2. Photograph of UTRC Boundary Layer
Wind Tunnel Test Section

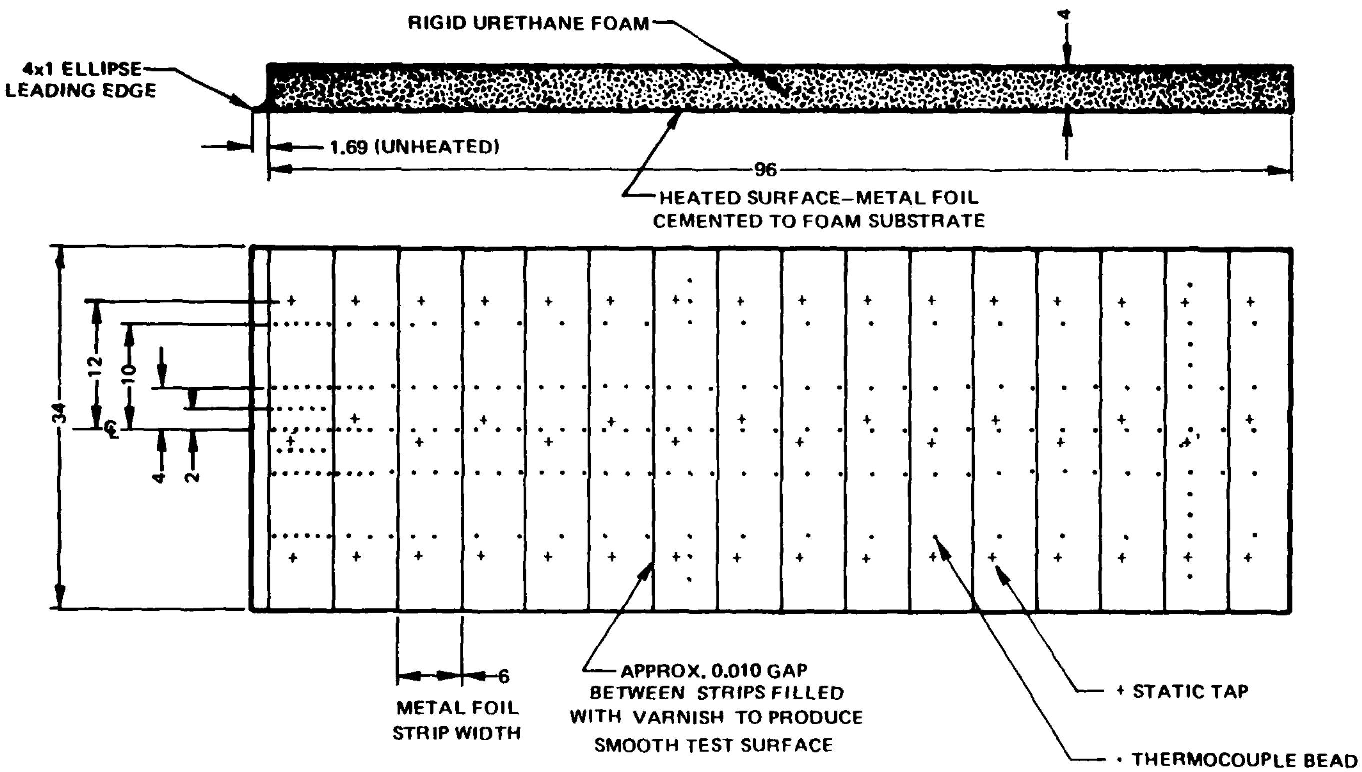

Figure 3. Instrumentation Diagram for the Uniform Heat Flux Flat Wall Model

79-05-70-4

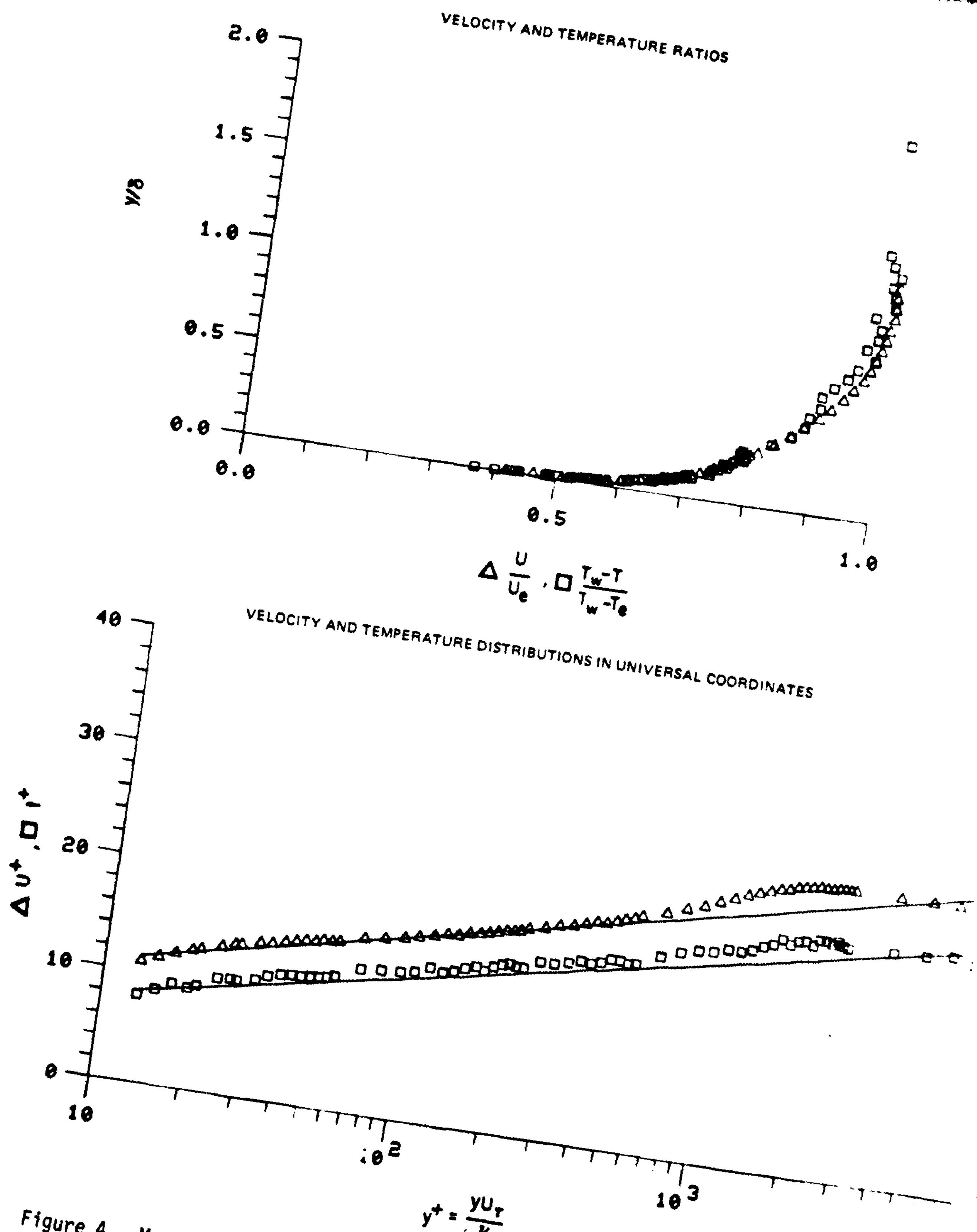

Figure 4. Mean Velocity and Temperature Profiles x = 68 in., Te = 1.6%

78-12-100-1

Mean Profile Data

x = 68 in., Te = 1.6[illegible]

N	Y INCHES	Y/ DELTA	U FT/SEC	T DEG.F	U/UE	THETA	U-UE / UTAU	U(+)	T(+)	Y(+)
1	.0073	.007	41.30	86.26	.421	.371	-14.898	10.616	7.672	13.250
2	.0083	.007	43.36	85.45	.442	.403	-14.352	11.364	8.544	15.257
3	.0094	.008	45.51	84.60	.464	.436	-13.794	11.922	9.256	17.046
4	.0106	.009	47.35	84.65	.482	.426	-13.313	12.403	9.047	19.215
5	.0113	.010	48.06	84.44	.490	.442	-13.123	12.593	9.387	20.460
6	.0132	.012	50.00	83.36	.509	.485	-12.617	13.099	10.281	23.914
7	.0146	.013	51.06	83.24	.520	.489	-12.334	13.382	10.380	26.445
8	.0153	.014	51.66	83.27	.526	.488	-12.179	13.537	10.356	27.720
9	.0176	.016	52.95	82.87	.539	.504	-11.645	13.871	10.685	31.868
10	.0194	.017	53.42	82.37	.544	.523	-11.722	13.994	11.103	35.121
11	.0214	.019	54.41	82.04	.554	.536	-11.462	14.254	11.380	38.736
12	.0232	.021	55.16	81.92	.562	.541	-11.266	14.450	11.477	41.990
13	.0249	.022	55.70	81.91	.567	.541	-11.124	14.592	11.485	45.063
14	.0268	.024	56.15	81.83	.572	.544	-11.007	14.709	11.553	48.497
15	.0285	.025	56.82	81.71	.579	.549	-10.832	14.884	11.652	51.570
16	.0304	.027	57.06	81.54	.581	.556	-10.769	14.947	11.793	55.005
17	.0322	.029	57.40	81.34	.585	.564	-10.680	15.036	11.957	56.258
18	.0366	.035	59.29	80.24	.604	.607	-10.184	15.532	12.874	70.168
19	.0454	.041	60.37	80.03	.615	.615	-9.901	15.815	13.045	82.116
20	.0524	.047	61.65	79.94	.628	.618	-9.568	16.148	13.117	94.772
21	.0586	.052	62.44	79.73	.636	.626	-9.361	16.355	13.293	105.979
22	.0657	.059	63.60	79.02	.648	.654	-9.056	16.660	13.880	118.912
23	.0725	.065	64.57	79.39	.658	.640	-8.803	16.913	13.580	131.104
24	.0787	.070	65.19	78.99	.664	.656	-8.640	17.076	13.911	142.311
25	.0854	.076	66.02	78.53	.673	.673	-8.422	17.294	14.287	154.427
26	.0925	.083	66.60	78.13	.678	.687	-8.270	17.446	14.579	167.256
27	.0986	.088	67.23	78.53	.685	.673	-8.104	17.612	14.286	178.282
28	.1053	.094	67.83	77.97	.691	.695	-7.948	17.768	14.756	190.393
29	.1124	.100	68.49	77.70	.698	.706	-7.776	17.940	14.979	203.227
30	.1166	.106	68.98	77.44	.703	.716	-7.645	18.071	15.192	214.434
31	.1255	.112	69.24	77.70	.705	.706	-7.579	18.137	14.963	226.906
32	.1327	.118	70.17	77.71	.715	.706	-7.335	18.381	14.971	239.920
33	.1494	.133	71.33	76.75	.727	.743	-7.032	18.684	15.769	270.107
34	.1672	.149	72.67	76.74	.740	.743	-6.679	19.037	15.773	302.262
35	.1845	.165	73.35	76.45	.747	.755	-6.501	19.215	16.016	333.557
36	.2026	.181	74.45	76.11	.758	.768	-6.213	19.503	16.302	366.270
37	.2194	.196	75.70	76.25	.771	.762	-5.886	19.630	16.178	396.638
38	.2377	.212	76.13	75.89	.775	.777	-5.773	19.943	16.479	429.717
39	.2544	.227	77.18	75.43	.786	.795	-5.498	20.218	16.863	459.903
40	.2725	.243	78.20	75.43	.797	.795	-5.232	20.484	16.859	492.621
41	.2894	.258	78.68	75.67	.801	.785	-5.106	20.610	16.667	523.169
42	.3076	.275	79.86	75.59	.814	.789	-4.795	20.921	16.732	556.267
43	.3675	.328	82.06	74.49	.836	.831	-4.215	21.501	17.642	664.341
44	.4275	.382	84.49	73.71	.861	.862	-3.584	22.132	18.291	772.796
45	.4875	.435	86.40	73.22	.880	.881	-3.084	22.632	18.698	881.251
46	.5476	.489	88.40	73.09	.901	.886	-2.558	23.158	18.804	989.887
47	.6074	.542	90.14	72.70	.918	.901	-2.103	23.613	19.125	1097.980
48	.6675	.596	91.82	72.70	.935	.901	-1.664	24.052	19.126	1206.616
49	.7274	.649	93.24	72.28	.950	.918	-1.292	24.424	19.476	1314.690
50	.7876	.703	94.42	71.77	.962	.938	-.982	24.734	19.901	1423.306
51	.8474	.756	95.34	71.44	.971	.951	-.741	24.975	20.176	1531.800
52	.9073	.810	95.93	70.79	.977	.976	-.587	25.129	20.709	1640.274
53	.9676	.864	96.73	71.17	.985	.961	-.378	25.338	20.395	1749.271
54	1.0276	.917	97.21	70.78	.990	.976	-.251	25.465	20.719	1857.526
55	1.0876	.971	97.54	70.70	.994	.980	-.164	25.552	20.792	1965.981
56	1.1476	1.024	97.95	71.01	.998	.967	-.058	25.658	20.529	2074.436
57	1.2073	1.078	97.92	70.27	.997	.996	-.065	25.651	21.142	2182.349
58	1.2676	1.131	98.05	70.31	.999	.995	-.032	25.684	21.109	2291.346
59	1.3272	1.185	98.13	70.46	1.000	.988	-.011	25.705	20.967	2399.078
60	1.3874	1.238	98.20	70.16	1.000	1.000	.008	25.724	21.216	2507.894
61	1.4474	1.292	98.16	70.54	1.000	.986	.004	25.720	20.921	2616.349
62	1.5075	1.345	98.25	70.74	1.001	.978	.020	25.736	20.753	2724.985
63	2.1325	1.903	98.30	70.51	1.001	.987	.033	25.749	20.942	3854.724
64	2.7576	2.461	98.20	70.38	1.000	.992	.007	25.723	21.055	4984.644
65	3.3825	3.019	98.16	70.14	1.000	1.002	.003	25.719	21.252	6114.203
66	4.0074	3.577	98.27	70.59	1.001	.984	.026	25.742	20.878	7243.761

Table 1

RUN NO. 3. POINT 2.

BOUNDARY LAYER PROPERTIES

	LINEAR INTERPOLATION TO WALL	STANDARD SUBLAYER FUNCTION FROM WALL TO Y+=30
FREE STREAM VELOCITY =	98.170	98.170
FREE STREAM TEMPERATURE =	70.180	
WALL TEMPERATURE =	95.750	
WALL HEAT FLUX =	.07954	
FREE STREAM DENSITY =	.07552	
FREE STREAM KINEMATIC VISCOSITY =	.0001619	
DENSITY OF FLUID AT WALL =	.07204	
KINEMATIC VISCOSITY OF FLUID AT WALL =	.0001760	
WALL/FREE STREAM DENSITY RATIO =	.95396	
LOCATION REYNOLDS NUMBER (REX) =	3435559.84	
INPUT VALUE OF VELOCITY DELTA =	1.30000	
INPUT VALUE OF TEMPERATURE DELTA =	1.30000	
CALCULATED DELTA =		1.12046
DELTA 99.5% INPUT =	.00000	
DISPLACEMENT THICKNESS (DELSTAR) =	.15429	.15443
MOMENTUM THICKNESS (THETA) =	.10938	.10967
ENERGY-DISSIPATION THICKNESS =	.19539	.19556
ENTHALPY THICKNESS =	.00597	.00598
SHAPE FACTOR 12 (DELSTAR/THETA) =	1.41057	1.40819
SHAPE FACTOR 32 (ENERGY/THETA) =	1.78634	1.78327
MOMENTUM THICKNESS REYNOLDS NUMBER =	5526.16	5540.66
DISPLACEMENT THICKNESS REYNOLDS NUMBER =	7795.01	7602.27
SKIN FRICTION COEFFICIENT =	.002865	
FRICTION VELOCITY =	3.81748	
LAW OF THE WALL CONSTANT (K) =	.41000	
LAW OF THE WALL CONSTANT (C) =	5.00000	
WAKE STRENGTH =		.44004
CLAUSERS 'DELTA' INTEGRAL =	-3.62559	-3.81767
CLAUSERS 'G' INTEGRAL =	24.97566	24.86843
DISPLACEMENT THICKNESS - CONSTANT DENSITY =	.14465	.14845
MOMENTUM THICKNESS - CONSTANT DENSITY =	.11055	.11085
SHAPE FACTOR 12 - CONSTANT DENSITY =	1.30848	1.33924

LOCATION -X- 68.00000

Te = 1.6%

Table 2

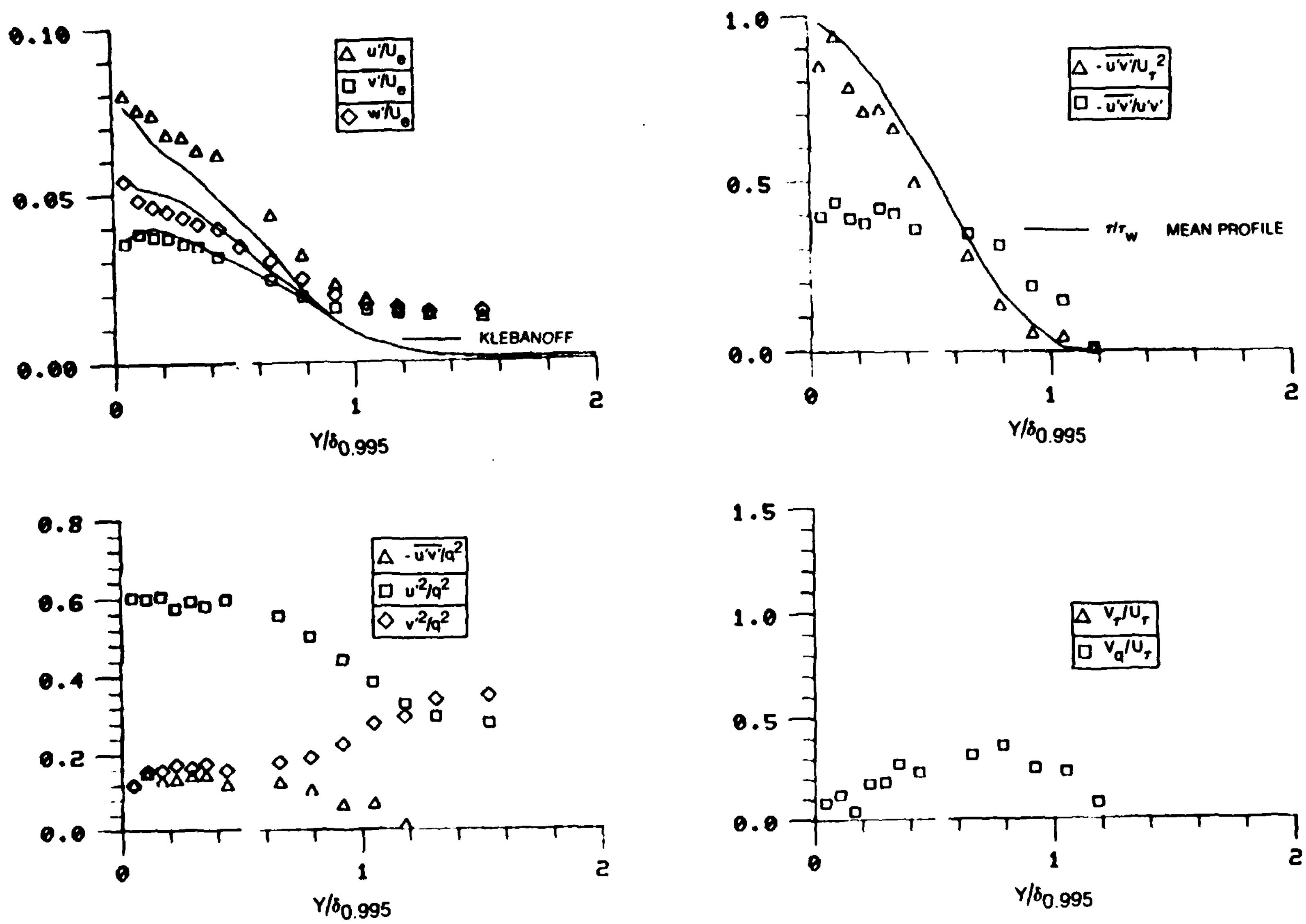

Figure 5A. Boundary Layer Turbulence Quantities $x = 68$ in, $T_e = 1.6\%$

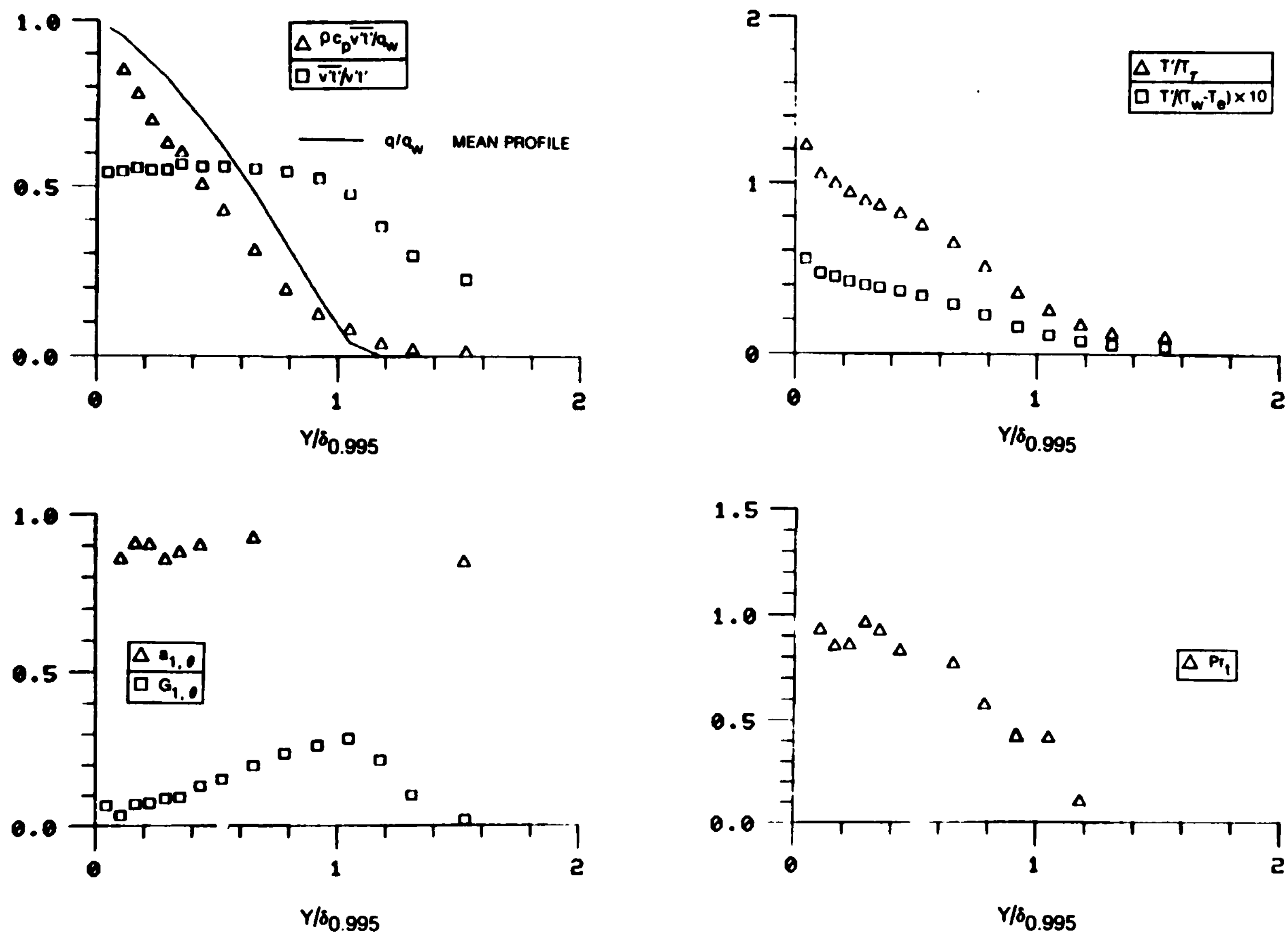

Figure 5B. Boundary Layer Turbulence Quantities $x = 68$ in, $T_e = 1.6\%$

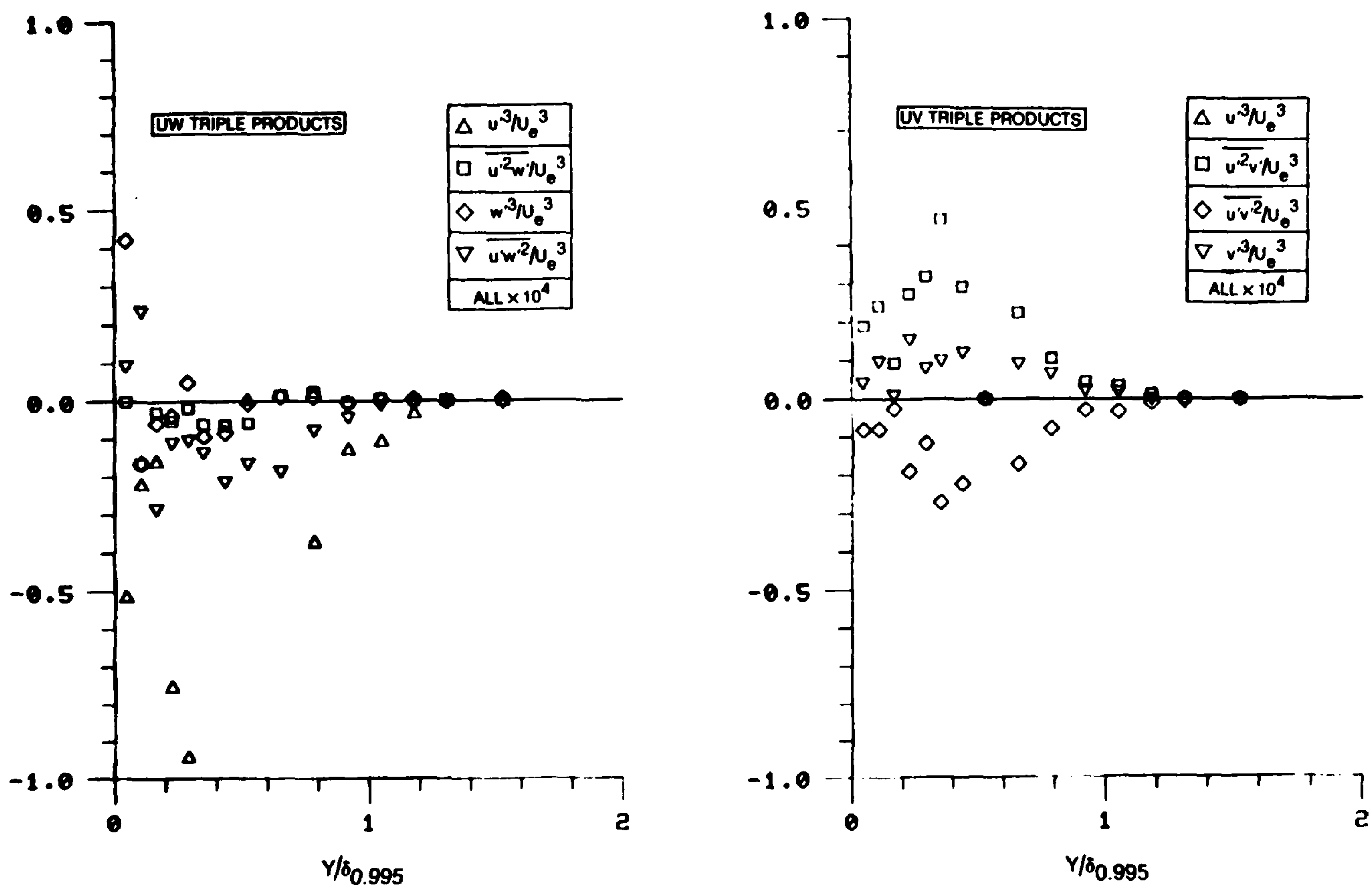

Figure 5C. Boundary Layer Triple Product Distributions $x = 68$ in, $T_e = 1.6\%$

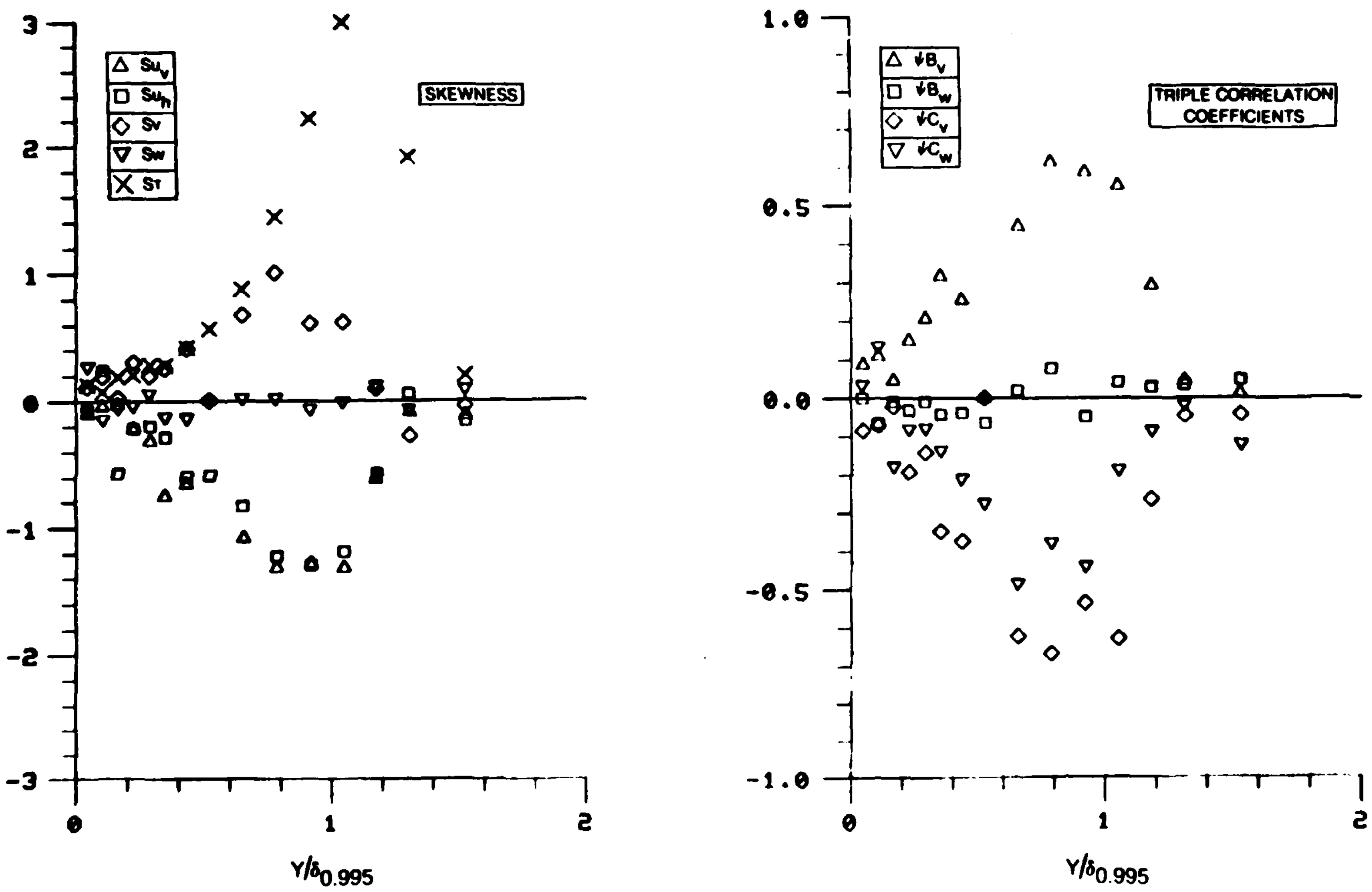

Figure 5D. Boundary Layer Skewness and Triple Product Correlation Coefficient Distributions $x = 68$ in, $T_e = 1.6\%$

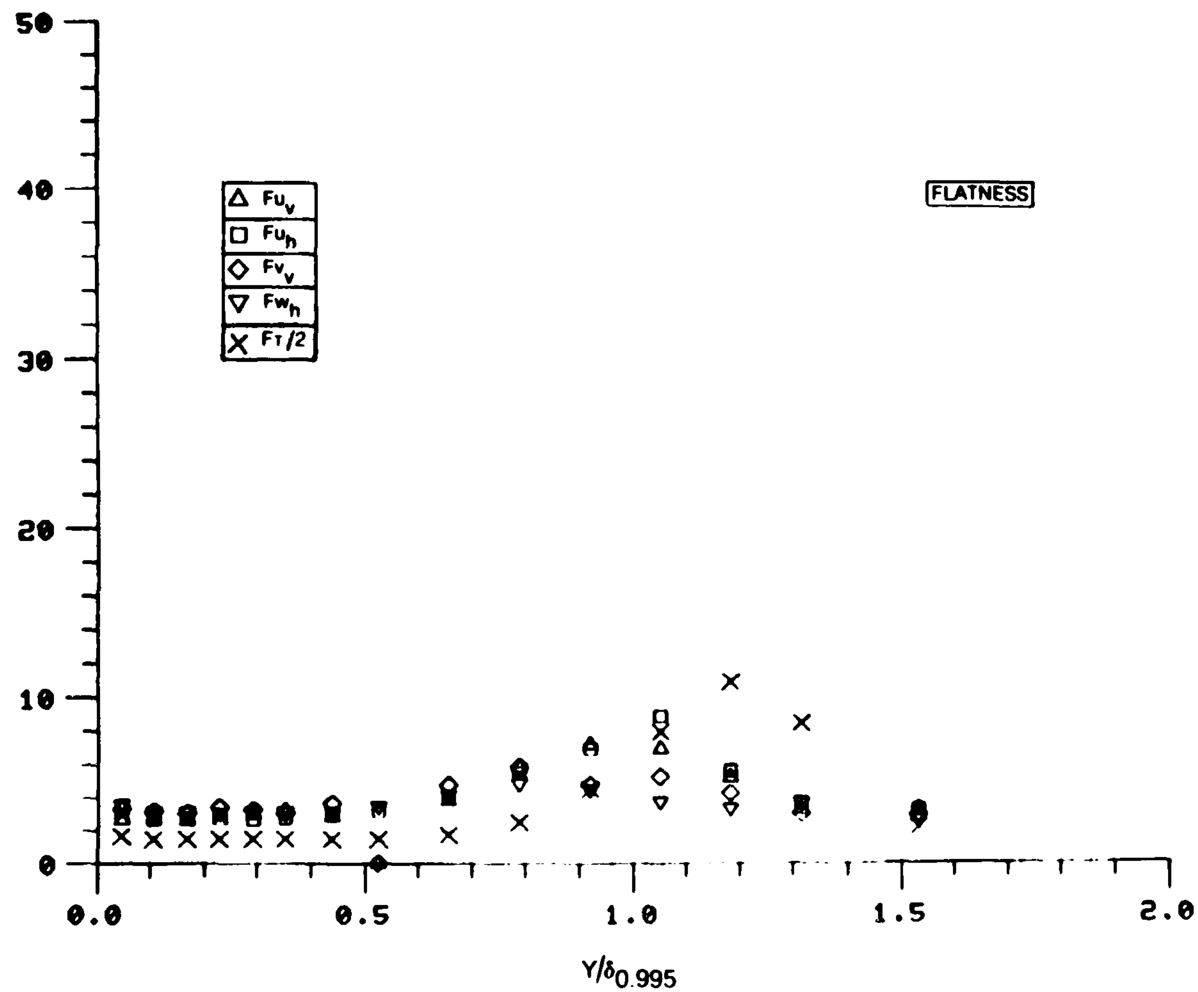

Figure 5E. Boundary Layer Flatness Distributions $x = 68$ in, $T_e = 1.6\%$

Fluctuating Profile Data

x = 68 in, Te = 1.6%

N	Y: INCHES	Y/DELTA	U'/UE	V'/UE	W'/UE	$\sqrt{\overline{U'V'}}$/UE	$\overline{U'V'}$/UTAU	$\overline{U'V'}$/U'V'	C/UE
1	4.000	3.500	.0137	.0179	.0153	.0050	-.0169	-.0960	.0272
2	.050	.044	.0796	[illegible]	.0541	.0353	.644[illegible]	.3574	.1726
3	.125	.105	.0751	.0382	.0462	.0371	.9339	.4265	.0571
4	.190	.166	.0736	.0374	.046[illegible]	.0339	.76[illegible]	.3657	[illegible]
5	.260	.227	.0677	.0371	.044[illegible]	.0323	.70[illegible]	.3762	[illegible]
6	.330	.289	.067[illegible]	.0351	.043[illegible]	.0324	.7124	.4[illegible]	[illegible]
7	.400	.350	.0627	.0344	.040[illegible]	.0311	.6560	.4[illegible]	[illegible]
8	.500	.437	.0612	.0314	.03[illegible]	.0269	.4527	[illegible]	.0754
9	.600	.525	.0254	.0000	.0340	.0000	.0000	[illegible]	.0425
10	.750	.656	[illegible]	.0245	.0240	.0202	.2774	.3447	[illegible]
11	.900	.787	.0316	.0192	.0245	.0135	.1[illegible]	.3105	[illegible]
12	1.050	.919	.0226	.0160	.0196	.0065	[illegible]	.1516	[illegible]
13	1.200	1.050	.0160	.0153	.0169	.0074	[illegible]	.1476	[illegible]
14	1.350	1.181	.0147	.0140	.015[illegible]	.0024	[illegible]	.0094	[illegible]
15	1.500	1.312	.0131	.0141	.0145	.0036	-.0066	-.0677	[illegible]
16	1.750	1.531	.012[illegible]	.0140	.0144	.0046	-.015[illegible]	-.1257	[illegible]
17	4.000	3.500	.012[illegible]	.0163	.0141	.0046	-.01[illegible]	-.0094	[illegible]
18	.000	.000	.0000	.0000	.0000	.0000	.0000	.0000	[illegible]

N	Y: INCHES	Y/DELTA	$\overline{V'U'}$/C2	U'2/C2	V'2/C2	W'2/C2	VTAU/UTAU	VG/UTAU	$\overline{V'T'}$RHOCP/QWALL
1	4.000	3.500	-.0336	.2537	.4316	.3146	[illegible]	.0345	.0028
2	.050	.044	.116[illegible]	.0716	.119[illegible]	.2785	[illegible]	[illegible]	.646[illegible]
3	.125	.105	.1456	.5967	.15[illegible]	.2467	[illegible]	[illegible]	[illegible]
4	.190	.166	.1262	.0642	.1562	.2395	[illegible]	.0413	[illegible]
5	.260	.227	.13[illegible]	.5553	.1723	.2525	[illegible]	.1[illegible]	[illegible]
6	.330	.289	.1366	.5666	.1623	.2445	[illegible]	.1[illegible]	[illegible]
7	.400	.350	.1467	.5794	.1746	.2466	[illegible]	.2[illegible]	[illegible]
8	.500	.437	.1151	.5945	.1563	.2487	[illegible]	.2[illegible]	[illegible]
9	.600	.525	.0000	.3583	.0000	.6417	[illegible]	[illegible]	[illegible]
10	.750	.656	.1210	.5540	.1777	.2674	[illegible]	.3166	[illegible]
11	.900	.787	.0957	.5014	.1904	.3063	[illegible]	.3[illegible]	[illegible]
12	1.050	.919	.0637	.4404	.224[illegible]	.3355	[illegible]	.2[illegible]	[illegible]
13	1.200	1.050	.0639	.3841	.2772	.3387	[illegible]	.2[illegible]	[illegible]
14	1.350	1.181	.00[illegible]	.3284	.2964	.3752	[illegible]	[illegible]	[illegible]
15	1.500	1.312	-.0224	.2974	.3404	.3622	[illegible]	-.[illegible]	[illegible]
16	1.750	1.531	-.040[illegible]	.2797	.3508	.3659	[illegible]	-.00[illegible]	[illegible]
17	4.000	3.500	-.034[illegible]	.2513	.4291	.3196	[illegible]	[illegible]	[illegible]
18	.000	.000	.0000	.0000	.0003	.0000	.0000	.0000	[illegible]

N	INCHES	DELTA	$\overline{V'T'}$/V'T'	T'/TTAU	T'/(TW-TE)	A10	G10	PRT
1	4.000	3.500	.0550	.0065	.0043	.2247	-.0075	-5.1615
2	.050	.044	.5416	1.2264	.0549	1.1025	.0654	.9272
3	.125	.105	.5464	1.0489	.0472	.6541	.0330	.8479
4	.190	.166	.5554	.9900	.0445	.9045	.0[illegible]	.8[illegible]
5	.260	.227	.5466	.9364	.042[illegible]	.9003	.0741	.96[illegible]
6	.330	.289	.5466	.8876	.0399	.8513	.0680	.9233
7	.400	.350	.5646	.8614	.0387	.8756	.0930	.8266
8	.500	.437	.5573	.6139	.0366	.8967	.12[illegible]	[illegible]
9	.600	.525	.5564	.7446	.0335	.0000	.1[illegible]	.76[illegible]
10	.750	.656	.5524	.6428	.0269	.9193	.1681	.59[illegible]
11	.900	.787	.544[illegible]	.5022	.0226	1.0803	.2350	.8120
12	1.050	.919	.5234	.3509	.0153	1.5697	.2643	.41[illegible]
13	1.200	1.050	.47[illegible]	.2464	.0111	1.6204	.2856	.0976
14	1.350	1.181	.3867	.1647	.0074	3.3804	.2161	-.4[illegible]
15	1.500	1.312	.2939	.1165	.0053	1.5145	.1[illegible]	-1.2[illegible]
16	1.750	1.531	.22[illegible]	.0979	.0044	.8422	.0[illegible]	-2.6[illegible]
17	4.000	3.500	[illegible]	[illegible]	.0043	.4061	-.01[illegible]	[illegible]
18	.000	.000	.0000	.0000	.0000	.0000	.0000	[illegible]

Table 3A

Fluctuating Profile Data

x = 68 in., Te = 1.6%

N	Y: INCHES	Y/DELTA	U'3/UE3 x 10000	U'2V'/UE3 x 10000	V'3/UE3 x 10000	U'V'2/UE3 x 10000	[illegible] x 10000	[illegible] x 10000	[illegible]
1	4.000	3.500	.0064	.0019	.0055	-.0726	[illegible]	[illegible]	[illegible]
2	.050	.044	-.5168	.0013	.4242	-.0955	.1966	[illegible]	[illegible]
3	.120	.105	-.2241	-.1647	-.1655	[illegible]	.2457	[illegible]	[illegible]
4	.190	.166	-.1606	-.0295	-.0568	-.4797	.0939	[illegible]	[illegible]
5	.260	.227	-.7562	-.0026	-.0790	-.1069	[illegible]	[illegible]	[illegible]
6	.330	.289	-.9481	-.1195	-.0473	-.0997	[illegible]	[illegible]	[illegible]
7	.400	.350	-2.1948	-.0617	-.0927	-.1325	[illegible]	[illegible]	[illegible]
8	.500	.437	-1.49[illegible]	-.0032	-.0649	-.2287	[illegible]	[illegible]	[illegible]
9	.600	.525	.0000	-.0576	-.0057	-.1626	[illegible]	[illegible]	[illegible]
10	.750	.656	-1.0599	.0119	.0067	-.1651	[illegible]	[illegible]	[illegible]
11	.900	.787	-.37[illegible]	-.0014	-.0056	-.0728	[illegible]	[illegible]	[illegible]
12	1.050	.919	-.1326	-.0052	-.0064	-.0412	.0446	[illegible]	[illegible]
13	1.200	1.050	-.10[illegible]	[illegible]	[illegible]	-.0290	[illegible]	[illegible]	[illegible]
14	1.350	1.181	[illegible]	.0057	[illegible]	-.0269	.0127	[illegible]	[illegible]
15	1.500	1.312	-.0068	.0011	-.0017	-.0235	[illegible]	[illegible]	[illegible]
16	1.750	1.531	-.0029	.0011	-.0067	-.0231	[illegible]	[illegible]	[illegible]
17	4.000	3.500	.0039	.0006	-.0056	-.0323	[illegible]	[illegible]	[illegible]
18	.000	.000	.0000	.0000	.0000	.0000	[illegible]	[illegible]	[illegible]

N	Y: INCHES	Y/DELTA	SU V	SU W	SV	SW	ST	PSI[illegible] V	PSI[illegible] W
1	4.000	3.500	.2967	-.0014	.0484	[illegible]	[illegible]	[illegible]	[illegible]
2	.050	.044	-.1026	-.0639	.1051	.2665	[illegible]	[illegible]	[illegible]
3	.120	.105	[illegible]	-.0730	.1616	-.1422	[illegible]	.1[illegible]	[illegible]
4	.190	.166	[illegible]	-.0797	[illegible]	-.0619	[illegible]	[illegible]	[illegible]
5	.260	.227	-.22[illegible]	-.2166	.2969	-.0421	[illegible]	[illegible]	[illegible]
6	.330	.289	-.3175	-.2061	.1567	.0566	[illegible]	[illegible]	[illegible]
7	.400	.350	-.7578	-.2033	.2500	-.1265	[illegible]	[illegible]	[illegible]
8	.500	.437	-.6546	-.0042	[illegible]	-.1739	.4126	[illegible]	[illegible]
9	.600	.525	.0000	-.0867	.0000	-.0124	.5576	[illegible]	[illegible]
10	.750	.656	-1.0656	-.0739	.6655	.0195	.6747	[illegible]	[illegible]
11	.900	.787	-1.3156	-1.0330	.9933	.0218	1.4367	.61[illegible]	[illegible]
12	1.050	.919	-1.2870	-1.3000	.5998	-.0647	2.2[illegible]	[illegible]	[illegible]
13	1.200	1.050	-1.3151	-1.1852	.6100	-.0365	2.975[illegible]	[illegible]	[illegible]
14	1.350	1.181	-.6172	-.5830	.0918	.1199	3.084[illegible]	.29[illegible]	[illegible]
15	1.500	1.312	-.0969	.1525	-.2775	-.0659	1.9[illegible]	[illegible]	[illegible]
16	1.750	1.531	-.13[illegible]1	-.1690	-.0443	.0916	.1930	.01[illegible]	[illegible]
17	4.000	3.500	.1677	-.3578	-.0231	-.1922	[illegible]	[illegible]	[illegible]
18	.000	.000	.0000	.0000	.0000	.0000	[illegible]	[illegible]	[illegible]

N	Y: INCHES	Y/DELTA	PSICV	PSICW	FU V	FU W	FT V	FT W	FT
1	4.000	3.500	.0909	-.0819	3.0503	3.0553	2.6930	2.7226	3.6[illegible]
2	.050	.044	-.0647	[illegible]	2.6887	2.7409	3.31[illegible]	3.5675	[illegible]
3	.120	.105	-.0701	.1170	2.7296	2.6472	3.1473	3.1850	[illegible]
4	.190	.166	-.0240	-.1772	2.7029	2.6810	[illegible]	3.1284	[illegible]
5	.260	.227	-.1947	-.0799	2.7011	2.7413	3.4140	3.0740	.9275
6	.330	.289	-.1424	-.0767	3.0205	2.6665	[illegible]	[illegible]	[illegible]
7	.400	.350	-.3469	-.1341	3.1547	2.7872	3.0947	3.1476	[illegible]
8	.500	.437	-.3731	-.2113	2.8791	2.9526	[illegible]	3.1611	[illegible]
9	.600	.525	.0000	-.2741	.0000	3.1734	[illegible]	3.4610	[illegible]
10	.750	.656	-.6238	-.4836	3.8277	3.9672	4.7195	4.1736	[illegible]
11	.900	.787	-.6677	-.3769	5.8453	5.5369	5.7997	4.8634	[illegible]
12	1.050	.919	-.5341	-.4766	7.1766	6.9262	4.75[illegible]	4.5045	[illegible]
13	1.200	1.050	-.6261	-.1867	6.8997	8.6146	5.2870	3.7637	[illegible]
14	1.350	1.181	-.2651	-.0826	5.1601	5.0062	4.2715	[illegible]	[illegible]
15	1.500	1.312	-.0440	-.0157	3.2720	3.6776	2.982[illegible]	3.6577	[illegible]
16	1.750	1.531	[illegible]	-.0192	3.2755	[illegible]	[illegible]	[illegible]	[illegible]
17	4.000	3.500	-.0372	-.0936	2.9373	3.0763	2.6397	3.0224	3.6[illegible]
18	.000	.000	.0000	.0000	.0000	.0000	.0000	.0000	.0000

Table 3B

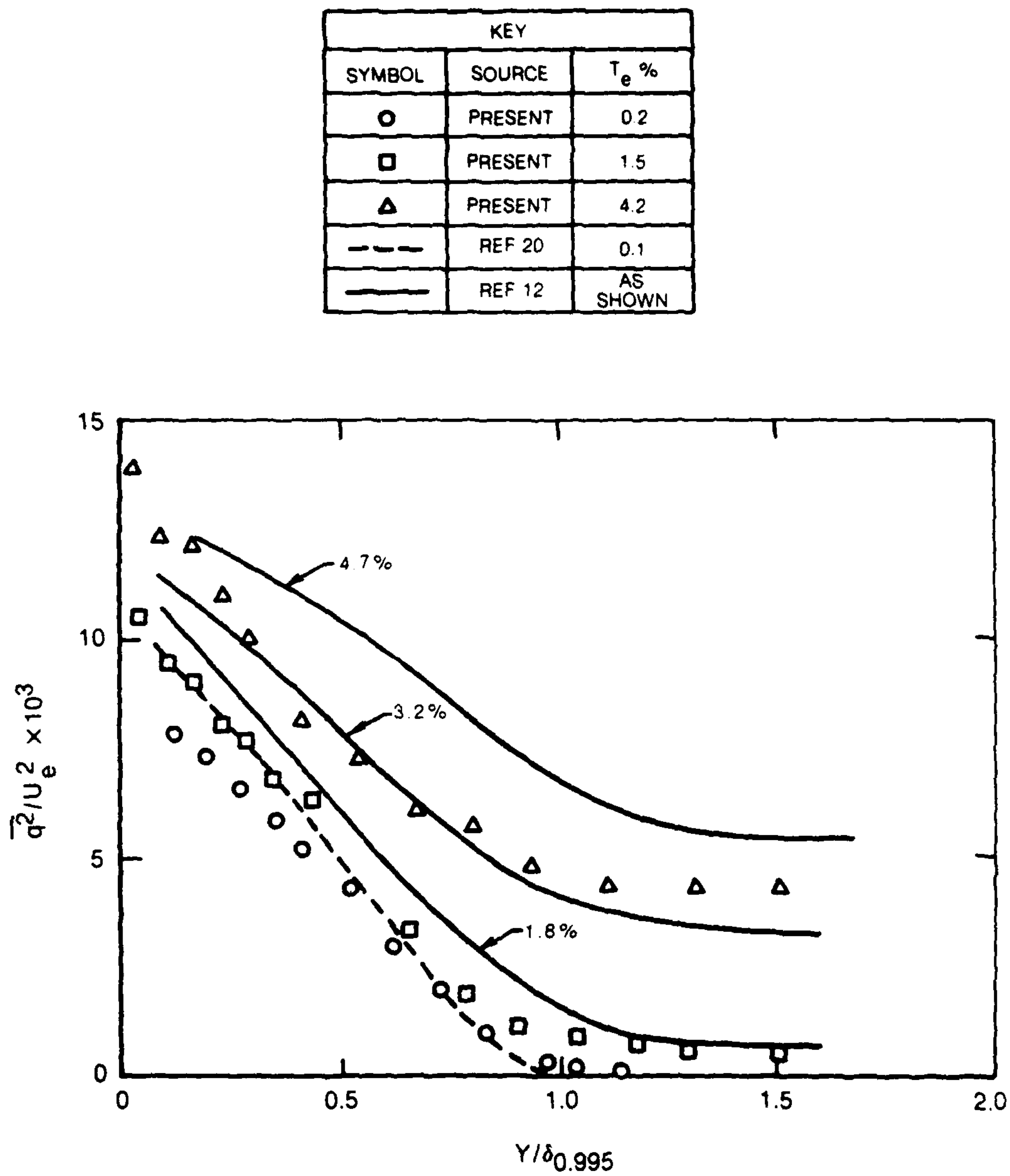

Figure 6. Boundary Layer Turbulent Kinetic Energy Distribution

82-10-71-13

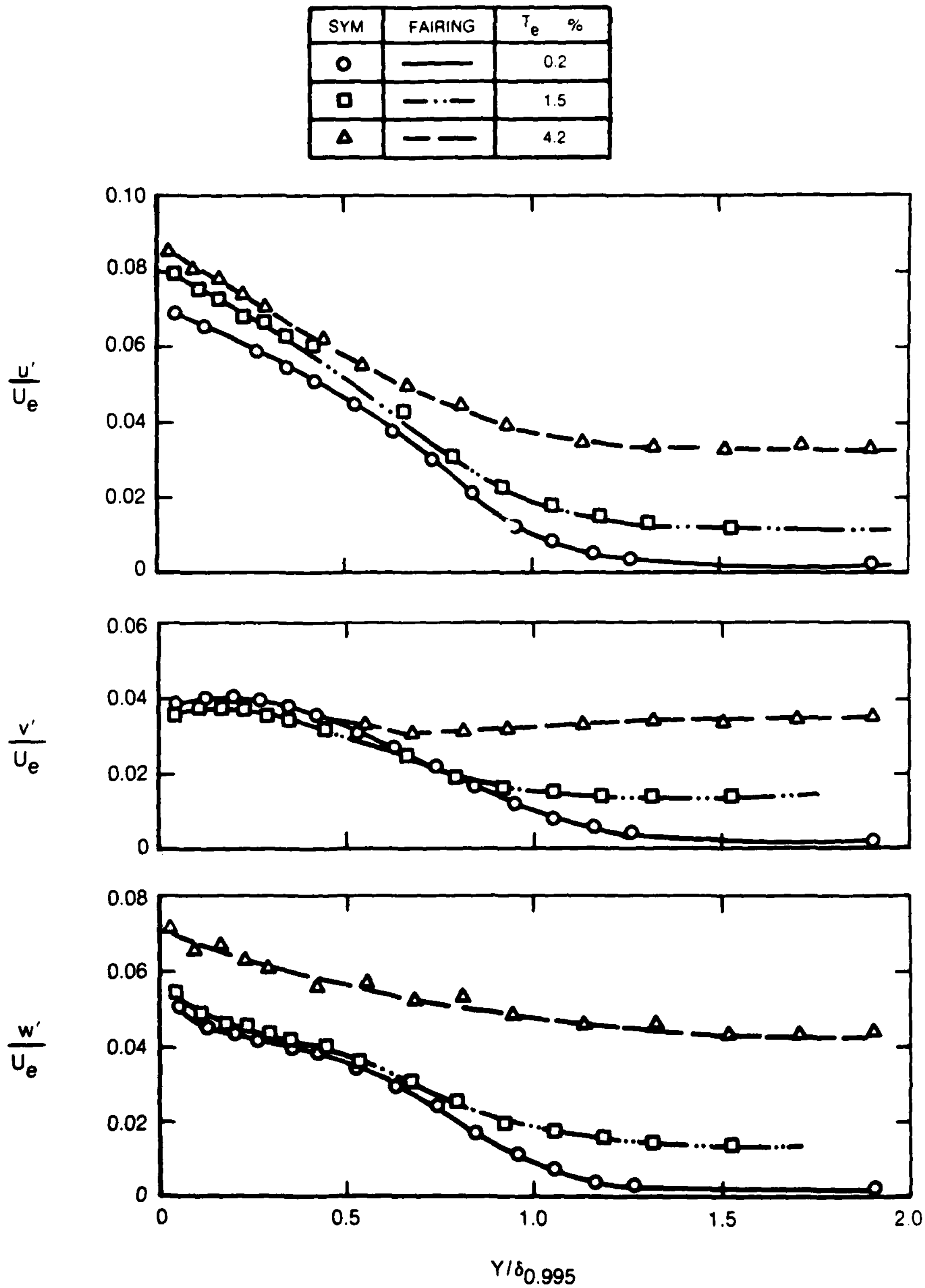

Figure 7. Distribution of the Components of Boundary Layer Turbulence

82-10-71-12

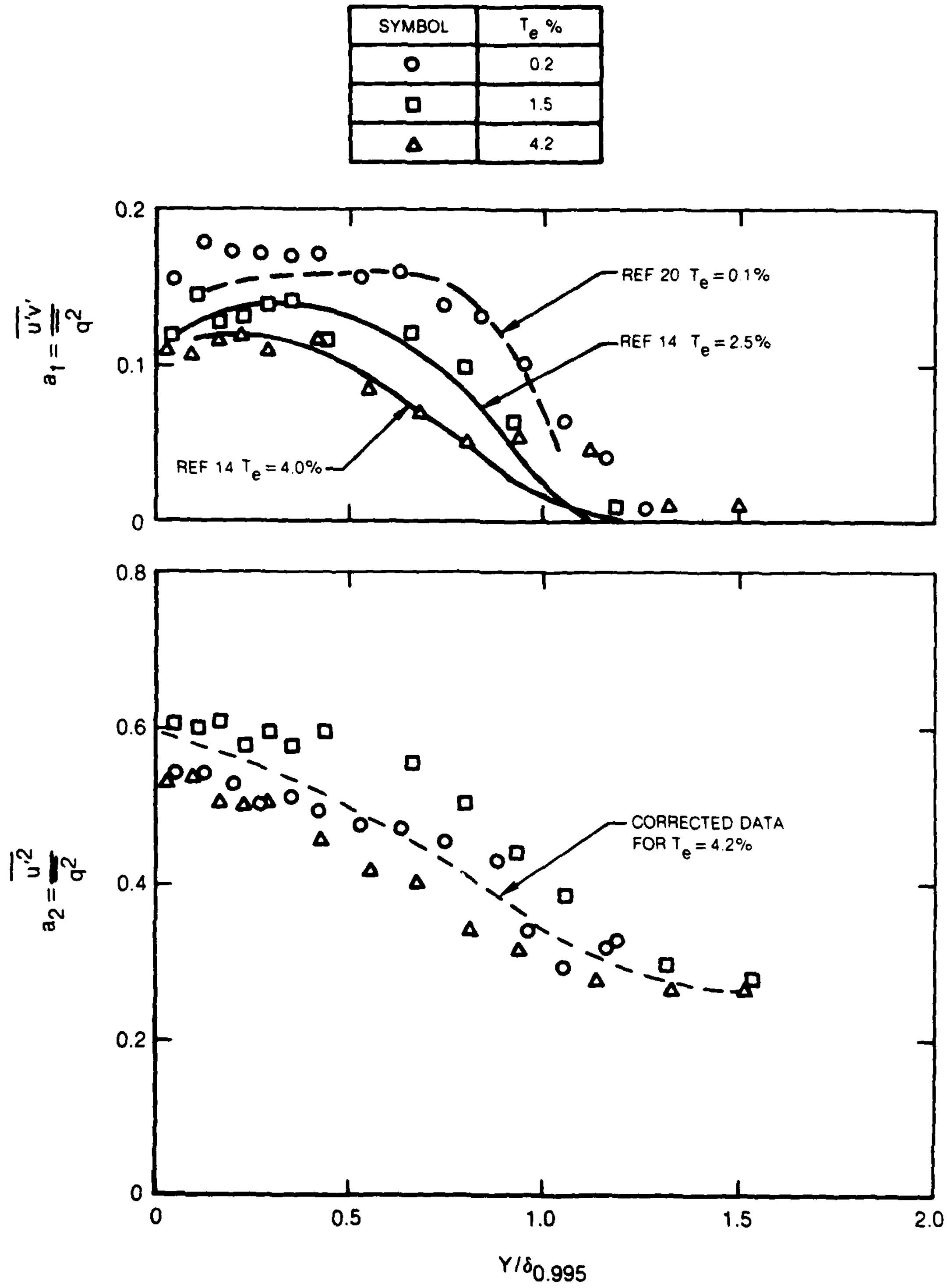

Figure 8A. Distribution of the Turbulence Structural Coefficients a_1 and a_2 Across the Boundary Layer

82-10-71-11

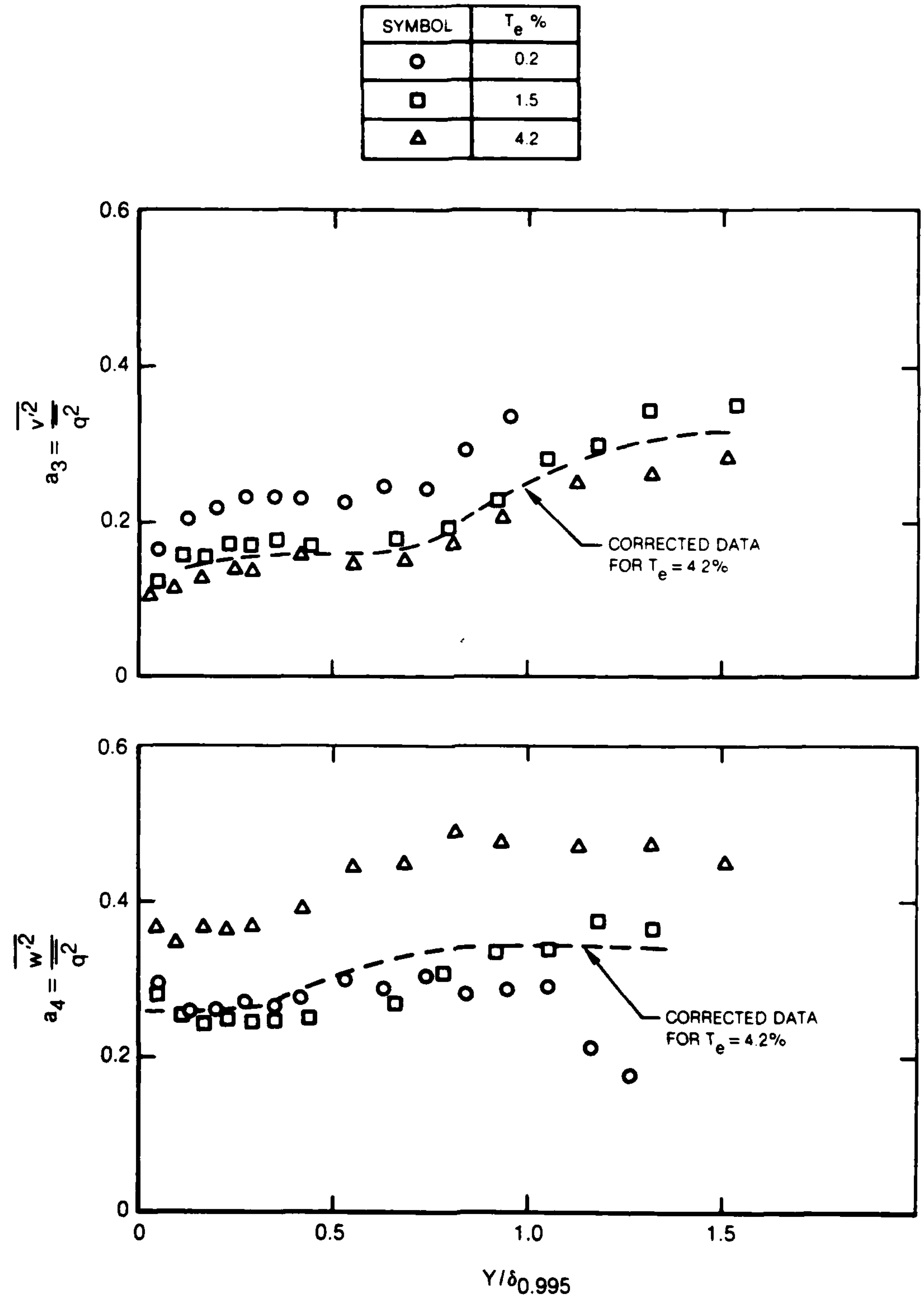

Figure 8B. Distribution of the Turbulence Structural Coefficients a_3 and a_4 Across the Boundary Layer

82-10-71-10

KEY	
SYM	SOURCE
●	PRESENT DATA
△	CHARNAY, et al (10)
▽	CHARNAY, et al (12)
□	HANCOCK (14)
◇	HUFFMAN (11)
○	EVANS (24)

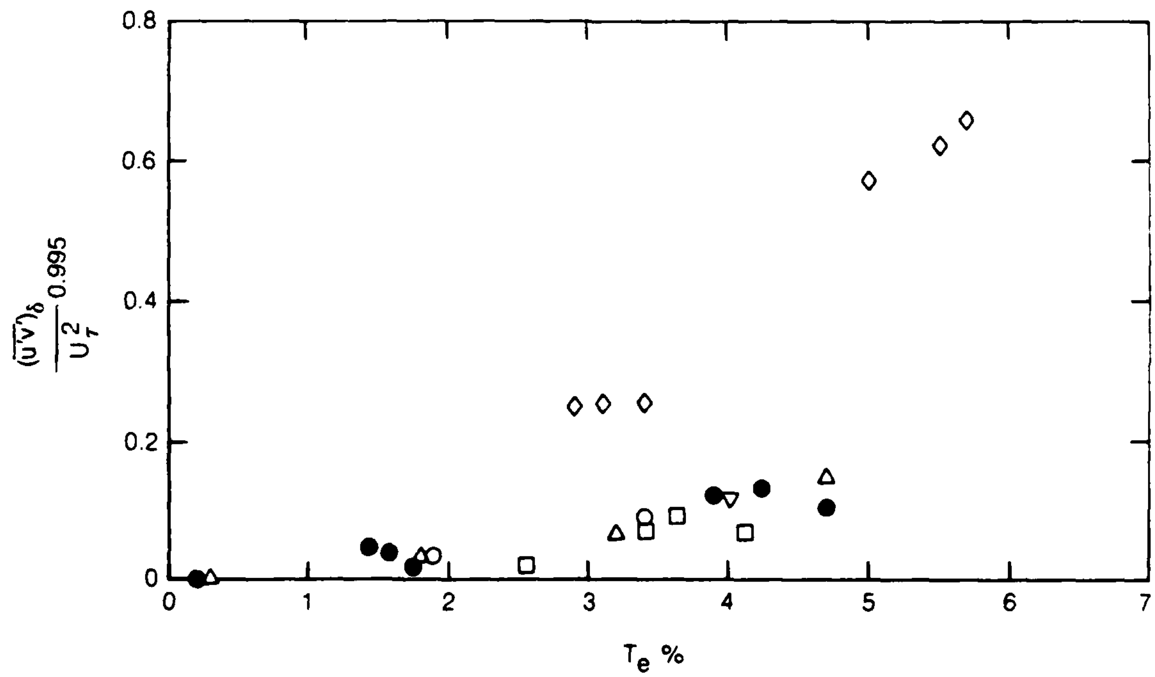

Figure 9. Influence of Free-Stream Turbulence on the Turbulent Shear Stress at $\delta_{0.995}$

82-10-71-9

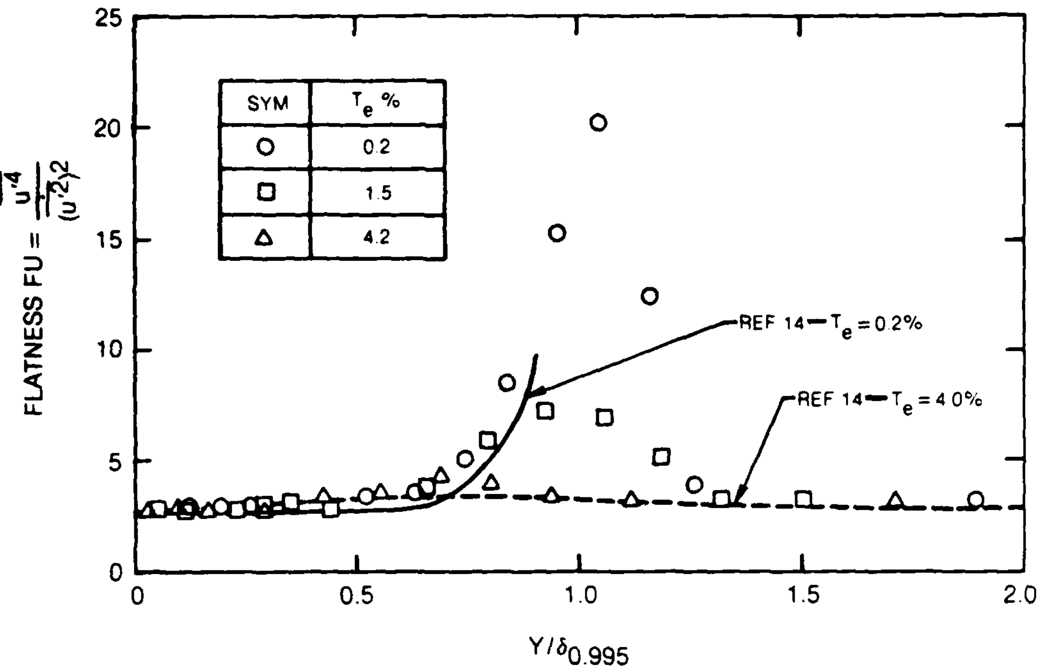

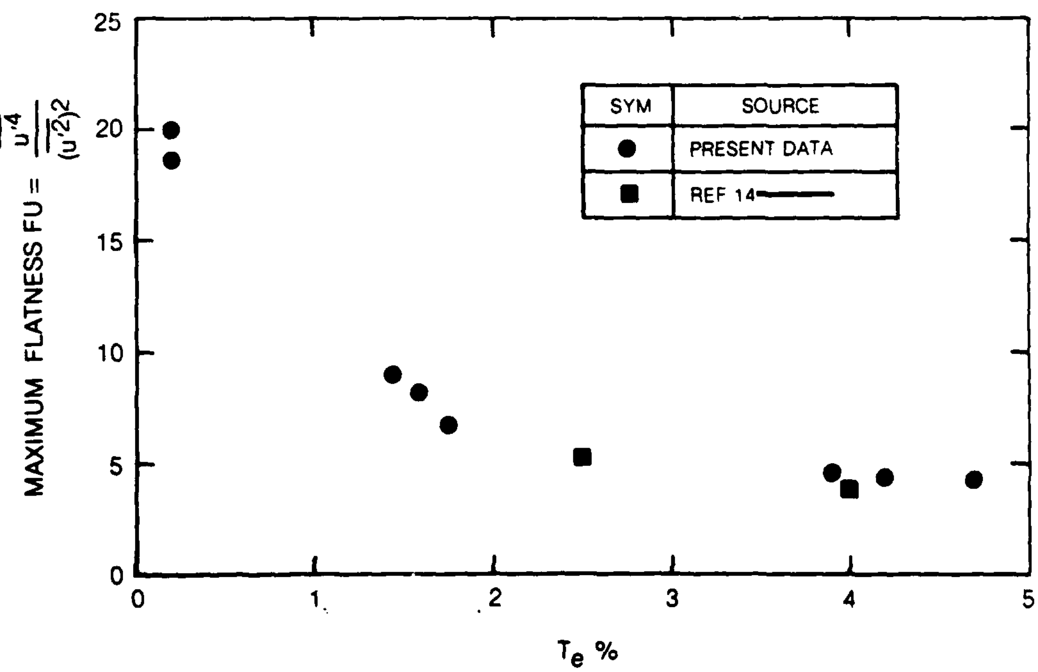

Figure 10. Effect of Free-Stram Turbulence on the u' Flatness Factor Distributions

82-10-71-8

SYMBOL CODE		
DATA	EQ 17	T_e %
○	———	0.2
▲	– – – –	1.4
□	—·—·—	4.0

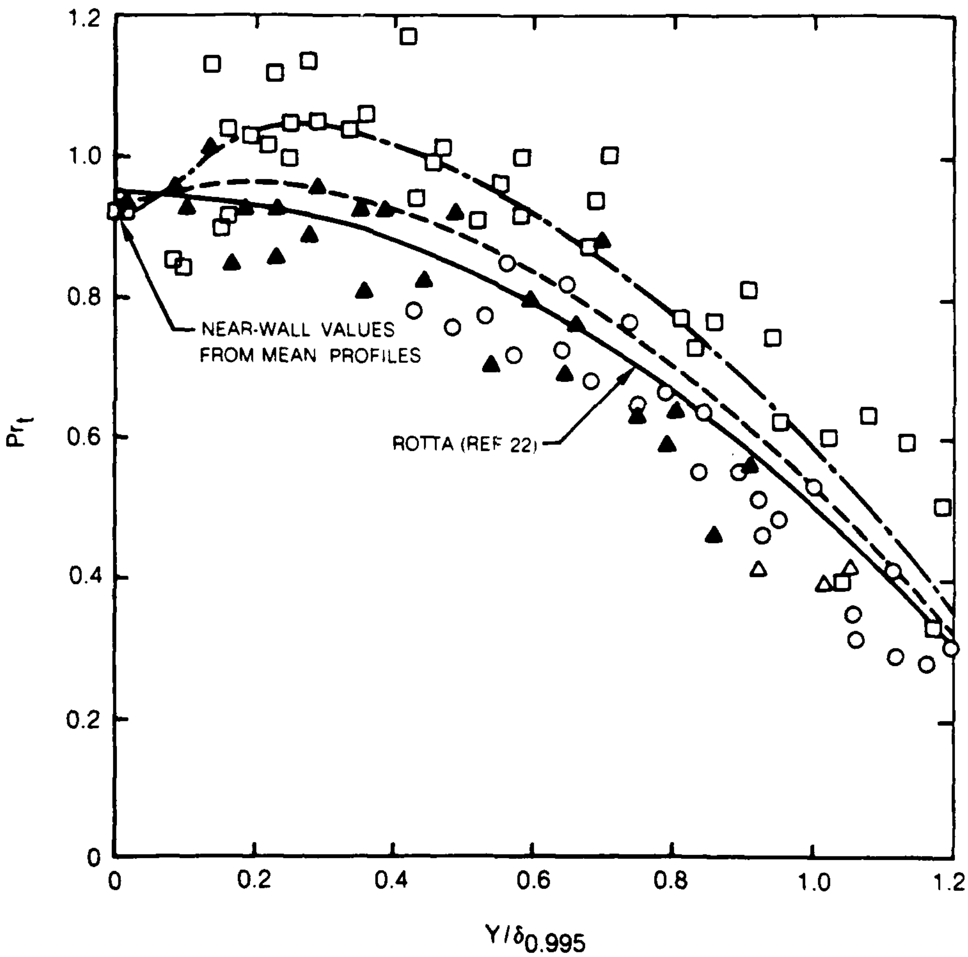

Figure 11. Effect of Free-Stream Turbulence on the Turbulent Prandtl Number Distribution

82-10-71-7

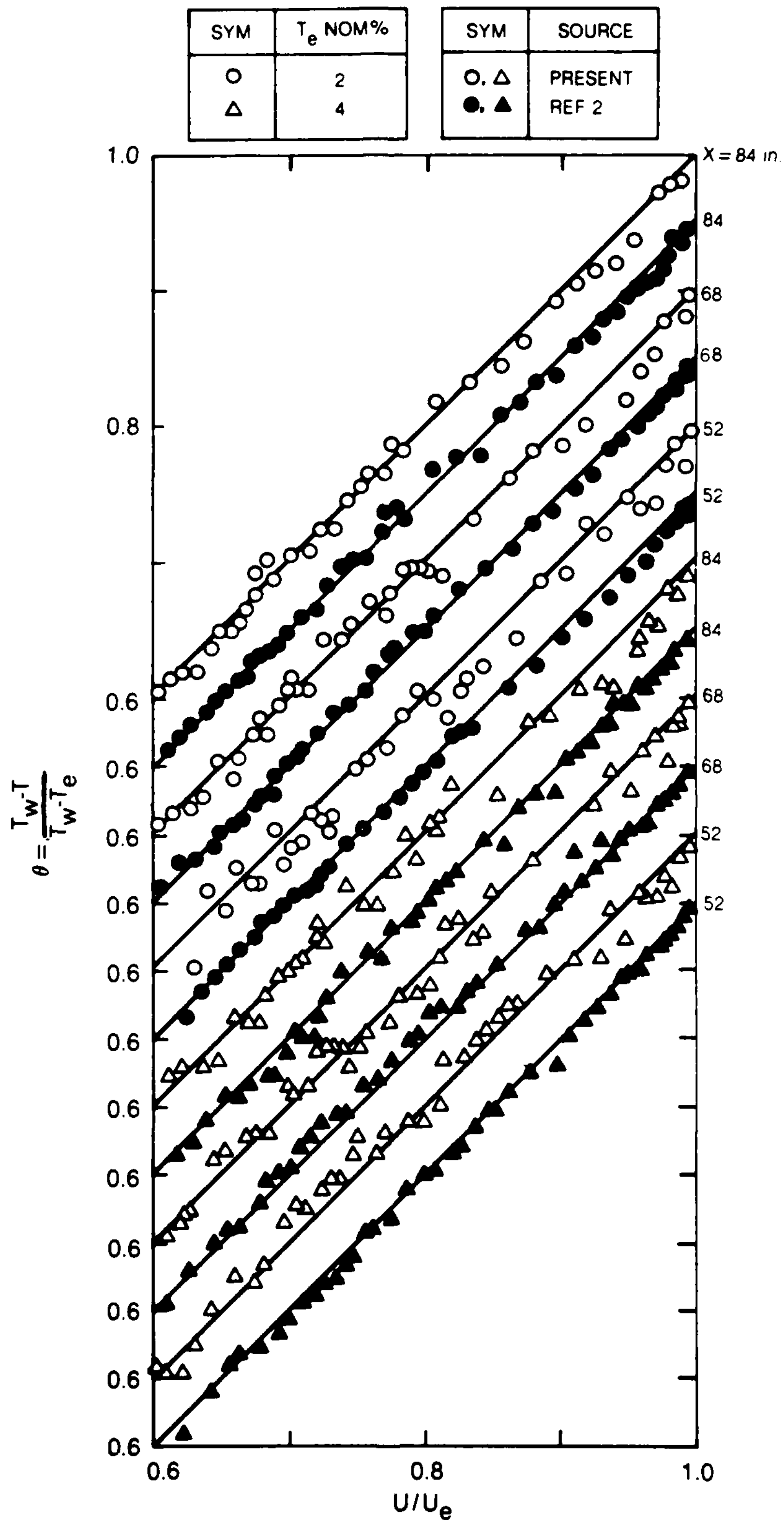

Figure 12. Mean Velocity and Temperature Profiles for Various Free-Stream Turbulence Levels

82-10-71-1

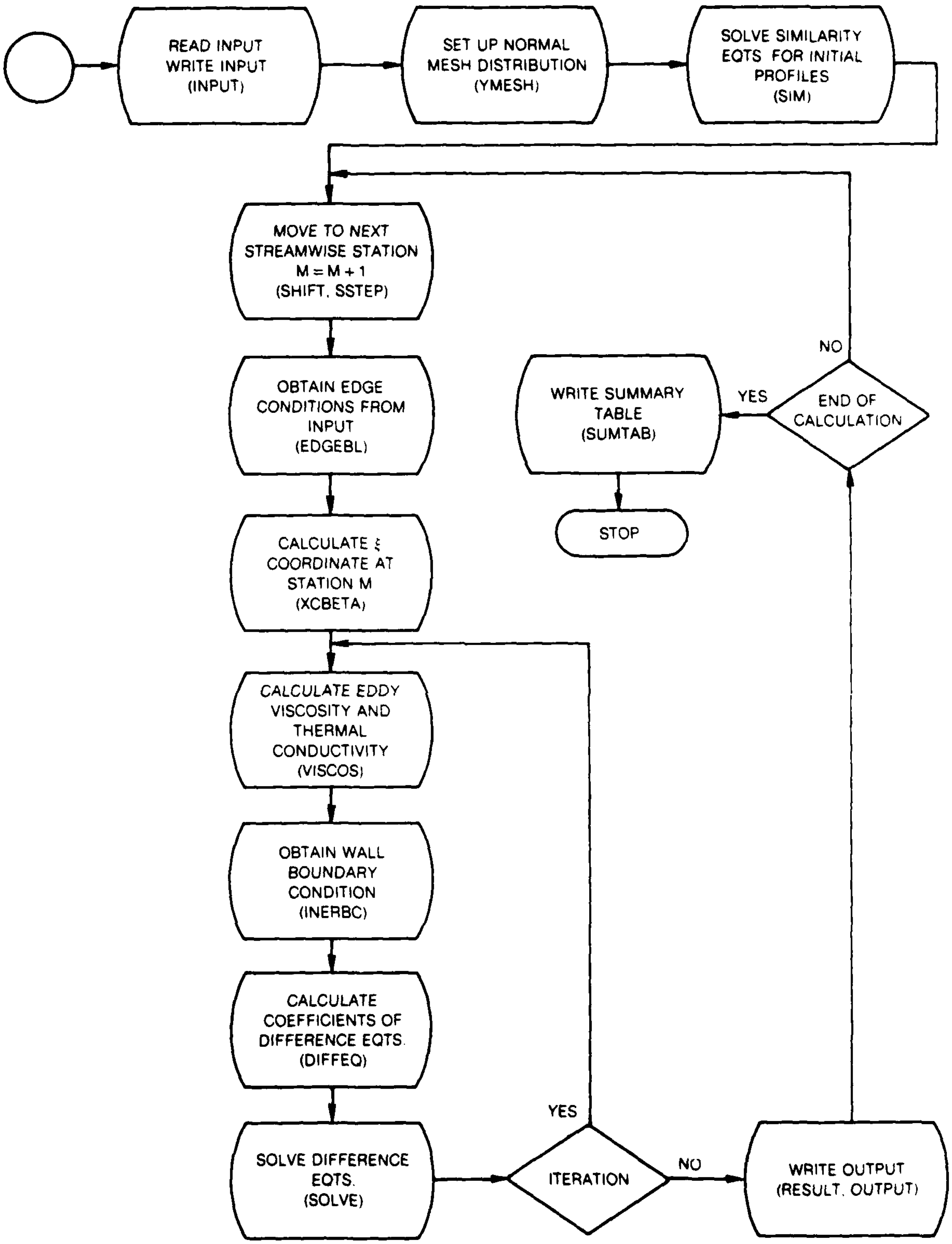

Figure 13. Flow Chart for ABLE Code - Module MAIN

82-11-79-2

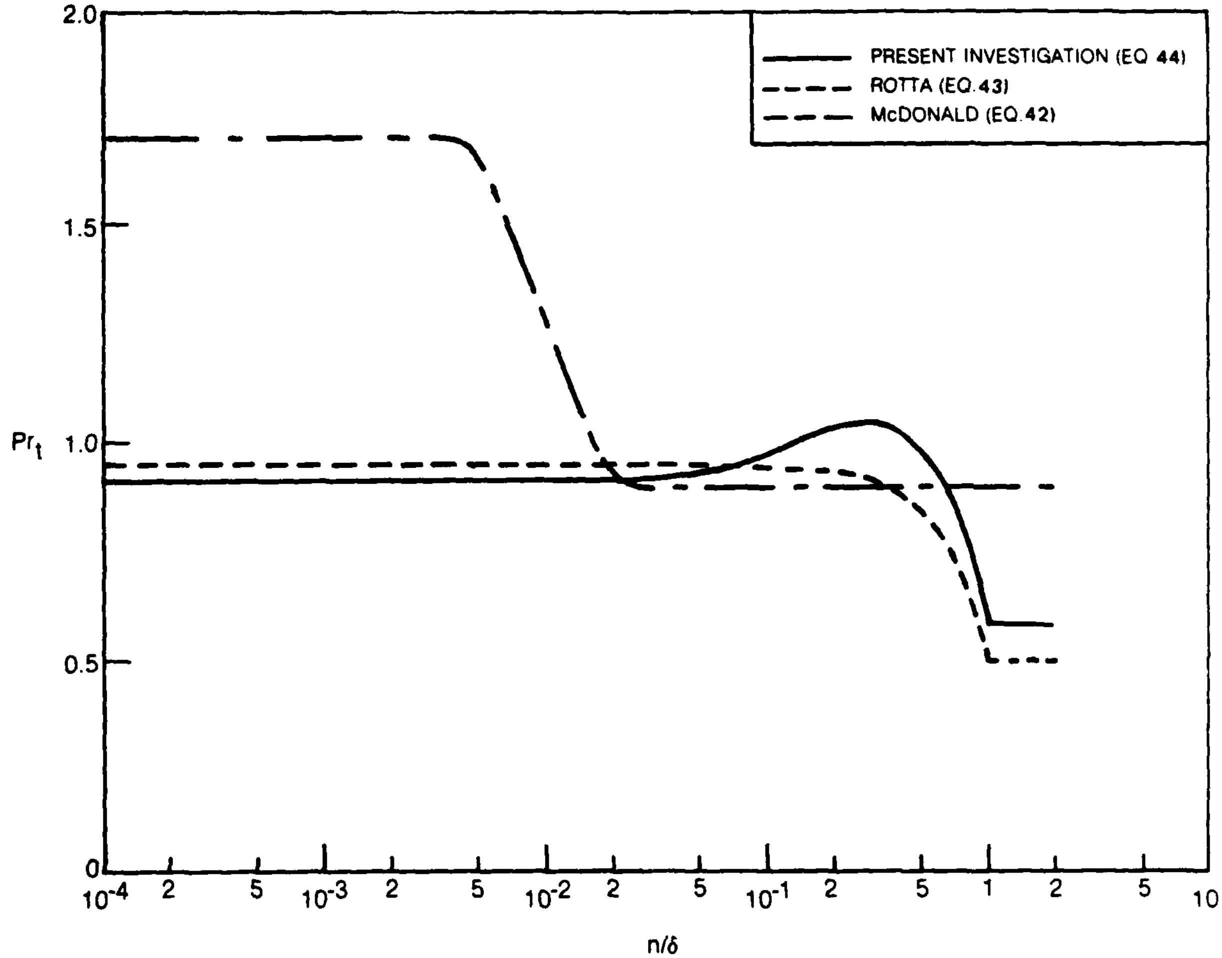

Figure 14. Comparison of Turbulent Prandtl Number Distributions for Flow with 2% Freestream Turbulence

82-11-79-22

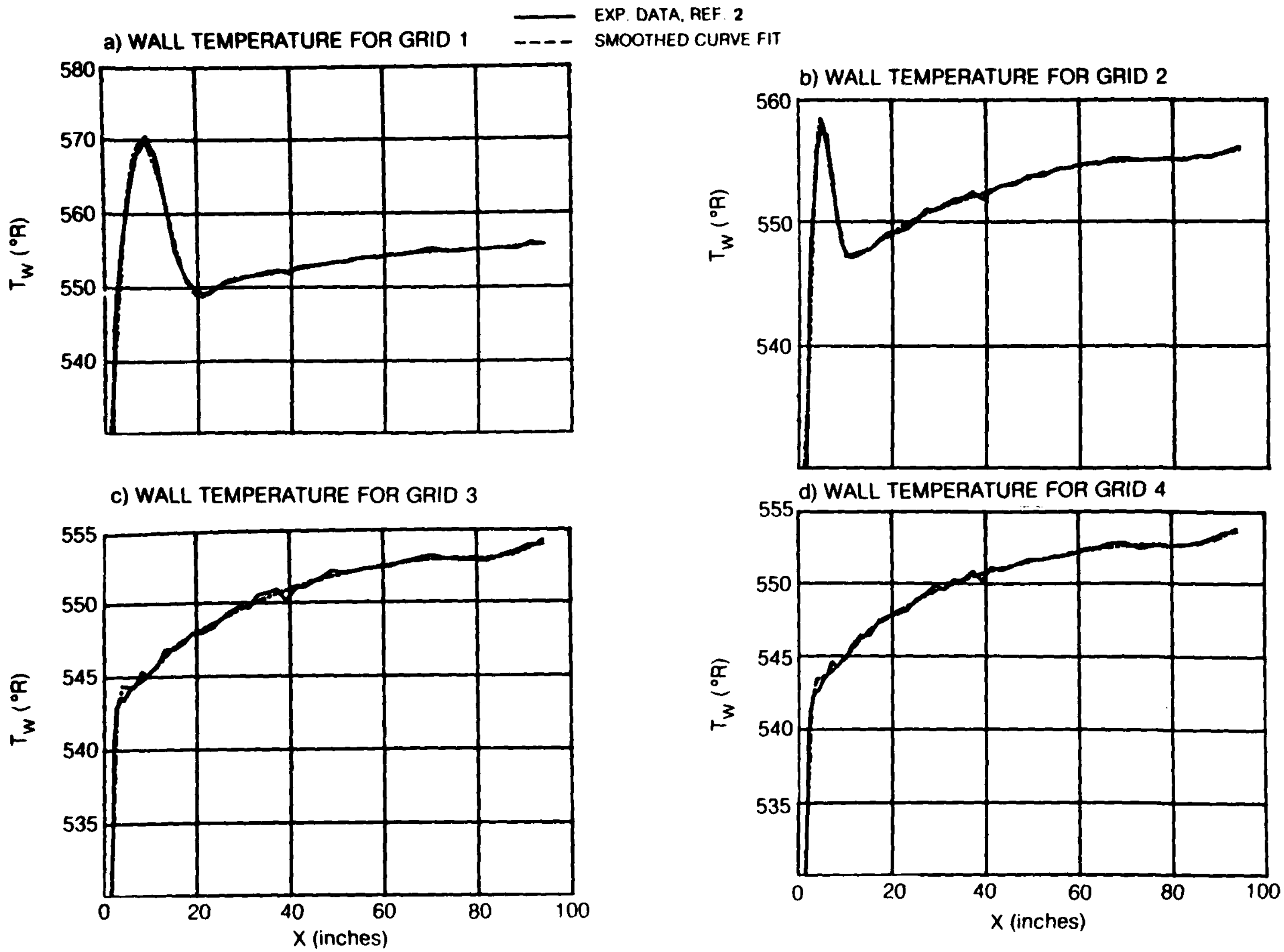

Figure 15. *Numerically Smoothed* Experimental Wall Temperature Distribution

82-11-79-3

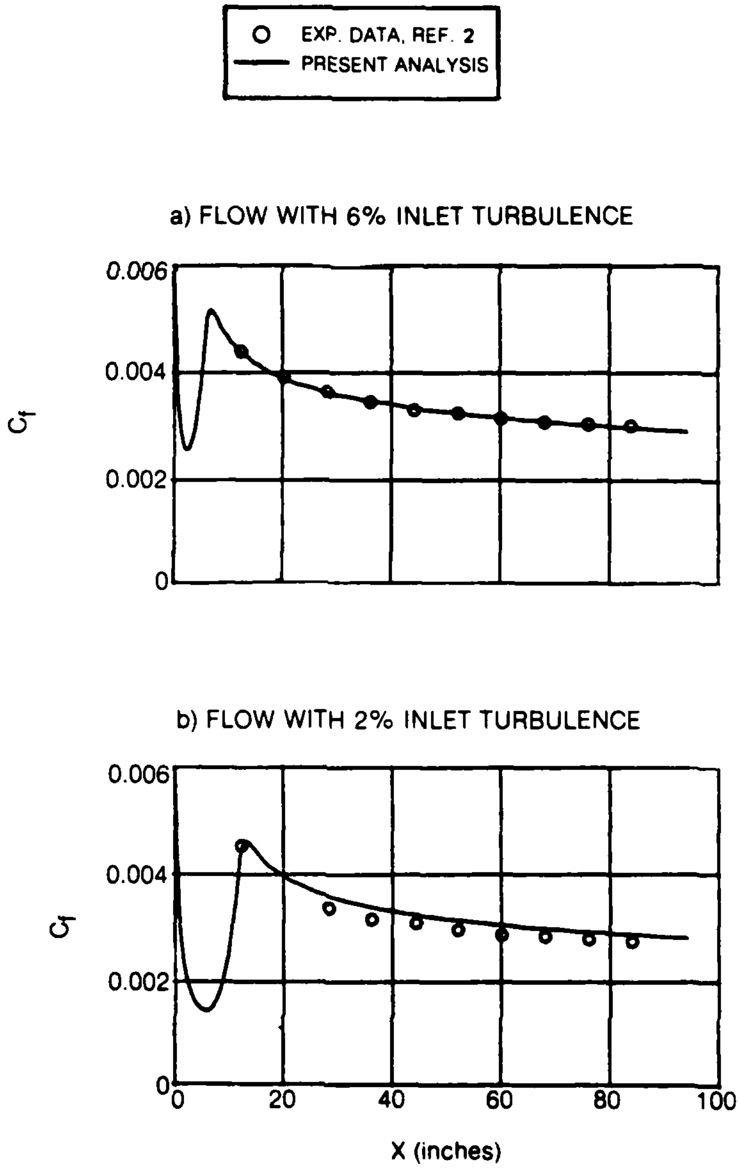

Figure 16. Comparison of Theoretical Skin Friction with Experimental Data for Different Inlet Turbulence Levels

82-11-79-4

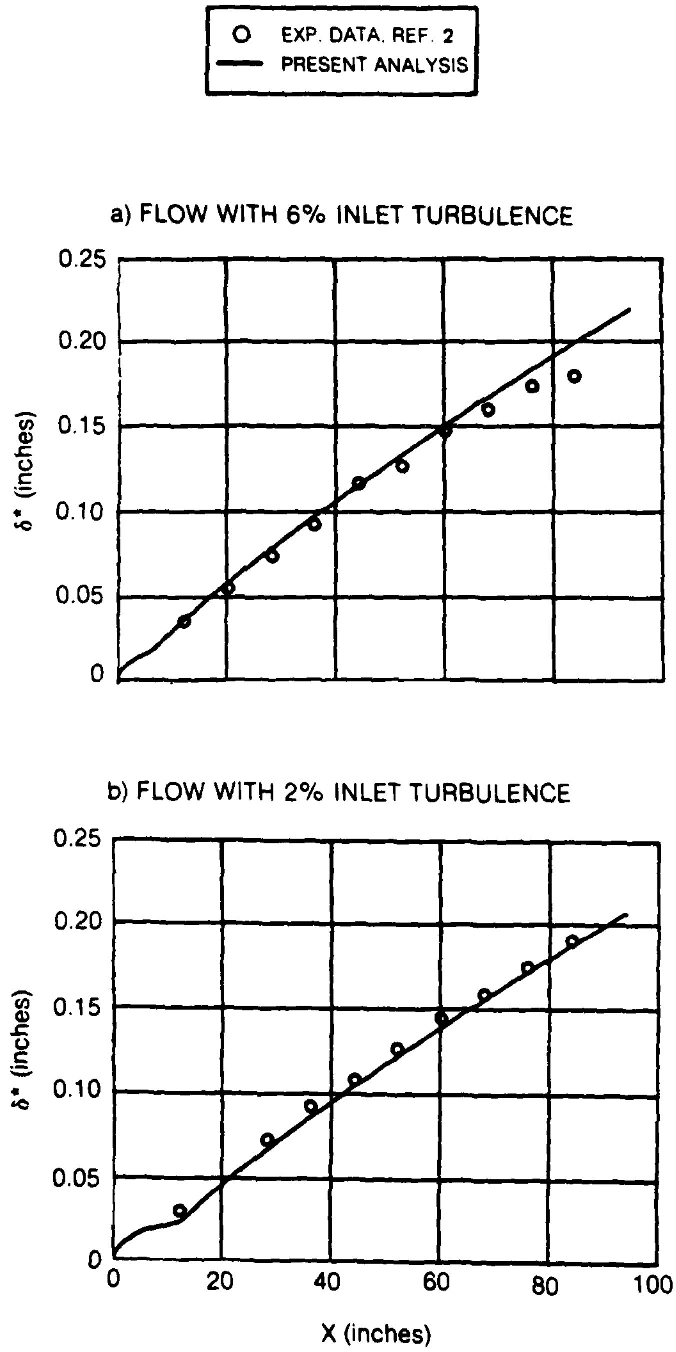

Figure 17. Comparison of Theoretical Displacement Thickness with Experimental Data for Different Inlet Turbulence Levels

82-11-79-5

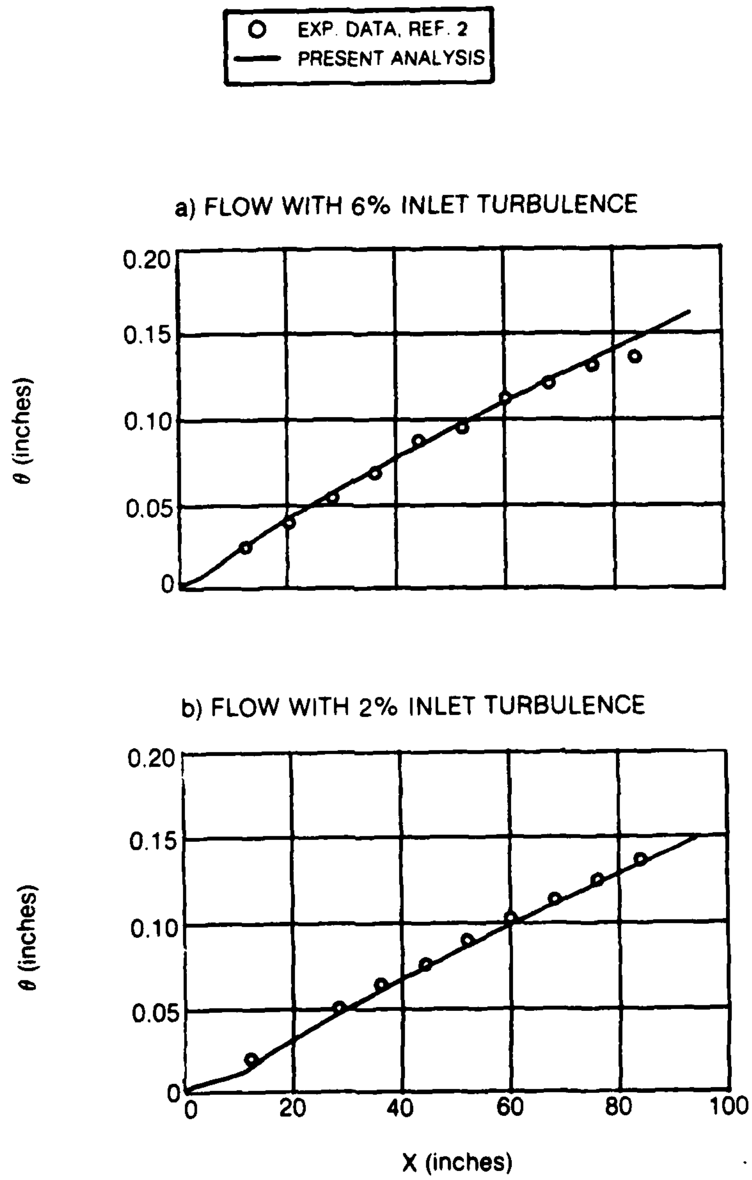

Figure 18. Comparison of Theoretical Momentum Thickness with Experimental Data for Different Inlet Turbulence Levels

82-11-79-6

INLET TURBULENCE	δ (inches)	
6%	1.256	□ EXP. DATA, REF. 2
2%	1.055	—— PRESENT ANALYSIS

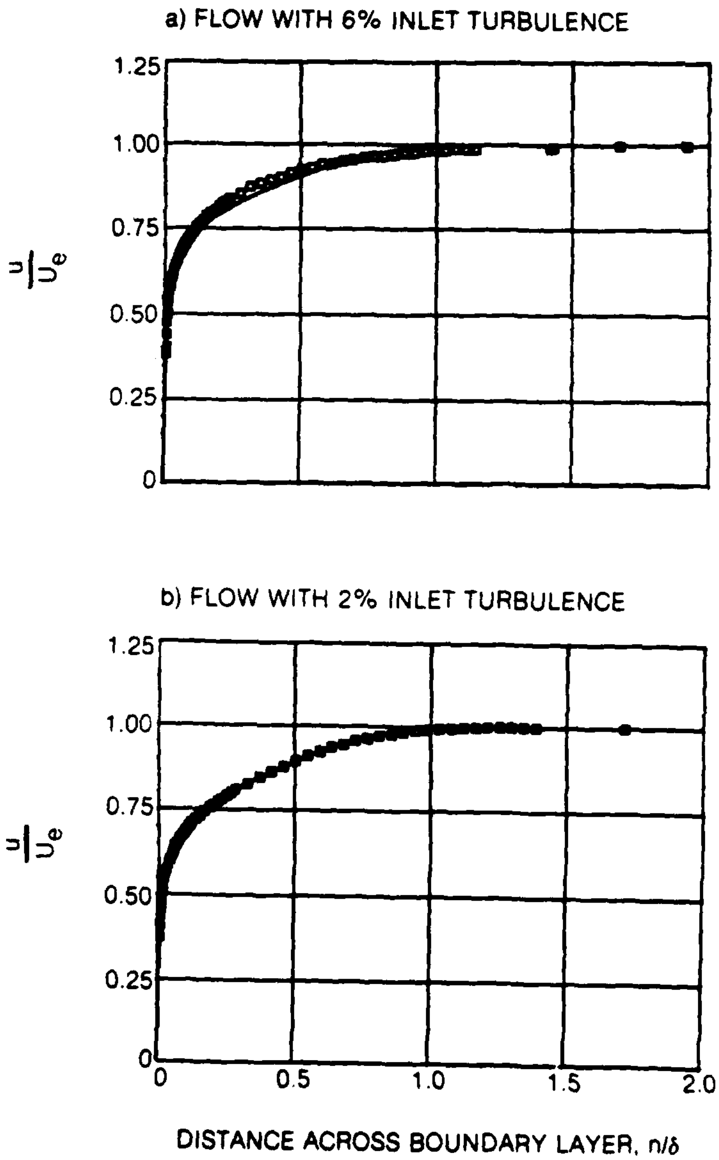

Figure 19. Comparison of Theoretical Mean Velocity With Experimental Data at X = 68 inches for Different Inlet Turbulence Levels

82-11-79-7

INLET TURBULENCE	δ (inches)	
6%	1.256	□ EXP. DATA, REF. 2
2%	1.055	—— PRESENT ANALYSIS

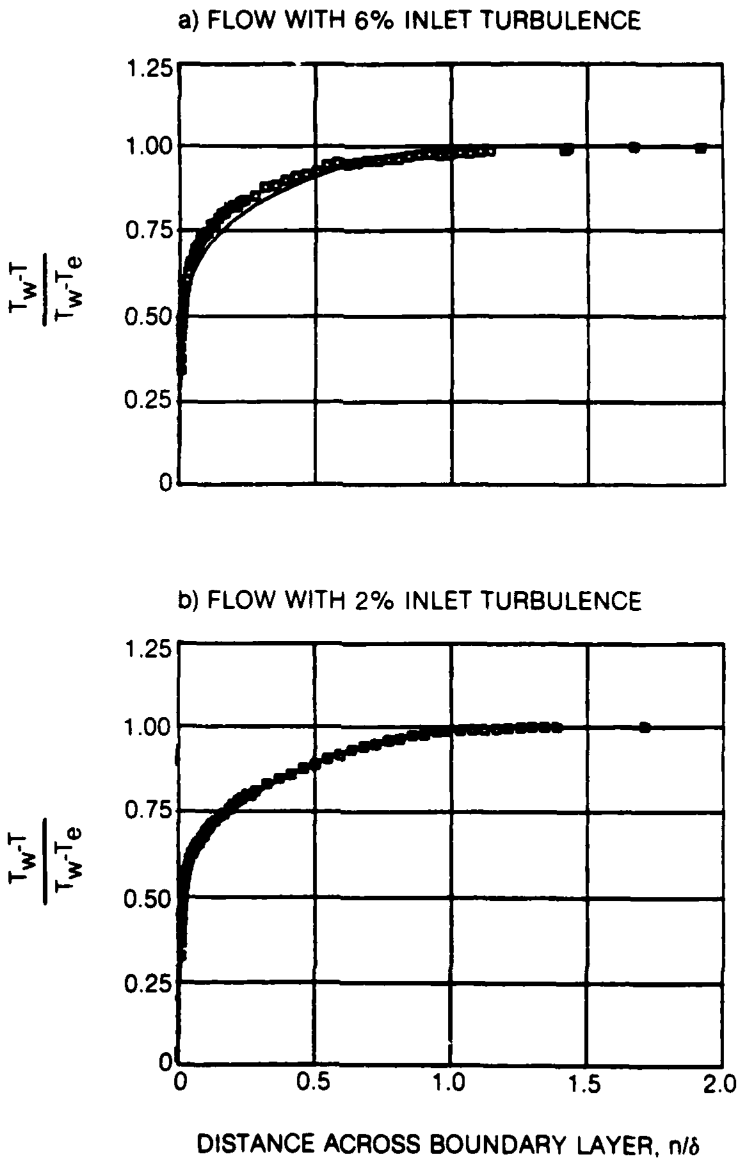

Figure 20. Comparison of Theoretical Mean Temperature with Experimental Data at X = 68 inches for Different Inlet Turbulence Levels

82-11-79-8

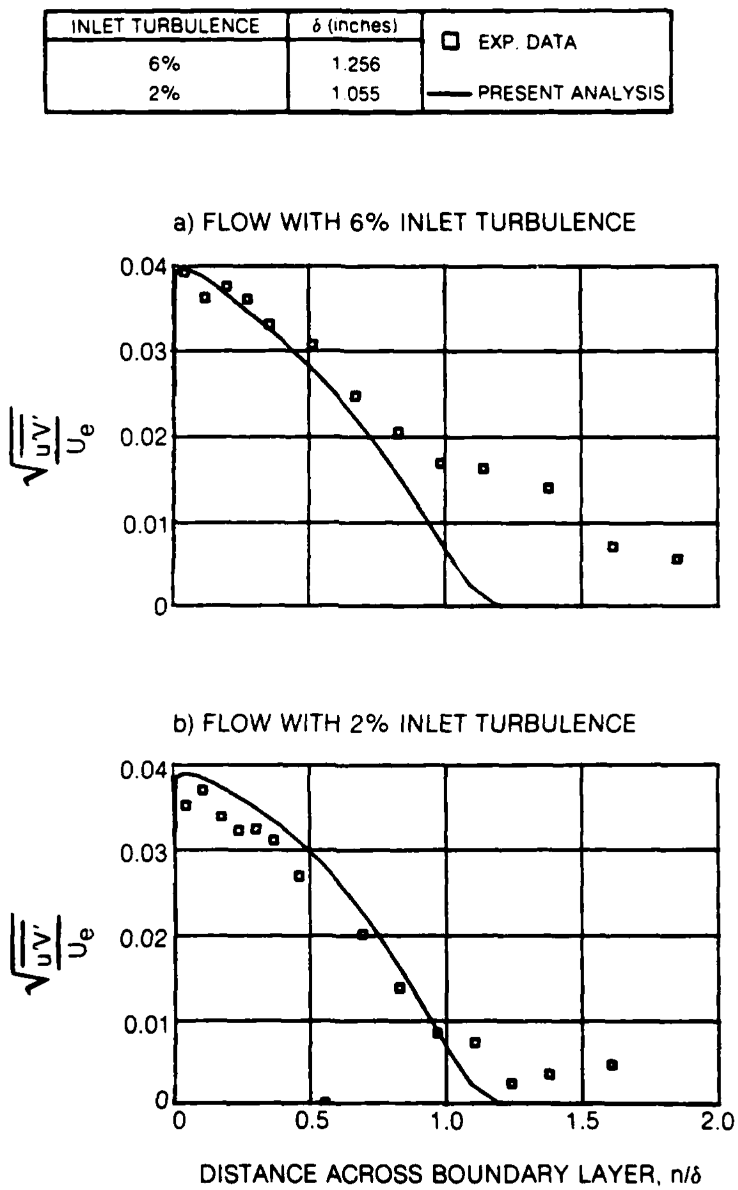

Figure 21. Comparison of Theoretical Reynolds Shear Stress with Experimental Data at X = 68 inches for Different Inlet Turbulence Levels

82-11-79-9

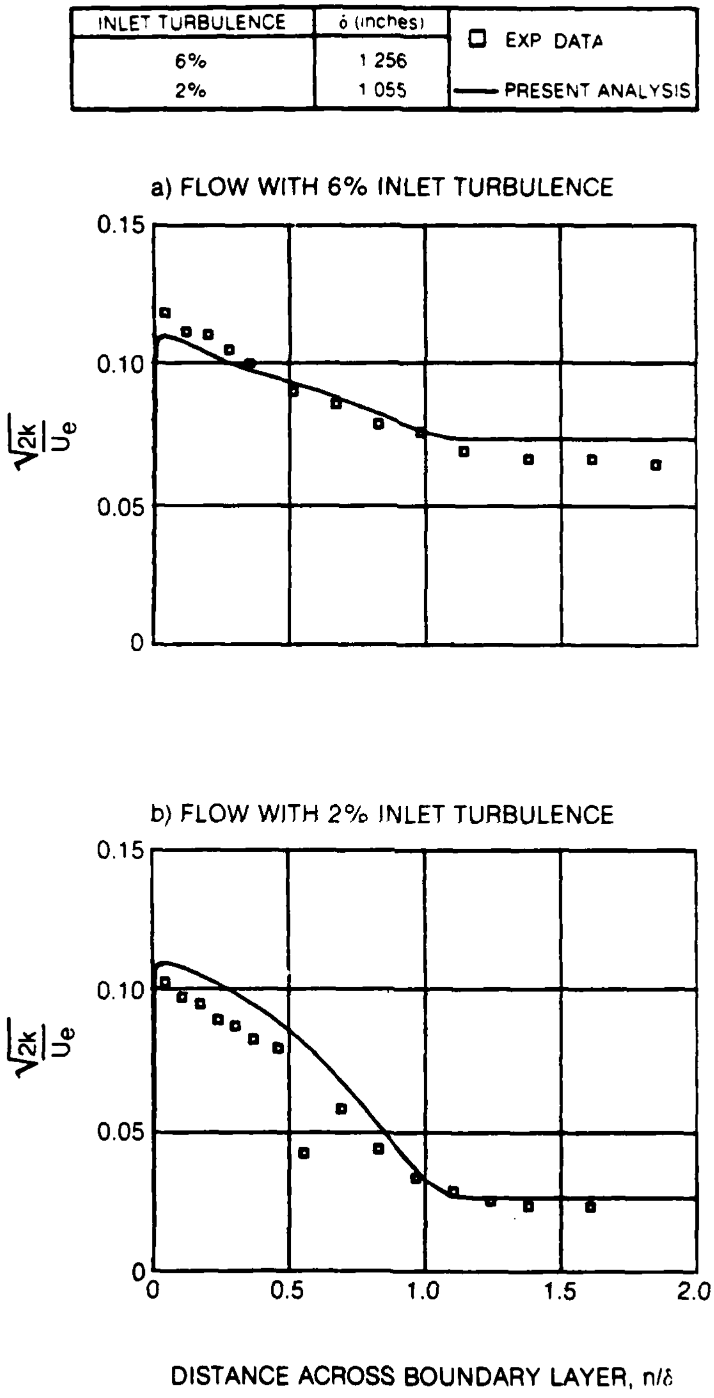

Figure 22. Comparison of Theoretical Turbulent Kinetic Energy with Experimental Data at X = 68 inches for Different Inlet Turbulence Levels

82-11-79-10

INLET TURBULENCE	δ (inches)	
6%	1 256	□ EXP. DATA
2%	1 055	—— PRESENT ANALYSIS

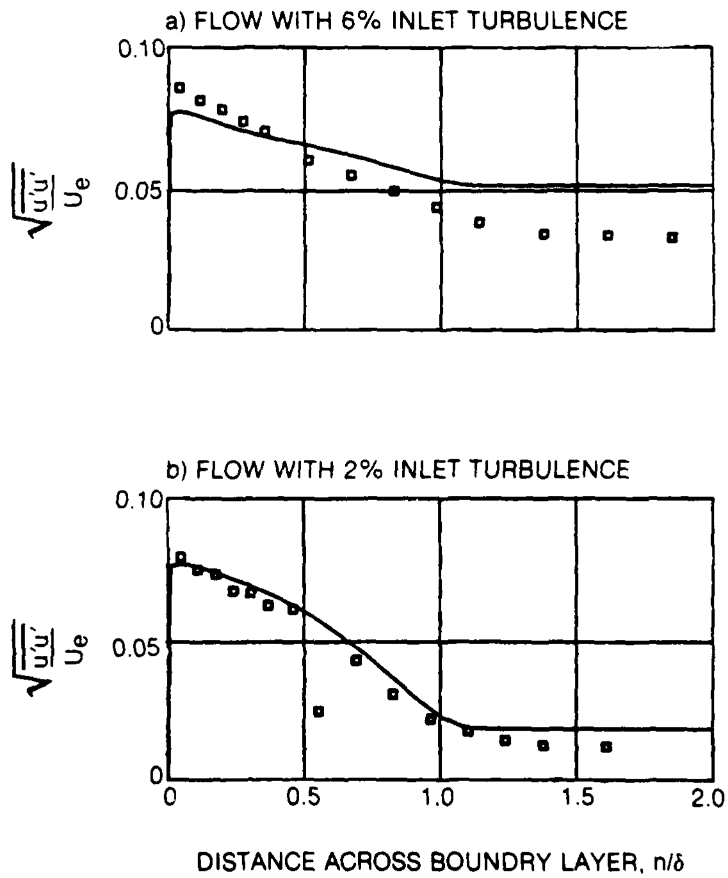

Figure 23. Comparison of Theoretical Component of Turbulent Intensity, $\overline{u'v'}$, with Experimental Data at X = 68 inches for Different Inlet Turbulence Levels

INLET TURBULENCE	δ (inches)	
6%	1 256	□ EXP. DATA
2%	1 055	—— PRESENT ANALYSIS

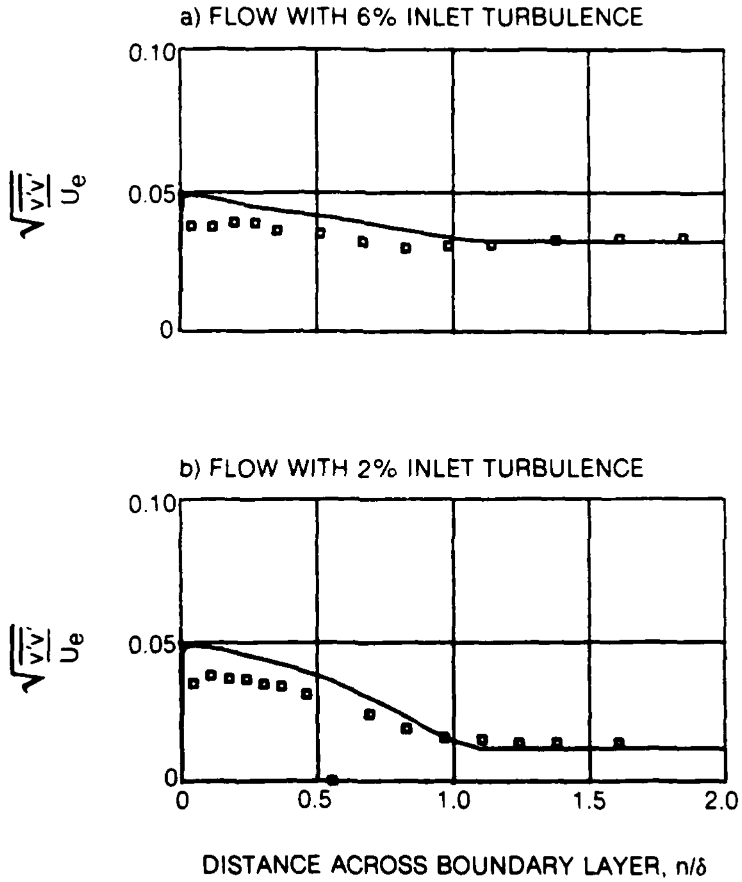

Figure 24. Comparison of Theoretical Component of Turbulent Intensity, $\overline{v'v'}$, with Experimental Data at X = 68 inches for Different Inlet Turbulence Levels

82-11-79-12

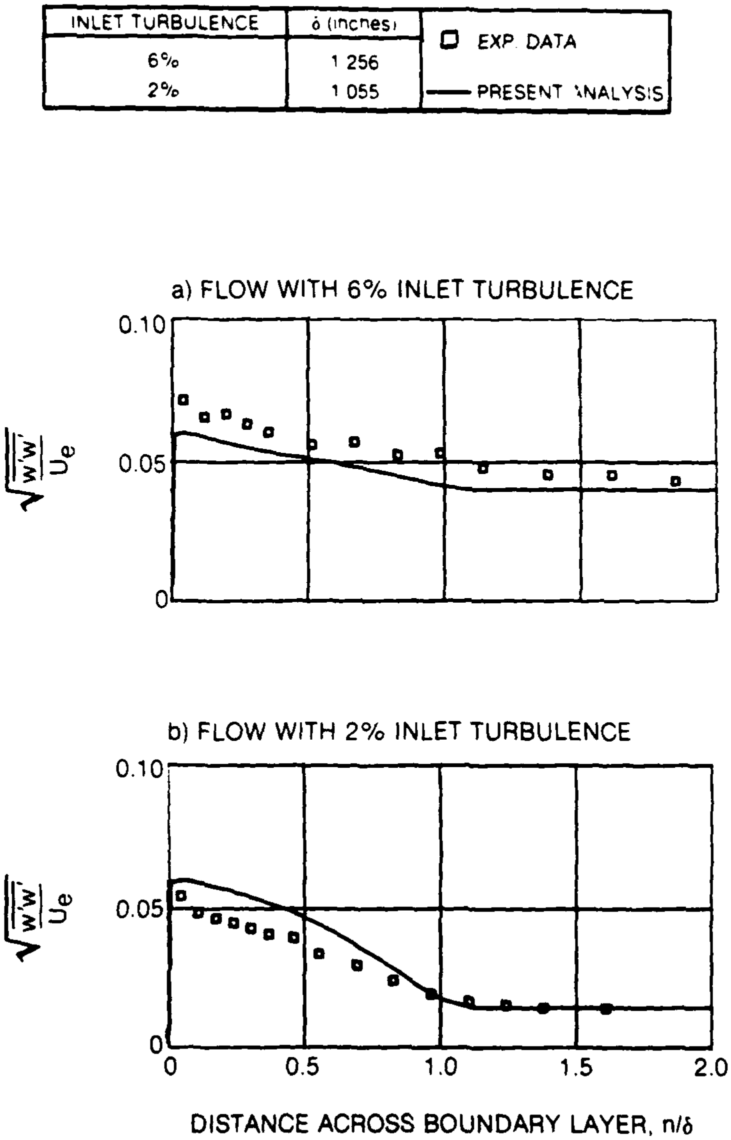

Figure 25. Comparison of Theoretical Component of Turbulent Intensity, $\overline{w'w'}$, with Experimental Data at X = 68 inches for Different Turbulence Levels

82-11-79-13

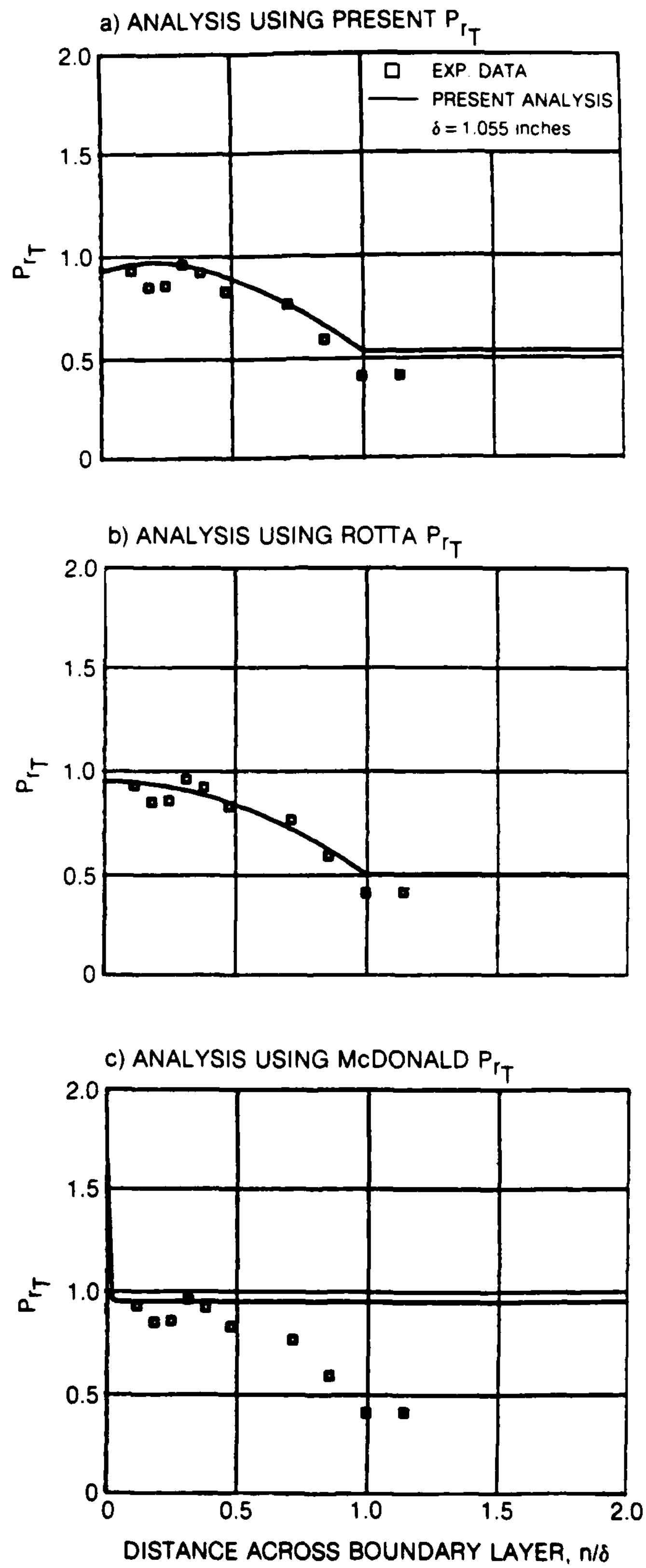

Figure 26a. Comparison of Theoretical Turbulent Prandtl Number with Experimental Data at X = 68 inches for 2% Inlet Turbulence Level

82-11-79-14

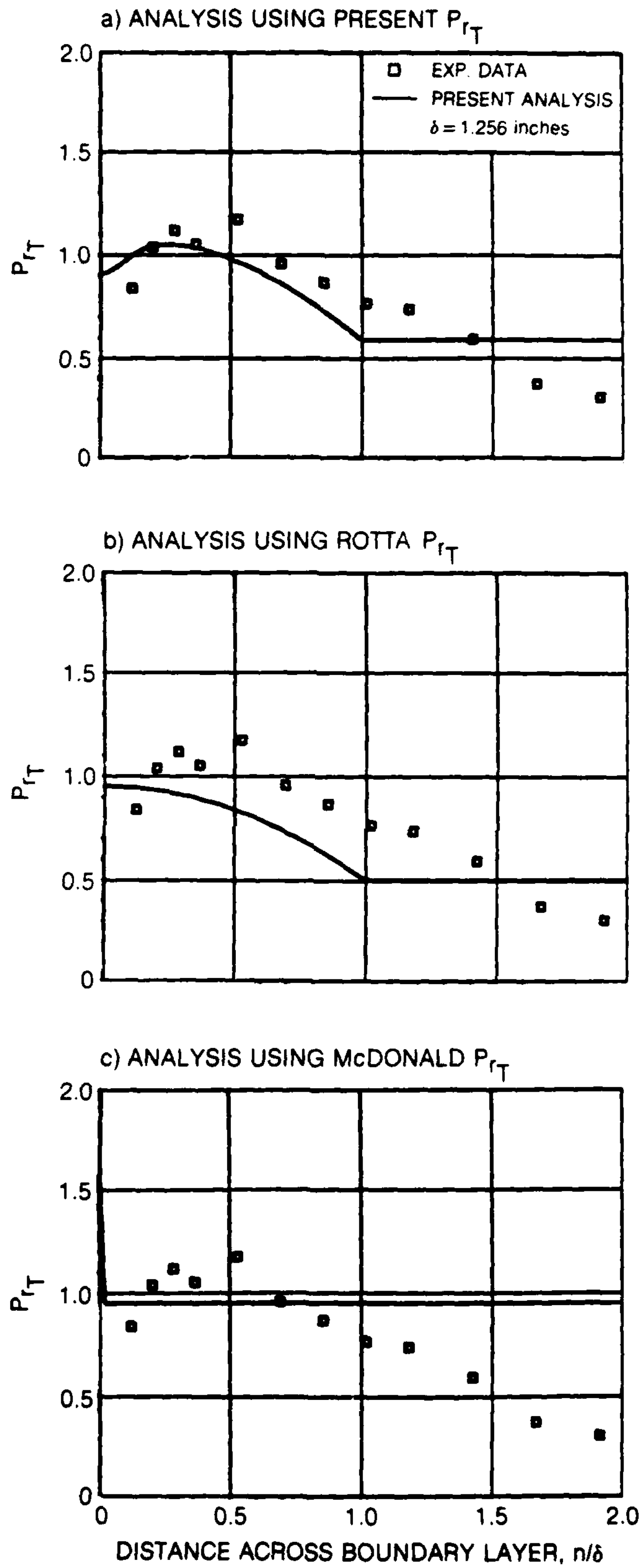

Figure 26b. Comparison of Theoretical Turbulent Prandtl Number with Experimental Data at X = 68 inches for 6% Inlet Turbulence Level

82-11-79-15

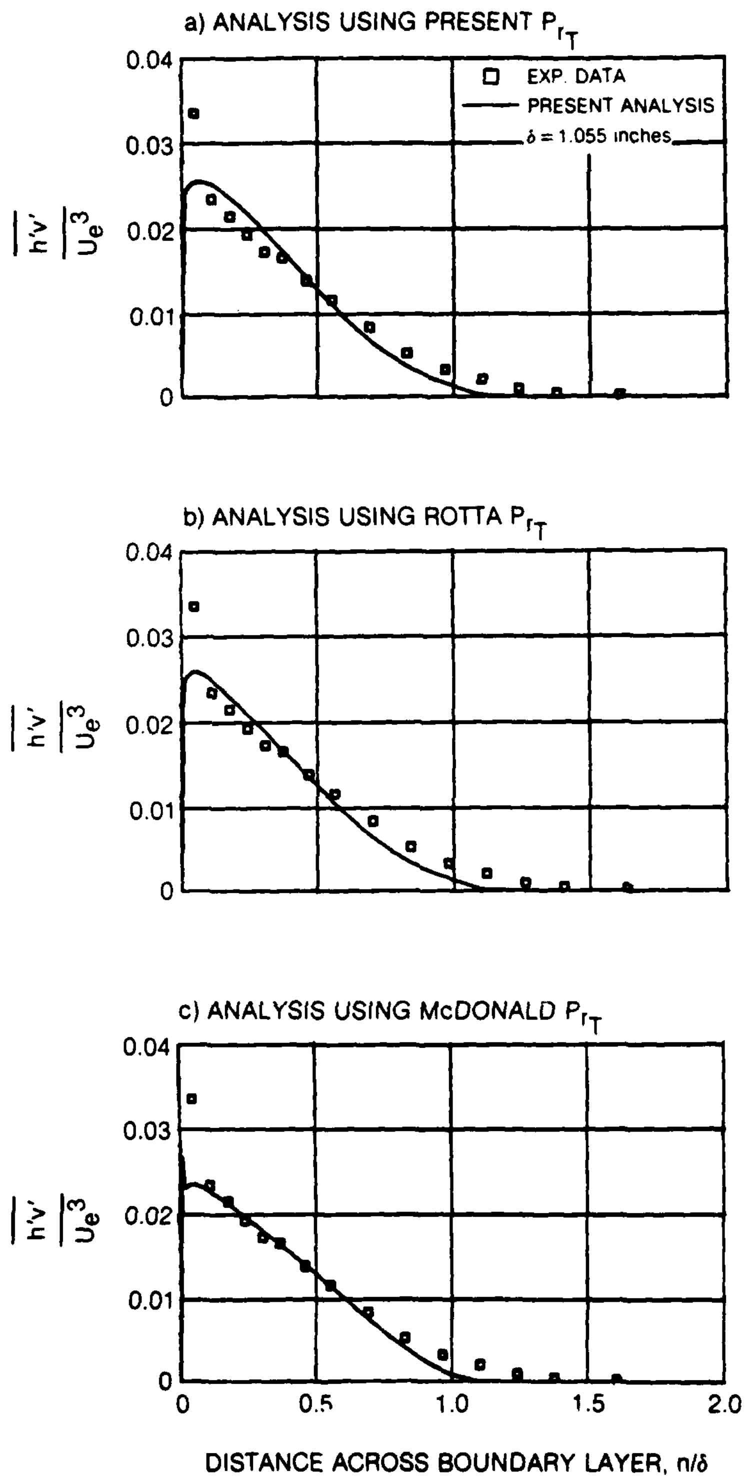

Figure 27a. Comparison of Theoretical Thermal Heat Flux with Experimental Data at X = 68 inches for a 2% Inlet Turbulence Level

82-11-79-16

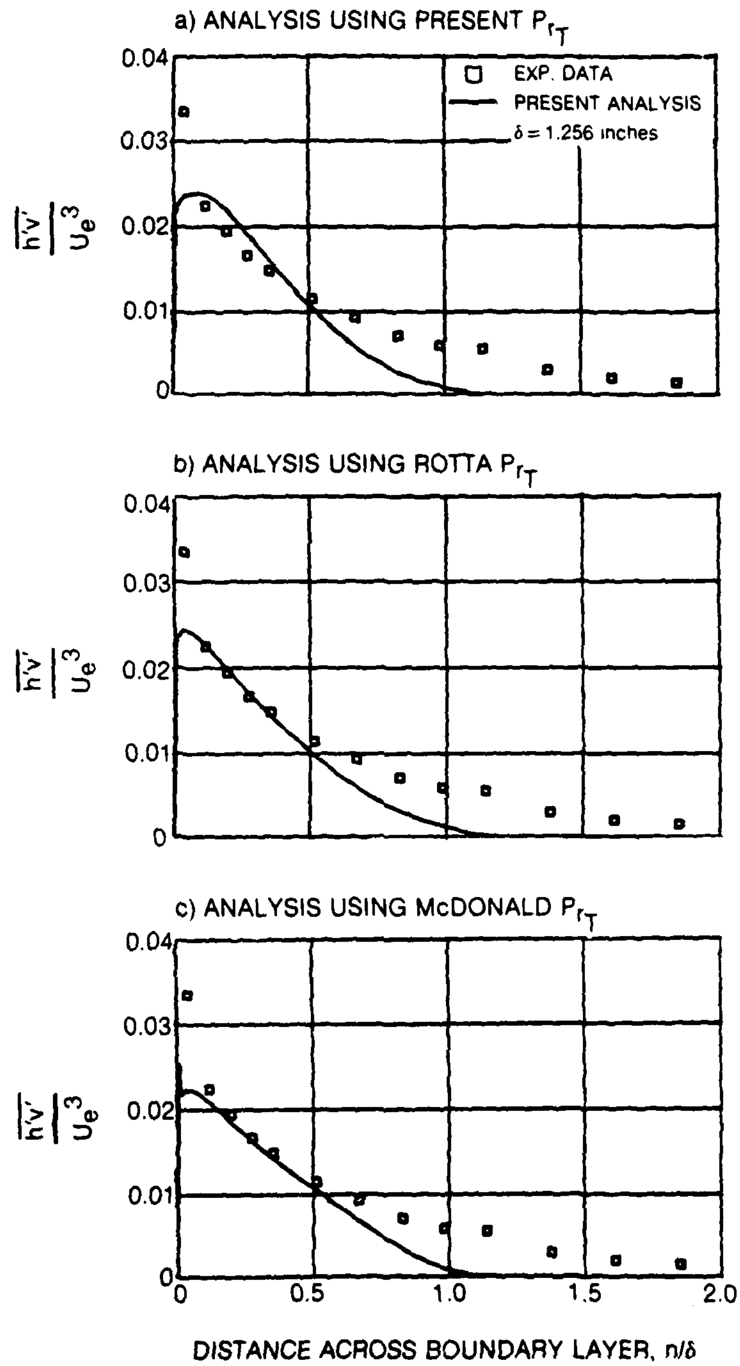

Figure 27b. Comparison of Theoretical Thermal Heat Flux with Experimental Data at X = 68 inches for a 6% Inlet Turbulence Level

82-11-79-17

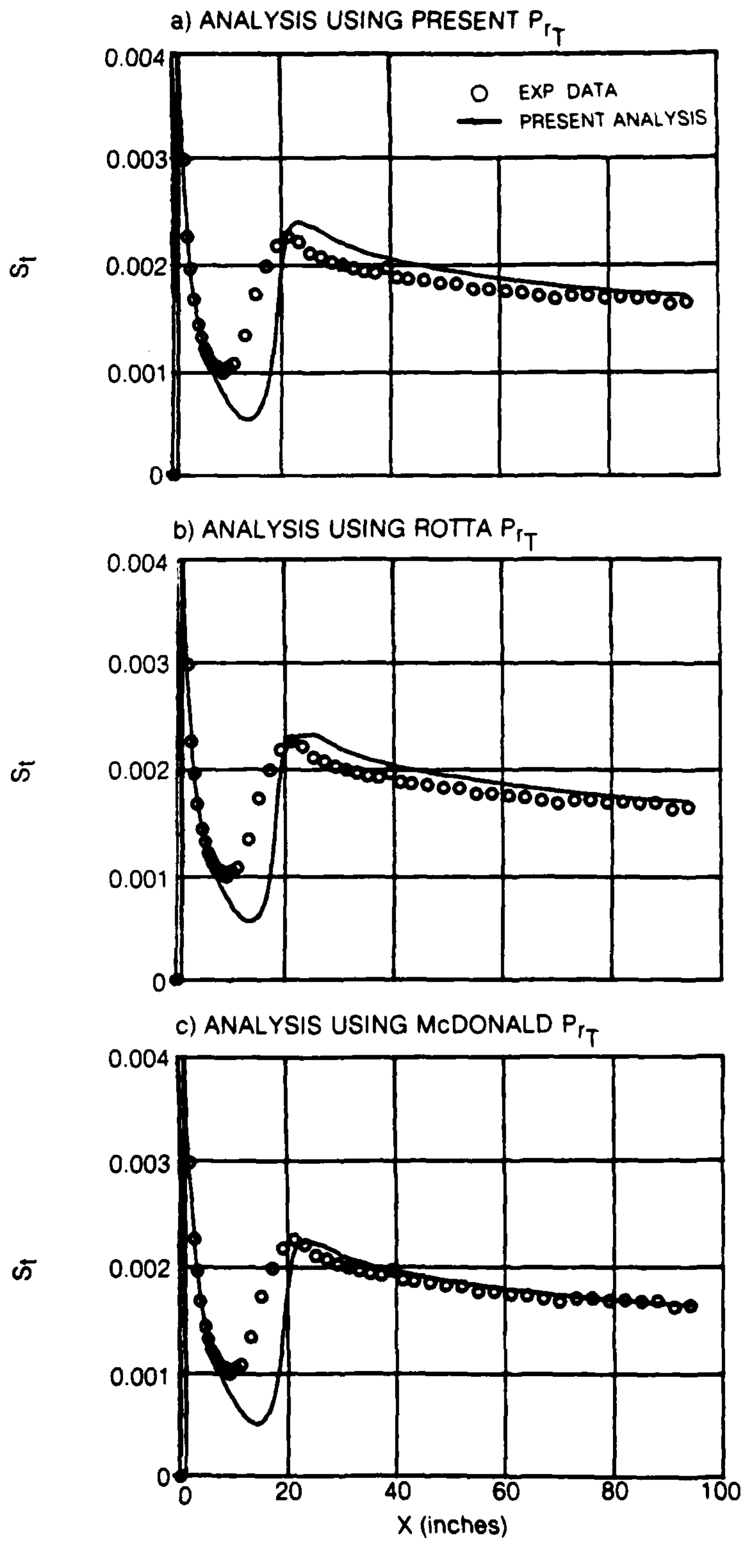

Figure 28a. Comparison of Theoretical Stanton Number with Experimental Data for 1% Inlet Turbulence Level

82-11-79-18

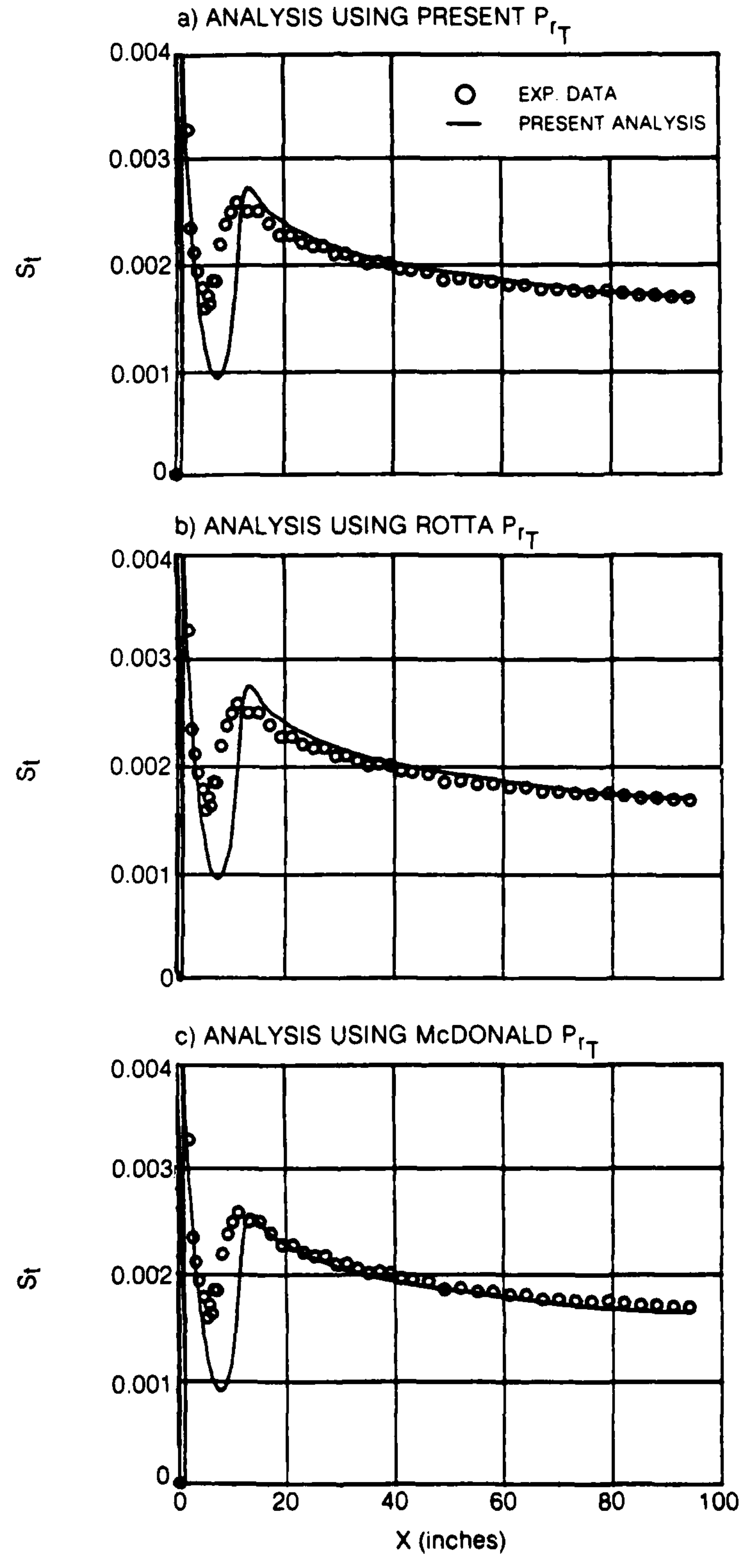

Figure 28b. Comparison of Theoretical Stanton Number with Experimental Data for 2% Inlet Turbulence Level

82-11-79-19

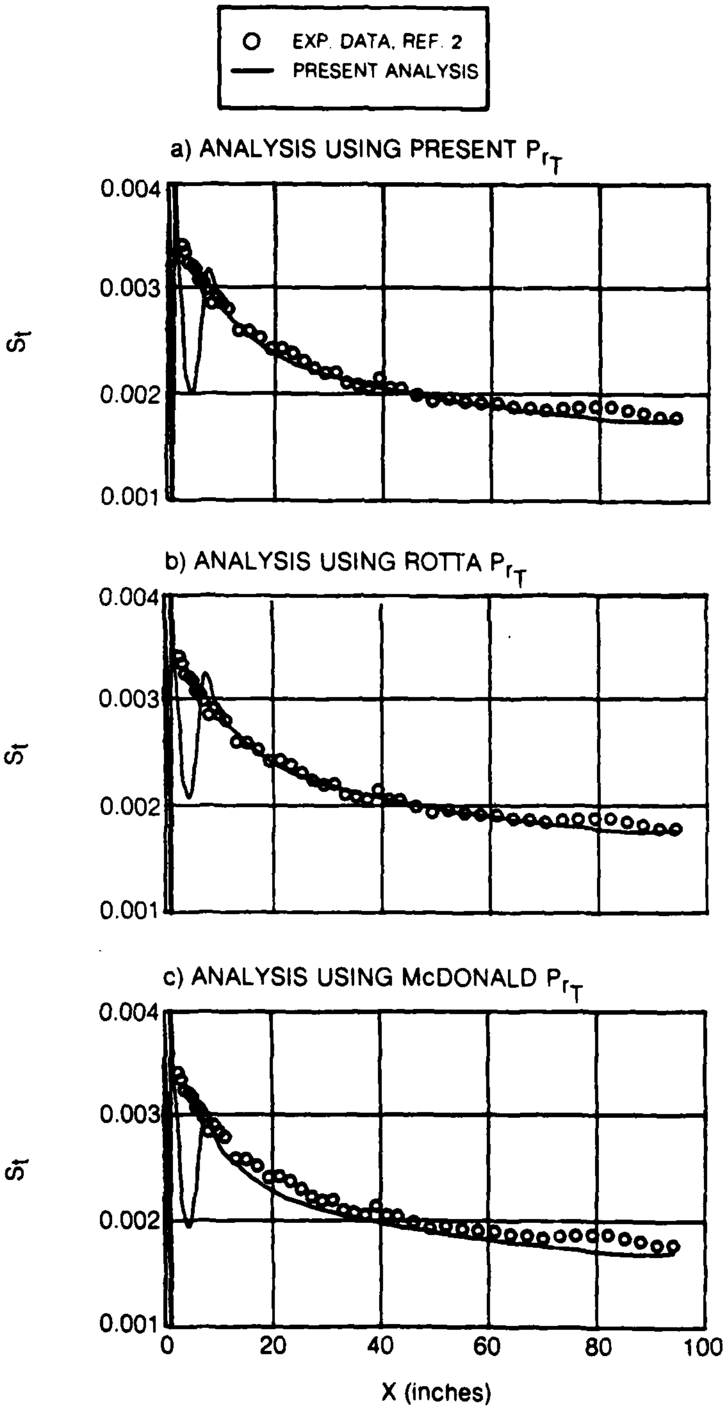

Figure 28c. Comparison of Theoretical Stanton Number with Experimental Data for 4% Inlet Turbulence Level

82-11-79-20

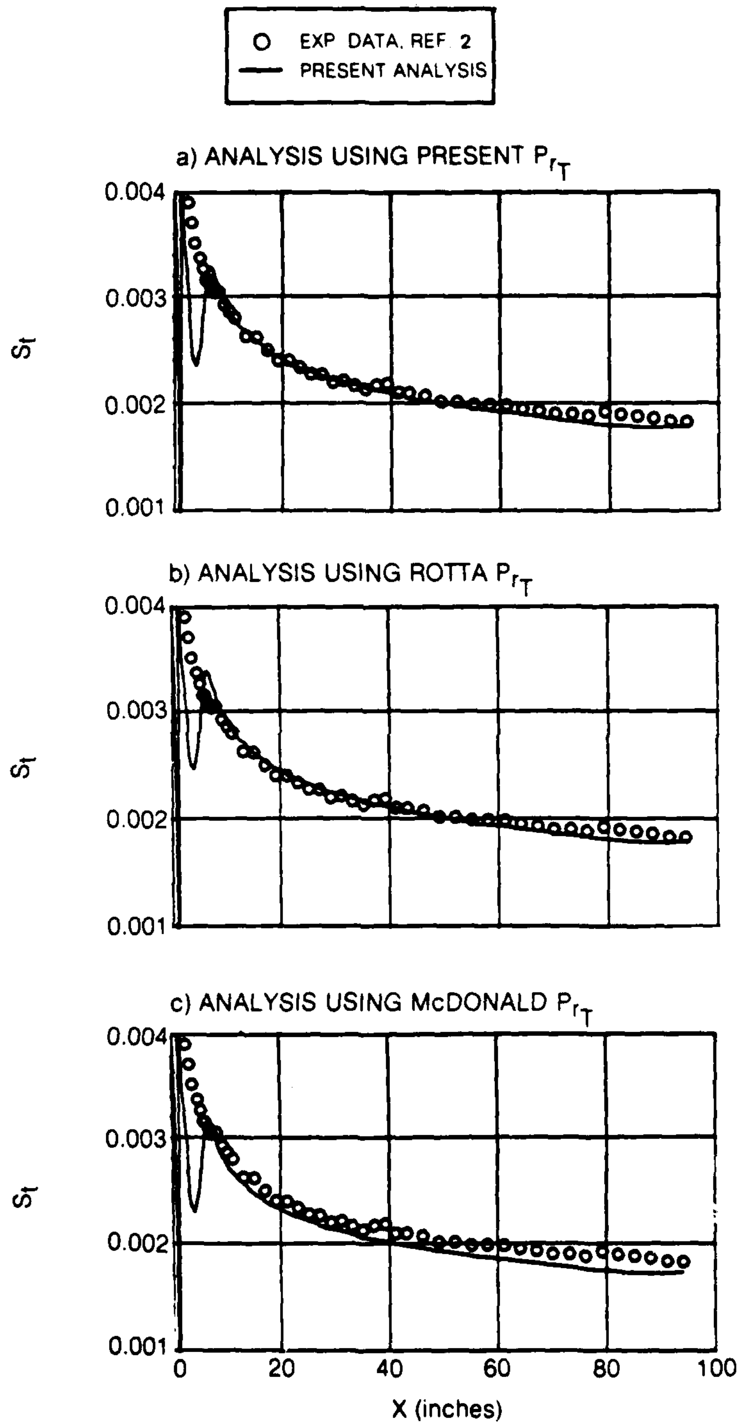

Figure 28d. Comparison of Theoretical Stanton Number with Experimental Data for 6% Inlet Turbulence Level

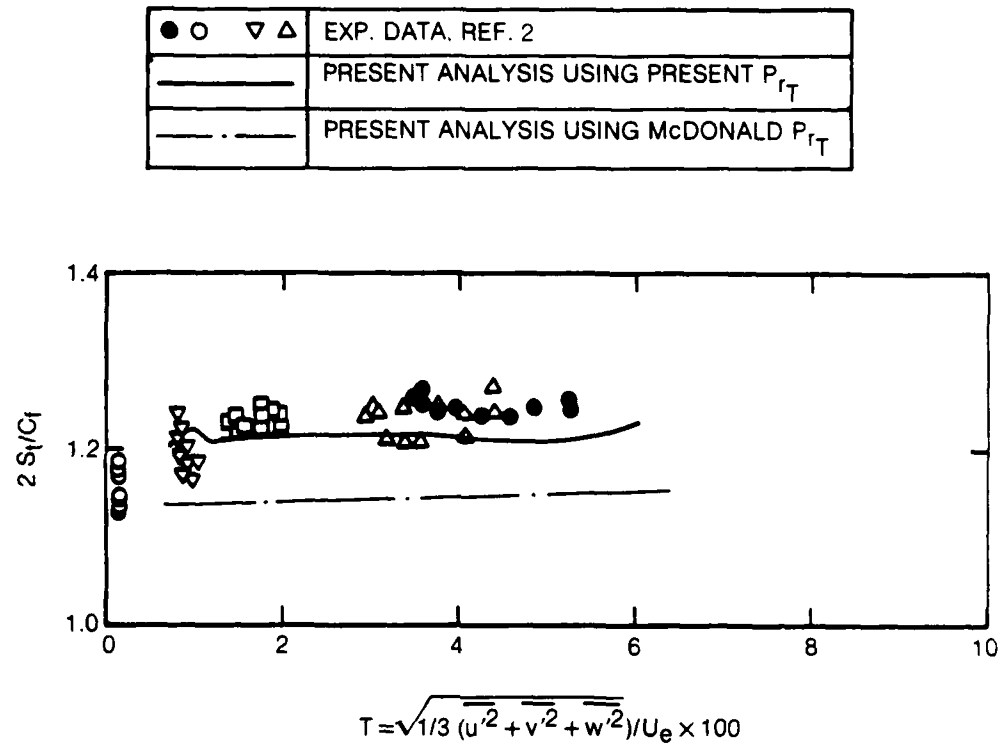

Figure 29. Theoretical Prediction of Reynolds Analogy Factor - Varying Edge Turbulence Levels

82-11-79-1

APPENDIX A - ERROR ANALYSIS

In this program mean velocity (U) profiles were determined by means of Pitot, single wire, x wire and 3 sensor hot wire probes. Mean temperatures (T) were measured by both 3 sensor hot wire and thermocouple probes. Fluctuating velocities and Reynolds stress distributions (u', v', w', $\overline{u'v'}$) were determined both with x wire and 3 wire techniques.

Assessment of absolute errors for the analog signals measured in this program would be a relatively straightforward matter. For example, the possible errors in measured pressures from the pitot probes or the recorded, digitized voltages from the hot-wire anemometer can be computed from the individual expected uncertainties. Computation of the absolute errors of the measured physical quantities (e.g., u', v', t'), however, is practically impossible because the true accuracy of factors such as Pitot probe wall proximity corrections, Pitot probe turbulence corrections, hot wire wall radiation effects, high turbulence sensor cross-talk, etc. are unknown. For this reason the uncertainties for the various quantities measured for this program will be assessed by (1) comparing the measured quantities with independently determined or computed results or (2) comparisons of like quantities measured using different probes and instrumentation techniques.

Mean velocity and temperature profile data obtained with different measurement techniques (four techniques for velocity, two techniques for temperature) are presented in Fig. A-1. These profile data were all obtained at X = 84 inches at three levels of free-stream turbulence. In-depth descriptions of the Pitot and thermocouple probes and data systems used for the mean velocity and temperature profiles are provided in Ref. 2. These probes were designed and constructed specifically for these types of boundary layer flows and a number of well established near-wall correction terms (see Ref. 2) were applied to the data. In addition, a number of comparison checks (see Refs. 1 and 2) showed that these mean profile data were very accurate. For these reasons the mean velocity profiles from the Pitot probe and the mean temperature profiles from the thermocouple probe were selected as the "true" respective profiles. For the data of Fig. A-1 all the other velocity profile measurements were compared to the Pitot probe data while the triple sensor temperature data were compared to the temperature profiles from the thermocouple probe.

An examination of the mean velocity profile data of Fig. A-1 indicates that 85 percent of all the measurements fell within ± 3 percent of the "true" Pitot profile. Only one set of data, the vertical x probe results for Te = 0.2 percent, had any discrepancies larger than 5 percent. Discrepancies in the mean temperature profile measurements were slightly larger than those for the velocity measurements with only 70 percent of the measurements falling within ± 5 percent of the thermocouple probe profile. The 3 sensor probe temperature data also showed a clear bias to read slightly lower temperatures than the thermocouple probe. The relatively larger errors for the temperature profiles as compared to the velocity profiles is not surprising. Because of the relatively large size of the 3 sensor probes they span a gradient of both velocity and temperature in the boundary layer flow. The data reduction system

is forced to assume that a single effective velocity and flow temperature apply over the entire probe.

Plots of the average bias $\overline{(x_i-\bar{x})}$ and standard error $\sqrt{\overline{(x_i-\bar{x})^2}}$ (x_i is the measured quantity and $\bar{x}$ is the "true") quantity at a given profile location) for the various profiles are given in Fig. A-2. These results are plotted as a function of the ratio between the overall boundary layer thickness and the probe sensor height (h). The overall profile errors are plotted in Fig. A-2, were largest for the thinnest boundary layers (with the relatively steepest velocity and temperature gradients). In addition, the largest local bias errors of Fig. A-1 were located near the wall where the steepest gradients exist. This result has led to the conclusion that the local gradients across the sensor arrays were a significant cause of the discrepancies between the x-type probe mean data and the "true" profiles.

Distribtuions of the various measurements of the streamwise and vertical velocity fluctuations and the Reynolds stress distributions are given in Figs. A-3 and A-4. No "true" or best distributions of these quantities are known for these profiles and so the data at a given location in a profile were compared with the average of all the like data taken at that location. The plots of Figs. A-3 and A-4, then, show distributions of the inconsistencies between the various measurement techniques for the various profiles. The agreement between the separate measurements for u'/U_e and v'/U_e were generally very good ($\pm \approx 1/2$ percent for u'/U_e and $\pm \approx 1/5$ percent for v'/U_e). If the average levels of u'/U_e and v'/U_e are approximated as 0.06 and 0.04 respectively the above inconsistencies are equivalent to ± 8 percent and ± 5 percent uncertainties in the fluctuating velocities (u' and v') themselves. Note that for the u'/U_e plot of Fig. A-3 data were included for a "single horizontal wire". These particular data were obtained with an analog data system consisting of a polynomial linearizer and a true RMS voltmeter. All the other data of Fig. A-3 were obtained with the previously described analog-digital system. The consistency between the measurements for these two very different techniques is excellent. The largest inconsistencies were observed for the Reynolds stress distributions of Fig. A-4. This is not at all surprising as it is far more difficult to measure correlated than single fluctuating quantities. For these Reynolds stress data a ± 15 percent inconsistency band encompasses nearly all the measurements.

Plots of the average "bias" and "standard error" for the fluctuating quantities of Fig. II-3 and II-4 are presented in Fig. A-5. The overall profile errors for the stress measurements were clearly much larger than the errors for the individual velocity fluctuations. Unlike the mean profile results of Fig. A-2 the uncertainties of the fluctuating quantities for the various boundary layer thicknesses were nearly constant.

TYPE PROBE	SINGLE HORIZ	TRI-X	X-H	X-V
SYMBOL	○	□	▽	△

T_e %	0 2	1 4	3 9
SYMBOLS	OPEN	HALF FILLED	SOLID

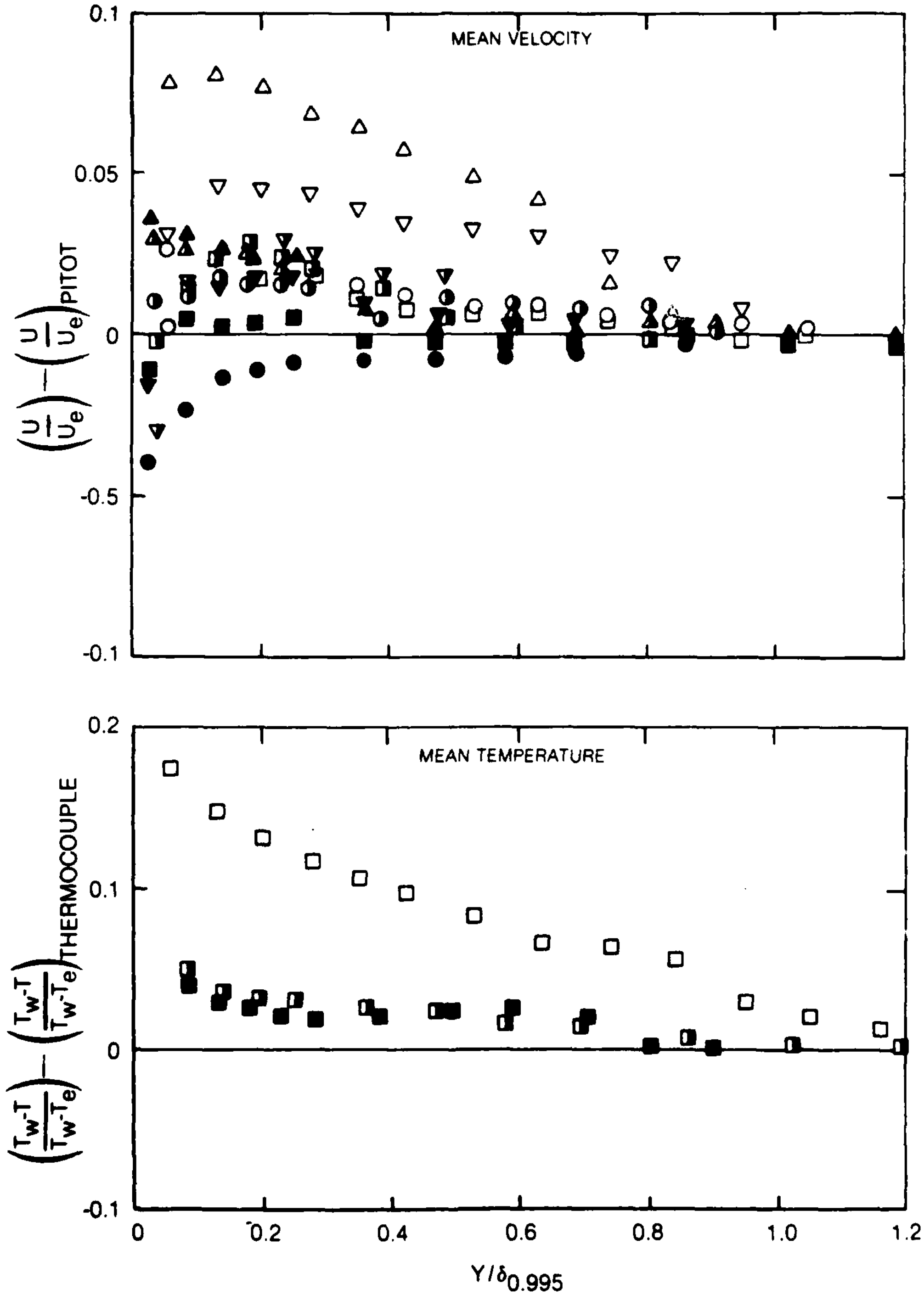

Figure A-1. Discrepancies Between Various Local Measurements of Mean Velocity and Temperature Profile Data

82-10-71-6

AD-A127 799 THE EFFECTS OF FREE-STREAM TURBULENCE ON THE TURBULENCE STRUCTURE AND HEA..(U) UNITED TECHNOLOGIES RESEARCH CENTER EAST HARTFORD CT M F BLAIR ET AL. NOV 82 2/2

UNCLASSIFIED UTRC/R82-915634-2 AFOSR-TR-83-0355 F/G 20/4 NL

END
DATE
FILMED
5-83
DTIC

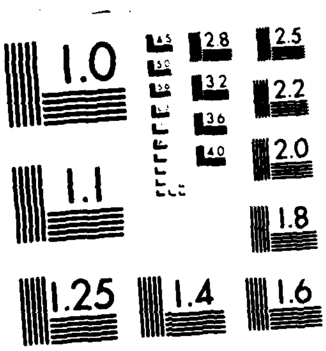

MICROCOPY RESOLUTION TEST CHART
NATIONAL BUREAU OF STANDARDS 1963 A

MEASURED QUANTITY	U/U_e			T_w-T/T_w-T_e
TYPE PROBE	TRI-X	X-H	X-V	TRI-X
SYMBOL	□	▽	△	◇

T_e %	0.2	1.4	3.9
SYMBOLS	OPEN	HALF FILLED	SOLID

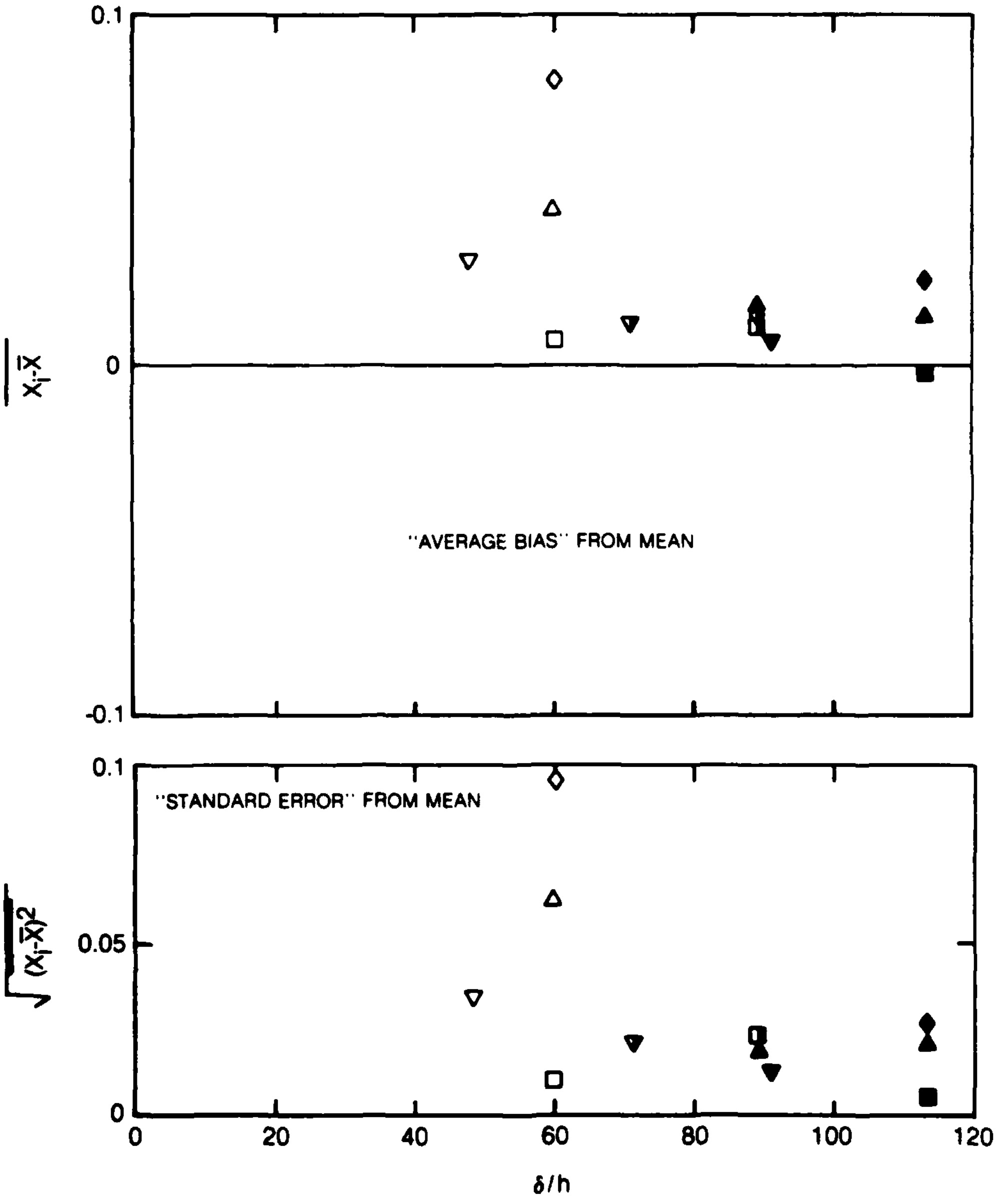

Figure A-2. Overall Discrepancies Between Different Mean Measurement Techniques for Various Profiles

82-10-71-5

TYPE PROBE	SINGLE HORIZ	TRI-X	X-H	X-V_1	X-V_2
SYMBOL	○	□	▽	△	◬

T_e %	0.2	1.4	3.9
SYMBOL	OPEN	HALF FILLED	SOLID

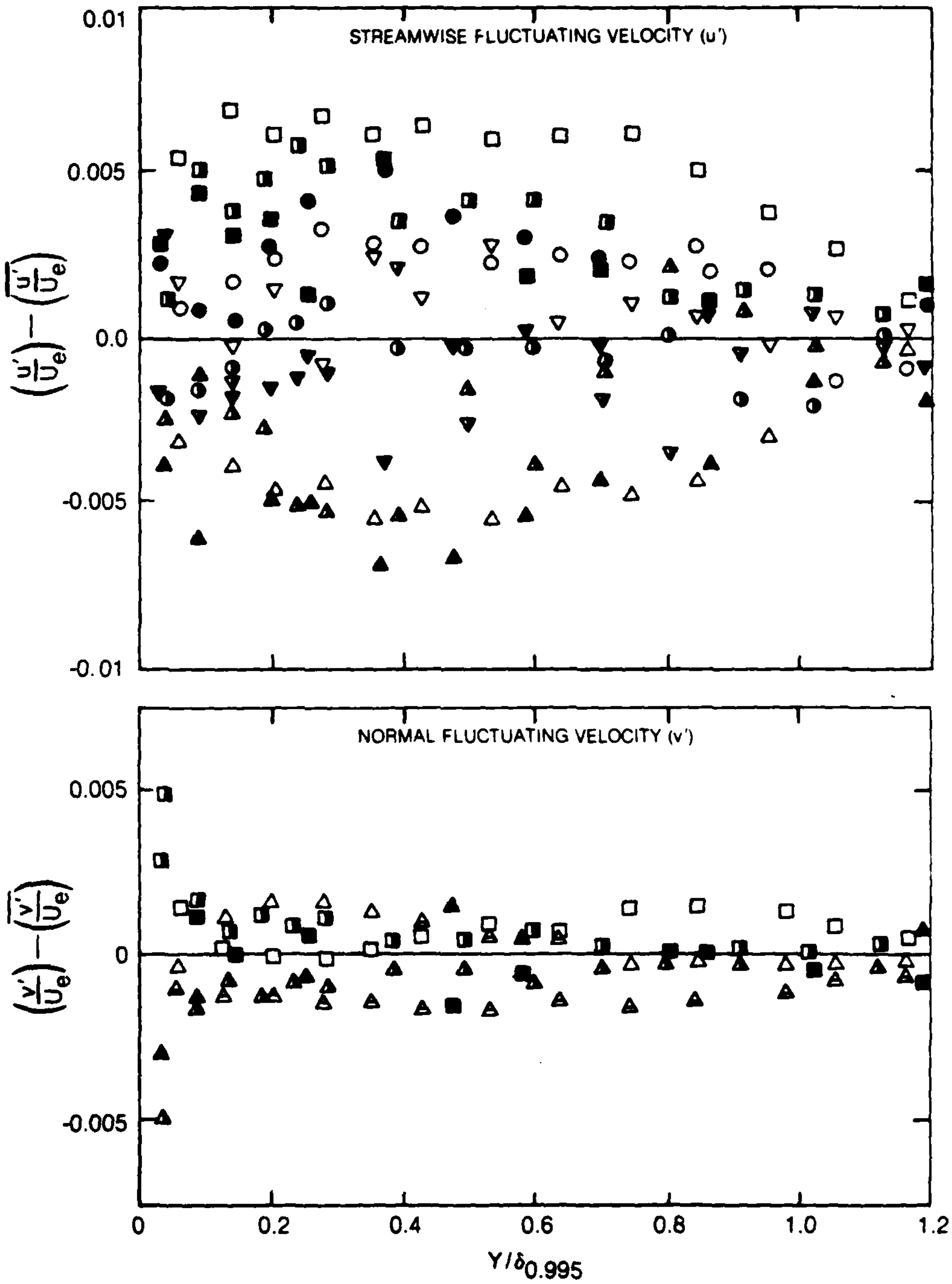

Figure A-3. Discrepancies Between Various Local Measurements of Fluctuating Velocity Components

82-10-71-4

TYPE PROBE	TR-X	$X\text{-}V_1$	$X\text{-}V_2$
SYMBOL	○	△	▲

T_e %	0.2	0.14	3.9
SYMBOL	OPEN	HALF FILLED	SOLID

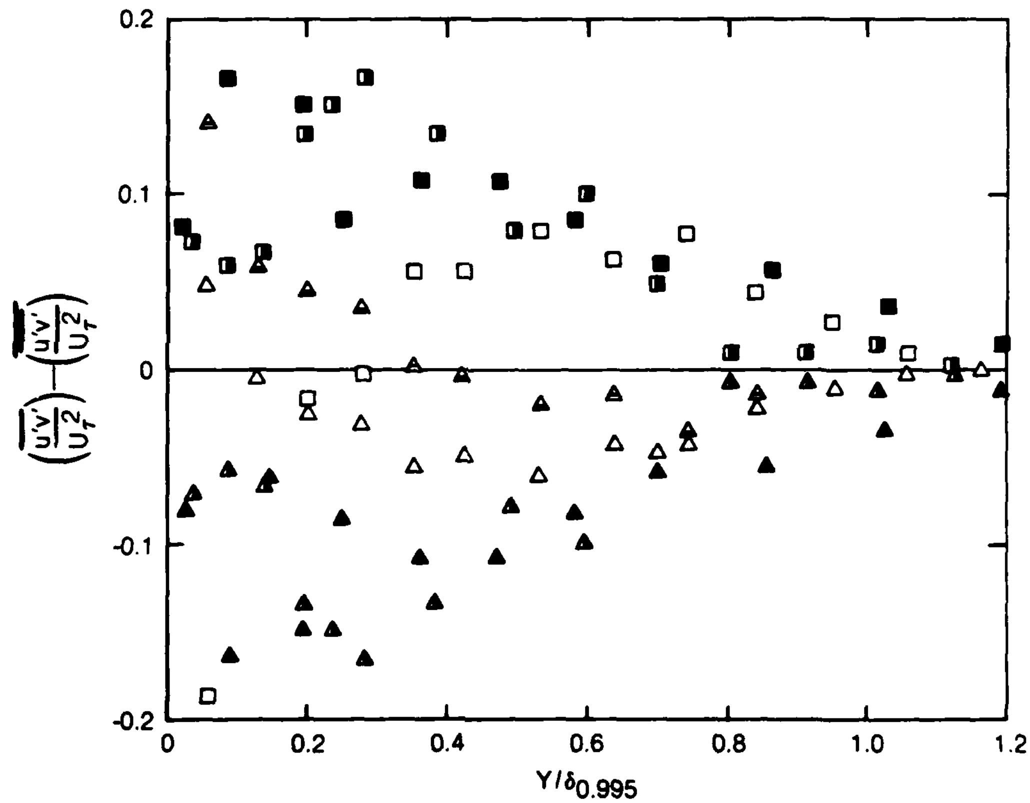

Figure A-4. Discrepancies Between Various Local Turbulent Shear Stress Measurements

82-10-71-3

MEASURED QUANTITY	u'/U_e			v'/U_e		$\overline{u'v'}/U_T^2$	
TYPE PROBE	TRI-X	X-H	X-V	TRI-X	X-V	TRI-X	
SYMBOL	□	▽	△	◇	◸	◹	○

T_e %	0.2	1.4	3.9
SYMBOLS	OPEN	HALF FILLED	SOLID

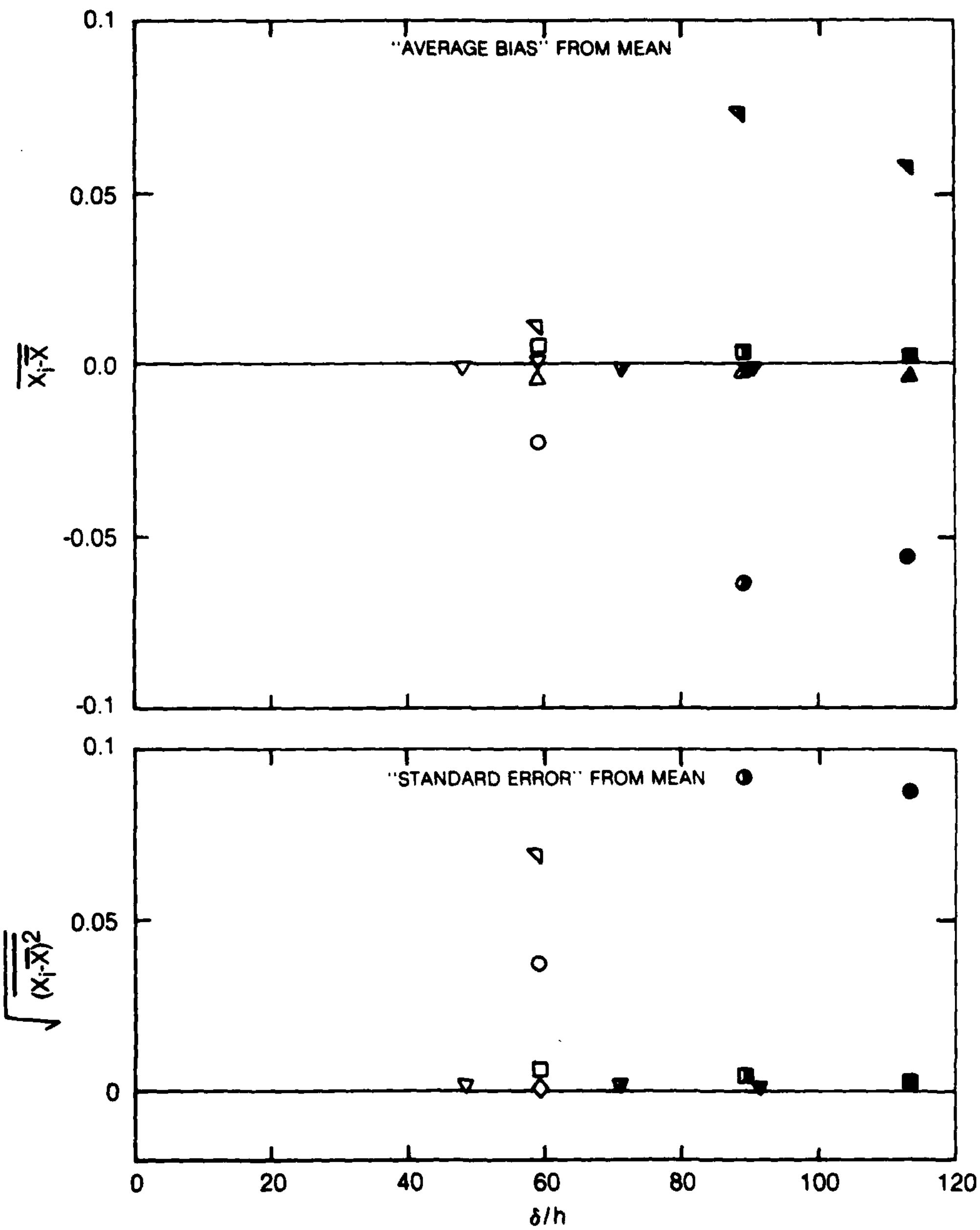

Figure A-5. Overall Discrepancies Between Different Fluctuating Measurement Techniques for Various Profiles

82-10-71-2

APPENDIX B - EXPERIMENTAL PROFILE DATA

All data for each profile are grouped together as follows:

a) mean profile data
b) mean profile data tabulation
c) boundary layer property tabulation
d) fluctuating profile plots (A-E)
e) fluctuating profile data tabulation (A-B).

The profile data are presented in the following order:

	X	Te%
1	52	0.2
2	68	0.2
3	84	0.2
4	52	1.8
5	68	1.6
6	84	1.4
7	52	4.7
8	68	4.2
9	84	3.9

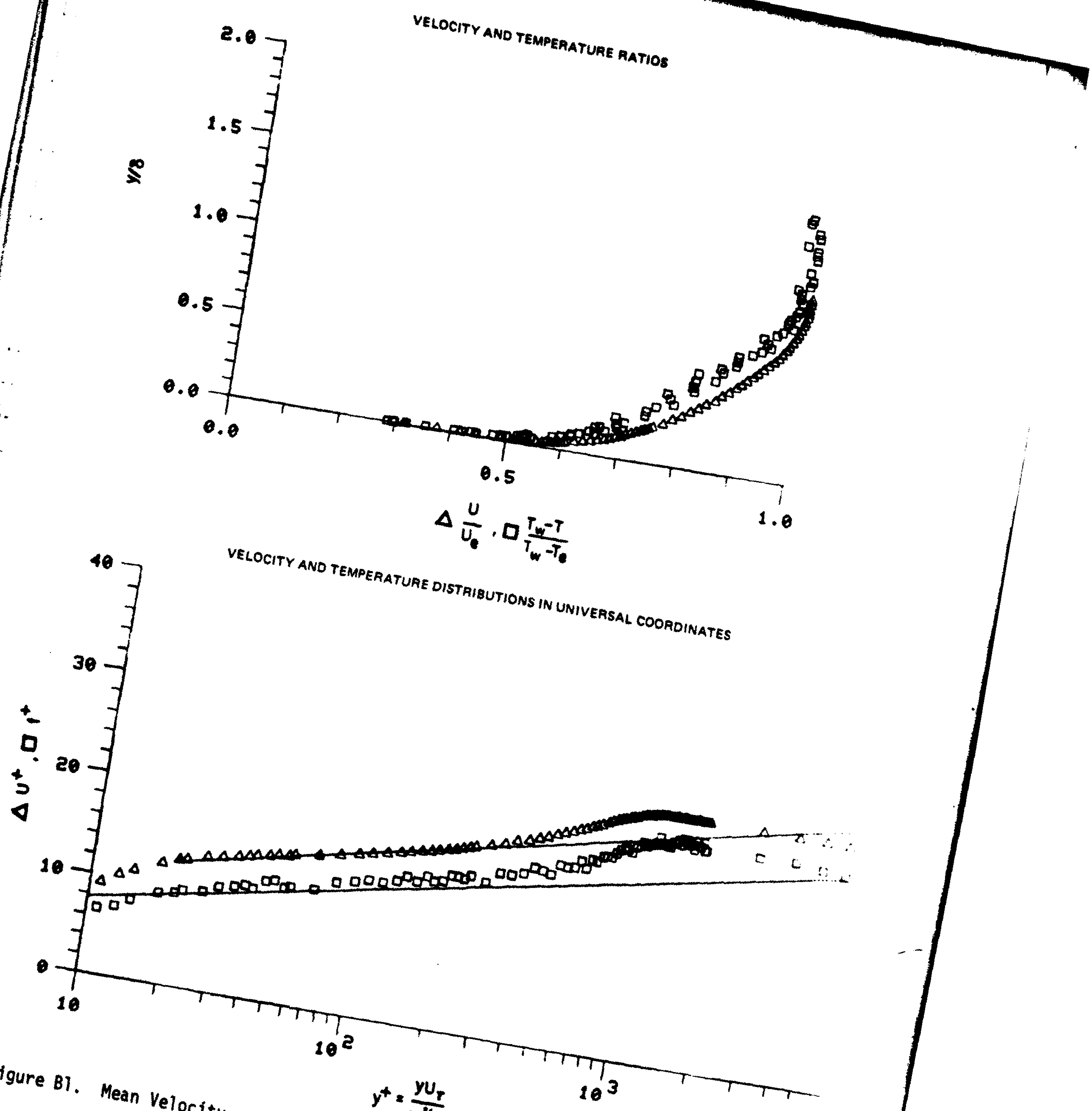

Figure B1. Mean Velocity and Temperature Profiles x = 52 in., Te = 0.2%

78-12-100-1

Mean Profile Data

x = 52 in., Te = 0.2%

N	Y INCHES	Y/ DELTA	U FT/SEC	T DEG.F	U/UE	THETA	U-UE UTAU	U(+)	T(+)	Y(+)
1	.0033	.006	31.10	82.76	.314	.286	-16.897	7.747	6.389	6.466
2	.0043	.007	31.65	82.61	.320	.295	-16.758	7.885	6.596	8.436
3	.0056	.009	37.10	82.57	.375	.297	-15.401	9.242	6.641	10.969
4	.0065	.011	41.20	82.22	.417	.319	-14.379	10.264	7.129	12.722
5	.0073	.012	44.03	81.64	.445	.355	-13.674	10.969	7.920	14.261
6	.0092	.015	48.40	80.80	.469	.407	-12.586	12.057	9.081	17.962
7	.0106	.018	50.62	80.59	.512	.419	-12.032	12.611	9.369	20.712
8	.0113	.019	51.30	80.31	.519	.437	-11.864	12.760	9.749	22.074
9	.0135	.022	53.40	80.17	.540	.445	-11.340	13.303	9.941	26.360
10	.0154	.026	54.76	79.66	.554	.476	-11.002	13.642	10.639	30.061
11	.0175	.029	55.74	79.43	.563	.491	-10.757	13.886	10.965	34.153
12	.0191	.032	56.44	79.28	.571	.500	-10.584	14.059	11.164	37.270
13	.0204	.034	57.12	79.42	.577	.492	-10.413	14.231	10.980	39.803
14	.0227	.038	57.91	78.72	.585	.535	-10.218	14.426	11.942	44.284
15	.0245	.041	58.55	78.58	.592	.543	-10.056	14.586	12.132	47.790
16	.0267	.044	59.26	78.98	.599	.518	-9.880	14.764	11.574	52.077
17	.0282	.047	59.74	78.82	.604	.528	-9.761	14.883	11.802	54.999
18	.0344	.057	61.33	78.70	.620	.536	-9.366	15.277	11.969	67.078
19	.0415	.069	62.99	77.96	.637	.580	-8.951	15.692	12.946	80.911
20	.0485	.080	64.26	77.72	.650	.596	-8.629	16.014	13.312	94.548
21	.0543	.090	65.41	77.44	.661	.613	-8.350	16.294	13.692	105.845
22	.0615	.102	66.56	77.43	.673	.614	-8.057	16.586	13.709	119.875
23	.0665	.113	67.65	77.20	.684	.626	-7.792	16.852	14.028	133.513
24	.0745	.123	68.45	76.78	.692	.654	-7.591	17.052	14.605	145.203
25	.0813	.134	69.45	76.94	.702	.644	-7.341	17.302	14.376	158.451
26	.0867	.147	70.23	76.48	.710	.672	-7.148	17.495	15.016	172.668
27	.0945	.156	70.96	76.78	.717	.654	-6.967	17.677	14.600	184.167
28	.1019	.168	71.90	76.65	.727	.662	-6.731	17.913	14.781	196.584
29	.1085	.179	72.65	76.16	.734	.692	-6.544	18.099	15.448	211.443
30	.1146	.189	73.32	76.16	.741	.692	-6.379	18.264	15.454	223.327
31	.1215	.201	73.99	76.19	.748	.690	-6.211	18.433	15.414	236.770
32	.1264	.212	74.63	75.97	.754	.704	-6.051	18.592	15.717	250.213
33	.1456	.241	76.37	76.24	.772	.687	-5.617	19.026	15.348	283.723
34	.1632	.270	77.81	75.40	.787	.739	-5.260	19.384	16.499	318.012
35	.1806	.299	79.41	75.38	.803	.740	-4.862	19.782	16.527	351.911
36	.1965	.328	80.73	75.12	.816	.756	-4.531	20.112	16.879	382.765
37	.2158	.357	82.05	74.63	.829	.786	-4.202	20.441	17.556	420.489
38	.2335	.386	83.34	74.74	.843	.779	-3.881	20.763	17.402	454.973
39	.2504	.414	84.73	74.86	.857	.772	-3.535	21.108	17.235	487.899
40	.2684	.444	85.81	74.10	.867	.819	-3.266	21.378	18.282	522.967
41	.2853	.472	87.00	74.16	.879	.815	-2.971	21.672	18.194	555.892
42	.3034	.502	88.15	74.10	.891	.818	-2.684	21.960	18.279	591.155
43	.3183	.526	89.00	73.57	.900	.851	-2.473	22.171	19.011	620.164
44	.3332	.551	89.90	74.06	.909	.821	-2.247	22.397	18.343	649.213
45	.3481	.575	90.60	73.36	.916	.864	-2.024	22.619	19.297	678.242
46	.3631	.600	91.59	73.45	.926	.856	-1.828	22.816	19.170	707.466
47	.3789	.626	92.38	73.03	.934	.884	-1.629	23.014	19.745	738.248
48	.3932	.650	93.24	72.99	.943	.887	-1.415	23.228	19.800	766.108
49	.4085	.675	93.98	73.00	.950	.886	-1.231	23.412	19.797	795.916
50	.4233	.700	94.66	72.62	.957	.909	-1.062	23.582	20.312	824.750
51	.4384	.725	95.16	72.36	.962	.926	-.938	23.706	20.671	854.168
52	.4537	.750	95.82	72.11	.969	.941	-.772	23.872	21.012	883.976
53	.4684	.774	96.27	72.24	.973	.933	-.660	23.983	20.638	912.616
54	.4833	.799	96.77	72.36	.978	.925	-.536	24.108	20.666	941.644
55	.4986	.824	97.32	72.00	.984	.948	-.398	24.245	21.163	971.453
56	.5133	.848	97.61	71.83	.987	.956	-.326	24.317	21.399	1000.092
57	.5287	.874	97.97	71.57	.990	.974	-.237	24.407	21.752	1030.095
58	.5433	.898	98.22	71.74	.993	.964	-.176	24.467	21.527	1058.539
59	.5583	.923	98.46	71.67	.995	.968	-.114	24.530	21.624	1087.763
60	.5733	.948	98.67	71.55	.997	.975	-.062	24.581	21.786	1116.986
61	.5886	.973	98.77	71.48	.998	.980	-.038	24.606	21.882	1146.794
62	.6034	.997	98.77	71.05	.998	1.006	-.038	24.605	22.472	1175.628
63	.6183	1.022	98.88	71.41	1.000	.984	-.010	24.634	21.976	1204.657
64	.6334	1.047	98.92	71.47	1.000	.980	-.002	24.642	21.693	1234.076
65	.6488	1.072	98.97	71.48	1.000	.980	.011	24.655	21.686	1264.079
66	.6639	1.097	99.03	71.58	1.001	.973	.027	24.670	21.739	1293.497
67	.6784	1.121	99.07	71.25	1.001	.994	.036	24.680	22.197	1321.747
68	.6933	1.146	99.02	71.20	1.001	.997	.024	24.668	22.264	1350.776
69	.7083	1.171	98.96	71.00	1.000	1.009	.008	24.652	22.540	1379.999
70	.7238	1.196	99.08	71.33	1.002	.989	.038	24.682	22.090	1410.197
71	.7386	1.221	99.03	70.91	1.001	1.015	.026	24.670	22.664	1439.421
72	.7534	1.245	98.99	70.88	1.001	1.017	.016	24.659	22.707	1467.865
73	.7687	1.271	99.02	71.18	1.001	.998	.024	24.666	22.288	1497.673
74	.7834	1.295	98.94	71.21	1.000	.996	.005	24.649	22.252	1526.312
75	.7984	1.320	99.05	71.19	1.001	.997	.031	24.675	22.273	1555.536
76	.8135	1.345	99.11	71.52	1.002	.977	.048	24.691	21.624	1584.954
77	.8285	1.369	98.99	70.86	1.001	1.018	.017	24.661	22.727	1614.178
78	.8433	1.394	98.95	71.17	1.000	.998	.006	24.650	22.299	1643.012
79	.8587	1.419	98.96	71.23	1.000	.995	.009	24.652	22.228	1673.015
80	.8733	1.443	98.96	70.89	1.001	1.016	.014	24.657	22.697	1701.459
81	.8887	1.469	99.04	71.52	1.001	.977	.031	24.674	21.630	1731.462
82	.9037	1.494	98.99	71.46	1.001	.981	.017	24.661	21.914	1760.686
83	1.4283	2.361	98.96	71.29	1.000	.992	.008	24.652	22.148	2782.734
84	1.9533	3.228	98.96	71.21	1.000	.997	.009	24.653	22.256	3805.562
85	2.4783	4.096	98.91	71.51	1.000	.978	-.003	24.641	21.636	4828.390
86	3.0033	4.964	99.01	71.64	1.001	.970	.021	24.665	21.657	5851.218

Table B1

RUN NO. 3. POINT 3.

BOUNDARY LAYER PROPERTIES

	LINEAR INTERPOLATION TO WALL	STANDARD SUBLAYER FUNCTION FROM WALL TO Y+=35
FREE STREAM VELOCITY =	98.922	98.922
FREE STREAM TEMPERATURE =	71.150	
WALL TEMPERATURE =	87.410	
WALL HEAT FLUX =	.05120	
FREE STREAM DENSITY =	.07523	
FREE STREAM KINEMATIC VISCOSITY =	.0001628	
DENSITY OF FLUID AT WALL =	.07300	
KINEMATIC VISCOSITY OF FLUID AT WALL =	.0001717	
WALL/FREE STREAM DENSITY RATIO =	.97028	
LOCATION REYNOLDS NUMBER (REX) =	2633499.75	
INPUT VALUE OF VELOCITY DELTA =	.61000	
INPUT VALUE OF TEMPERATURE DELTA =	.67000	
CALCULATED DELTA =		.60504
DELTA 99.5% INPUT =	.00000	
DISPLACEMENT THICKNESS (DELSTAR) =	.09026	.09063
MOMENTUM THICKNESS (THETA) =	.06280	.06260
ENERGY-DISSIPATION THICKNESS =	.11090	.11078
ENTHALPY THICKNESS =	.00274	.00273
SHAPE FACTOR 12 (DELSTAR/THETA) =	1.43730	1.44315
SHAPE FACTOR 32 (ENERGY/THETA) =	1.76594	1.76410
MOMENTUM THICKNESS REYNOLDS NUMBER =	3180.47	3180.34
DISPLACEMENT THICKNESS REYNOLDS NUMBER =	4571.29	4589.72
SKIN FRICTION COEFFICIENT =	.003195	
FRICTION VELOCITY =	4.01412	
LAW OF THE WALL CONSTANT (K) =	.41000	
LAW OF THE WALL CONSTANT (C) =	5.00000	
WAKE STRENGTH =		.49082
CLAUSERS 'DELTA' INTEGRAL =	-2.07555	-2.16672
CLAUSERS 'G' INTEGRAL =	14.68922	14.91446
DISPLACEMENT THICKNESS - CONSTANT DENSITY =	.08589	.08792
MOMENTUM THICKNESS - CONSTANT DENSITY =	.06337	.06336
SHAPE FACTOR 12 - CONSTANT DENSITY =	1.35544	1.38758

LOCATION -X- 52.00000

Te = 0.2%

Table B2

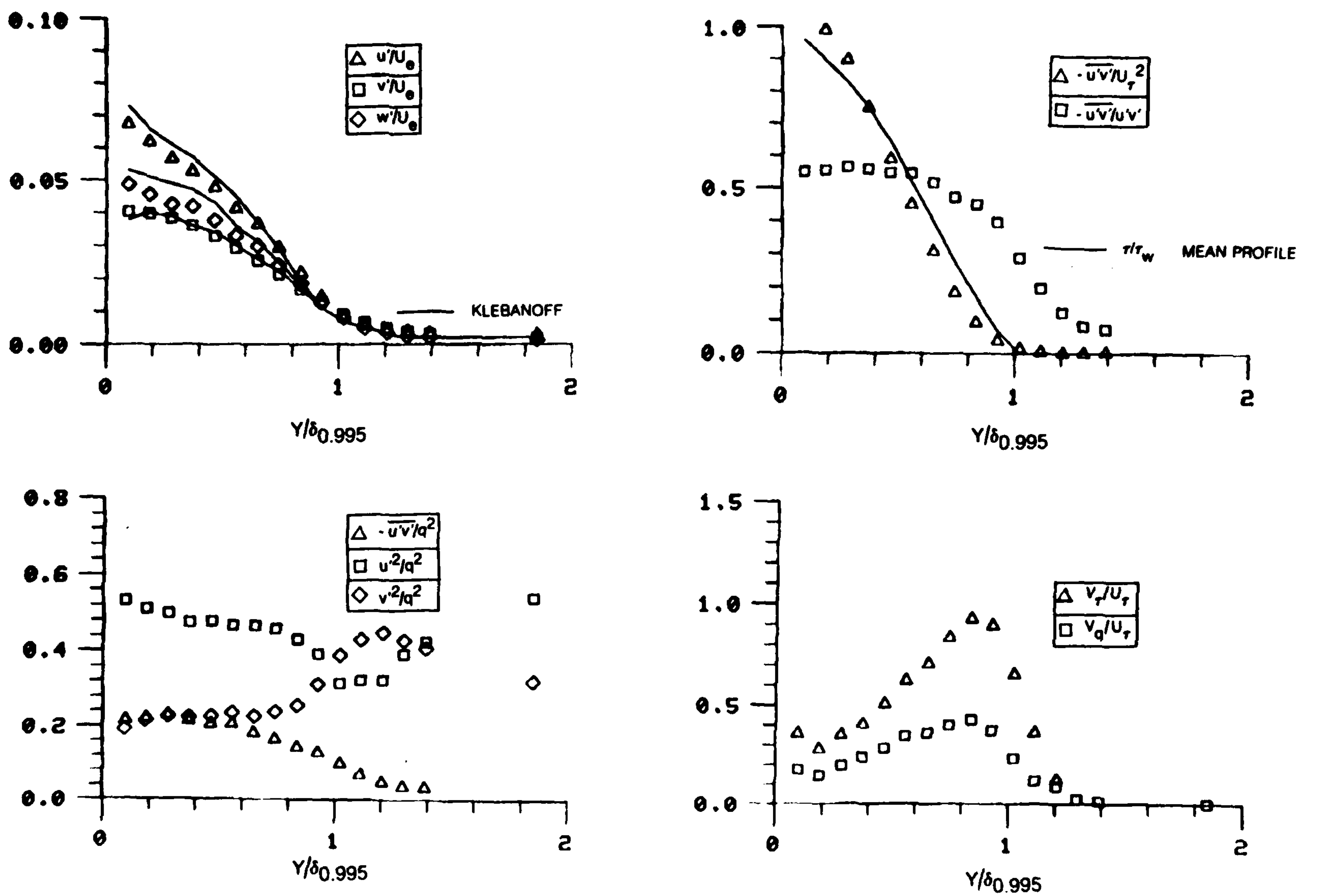

Figure B2A. Boundary Layer Turbulence Quantities $x = 52$ in, $T_e = 0.2\%$

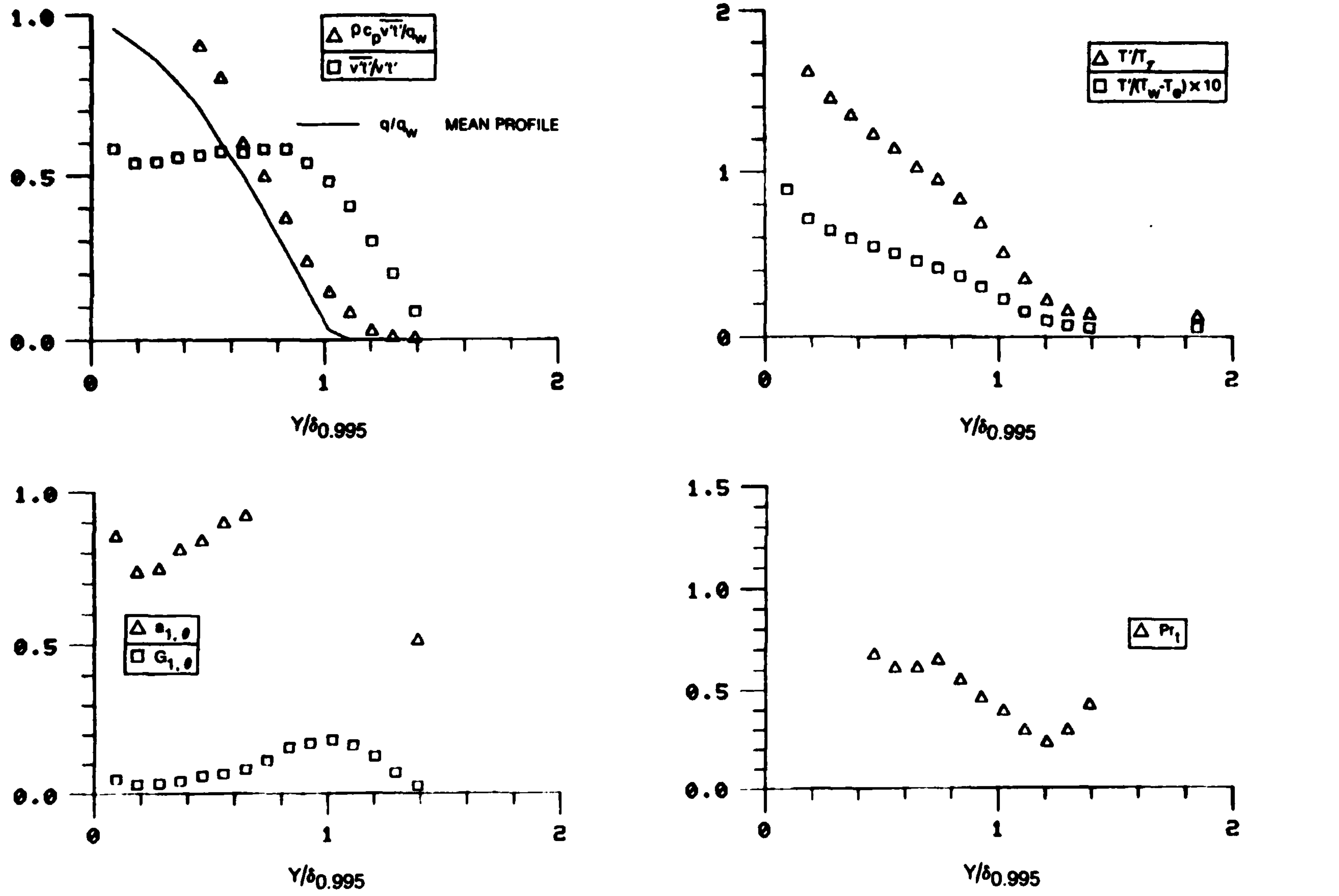

Figure B2B. Boundary Layer Turbulence Quantities, x = 52 in, T_e = 0.2%

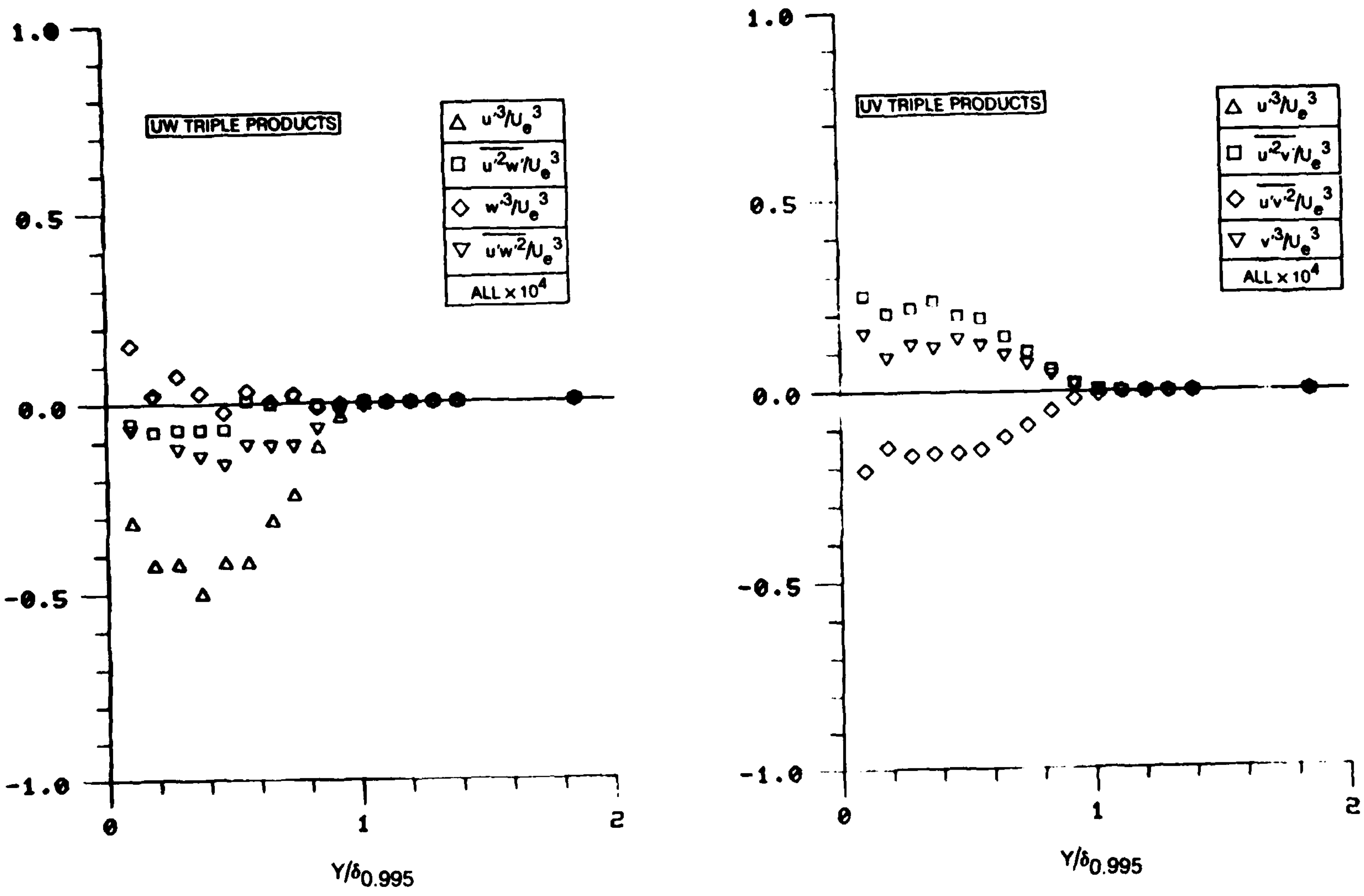

Figure B2C. Boundary Layer Triple Product Distributions $x = 52$ in, $T_e = 0.2\%$

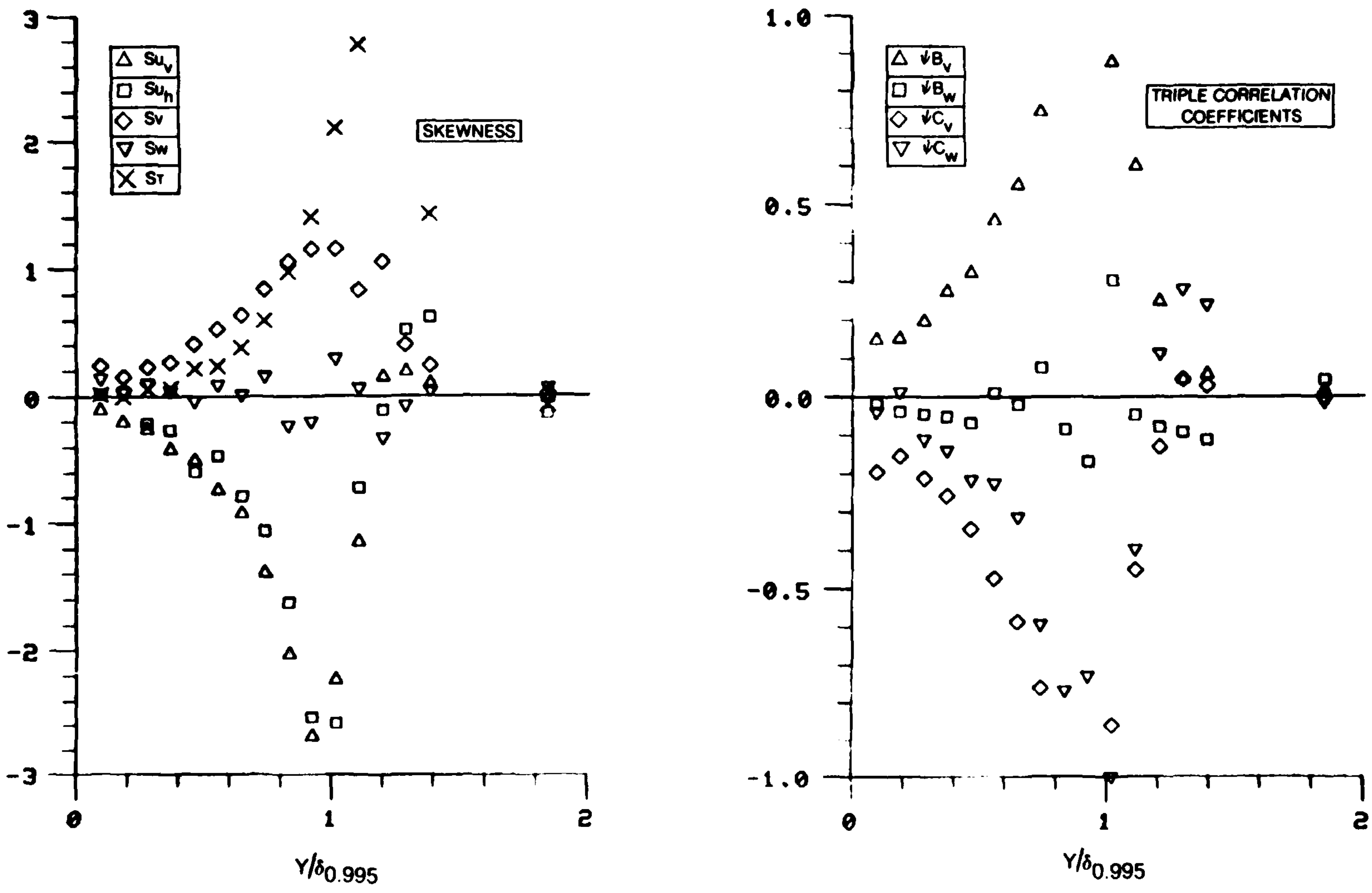

Figure B2D. Boundary Layer Skewness and Triple Product Correlation Coefficient Distributions $x = 52$ in, $T_e = 0.2\%$

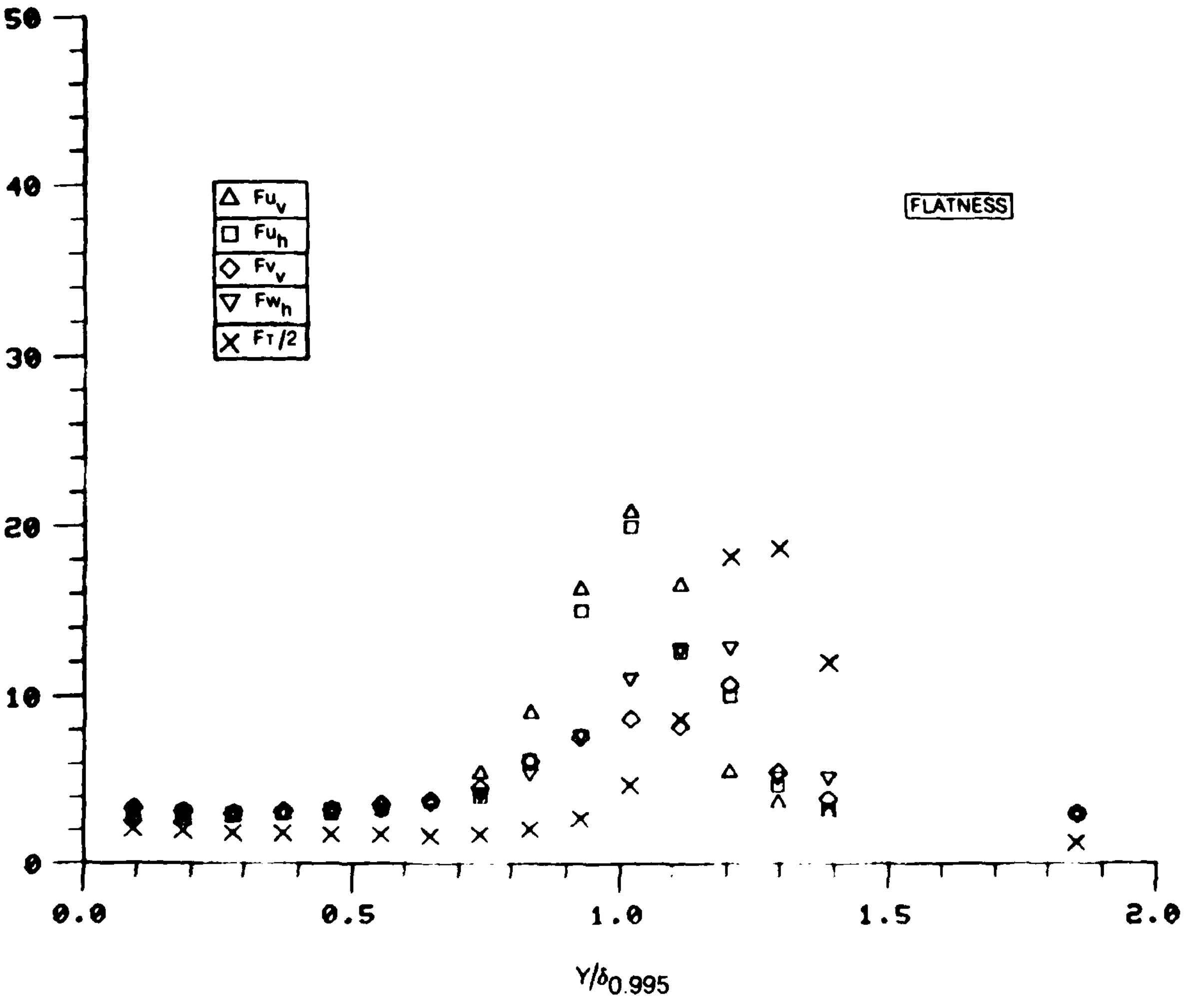

Figure B2E. Boundary Layer Flatness Distributions $x = 52$ in, $T_e = 0.2\%$

Fluctuating Profile Data

x = 52 in, Te = 0.2%

N	Y: INCHES	Y/ DELTA	U'/UE	V'/UE	W'/UE	$\sqrt{\overline{U'V'}}$/UE	$\overline{U'V'}$/ UTAU2	$\overline{U'V'}$/U'V'	Q/UE
1	3.000	5.556	.0011	.0016	.0000	.0002	-.0000	-.0101	.0019
2	.050	.093	.0672	.0403	.0466	.0427	1.1057	.5476	.0922
3	.100	.185	.0617	.0398	.0456	.0404	.9912	.5565	.0865
4	.150	.278	.0567	.0362	.0423	.0385	.8960	.5656	.0804
5	.200	.370	.0522	.0357	.0419	.0351	.7479	.5592	.0759
6	.250	.463	.0476	.0327	.0377	.0312	.5861	.5496	.0689
7	.300	.556	.0409	.0269	.0329	.0272	.4465	.5451	.0600
8	.350	.648	.0360	.0251	.0295	.0225	.3068	.5171	.0529
9	.400	.741	.0291	.0210	.0239	.0174	.1837	.4712	.0431
10	.450	.833	.0214	.0165	.0184	.0124	.0931	.4525	.0327
11	.500	.926	.0141	.0126	.0123	.0080	.0391	.3967	.0226
12	.550	1.019	.0081	.0090	.0079	.0045	.0123	.2911	.0144
13	.600	1.111	.0055	.0064	.0048	.0026	.0040	.1954	.0097
14	.650	1.204	.0042	.0050	.0035	.0016	.0015	.1246	.0074
15	.700	1.296	.0037	.0038	.0025	.0011	.0007	.0827	.0059
16	.750	1.389	.0033	.0032	.0021	.0009	.0005	.0733	.0057
17	1.000	1.852	.0028	.0021	.0014	.0004	-.0001	-.0216	.0036
18	3.000	5.556	.0023	.0016	.0011	.0005	-.0001	-.0498	.0031

N	Y: INCHES	Y/ DELTA	$\overline{V'U'}$/Q2	U'2/Q2	V'2/Q2	W'2/Q2	VTAU/ UTAU	VC/ UTAU	$\overline{V'T'}$RHO*CP/ QWALL
1	3.000	5.556	-.0144	.3261	.6739	.0000	.1930	.0021	.0019
2	.050	.093	.2145	.5312	.1909	.2779	.3548	.1723	
3	.100	.185	.2188	.5099	.2121	.276	.2753	.1469	
4	.150	.278	.2286	.4971	.2261	.2768	.3522	.1941	
5	.200	.370	.2142	.4744	.2215	.3041	.4059	.2376	
6	.250	.463	.2043	.4762	.2253	.2985	.5053	.2845	.8996
7	.300	.556	.2058	.4662	.2328	.3009	.6197	.3420	.7969
8	.350	.648	.1808	.4637	.2250	.3113	.7033	.3589	.5959
9	.400	.741	.1629	.4558	.2169	.3074	.8136	.4027	.4914
10	.450	.833	.1435	.4298	.2539	.3163	.9265	.4266	.3669
11	.500	.926	.1266	.3914	.3123	.2962	.8932	.3730	.2328
12	.550	1.019	.0971	.3145	.3895	.2960	.6531	.2312	.1424
13	.600	1.111	.0693	.3225	.4307	.2468	.3620	.1171	.0796
14	.650	1.204	.0466	.3243	.4477	.2280	.1237	.0915	.0224
15	.700	1.296	.0355	.3902	.4273	.1625	-.0559	.0229	.0074
16	.750	1.389	.0331	.4249	.4045	.1706	-.0443	.0115	.0021
17	1.000	1.852	-.0104	.5391	.3193	.1416	-.0131	.0007	-.000[illegible]
18	3.000	5.556	-.0255	.5770	.2831	.1399	.0540	.0006	-.0003

N	Y: INCHES	Y/ DELTA	$\overline{V'T'}$/V'T'	T'/TTAU	T'/(TW-TE)	A18	G18	PRT
1	3.000	5.556	-.0385	.1470	.0065	-.8704	.0012	-1.5202
2	.050	.093	.5613	2.0110	.0891	.8526	.0496	
3	.100	.185	.5389	1.6112	.0714	.7351	.0312	
4	.150	.278	.5404	1.4474	.0641	.7457	.0327	
5	.200	.370	.5535	1.3417	.0594	.8058	.0426	
6	.250	.463	.5604	1.2262	.0543	.8372	.0599	.6707
7	.300	.556	.5726	1.1399	.0505	.8978	.0654	.6062
8	.350	.648	.5697	1.0209	.0452	.9203	.0800	.6041
9	.400	.741	.5780	.9421	.0417	1.0504	.1096	.6456
10	.450	.833	.5789	.8292	.0367	1.2202	.1562	.5457
11	.500	.926	.5384	.6800	.0301	1.4047	.1718	.4556
12	.550	1.019	.4797	.5065	.0224	1.8409	.1820	.3898
13	.600	1.111	.4029	.3464	.0153	2.2637	.1622	.2886
14	.650	1.204	.2960	.2164	.0096	1.7649	.1272	.2274
15	.700	1.296	.1995	.1539	.0068	1.2742	.0716	.2876
16	.750	1.389	.0858	.1294	.0057	.5113	.0268	.4156
17	1.000	1.852	-.0108	.1200	.0053	-.2405	-.0017	-1.8186
18	3.000	5.556	-.0079	.1123	.0050	-.0799	.0000	-3.0404

Table B3A

Fluctuating Profile Data

x = 52 in., Te = 0.2%

N	Y: INCHES	Y/ DELTA	U'3/UE3 x 10000	U'2W'/ UE3 x 10000	W'3/UE3 x 10000	U'W'2/ UE3 x 10000	U'2V'/ UE3 x 10000	U'V'2/ UE3 x 10000	V'3/UE3 x 10000
1	3.000	5.556	-.0000	.0000	.0000	.0000	.0000	-.0000	.0000
2	.050	.093	-.3162	-.0502	.1535	-.0659	.2503	-.2049	.1539
3	.100	.185	-.4296	-.0758	.0236	.0188	.2058	-.1456	.0939
4	.150	.278	-.4271	-.0677	.0730	-.1162	.2195	-.1677	.1269
5	.200	.370	-.5037	-.0664	.0291	-.1354	.2366	-.1623	.1168
6	.250	.463	-.4229	-.0693	-.0218	-.1587	.1990	-.1604	.1433
7	.300	.556	-.4237	.0058	.0337	-.1068	.1947	-.1525	.1264
8	.350	.648	-.3132	-.0047	.0040	-.1094	.1453	-.1200	.0993
9	.400	.741	-.2465	.0198	.0222	-.1100	.1064	-.0873	.0767
10	.450	.833	-.1204	-.0067	-.0138	-.0653	.0566	-.0507	.0473
11	.500	.926	-.0403	-.0060	-.0038	-.0185	.0211	-.0208	.0229
12	.550	1.019	-.0077	.0022	.0014	-.0057	.0039	-.0049	.0064
13	.600	1.111	-.0013	-.0000	.0001	-.0006	.0009	-.0009	.0021
14	.650	1.204	.0001	-.0001	-.0002	.0001	.0002	-.0001	.0017
15	.700	1.296	.0001	-.0000	-.0000	.0001	.0000	.0000	.0000
16	.750	1.389	.0000	-.0000	.0000	.0000	.0000	.0000	.0001
17	1.000	1.852	-.0000	.0000	.0000	-.0000	.0000	.0000	.0000
18	3.000	5.556	-.0000	-.0000	.0000	-.0000	.0000	.0000	.0000

N	Y: INCHES	Y/ DELTA	SU V	SU H	SV	SW	ST	PSIBV	PSIBW
1	3.000	5.556	-.0089	.0000	.1593	.0000	-.3002	-.0024	.0000
2	.050	.093	-.1185	.0052	.2349	.1338	.0078	.1497	-.0195
3	.100	.185	-.2137	.0304	.1462	.0263	-.0091	.1506	-.0364
4	.150	.278	-.2698	-.2203	.2255	.0999	.0528	.1961	-.0446
5	.200	.370	-.4216	-.2672	.2630	.0429	.0628	.2753	-.0518
6	.250	.463	-.5138	-.5973	.4093	-.0416	.2129	.3215	-.0661
7	.300	.556	-.7500	-.4706	.5202	.0915	.2332	.4568	.0103
8	.350	.648	-.9242	-.7918	.6275	.0063	.3772	.5525	-.0207
9	.400	.741	-1.3927	-1.0619	.6290	.1506	.5875	.7468	.0787
10	.450	.833	-2.0364	-1.6232	1.0497	-.2327	.9722	1.0512	-.0837
11	.500	.926	-2.6934	-2.5342	1.1390	-.2045	1.3906	1.2750	-.1693
12	.550	1.019	-2.2307	-2.5805	1.1372	.2927	2.0928	.8817	.3076
13	.600	1.111	-1.1474	-.7285	.8223	.0555	2.7547	.6047	-.0436
14	.650	1.204	.1456	-.1128	1.0417	-.3304	3.7660	.2507	-.0767
15	.700	1.296	.1866	.5162	.3969	-.0802	3.1489	.0471	-.0699
16	.750	1.389	.0864	.6099	.2289	.0367	1.4124	.0622	-.1112
17	1.000	1.852	-.0262	-.1436	.0079	.0576	-.0760	.0183	.0479
18	3.000	5.556	-.1217	-.2463	.0061	.0468	-.0199	.0211	-.0124

N	Y: INCHES	Y/ DELTA	PSICV	PSICW	FU V	FU H	FU V	FU H	FT
1	3.000	5.556	.0500	.0000	3.0487	.0000	3.1967	.0000	2.9469
2	.350	.093	-.1956	-.0361	2.7187	2.6631	3.3205	3.1692	4.1137
3	.100	.185	-.1564	.0133	2.7937	2.6363	3.1392	3.1656	3.9857
4	.150	.278	-.2113	-.1093	2.8492	2.8241	3.0121	3.1038	3.6762
5	.200	.370	-.2579	-.1384	2.9966	2.9831	3.1390	3.0835	3.5993
6	.250	.463	-.3446	-.2147	3.1500	3.0313	3.2569	3.3060	3.4238
7	.300	.556	-.4743	-.2269	3.5947	3.2109	3.5752	3.2326	3.4355
8	.350	.648	-.5865	-.3116	3.8225	3.7721	3.8738	3.6986	3.2851
9	.400	.741	-.7598	-.5931	5.4175	4.0350	4.6076	4.2489	3.4415
10	.450	.833	-1.0323	-.7693	9.0202	6.2371	6.1534	5.5371	4.2209
11	.500	.926	-1.1411	-.7286	16.2345	14.9672	7.6221	7.7329	5.5655
12	.550	1.019	-.8598	-.9994	20.7781	19.8866	8.6562	11.1158	9.4444
13	.600	1.111	-.4516	-.3982	16.5380	12.6038	6.2341	12.6563	17.35[illegible]
14	.650	1.204	-.1306	.1146	5.5241	8.9953	10.6298	12.9152	36.3162
15	.700	1.296	.0495	.2824	3.6986	4.6467	5.5041	5.2091	37.322[illegible]
16	.750	1.389	.0338	.2456	3.1782	3.2838	3.9224	5.2674	24.0679
17	1.000	1.852	.0022	-.0101	3.0145	3.0273	3.0345	2.8938	2.4904
18	3.000	5.556	.0672	-.0366	3.1378	2.8422	3.0933	2.7387	2.6326

Table B3B

VELOCITY AND TEMPERATURE RATIOS

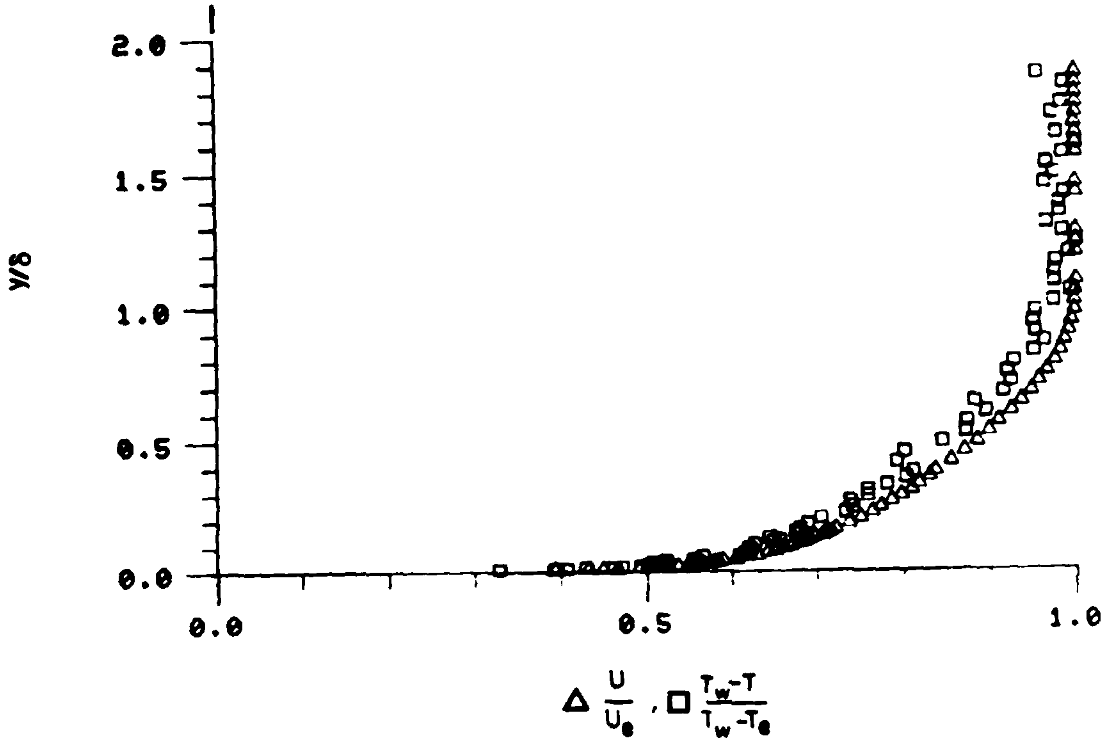

VELOCITY AND TEMPERATURE DISTRIBUTIONS IN UNIVERSAL COORDINATES

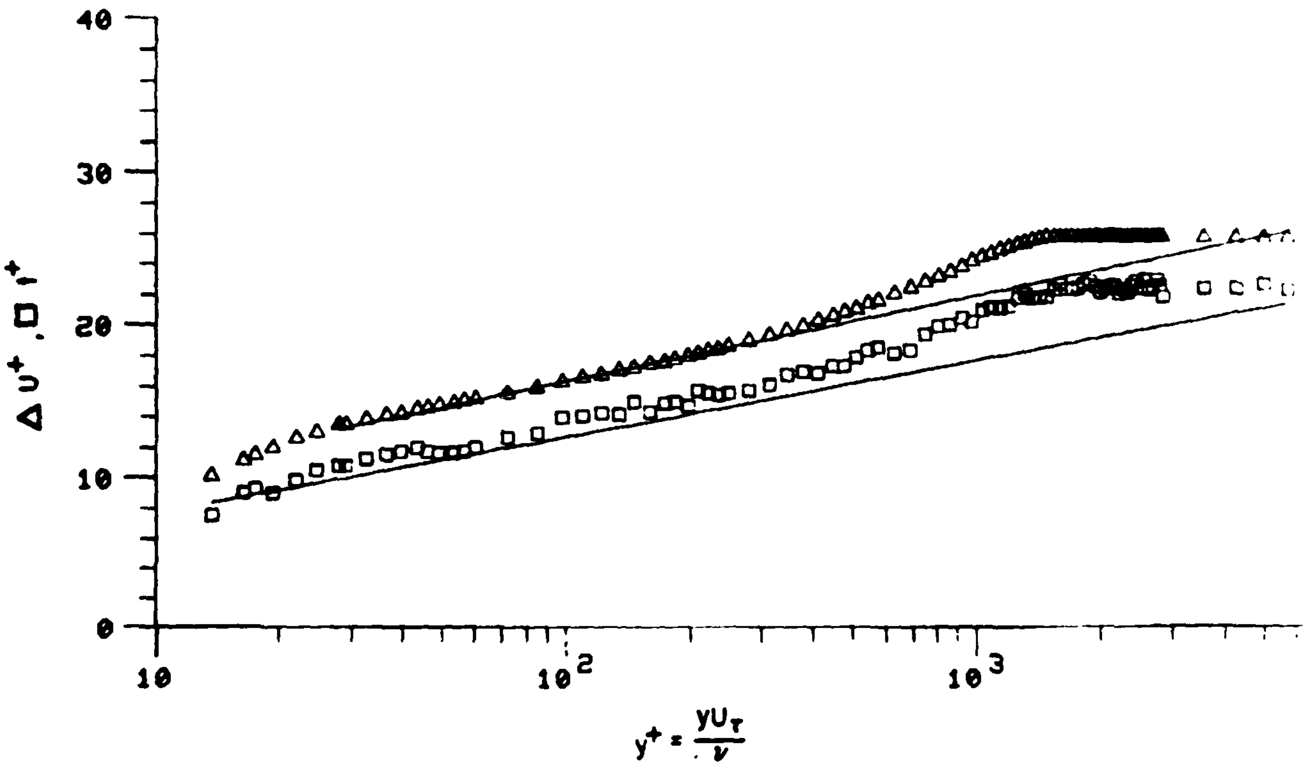

Figure B3. Mean Velocity and Temperature Profiles x = 68 in., Te = 0.2%

78-12-100-1

Mean Profile Data

x = 68 in., Te = 0.2%

N	Y INCHES	Y/DELTA	U FT/SEC	T DEG.F	U/UE	THETA	U-UE UTAU	U(+)	T(+)	Y(+)
1	.0044	.004	28.21	84.10	.284	.272	-18.616	7.470	5.960	8.086
2	.0054	.005	30.06	84.18	.303	.266	-18.322	7.964	5.647	9.913
3	.0072	.007	37.62	82.88	.379	.344	-16.323	9.963	7.556	13.199
4	.0084	.008	41.56	82.20	.419	.385	-15.274	11.012	8.453	15.390
5	.0095	.009	44.32	81.93	.446	.402	-14.550	11.736	8.813	17.396
6	.0114	.011	47.17	81.34	.475	.437	-13.795	12.491	9.592	20.867
7	.0134	.013	49.39	81.15	.498	.448	-13.208	13.078	9.834	24.518
8	.0155	.015	50.89	81.01	.513	.456	-12.810	13.476	10.014	26.352
9	.0172	.017	51.95	81.19	.523	.446	-12.529	13.757	9.789	31.456
10	.0185	.018	52.49	80.61	.529	.481	-12.386	13.900	10.551	33.829
11	.0205	.020	53.28	80.19	.537	.506	-12.176	14.110	11.097	37.460
12	.0224	.022	54.13	80.63	.545	.479	-11.952	14.334	10.516	40.949
13	.0245	.024	54.87	80.23	.553	.504	-11.755	14.531	11.051	44.783
14	.0262	.026	55.35	79.99	.558	.518	-11.629	14.657	11.360	47.886
15	.0323	.032	56.89	79.20	.573	.565	-11.220	15.066	12.401	59.023
16	.0396	.039	58.67	79.63	.591	.539	-10.749	15.537	11.840	72.350
17	.0464	.046	59.96	79.24	.604	.563	-10.407	15.879	12.352	84.764
18	.0524	.052	60.79	78.81	.612	.589	-10.190	16.096	12.918	95.718
19	.0595	.059	62.13	78.89	.626	.584	-9.832	16.454	12.814	108.680
20	.0663	.065	62.88	78.84	.633	.587	-9.636	16.650	12.678	121.094
21	.0723	.071	63.75	78.25	.642	.622	-9.405	16.881	13.645	132.048
22	.0795	.078	64.45	78.26	.649	.621	-9.218	17.068	13.637	145.192
23	.0866	.085	65.27	78.30	.658	.619	-9.002	17.284	13.581	158.154
24	.0923	.091	65.91	78.00	.664	.637	-8.833	17.453	13.980	168.561
25	.0994	.098	66.51	77.93	.670	.641	-8.674	17.612	14.071	181.523
26	.1063	.105	67.28	77.75	.678	.652	-8.469	17.817	14.300	194.119
27	.1126	.111	67.89	77.63	.684	.659	-8.307	17.979	14.466	205.621
28	.1198	.118	68.54	77.72	.691	.654	-8.135	18.151	14.348	218.765
29	.1266	.125	68.95	77.87	.695	.645	-8.028	18.258	14.154	231.180
30	.1434	.141	70.09	77.02	.706	.695	-7.726	18.560	15.263	261.880
31	.1611	.159	71.50	77.23	.720	.683	-7.353	18.933	14.984	294.164
32	.1787	.176	72.76	77.19	.733	.686	-7.013	19.273	15.046	326.395
33	.1965	.194	73.85	76.96	.744	.700	-6.729	19.557	15.352	358.791
34	.2134	.210	74.82	76.75	.754	.735	-6.472	19.814	16.141	389.645
35	.2315	.228	75.79	76.40	.763	.733	-6.217	20.069	16.082	422.688
36	.2483	.245	76.66	76.28	.772	.740	-5.962	20.304	16.236	453.359
37	.2664	.262	77.65	76.23	.782	.743	-5.723	20.563	16.300	486.403
38	.2834	.279	78.50	75.73	.791	.773	-5.498	20.788	16.967	517.439
39	.3014	.297	79.38	75.47	.800	.788	-5.266	21.020	17.298	550.300
40	.3312	.326	80.75	75.35	.813	.796	-4.904	21.382	17.459	604.704
41	.3614	.356	82.05	75.12	.827	.809	-4.559	21.727	17.765	659.838
42	.3914	.385	83.61	74.99	.842	.818	-4.145	22.141	17.942	714.607
43	.4214	.415	84.72	75.11	.854	.810	-3.851	22.435	17.775	769.376
44	.4513	.444	85.95	75.00	.866	.817	-3.525	22.761	17.921	823.962
45	.4814	.474	87.12	74.62	.878	.839	-3.217	23.069	18.423	878.914
46	.5116	.504	88.26	74.16	.889	.866	-2.908	23.378	19.004	934.046
47	.5419	.534	89.32	74.37	.900	.854	-2.633	23.653	18.747	989.365
48	.5713	.563	90.46	74.54	.911	.844	-2.326	23.960	18.531	1043.038
49	.6015	.592	91.30	74.13	.920	.869	-2.109	24.177	19.069	1098.172
50	.6316	.622	92.36	73.49	.931	.907	-1.824	24.462	19.909	1153.124
51	.6614	.651	93.21	73.48	.939	.908	-1.603	24.683	19.918	1207.528
52	.6914	.681	94.22	73.76	.949	.890	-1.337	24.949	19.526	1262.296
53	.7216	.711	95.02	73.53	.957	.905	-1.124	25.162	19.855	1317.431
54	.7514	.740	95.69	73.22	.964	.923	-.945	25.341	20.258	1371.834
55	.7814	.770	96.38	73.09	.971	.931	-.763	25.523	20.437	1426.603
56	.8116	.799	96.97	73.24	.977	.922	-.606	25.680	20.232	1481.737
57	.8415	.829	97.51	72.95	.982	.940	-.464	25.822	20.624	1536.324
58	.8714	.858	97.94	72.39	.987	.973	-.352	25.934	21.355	1590.910
59	.9013	.888	98.27	72.52	.990	.965	-.264	26.022	21.186	1645.497
60	.9313	.917	98.56	72.35	.993	.975	-.186	26.100	21.406	1700.266
61	.9614	.947	98.84	72.52	.996	.965	-.111	26.175	21.179	1755.217
62	.9915	.976	99.00	72.10	.997	.990	-.071	26.215	21.736	1810.169
63	1.0214	1.006	99.07	72.15	.998	.987	-.053	26.233	21.664	1864.755
64	1.0514	1.035	99.19	72.58	.999	.962	-.020	26.266	21.105	1919.524
65	1.0815	1.065	99.20	72.51	.999	.966	-.016	26.270	21.191	1974.475
66	1.1114	1.095	99.22	72.26	1.000	.981	-.012	26.274	21.524	2029.062
67	1.1413	1.124	99.27	72.70	1.000	.954	.003	26.289	20.944	2083.648
68	1.1713	1.154	99.25	72.33	1.000	.977	-.003	26.283	21.438	2138.417
69	1.2015	1.183	99.27	72.51	1.000	.966	.001	26.287	21.196	2193.551
70	1.2314	1.213	99.29	72.32	1.000	.977	.006	26.292	21.442	2248.138
71	1.2614	1.242	99.20	71.88	.999	1.003	-.016	26.269	22.022	2302.906
72	1.2913	1.272	99.23	72.06	1.000	.993	-.009	26.277	21.786	2357.493
73	1.3212	1.301	99.26	72.09	1.000	.991	-.001	26.285	21.751	2412.079
74	1.3514	1.331	99.25	72.26	1.000	.981	-.004	26.282	21.526	2467.213
75	1.3813	1.360	99.18	71.97	.999	.998	-.023	26.263	21.909	2521.800
76	1.4114	1.390	99.28	72.05	1.000	.993	.004	26.290	21.804	2576.751
77	1.4414	1.420	99.26	72.54	1.000	.964	-.002	26.284	21.161	2631.520
78	1.4715	1.449	99.14	72.41	.999	.972	-.033	26.253	21.323	2686.472
79	1.5014	1.479	99.15	72.10	.999	.990	-.031	26.255	21.732	2741.058
80	1.8766	1.848	99.09	72.34	.998	.976	-.046	26.240	21.423	3426.035
81	2.2513	2.217	99.12	71.92	.999	1.001	-.037	26.249	21.975	4110.099
82	2.6265	2.587	99.27	72.16	1.000	.987	.002	26.288	21.661	4795.076
83	3.0014	2.956	99.18	72.38	.999	.974	-.023	26.263	21.370	5479.505

Table B4

RUN NO. 3. POINT 2.

BOUNDARY LAYER PROPERTIES

	LINEAR INTERPOLATION TO WALL	STANDARD SUBLAYER FUNCTION FROM WALL TO Y+=35
FREE STREAM VELOCITY =	99.171	99.171
FREE STREAM TEMPERATURE =	73.270	
WALL TEMPERATURE =	90.270	
WALL HEAT FLUX =	.05020	
FREE STREAM DENSITY =	.07493	
FREE STREAM KINEMATIC VISCOSITY =	.0001639	
DENSITY OF FLUID AT WALL =	.07262	
KINEMATIC VISCOSITY OF FLUID AT WALL =	.0001733	
WALL/FREE STREAM DENSITY RATIO =	.96909	
LOCATION REYNOLDS NUMBER (REX) =	3428173.22	
INPUT VALUE OF VELOCITY DELTA =	.90000	
INPUT VALUE OF TEMPERATURE DELTA =	.97000	
CALCULATED DELTA =		.81093
DELTA 99.5% INPUT =	.00000	
DISPLACEMENT THICKNESS (DELSTAR) =	.12319	.12306
MOMENTUM THICKNESS (THETA) =	.08551	.08564
ENERGY-DISSIPATION THICKNESS =	.15118	.15148
ENTHALPY THICKNESS =	.00370	.00371
SHAPE FACTOR 12 (DELSTAR/THETA) =	1.44071	1.43351
SHAPE FACTOR 32 (ENERGY/THETA) =	1.76804	1.76469
MOMENTUM THICKNESS REYNOLDS NUMBER =	4310.75	4327.68
DISPLACEMENT THICKNESS REYNOLDS NUMBER =	6210.57	6203.78
SKIN FRICTION COEFFICIENT =	.002940	
FRICTION VELOCITY =	3.86252	
LAW OF THE WALL CONSTANT (K) =	.41000	
LAW OF THE WALL CONSTANT (C) =	5.00000	
WAKE STRENGTH =		.57972
CLAUSERS 'DELTA' INTEGRAL =	-2.88141	-3.06592
CLAUSERS 'G' INTEGRAL =	21.95430	21.63072
DISPLACEMENT THICKNESS - CONSTANT DENSITY =	.11569	.11941
MOMENTUM THICKNESS - CONSTANT DENSITY =	.08625	.08660
SHAPE FACTOR 12 - CONSTANT DENSITY =	1.34363	1.37890

LOCATION -X- 68.00000

Te = 0.2%

Table B5

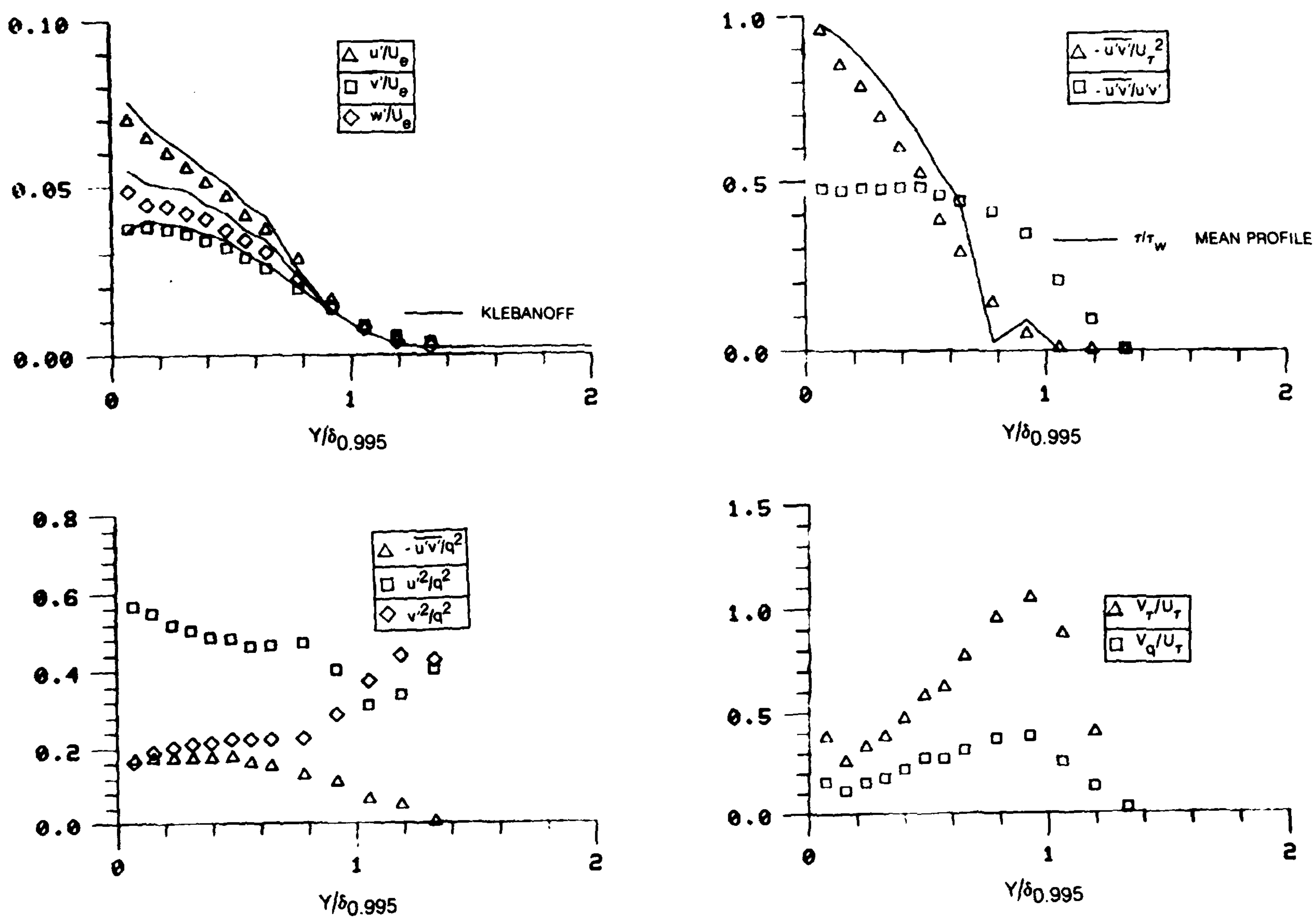

Figure B4A. Boundary Layer Turbulence Quantities $x = 68$ in, $T_e = 0.2\%$

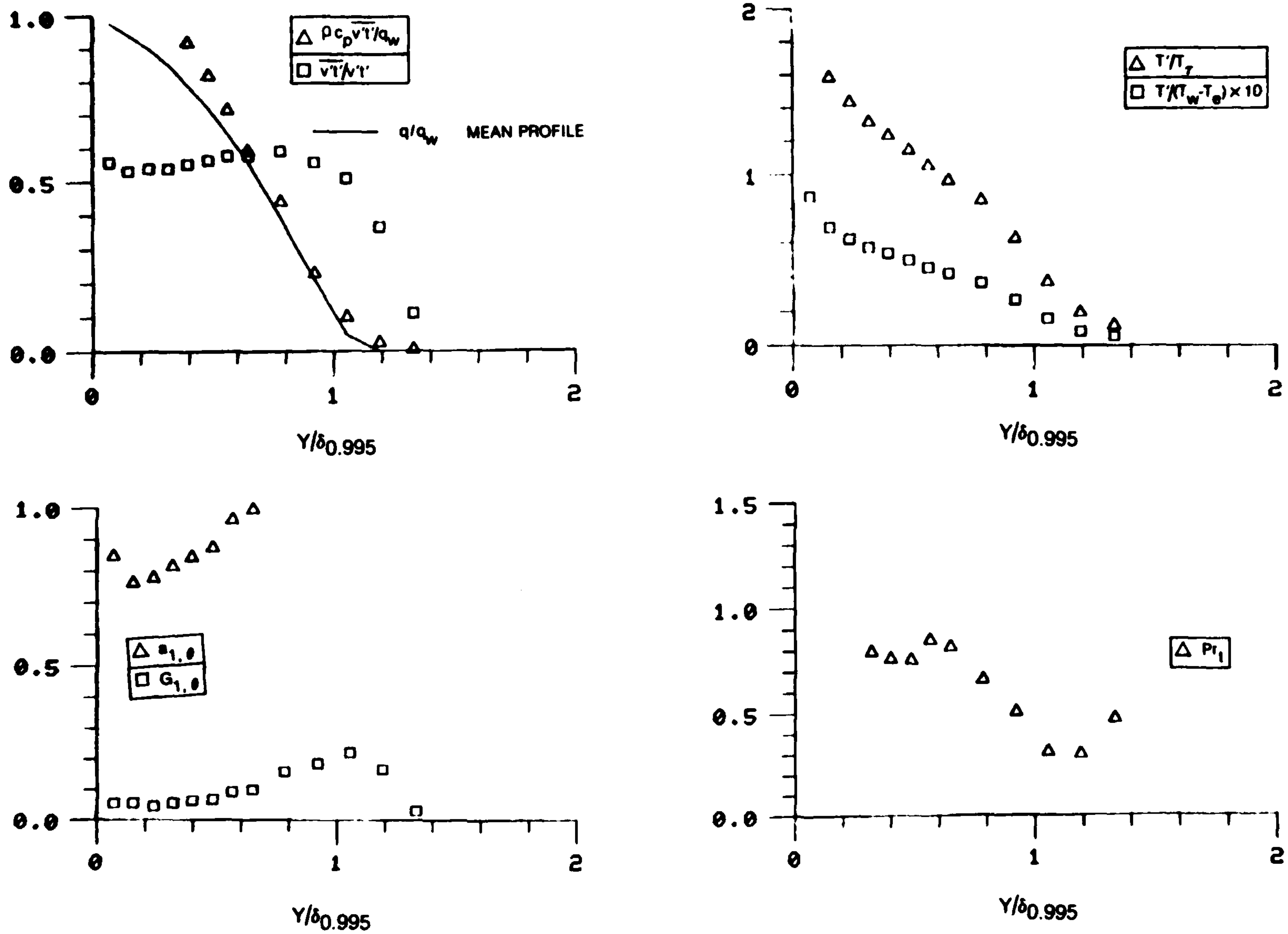

Figure B4B. Boundary Layer Turbulence Quantities, x = 68 in, T_e = 0.2%

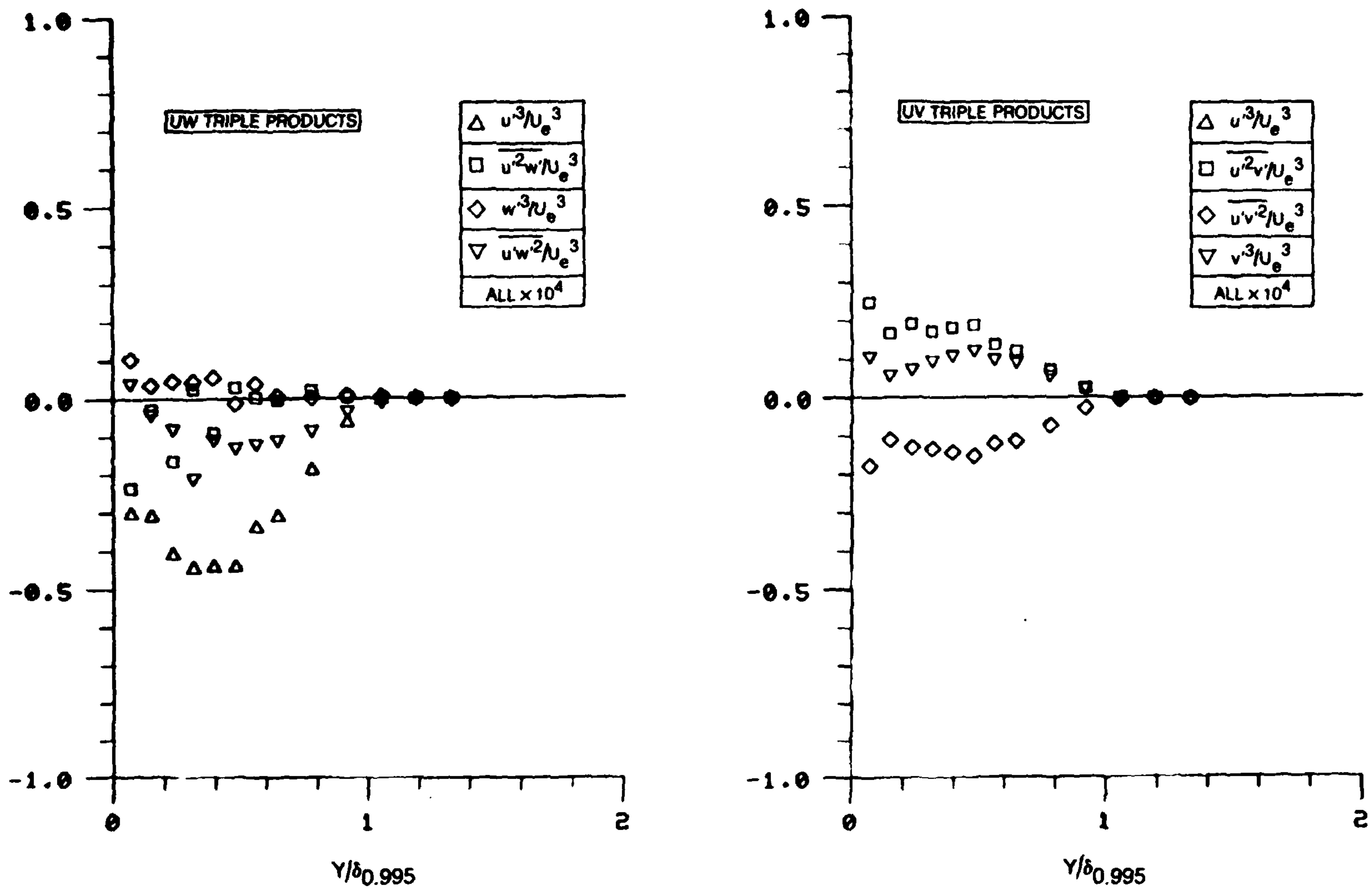

Figure B4C. Boundary Layer Triple Product Distributions $x = 68$ in, $T_e = 0.2\%$

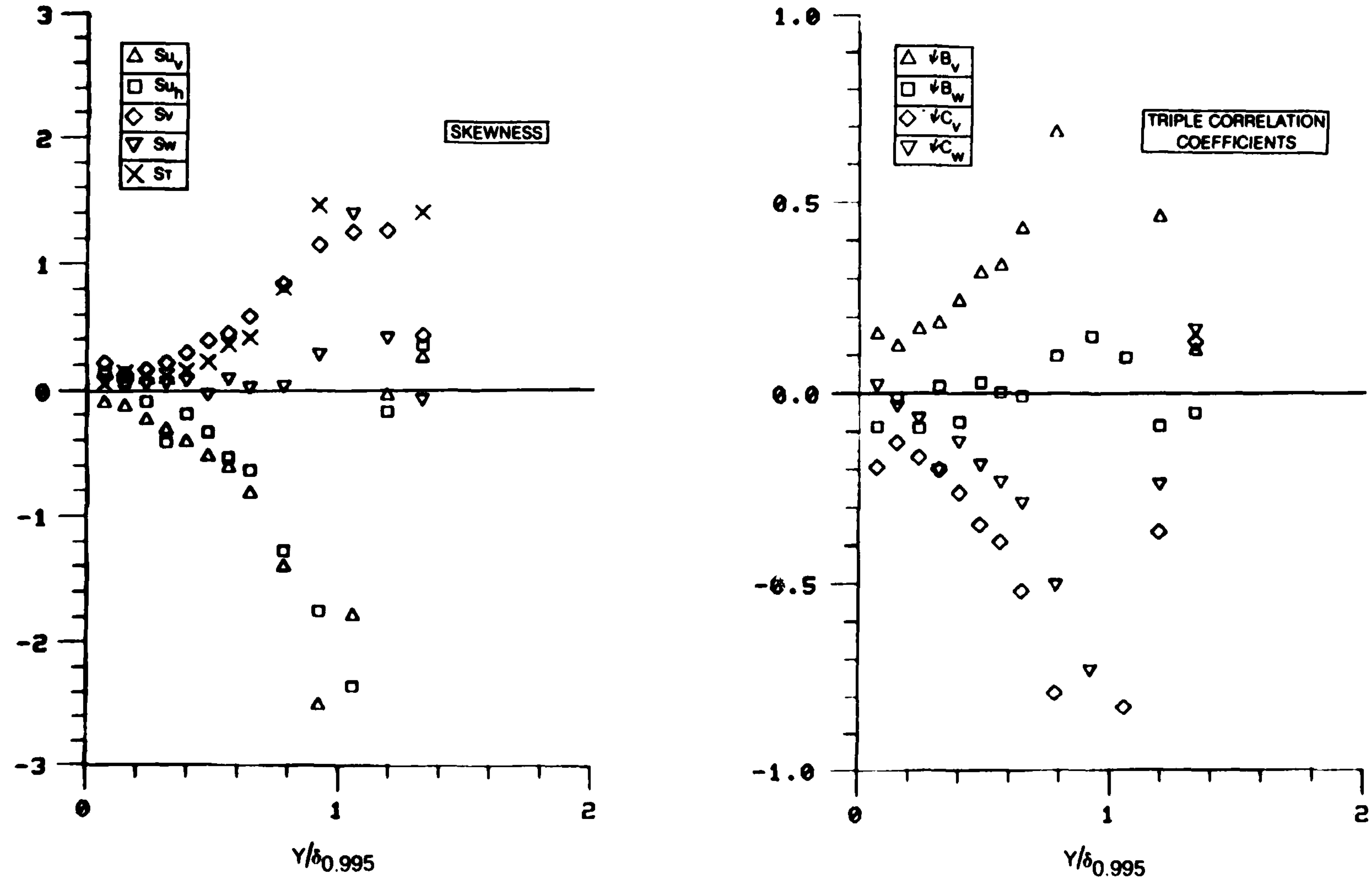

Figure B4D. Boundary Layer Skewness and Triple Product Correlation Coefficient Distributions $x = 68$ in, $T_e = 0.2\%$

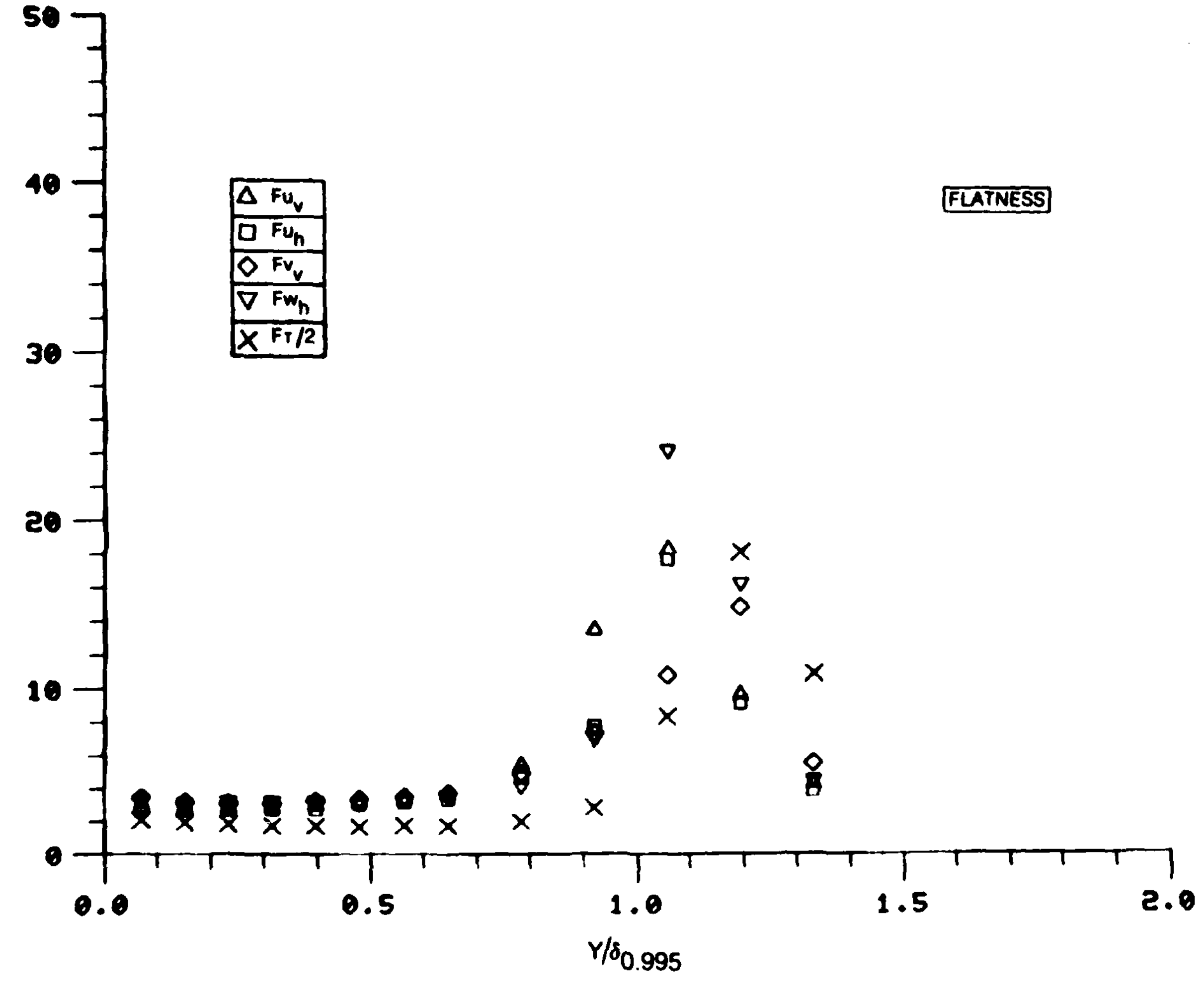

Figure B4E. Boundary Layer Flatness Distributions $x = 68$ in, $T_e = 0.2\%$

Fluctuating Profile Data

x = 68 in., Te = 0.2%

N	Y: INCHES	Y/ DELTA	U'/UE	V'/UE	W'/UE	$\sqrt{\overline{U'V'}}$/UE	$\overline{U'V'}$/ UTAU2	$\overline{U'V'}$/U'V'	C/UE
1	3.000	4.110	.0026	.0019	.0011	.002	.0048	-.1956	.0034
2	.050	.068	.0700	.0374	.0485	.0362	.9599	.4797	.093[illegible]
3	.110	.151	.0643	.0378	.0444	.0360	.8518	.4719	.086[illegible]
4	.170	.233	.0599	.0373	.0442	.0346	.7857	.4807	.08[illegible]
5	.230	.315	.0556	.0360	.0420	.0324	.6914	.4766	.078[illegible]
6	.290	.397	.0511	.0339	.0404	.0304	.6051	.4813	.07[illegible]
7	.350	.479	.0470	.0318	.0368	.0282	.5238	.4835	.0677
8	.410	.562	.0410	.0284	.0339	.0242	.3841	.4582	.060[illegible]
9	.470	.644	.0370	.0255	.0303	.0210	.2894	.4419	.054[illegible]
10	.570	.761	.0280	.0194	.0223	.0146	.1401	.4100	.040[illegible]
11	.670	.918	.0163	.0138	.0142	.0085	.0469	.3461	.0256
12	.770	1.055	.0078	.0086	.0079	.0035	.0062	.2071	.014[illegible]
13	.870	1.192	.0047	.0054	.0038	.0018	.0021	.0930	.0061
14	.970	1.329	.0036	.0037	.0023	.0003	.0001	.0076	.00[illegible]
15	1.500	2.055	.0031	.0019	.0014	.0009	-.0005	-.1266	.0039
16	3.000	4.110	.0027	.0016	.0011	.0003	-.0001	-.0227	.003[illegible]
17	.000	.000	.0000	.0000	.0000	.0000	.0000	.0000	.000[illegible]
18	.000	.000	.0000	.0000	.0000	.0000	.0000	.0000	.000[illegible]

N	Y: INCHES	Y/ DELTA	$\overline{V'U'}$/Q2	U'2/Q2	V'2/Q2	W'2/Q2	VTAU/ UTAU	VC/ UTAU	$\overline{V'T'}$RHO*CP/ QWALL
1	3.000	4.110	.6413	.5756	.3090	.1154	-.0071	-.0004	.0000
2	.050	.068	.1669	.5658	.1621	.2721	.3851	.1622	
3	.110	.151	.1720	.5491	.1894	.2615	.2626	.1156	
4	.170	.233	.1725	.5176	.2002	.2822	.3329	.1559	
5	.230	.315	.1710	.5030	.2105	.2865	.3841	.1773	1.0114
6	.290	.397	.1708	.4846	.2128	.3026	.4719	.2223	.916[illegible]
7	.350	.479	.1742	.4826	.2212	.2962	.5841	.2780	.618[illegible]
8	.410	.562	.1606	.4627	.2223	.3150	.6199	.2724	.714[illegible]
9	.470	.644	.1501	.4656	.2222	.3123	.7707	.3182	.588[illegible]
10	.570	.761	.1289	.4724	.2266	.3010	.9548	.3706	.4387
11	.670	.918	.1067	.4032	.2886	.3062	1.0501	.3851	.22[illegible]
12	.770	1.055	.0634	.3112	.3739	.3149	.8799	.2564	.101[illegible]
13	.870	1.192	.0477	.3387	.4398	.2215	.3980	.1332	.025[illegible]
14	.970	1.329	.0035	.4024	.4272	.1704	-.7050	.0269	.0024
15	1.500	2.055	-.0472	.6340	.2446	.1214	.0365	.0024	-.00[illegible]
16	3.000	4.110	-.0097	.6742	.2242	.1016	-.1007	-.0020	.00[illegible]
17	.000	.000	.0000	.0000	.0000	.0000	.0000	.0000	.000[illegible]
18	.000	.000	.0000	.0000	.0000	.0000	.0000	.0000	.000[illegible]

N	Y: INCHES	Y/ DELTA	$\overline{V'T'}$/V'T'	T'/TTAU	T'/(TW-TE)	A10	G10	PRT
1	3.000	4.110	-.0007	.0997	.0043	.0000	.0000	.0000
2	.050	.068	.5591	2.0074	.0870	.8470	.0555	
3	.110	.151	.5326	1.5867	.0688	.7619	.0553	
4	.170	.233	.5366	1.4331	.0621	.7793	.0436	
5	.230	.315	.5392	1.3199	.0572	.8165	.0538	.7930
6	.290	.397	.5515	1.2348	.0535	.8462	.0637	.7628
7	.350	.479	.5626	1.1451	.0496	.8745	.0666	.7569
8	.410	.562	.5762	1.0541	.0457	.9637	.0933	.8496
9	.470	.644	.5773	.9665	.0419	.9954	.1002	.8172
10	.570	.781	.5912	.8448	.0366	1.1985	.1596	.6602
11	.670	.918	.5567	.6254	.0271	1.4081	.1866	.5079
12	.770	1.055	.5066	.3713	.0161	2.2007	.2208	.3105
13	.870	1.192	.3626	.1964	.0085	2.3548	.1667	.2992
14	.970	1.329	.1114	.1206	.0052	1.8659	.0295	.4731
15	1.500	2.055	-.0163	.1103	.0048	-.0569	.0020	1.8446
16	3.000	4.110	.0104	.1044	.0045	.0802	.0000	4.9663
17	.000	.000	.0000	.0000	.0000	.0000	.0000	.0000
18	.000	.000	.0000	.0000	.0000	.0000	.0000	.0000

Table B6A

Fluctuating Profile Data

x = 68 in., Te = 0.2%

N	Y: INCHES	Y/ DELTA	U'3/UE3 X 10000	U'2W'/ UE3 X 10000	W'3/UE3 X 10000	U'W'2/ UE3 X 10000	U'2V'/ UE3 X 10000	U'V'2/ UE3 X 10000	V'3/UE3 X 10000
1	3.000	4.110	-.0000	-.0000	-.0000	-.0000	.0000	-.0000	-.0000
2	.050	.068	-.3027	-.2350	.1026	.0427	.2473	-.1758	.1107
3	.110	.151	-.3062	-.0303	.0350	-.0389	.1669	-.1102	.0624
4	.170	.233	-.4099	-.1656	.0443	-.0778	.1947	-.1298	.0786
5	.230	.315	-.4445	.0270	.0462	-.2068	.1752	-.1326	.0966
6	.290	.397	-.4421	-.0908	.0561	-.1059	.1835	-.1427	.1117
7	.350	.479	-.4408	.0288	-.0140	-.1255	.1911	-.1530	.1255
8	.410	.562	-.3394	.0026	.0360	-.1169	.1372	-.1198	.1022
9	.470	.644	-.3092	-.0040	.0081	-.1057	.1239	-.1138	.0967
10	.570	.781	-.1871	.0234	.0041	-.0806	.0751	-.0702	.0606
11	.670	.918	-.0613	.0079	.0086	-.0280	.0261	-.0264	.0297
12	.770	1.055	-.0046	.0007	.0074	-.0056	.0037	-.0039	.0076
13	.670	1.192	-.0001	-.0001	.0002	-.0002	.0004	-.0005	.0000
14	.970	1.329	.0001	-.0000	-.0000	.0000	.0001	.0001	.0000
15	1.500	2.055	.0000	.0000	.0000	.0000	.0000	.0000	.0000
16	3.000	4.110	.0000	.0000	.0000	-.0000	-.0000	.0000	-.0000
17	.000	.000	.0000	.0000	.0000	.0000	.0000	.0000	.0000
18	.000	.000	.0000	.0000	.0000	.0000	.0000	.0000	.0000

N	Y: INCHES	Y/ DELTA	SU V	SU W	SV	SW	ST	PSIEV	PSIEW
1	3.000	4.110	-.1433	-.0034	-.0398	-.4208	.0273	.0090	-.1613
2	.050	.068	-.1066	.1372	.2109	.0843	.0529	.1552	-.0861
3	.110	.151	-.1398	.0548	.1158	.0355	.1333	.1211	-.0147
4	.170	.233	-.2381	-.0950	.1523	.0542	.1036	.1682	-.0900
5	.230	.315	-.3240	-.4190	.2117	.0649	.1094	.1828	.0179
6	.290	.397	-.4141	-.1899	.2855	.0846	.1525	.2407	-.0736
7	.350	.479	-.5299	-.3355	.3894	-.0251	.2221	.3149	.0306
8	.410	.562	-.6190	-.5386	.4446	.0937	.3597	.3339	.0025
9	.470	.644	-.6198	-.6776	.5799	.0328	.4162	.4319	-.0077
10	.570	.781	-1.3989	-1.2780	.8360	.0376	.8076	.6876	.1001
11	.670	.918	-2.5019	-1.7551	1.1376	.2880	1.4502	1.0418	.1522
12	.770	1.055	-1.7936	-2.3528	1.2399	1.3923	3.0275	1.0351	.0955
13	.870	1.192	-.0491	-.1697	1.2477	.4168	4.1170	.4643	-.0832
14	.970	1.329	.2494	.3479	.4267	-.0666	1.3920	.1169	-.0497
15	1.500	2.055	.1154	-.2066	.1025	.1279	-.1452	.0128	.0441
16	3.000	4.110	.2069	-.8690	-.0228	.0671	-.2043	-.0607	.0233
17	.000	.000	.0000	.0000	.0000	.0000	.0000	.0000	.0000
18	.000	.000	.0000	.0000	.0000	.0000	.0000	.0000	.0000

N	Y: INCHES	Y/ DELTA	PSICV	PSICW	FU V	FU W	FU V	FU W	FT
1	3.000	4.110	-.0267	-.2917	3.0291	3.2710	3.0379	3.7406	2.6773
2	.050	.068	-.1925	.0260	2.8096	2.6306	3.3938	3.3530	4.1134
3	.110	.151	-.1278	-.0291	2.7371	2.6681	3.1789	3.1543	3.6063
4	.170	.233	-.1675	-.0617	2.7174	2.6968	3.0549	3.2251	3.7141
5	.230	.315	-.1965	-.1963	2.8463	2.7914	3.1224	3.2488	3.4637
6	.290	.397	-.2617	-.1210	2.9808	2.7615	3.2415	3.2765	3.5706
7	.350	.479	-.3459	-.1838	3.1622	2.9865	3.3747	3.0655	3.3766
8	.410	.562	-.3895	-.2304	3.2922	3.1745	3.4584	3.3665	3.4265
9	.470	.644	-.5204	-.2833	3.6550	3.3490	3.7791	3.5881	3.4877
10	.570	.781	-.7887	-.5004	5.4422	4.6673	4.9047	4.1493	3.9211
11	.670	.918	-1.0312	-.7246	13.4379	7.7491	7.3122	7.0297	5.6717
12	.770	1.055	-.8292	-1.0129	18.1795	17.5620	10.7762	23.9625	16.6571
13	.670	1.192	-.3642	-.2370	9.5933	9.0941	14.7623	16.1623	30.0723
14	.970	1.329	.1385	.1726	4.2825	3.8376	5.5361	4.5272	21.6237
15	1.500	2.055	.0895	.0575	3.1115	2.5489	2.9376	2.9466	2.8134
16	3.000	4.110	.0143	-.2636	3.1062	2.9553	2.9922	3.0261	2.6764
17	.000	.000	.0000	.0000	.0000	.0000	.0000	.0000	.0000
18	.000	.000	.0000	.0000	.0000	.0000	.0000	.0000	.0000

Table B6B

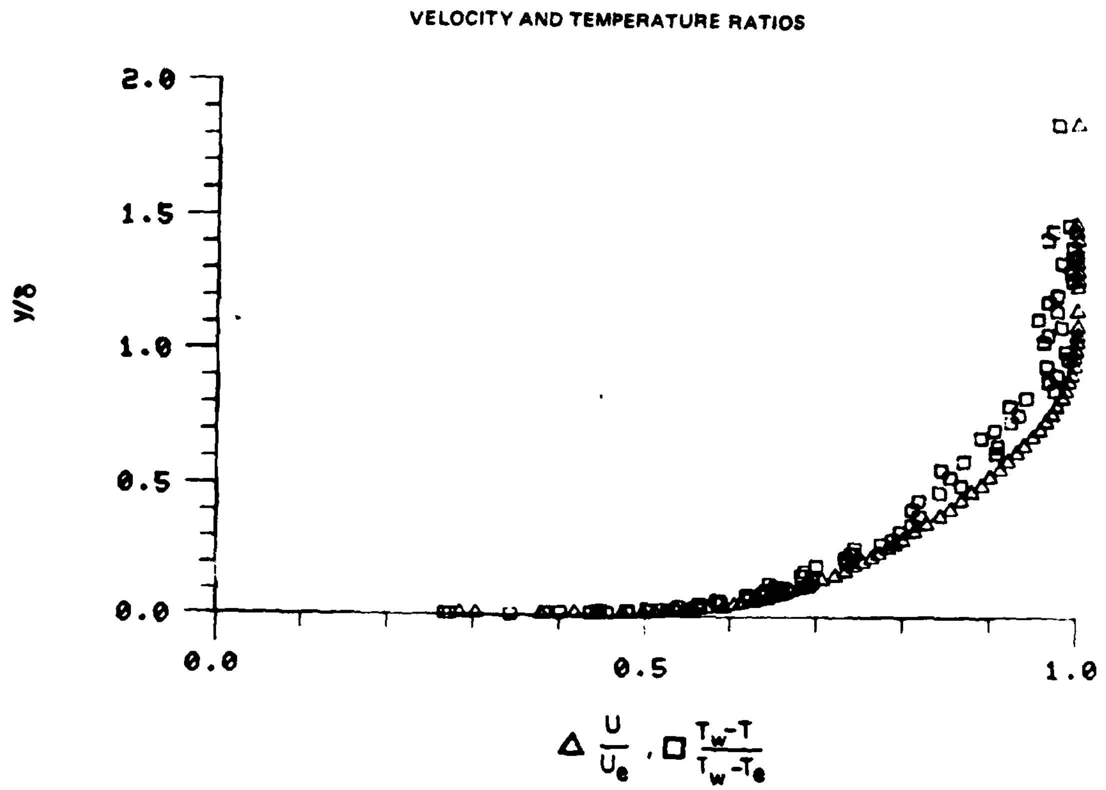

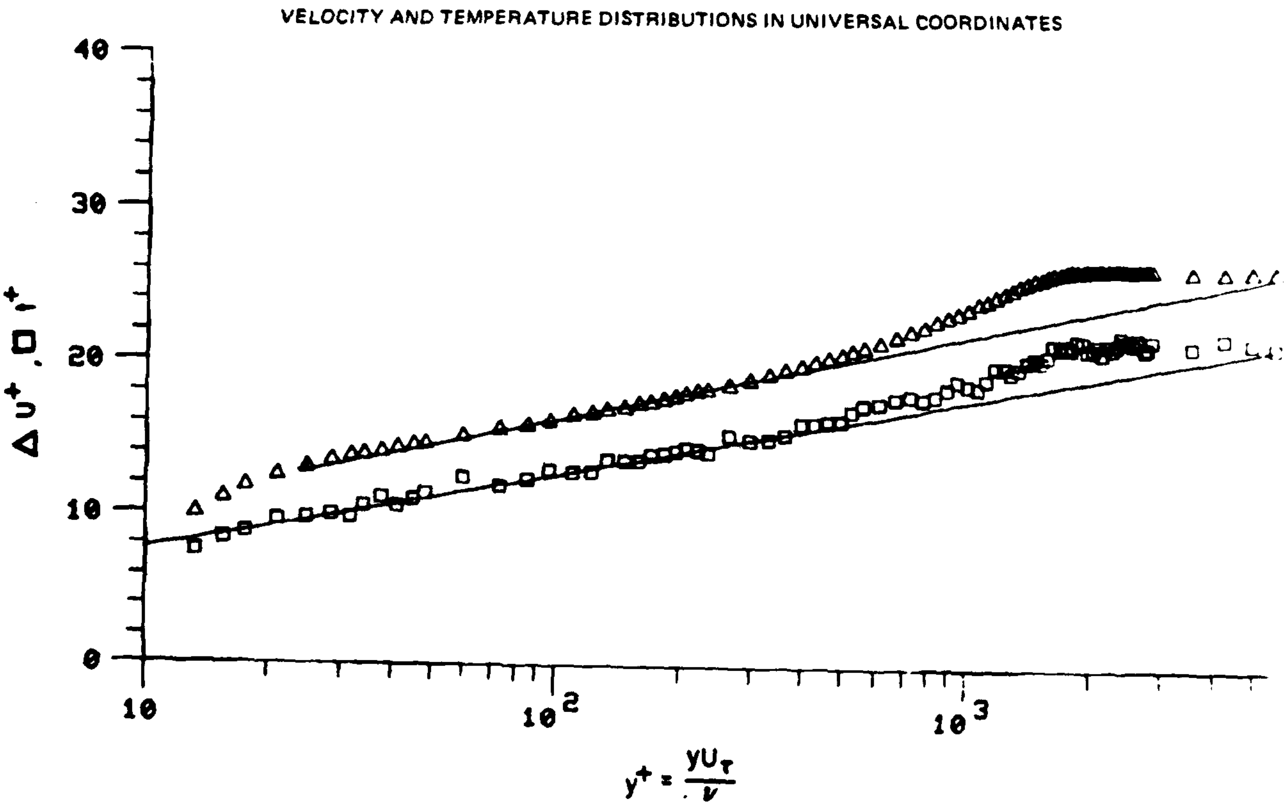

Figure B5. Mean Velocity and Temperature Profiles x = 84 in., Te = 0.2%

78-12-100-1

Mean Profile Data

x = 84 in., Te = 0.2%

N	Y INCHES	Y/DELTA	U FT/SEC	T DEG.F	U/UE	THETA	U-UE UTAU	U(+)	T(+)	Y(+)
1	.0073	.009	38.89	84.68	.392	.329	-15.608	10.068	7.495	13.615
2	.0086	.011	42.91	83.58	.433	.394	-14.566	11.109	6.977	16.402
3	.0094	.012	44.47	83.36	.448	.407	-14.163	11.512	9.272	17.515
4	.0103	.013	46.27	83.59	.467	.393	-13.695	11.980	8.963	19.168
5	.0118	.015	48.69	82.98	.491	.429	-13.068	12.607	9.773	21.974
6	.0132	.016	50.13	82.44	.505	.460	-12.704	12.971	10.495	24.575
7	.0150	.019	51.77	82.26	.522	.471	-12.272	13.403	10.739	27.918
8	.0156	.019	51.99	82.26	.524	.471	-12.215	13.460	10.743	29.032
9	.0174	.021	53.13	81.90	.536	.493	-11.921	13.754	11.227	32.376
10	.0196	.024	54.35	81.73	.546	.502	-11.603	14.072	11.449	36.462
11	.0213	.026	54.80	81.56	.553	.511	-11.467	14.166	11.651	39.620
12	.0232	.029	55.64	81.36	.561	.524	-11.270	14.405	11.942	43.149
13	.0247	.030	56.07	81.55	.565	.513	-11.158	14.517	11.695	45.936
14	.0263	.032	56.80	81.67	.573	.506	-10.969	14.706	11.538	48.905
15	.0286	.035	57.37	81.65	.578	.507	-10.823	14.853	11.565	53.180
16	.0303	.037	57.83	81.55	.583	.513	-10.702	14.973	11.696	56.337
17	.0342	.040	58.34	81.39	.588	.523	-10.570	15.105	11.914	59.667
18	.0386	.048	59.80	80.65	.603	.554	-10.193	15.483	12.632	71.755
19	.0456	.056	61.23	80.67	.617	.565	-9.824	15.851	12.872	84.757
20	.0525	.065	62.44	79.93	.630	.608	-9.509	16.167	13.865	97.574
21	.0586	.072	63.56	79.81	.641	.615	-9.213	16.462	14.020	108.904
22	.0654	.081	64.42	79.73	.650	.620	-8.996	16.679	14.139	121.535
23	.0723	.089	65.44	79.74	.660	.619	-8.733	16.942	14.114	134.352
24	.0763	.097	66.24	79.16	.668	.653	-8.525	17.151	14.893	145.497
25	.0857	.106	67.15	79.64	.677	.625	-8.290	17.366	14.249	159.242
26	.0925	.114	67.75	79.25	.683	.648	-8.134	17.541	14.773	171.873
27	.0983	.121	68.36	79.13	.689	.655	-7.978	17.696	14.933	182.646
28	.1056	.130	69.05	79.35	.696	.642	-7.798	17.877	14.641	196.206
29	.1125	.139	69.79	78.62	.704	.685	-7.606	18.070	15.627	209.023
30	.1183	.146	70.31	78.74	.709	.678	-7.471	18.204	15.465	219.796
31	.1257	.155	70.81	78.83	.714	.673	-7.342	18.333	15.343	233.541
32	.1327	.164	71.39	78.75	.720	.678	-7.191	18.484	15.452	246.544
33	.1496	.185	72.93	78.58	.735	.688	-6.794	18.882	15.682	277.935
34	.1672	.206	74.24	78.33	.749	.702	-6.454	19.221	16.005	310.627
35	.1844	.227	75.50	77.83	.761	.732	-6.128	19.547	16.679	342.576
36	.2024	.250	76.49	77.69	.771	.740	-5.871	19.804	16.865	376.010
37	.2193	.270	77.79	77.75	.784	.737	-5.535	20.140	16.794	407.402
38	.2374	.293	78.89	77.41	.795	.757	-5.251	20.425	17.247	441.022
39	.2547	.314	80.04	77.40	.807	.757	-4.953	20.723	17.256	473.157
40	.2724	.336	80.87	77.04	.816	.779	-4.737	20.936	17.747	506.034
41	.2897	.357	82.09	76.65	.828	.801	-4.423	21.252	18.261	538.169
42	.3075	.379	82.87	76.50	.836	.810	-4.220	21.455	18.469	571.232
43	.3371	.416	84.65	76.82	.854	.791	-3.759	21.917	18.040	626.214
44	.3673	.453	86.24	76.67	.870	.800	-3.347	22.328	18.235	682.310
45	.3975	.490	87.62	75.93	.884	.844	-2.989	22.686	19.232	738.406
46	.4276	.527	88.97	75.48	.897	.870	-2.640	23.035	19.834	794.316
47	.4576	.565	90.22	75.44	.910	.872	-2.317	23.358	19.881	850.412
48	.4879	.602	91.58	75.06	.923	.895	-1.965	23.710	20.400	906.722
49	.5175	.638	92.82	75.28	.936	.882	-1.645	24.031	20.095	961.304
50	.5477	.675	93.90	74.71	.947	.915	-1.364	24.311	20.664	1017.4[illegible]
51	.5777	.712	94.82	74.57	.956	.923	-1.126	24.549	21.051	1073.1[illegible]
52	.6077	.749	95.82	74.62	.966	.921	-.867	24.809	20.988	1128.649
53	.6377	.786	96.56	74.50	.974	.928	-.676	24.999	21.145	1184.573
54	.6675	.823	97.26	74.10	.981	.951	-.490	25.185	21.685	1239.926
55	.6974	.860	97.80	73.89	.986	.963	-.354	25.321	21.960	1295.465
56	.7275	.897	98.28	74.06	.991	.952	-.230	25.445	21.706	1351.375
57	.7577	.934	98.67	74.11	.995	.951	-.130	25.546	21.675	1407.471
58	.7874	.971	98.94	74.07	.998	.953	-.059	25.616	21.720	1462.639
59	.8177	1.008	98.99	73.70	.998	.975	-.046	25.630	22.223	1518.920
60	.8477	1.045	99.07	73.39	.999	.993	-.026	25.649	22.635	1574.645
61	.8775	1.082	99.14	73.71	1.000	.974	-.007	25.668	22.200	1629.998
62	.9075	1.119	99.20	73.71	1.000	.974	.007	25.682	22.206	1685.722
63	.9376	1.156	99.18	73.66	1.000	.977	.003	25.679	22.269	1741.633
64	.9674	1.193	99.13	73.41	1.000	.992	-.010	25.665	22.613	1796.966
65	.9977	1.230	99.14	73.27	1.000	1.000	-.008	25.667	22.792	1853.267
66	1.0276	1.267	99.12	73.54	.999	.984	-.013	25.662	22.435	1908.806
67	1.0575	1.304	99.19	73.85	1.000	.966	.086	25.681	22.025	1964.345
68	1.0677	1.341	99.18	73.60	1.000	.981	.001	25.677	22.354	2020.441
69	1.1176	1.378	99.19	73.58	1.000	.982	.006	25.681	22.383	2075.980
70	1.1476	1.415	99.15	73.51	1.000	.986	-.004	25.671	22.481	2131.704
71	1.1776	1.452	99.16	73.88	1.000	.964	-.002	25.673	21.980	2187.429
72	1.2073	1.489	99.24	73.71	1.001	.974	.018	25.693	22.204	2242.596
73	1.2375	1.526	99.22	73.84	1.000	.966	.012	25.687	22.032	2298.692
74	1.2675	1.563	99.10	73.52	.999	.985	-.020	25.656	22.458	2354.417
75	1.2976	1.600	99.14	73.28	1.000	1.000	-.009	25.666	22.785	2410.327
76	1.3272	1.637	99.17	73.65	1.000	.977	-.001	25.674	22.282	2465.308
77	1.3576	1.674	99.06	73.22	.999	1.003	-.028	25.647	22.868	2521.776
78	1.3875	1.711	99.10	73.73	.999	.973	-.020	25.656	22.184	2577.315
79	1.4177	1.748	99.11	73.55	.999	.983	-.017	25.658	22.417	2633.411
80	1.4477	1.785	99.12	73.25	.999	1.001	-.014	25.662	22.829	2689.135
81	1.4775	1.822	99.12	73.51	.999	.986	-.014	25.661	22.472	2744.488
82	1.5074	1.859	99.12	74.03	1.000	.955	-.013	25.663	21.780	2800.027
83	1.8824	2.321	99.08	73.63	.999	.979	-.024	25.652	22.312	3496.583
84	2.2576	2.784	99.05	73.63	.999	.979	-.030	25.645	22.309	4193.511
85	2.6325	3.246	99.18	73.41	1.000	.992	.001	25.676	22.613	4889.882
86	3.0077	3.709	99.05	73.70	.999	.975	-.031	25.644	22.216	5586.810

Table B7

RUN NO. 3. POINT 1.

BOUNDARY LAYER PROPERTIES

	LINEAR INTERPOLATION TO WALL	STANDARD SUBLAYER FUNCTION FROM WALL TO Y+=35
FREE STREAM VELOCITY =	99.264	99.264
FREE STREAM TEMPERATURE =	71.940	
WALL TEMPERATURE =	88.630	
WALL HEAT FLUX =	.05020	
FREE STREAM DENSITY =	.07512	
FREE STREAM KINEMATIC VISCOSITY =	.0001632	
DENSITY OF FLUID AT WALL =	.07283	
KINEMATIC VISCOSITY OF FLUID AT WALL =	.0001724	
WALL/FREE STREAM DENSITY RATIO =	.96956	
LOCATION REYNOLDS NUMBER (REX) =	4257589.31	
INPUT VALUE OF VELOCITY DELTA =	1.13000	
INPUT VALUE OF TEMPERATURE DELTA =	1.25000	
CALCULATED DELTA =		1.01545
DELTA 99.5% INPUT =	.00000	
DISPLACEMENT THICKNESS (DELSTAR) =	.15211	.15221
MOMENTUM THICKNESS (THETA) =	.10696	.10706
ENERGY-DISSIPATION THICKNESS =	.18910	.18914
ENTHALPY THICKNESS =	.00448	.00448
SHAPE FACTOR 12 (DELSTAR/THETA) =	1.42212	1.42180
SHAPE FACTOR 32 (ENERGY/THETA) =	1.76801	1.76676
MOMENTUM THICKNESS REYNOLDS NUMBER =	5421.16	5426.27
DISPLACEMENT THICKNESS REYNOLDS NUMBER =	7709.54	7715.06
SKIN FRICTION COEFFICIENT =	.002806	
FRICTION VELOCITY =	3.77632	
LAW OF THE WALL CONSTANT (K) =	.41000	
LAW OF THE WALL CONSTANT (C) =	5.00000	
WAKE STRENGTH =		.60112
CLAUSERS 'DELTA' INTEGRAL =	-3.76703	-3.86635
CLAUSERS 'G' INTEGRAL =	27.56274	27.56606
DISPLACEMENT THICKNESS - CONSTANT DENSITY =	.14552	.14765
MOMENTUM THICKNESS - CONSTANT DENSITY =	.10785	.10795
SHAPE FACTOR 12 - CONSTANT DENSITY =	1.34934	1.36957

LOCATION -X- 84.00000

Te = 0.2%

Table B8

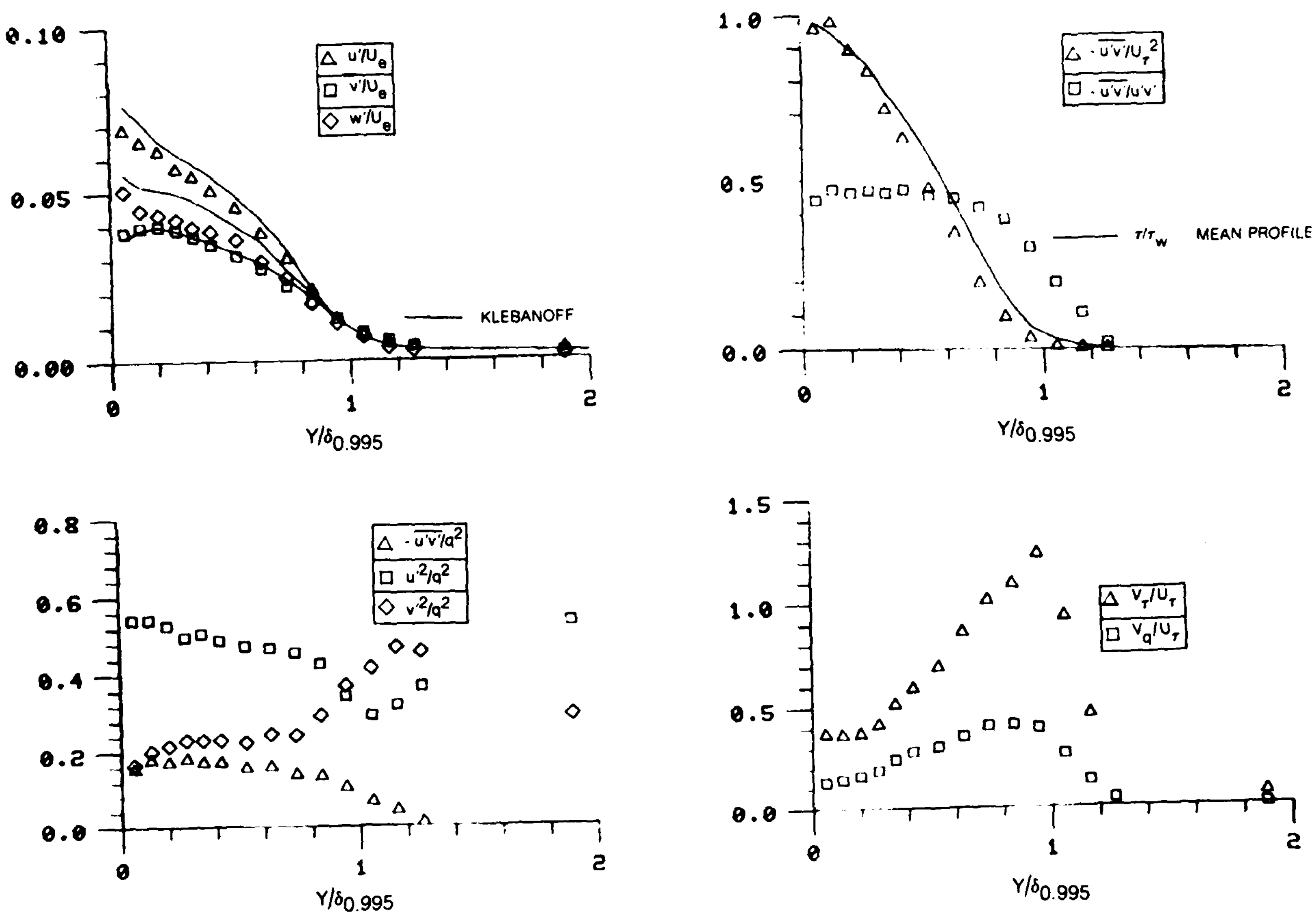

Figure B6A. Boundary Layer Turbulence Quantities $x = 84$ in, $T_\epsilon = 0.2\%$

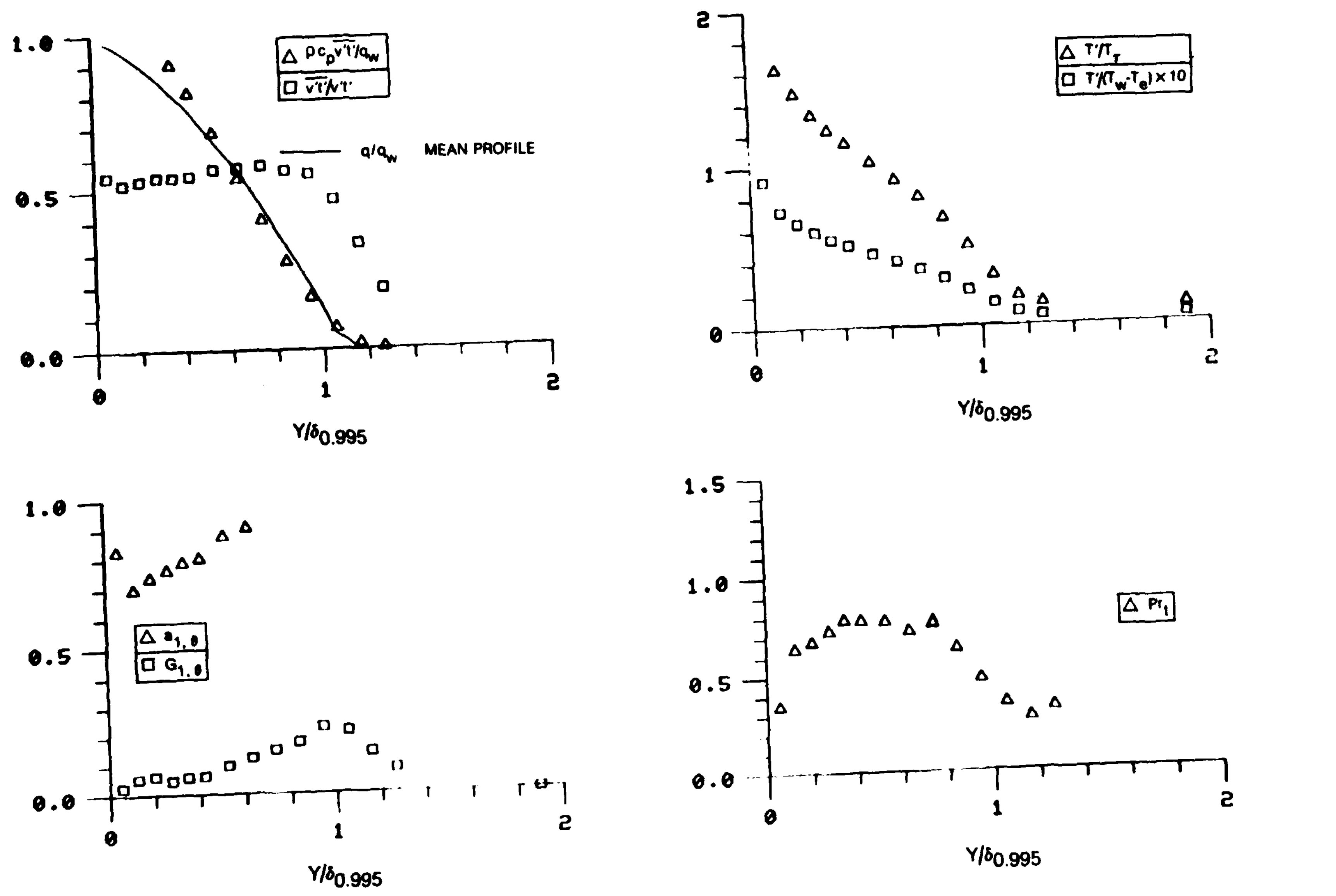

Figure B6B. Boundary Layer Turbulence Quantities, x = 84 in, T_e = 0.2%

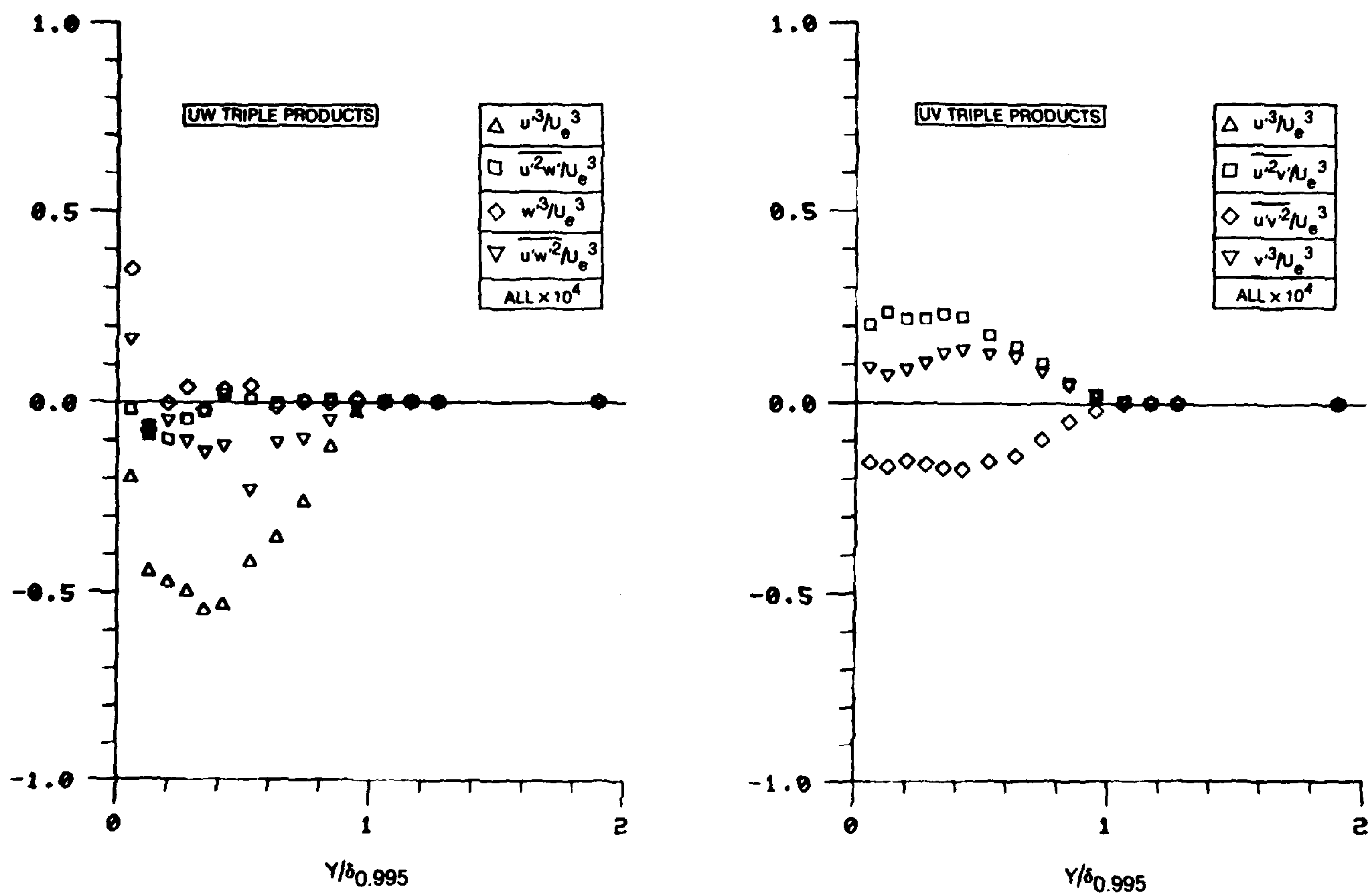

Figure B6C. Boundary Layer Triple Product Distributions $x = 84$ in, $T_e = 0.2\%$

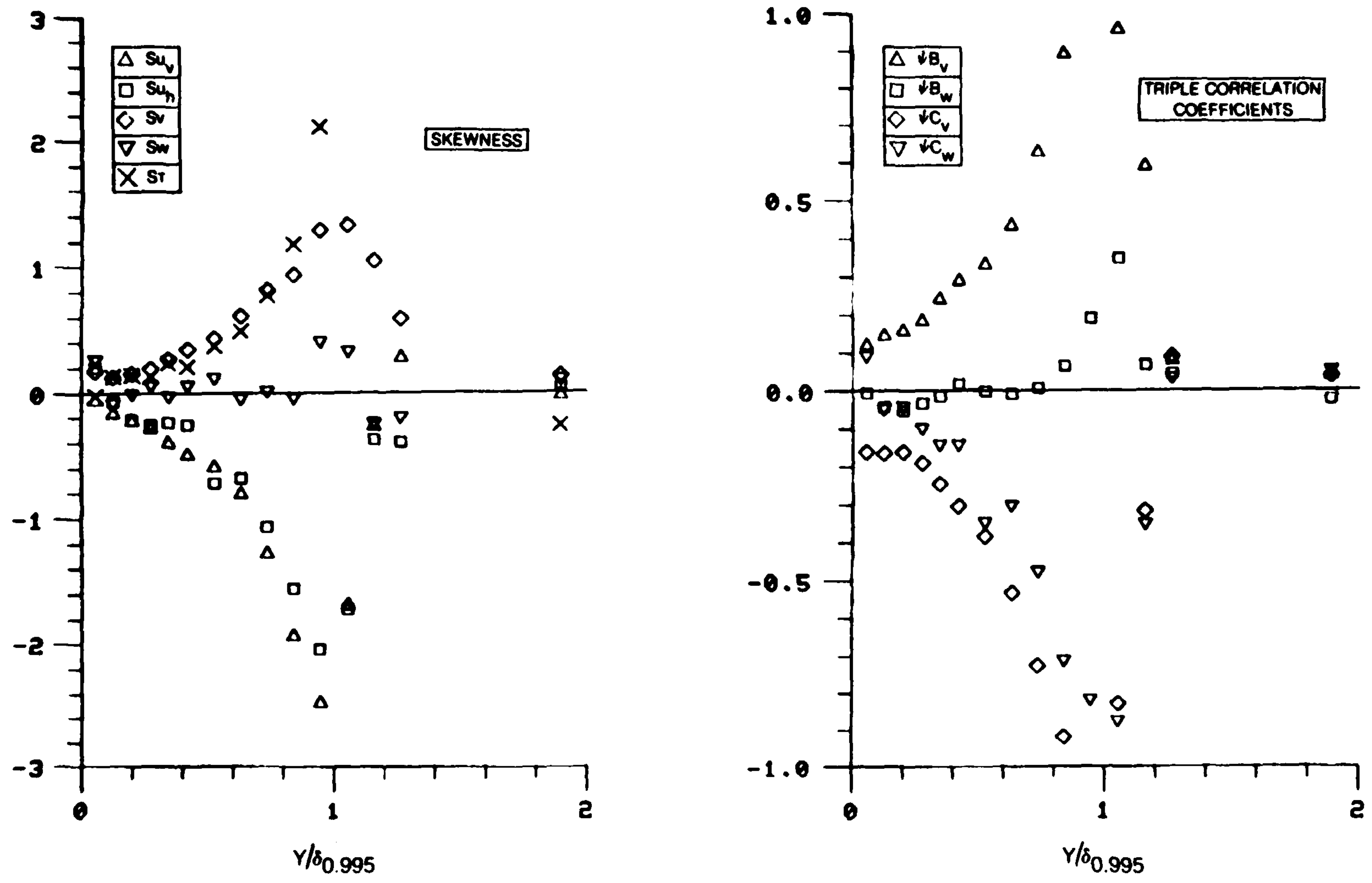

Figure B6D. Boundary Layer Skewness and Triple Product Correlation Coefficient Distributions $x = 84$ in, $T_e = 0.2\%$

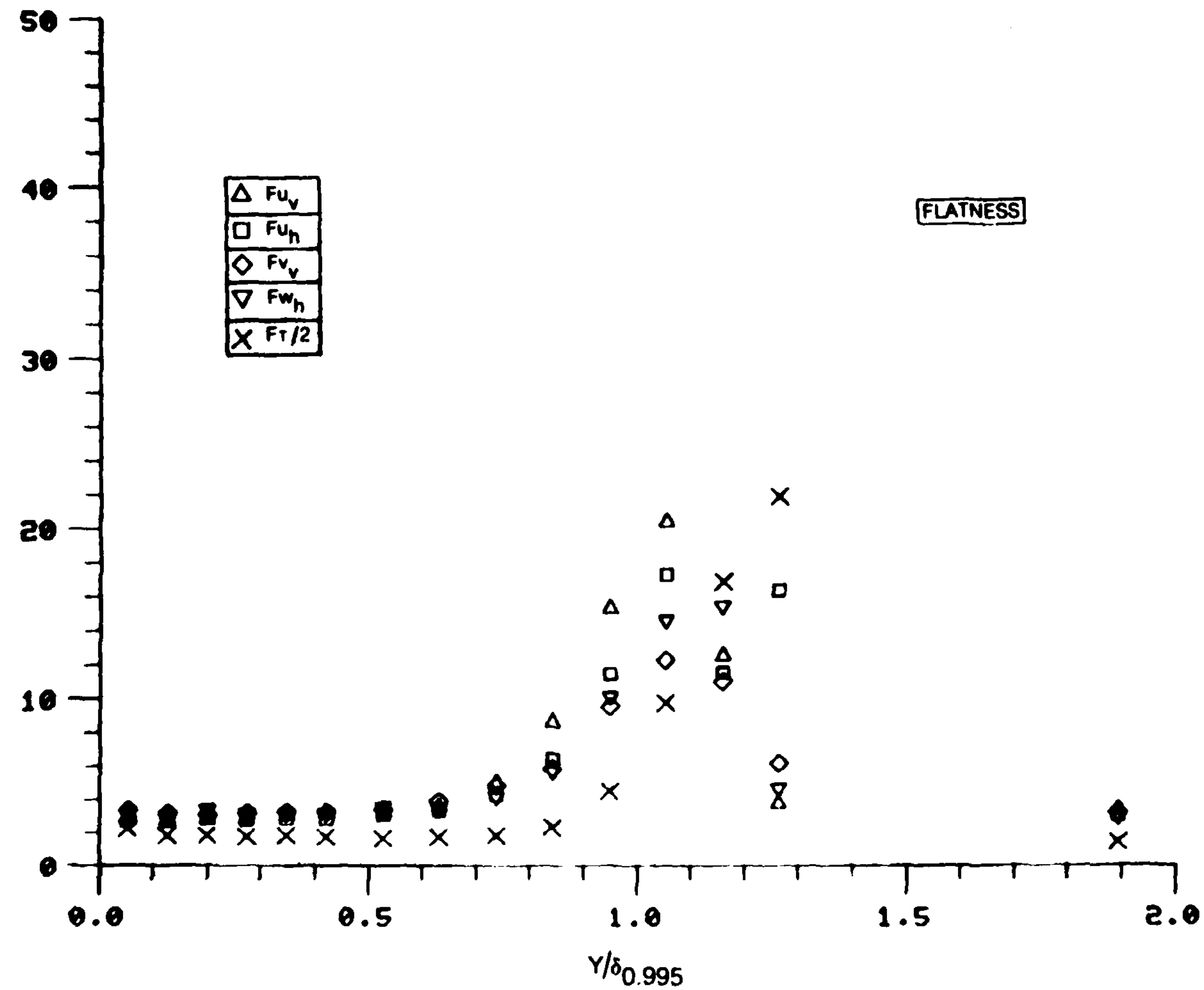

Figure B6E. Boundary Layer Flatness Distributions $x = 84$ in, $T_e = 0.2\%$

Fluctuating Profile Data

x = 84 in., Te = 0.2%

N	Y: INCHES	Y/ DELTA	U'/UE	V'/UE	W'/UE	$\sqrt{\overline{U'V'}}$/UE	$\overline{U'V'}$/ UTAU2	$\overline{U'V'}$/U'V'	C/UE
1	3.000	3.158	.0022	.0017	.0011	.0005	-.0002	-.0514	[illegible]
2	.050	.053	.0690	.0381	.0507	.0370	.9582	.4416	[illegible]
3	.120	.126	.0651	.0397	.0450	.0373	.9764	.4716	[illegible]
4	.190	.200	.0623	.0359	.0436	.0357	.8916	.4620	[illegible]
5	.260	.274	.0571	.0389	.0421	.0344	.8262	.4702	[illegible]
6	.330	.347	.0548	.0370	.0396	.0319	.7138	.4636	[illegible]
7	.400	.421	.0505	.0346	.0381	.0299	.6279	.4715	[illegible]
8	.500	.526	.0452	.0312	.0359	.0260	.4746	.4566	[illegible]
9	.600	.632	.0377	.0272	.0294	.0220	.3406	.4442	[illegible]
10	.700	.737	.0301	.0219	.0245	.0167	.1947	.4175	.0446
11	.800	.842	.0208	.0172	.0168	.0116	.0937	.3841	[illegible]
12	.900	.947	.0120	.0125	.0110	.0066	.0307	.2957	[illegible]
13	1.000	1.053	.0071	.0084	.0071	.0034	.0079	.1977	[illegible]
14	1.100	1.158	.0048	.0058	.0039	.0017	.0020	.1054	[illegible]
15	1.200	1.263	.0038	.0042	.0026	.0006	.0002	.0165	[illegible]
16	1.800	1.895	.0026	.0019	.0015	.0006	-.0003	-.0564	[illegible]
17	3.000	3.158	.0022	.0016	.0018	.0005	-.0002	-.0597	[illegible]
18	.000	.000	.0000	.0000	.0000	.0000	.0000	.0000	[illegible]

N	Y: INCHES	Y/ DELTA	$\overline{V'U'}$/Q2	U'2/Q2	V'2/Q2	W'2/Q2	VTAU/ UTAU	VC/ UTAU	$\overline{V'T'}$RHO*CP/ QWALL
1	3.000	3.158	-.0269	.5492	.3245	.1263	-.0311	.0020	[illegible]
2	.050	.053	.1555	.5416	.1654	.2930	.3702	.1326	
3	.120	.126	.1780	.5407	.2013	.2560	.3666	.1460	
4	.190	.200	.1724	.5271	.2156	.2573	.3712	.1617	
5	.260	.274	.1807	.4983	.2310	.2707	.4197	.1864	[illegible]
6	.330	.347	.1713	.5054	.2300	.2646	.5150	.2431	[illegible]
7	.400	.421	.1721	.4901	.2306	.2793	.5926	.2820	[illegible]
8	.500	.526	.1571	.4749	.2257	.2994	.6924	.3030	.6637
9	.600	.632	.1607	.4693	.2448	.2659	.8629	.3578	[illegible]
10	.700	.737	.1395	.4559	.2416	.3024	1.0112	.4046	[illegible]
11	.800	.842	.1321	.4280	.2923	.2797	1.0891	.4139	[illegible]
12	.900	.947	.1033	.3427	.3717	.2856	1.2316	.3923	[illegible]
13	1.000	1.053	.0661	.2938	.4153	.2909	.9351	.2661	[illegible]
14	1.100	1.158	.0403	.3189	.4686	.2125	.4590	.1336	[illegible]
15	1.200	1.263	.0079	.3666	.4566	.1766	-.7562	.0414	[illegible]
16	1.800	1.895	-.0261	.5307	.2892	.1801	.0569	.0036	[illegible]
17	3.000	3.158	-.0253	.4500	.2485	.3016	-.0117	.0001	[illegible]
18	.000	.000	.0000	.0000	.0000	.0000	.0000	.0000	[illegible]

N	Y: INCHES	Y/ DELTA	$\overline{V'T'}$/V'T'	T'/TTAU	T'/(TW-TE)	A16	G16	PRT
1	3.000	3.158	.0833	.1024	.0045	.6516	-.0023	.6734
2	.050	.053	.5444	2.0615	.0915	.8264	.0244	
3	.120	.126	.5201	1.6271	.0722	.7012	.0545	
4	.190	.200	.5298	1.4656	.0650	.7377	.0632	
5	.260	.274	.5406	1.3306	.0590	.7617	.0464	.7303
6	.330	.347	.5415	1.2324	.0547	.7871	.0585	.7829
7	.400	.421	.5452	1.1541	.0512	.8035	.0639	.7776
8	.500	.526	.5670	1.0261	.0455	.8787	.0968	.7701
9	.600	.632	.5704	.9138	.0405	.9054	.1267	.7215
10	.700	.737	.5756	.8058	.0358	1.0112	.1536	[illegible]
11	.800	.842	.5592	.6718	.0298	1.1645	.1795	.6324
12	.900	.947	.5472	.4940	.0219	1.5421	.2305	.4773
13	1.000	1.053	.4668	.3097	.0137	1.8759	.2157	.3478
14	1.100	1.158	.3262	.1819	.0081	1.7551	.1420	.2739
15	1.200	1.263	.1854	.1291	.0057	2.0844	.0823	.3211
16	1.800	1.895	-.0471	.1076	.0048	-.2175	.0000	-.6405
17	3.000	3.158	.0360	.1015	.0045	.2512	.0000	.4803
18	.000	.000	.0000	.0000	.0000	.0000	.0000	.0000

Table B9A

Flucutating Profile Data

x = 84 in., Te = 0.2%

N	Y: INCHES	Y/ DELTA	U'3/UE3 x 10000	U'2W'/UE3 x 10000	W'3/UE3 x 10000	U'W'2/UE3 x 10000	U'2V'/UE3 x 10000	U'V'2/UE3 x 10000	V'3/UE3 x 10000
1	3.000	3.158	-.0000	-.0000	-.0000	-.0000	.0000	-.0000	[illegible]
2	.050	.053	-.2000	-.0195	.3483	.1692	.2030	-.1576	[illegible]
3	.120	.126	-.4466	-.0863	-.0751	-.0601	.2356	-.1661	[illegible]
4	.190	.200	-.4751	-.0975	-.0028	-.0461	.2199	-.1525	[illegible]
5	.260	.274	-.5004	-.0455	.0402	-.0986	.2197	-.1607	[illegible]
6	.330	.347	-.5498	-.0260	-.0204	-.1306	.2336	-.1704	[illegible]
7	.400	.421	-.5351	.0209	.0315	-.1116	.2263	-.1734	[illegible]
8	.500	.526	-.4224	.0064	.0430	-.2266	.1763	-.1534	[illegible]
9	.600	.632	-.3568	-.0036	-.0145	-.1046	.1471	-.1388	[illegible]
10	.700	.737	-.2633	.0017	.0015	-.0934	.1033	-.0956	[illegible]
11	.800	.842	-.1194	.0059	-.0021	-.0463	.0516	-.0497	[illegible]
12	.900	.947	-.0303	.0040	.0063	-.0137	.0151	-.0187	[illegible]
13	1.000	1.053	-.0043	.0016	.0013	-.0035	.0032	-.0037	[illegible]
14	1.100	1.158	-.0002	.0001	-.0001	-.0003	.0007	-.0005	[illegible]
15	1.200	1.263	.0001	.0000	-.0000	.0000	.0000	.0001	[illegible]
16	1.800	1.895	-.0000	-.0000	.0000	.0000	.0000	.0000	[illegible]
17	3.000	3.158	-.0000	-.0000	.0000	.0000	.0000	-.0000	[illegible]
18	.000	.000	.0000	.0000	.0000	.0000	.0000	.0000	[illegible]

N	Y: INCHES	Y/ DELTA	SU V	SU W	SV	SW	ST	PSIBV	PSIBW
1	3.000	3.158	-.0762	-.1192	.0251	-.1439	-.0462	.0541	[illegible]
2	.050	.053	-.0668	.1911	.1691	.2628	-.0297	.1190	[illegible]
3	.120	.126	-.1739	-.0808	.1190	-.0842	.1291	.1463	[illegible]
4	.190	.200	-.2282	-.2274	.1447	-.0056	.1341	.1570	[illegible]
5	.260	.274	-.2913	-.2565	.1828	.0547	.1237	.1832	[illegible]
6	.330	.347	-.4106	-.2388	.2610	-.0316	.2323	.2416	[illegible]
7	.400	.421	-.5012	-.2656	.3398	.0569	.2047	.2903	[illegible]
8	.500	.526	-.6035	-.7265	.4264	.1152	.3694	.3330	[illegible]
9	.600	.632	-.8135	-.6898	.6010	-.0519	.4857	.4346	[illegible]
10	.700	.737	-1.2871	-1.0766	.8007	.0089	.7687	.6276	[illegible]
11	.800	.842	-1.9378	-1.5548	.9259	-.0425	1.1695	.8938	[illegible]
12	.900	.947	-2.4734	-2.0408	1.2815	.4098	2.1025	1.0480	[illegible]
13	1.000	1.053	-1.6924	-1.7197	1.3185	.3284	3.3168	.9614	[illegible]
14	1.100	1.158	-.2731	-.3822	1.0312	-.2437	3.8582	.5947	[illegible]
15	1.200	1.263	.2714	-.3934	.5785	-.1959	3.0526	.0844	[illegible]
16	1.800	1.895	-.0301	.0510	.1265	.1110	-.2624	.0464	[illegible]
17	3.000	3.158	-.0228	.3012	-.0544	.0108	-.0323	.0336	[illegible]
18	.000	.000	.0000	.0000	.0000	.0000	.0000	.0000	[illegible]

N	Y: INCHES	Y/ DELTA	PSICV	PSICW	FU V	FU W	FU V	FU W	FT
1	3.000	3.158	-.0350	-.0248	2.8612	3.2235	3.1822	3.1402	2.675[illegible]
2	.050	.053	-.1620	.0938	2.7604	2.6898	3.3532	3.2046	[illegible]
3	.120	.126	-.1652	-.0453	2.7397	2.6264	3.1962	3.0830	3.702[illegible]
4	.190	.200	-.1620	-.0373	2.8000	2.8050	3.0814	3.4321	3.670[illegible]
5	.260	.274	-.1915	-.0955	2.8634	2.7104	3.1670	3.1262	[illegible]
6	.330	.347	-.2438	-.1403	3.0764	2.8664	3.2216	3.1896	[illegible]
7	.400	.421	-.3047	-.1397	3.1711	2.8528	3.2629	3.1681	[illegible]
8	.500	.526	-.3829	-.3437	3.2803	3.1062	3.4158	3.5636	[illegible]
9	.600	.632	-.5318	-.3005	3.5625	3.3716	3.9022	3.5012	3.495[illegible]
10	.700	.737	-.7270	-.4737	5.0039	4.2738	4.8173	4.1945	3.734[illegible]
11	.800	.842	-.9180	-.7085	8.5440	6.4175	5.8260	5.6409	4.702[illegible]
12	.900	.947	-1.1102	-.8167	15.2169	11.4509	9.5023	10.0596	8.944[illegible]
13	1.000	1.053	-.8277	-.8747	20.3442	17.2446	12.2509	14.5481	[illegible]
14	1.100	1.158	-.3174	-.3472	12.4789	11.5225	10.9740	15.4552	[illegible]
15	1.200	1.263	.0942	.0386	3.7858	16.3031	6.2007	4.6586	43.5916
16	1.800	1.895	.0454	.0599	3.3259	3.0096	3.1408	2.9333	2.843[illegible]
17	3.000	3.158	-.0162	.0339	2.9652	2.8138	3.0064	2.4356	2.620[illegible]
18	.000	.000	.0000	.0000	.0000	.0000	.0000	.0000	[illegible]

Table B9B

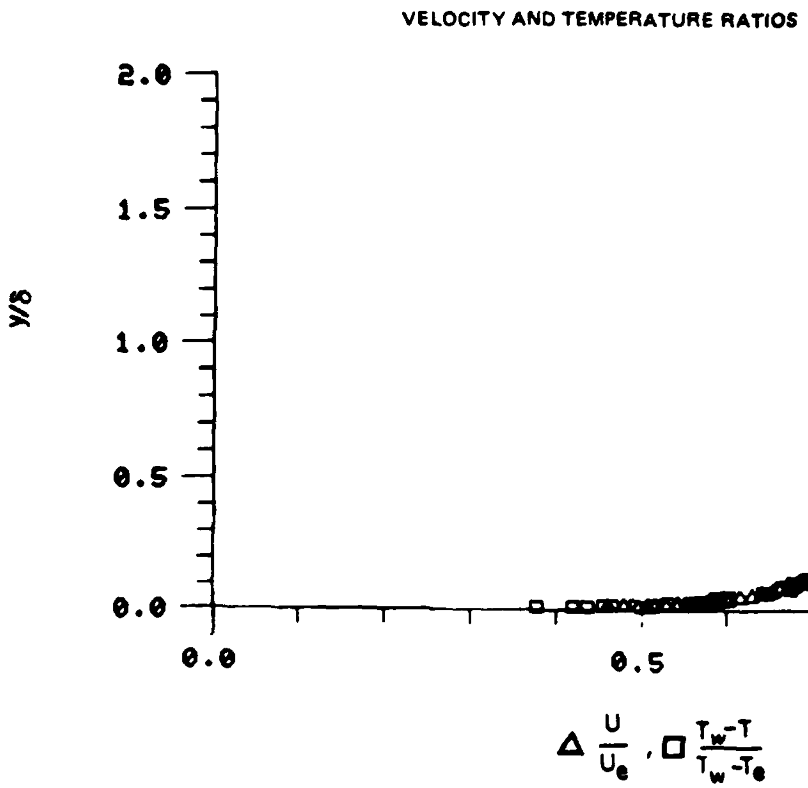

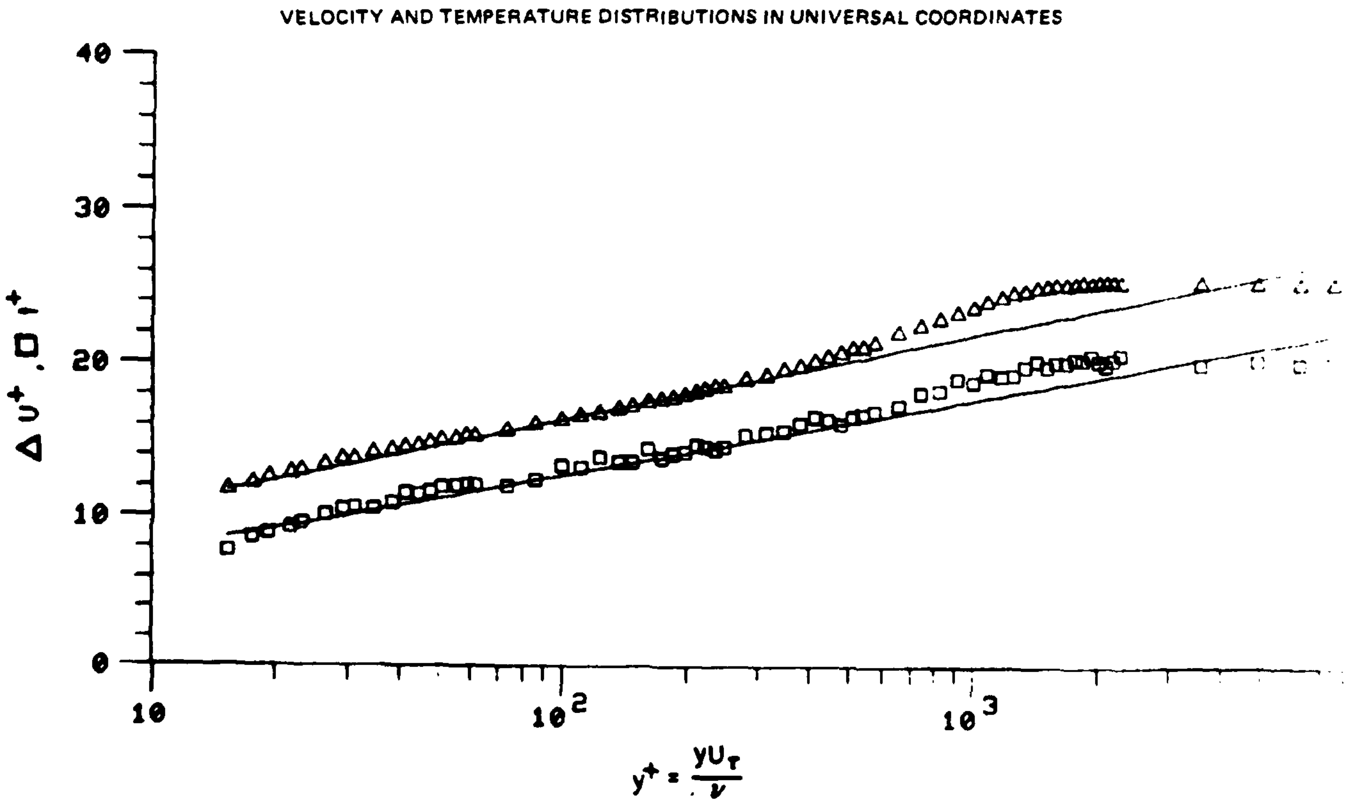

Figure B7. Mean Profile and Temperature Profiles x = 52 in., Te = 1.8%

78-12-100-1

Mean Profile Data

x = 52 in., Te = 1.8%

N	Y INCHES	Y/DELTA	U FT/SEC	T DEG.F	U/UE	THETA	U-UE UTAU	U(+)	T(+)	Y(+)
1	.0083	.010	45.17	85.92	.460	.377	-13.631	11.632	7.706	15.353
2	.0095	.011	47.06	84.89	.480	.420	-13.143	12.120	8.578	17.565
3	.0104	.012	48.69	84.47	.496	.437	-12.726	12.538	8.932	19.224
4	.0118	.014	49.76	84.04	.507	.455	-12.449	12.815	9.297	21.804
5	.0125	.014	50.48	83.78	.515	.466	-12.263	13.001	9.524	23.095
6	.0142	.016	51.92	83.12	.529	.494	-11.892	13.371	10.057	26.228
7	.0157	.016	53.07	82.66	.541	.513	-11.598	13.666	10.471	28.993
8	.0167	.019	53.20	82.58	.542	.516	-11.564	13.700	10.542	30.836
9	.0187	.022	54.51	82.67	.556	.513	-11.225	14.039	10.468	34.522
10	.0207	.024	55.32	82.23	.564	.531	-11.016	14.247	10.639	38.208
11	.0224	.026	55.94	81.45	.570	.563	-10.858	14.406	11.507	41.342
12	.0241	.028	56.57	81.62	.577	.556	-10.695	14.569	11.363	44.475
13	.0256	.030	57.08	81.40	.582	.565	-10.563	14.700	11.548	47.240
14	.0274	.032	57.78	81.09	.589	.578	-10.384	14.880	11.806	50.558
15	.0297	.034	58.06	80.89	.592	.587	-10.306	14.956	11.982	54.797
16	.0315	.036	58.83	80.82	.600	.590	-10.115	15.149	12.042	58.114
17	.0332	.038	59.05	80.80	.602	.590	-10.058	15.206	12.054	61.248
18	.0396	.046	60.31	80.89	.615	.586	-9.731	15.532	11.975	73.044
19	.0463	.053	61.74	80.51	.629	.602	-9.364	15.899	12.300	85.793
20	.0537	.062	62.83	79.40	.640	.648	-9.083	16.180	13.242	99.032
21	.0596	.069	64.08	79.54	.653	.643	-8.760	16.504	13.124	109.907
22	.0666	.077	64.84	78.76	.661	.675	-8.566	16.698	13.793	122.809
23	.0737	.085	65.95	79.03	.672	.664	-8.281	16.983	13.559	135.895
24	.0795	.092	66.56	79.04	.679	.664	-8.116	17.147	13.555	146.566
25	.0868	.100	67.49	78.10	.688	.703	-7.884	17.379	14.354	160.041
26	.0936	.108	68.22	78.72	.695	.677	-7.694	17.570	13.822	172.574
27	.0996	.115	68.72	78.42	.701	.689	-7.566	17.698	14.079	183.633
28	.1065	.123	69.44	78.31	.708	.694	-7.382	17.882	14.170	196.351
29	.1135	.131	70.20	77.80	.716	.715	-7.186	18.076	14.603	209.253
30	.1193	.138	70.75	77.86	.721	.712	-7.044	18.220	14.536	219.943
31	.1266	.146	71.44	78.06	.728	.704	-6.865	18.399	14.384	233.398
32	.1335	.154	71.67	77.87	.731	.712	-6.807	18.457	14.548	246.116
33	.1506	.174	73.49	77.05	.749	.747	-6.337	18.927	15.245	277.633
34	.1662	.194	74.34	76.84	.756	.755	-6.119	19.145	15.421	310.073
35	.1855	.214	75.82	76.70	.773	.761	-5.739	19.525	15.542	341.959
36	.2036	.235	76.75	76.10	.762	.786	-5.498	19.765	16.048	375.320
37	.2203	.254	77.86	75.62	.794	.806	-5.212	20.052	16.457	406.101
38	.2386	.275	79.03	75.80	.806	.798	-4.911	20.353	16.305	439.830
39	.2554	.295	80.00	76.10	.816	.786	-4.661	20.603	16.056	470.495
40	.2733	.315	81.09	75.64	.827	.805	-4.381	20.683	16.442	503.765
41	.2904	.335	81.56	75.42	.831	.814	-4.260	21.004	16.627	535.305
42	.3085	.356	82.82	75.18	.844	.824	-3.935	21.328	16.835	566.666
43	.3535	.408	85.04	74.74	.867	.843	-3.363	21.901	17.207	651.605
44	.3984	.459	87.00	73.75	.887	.884	-2.859	22.405	18.051	734.365
45	.4435	.511	88.78	72.57	.905	.891	-2.401	22.863	18.205	817.491
46	.4864	.563	90.26	72.71	.920	.927	-2.019	23.244	18.938	900.249
47	.5333	.615	91.61	72.69	.934	.920	-1.670	23.593	18.782	983.005
48	.5784	.667	93.03	72.24	.948	.947	-1.306	23.958	19.334	1066.132
49	.6234	.719	94.22	72.42	.960	.939	-1.000	24.264	19.183	1149.074
50	.6684	.771	95.27	72.35	.971	.942	-.729	24.534	19.241	1232.015
51	.7133	.823	95.90	71.69	.978	.970	-.566	24.698	19.799	1314.773
52	.7583	.874	96.55	71.28	.984	.987	-.400	24.864	20.149	1397.714
53	.8034	.926	97.19	71.63	.991	.972	-.235	25.029	19.653	1480.640
54	.8484	.978	97.39	71.36	.993	.983	-.183	25.081	20.079	1563.782
55	.8935	1.030	97.60	71.37	.995	.983	-.128	25.136	20.073	1646.908
56	.9384	1.082	97.89	71.02	.998	.997	-.054	25.209	20.370	1729.665
57	.9834	1.134	98.01	71.14	.999	.993	-.024	25.240	20.269	1812.607
58	1.0283	1.186	97.97	70.83	.999	1.006	-.034	25.229	20.536	1895.364
59	1.0734	1.238	98.15	71.19	1.000	.990	.013	25.276	20.222	1978.490
60	1.1184	1.290	98.19	71.61	1.001	.973	.022	25.286	19.867	2061.432
61	1.1635	1.342	98.22	71.13	1.001	.993	.030	25.294	20.275	2144.558
62	1.2084	1.393	98.19	70.68	1.001	1.012	.024	25.287	20.657	2227.315
63	1.9062	2.200	98.25	71.41	1.002	.981	.039	25.302	20.037	3517.150
64	2.6084	3.008	98.12	71.16	1.000	.992	.006	25.269	20.254	4807.722
65	3.3087	3.815	98.10	71.33	1.000	.985	.000	25.264	20.106	6098.479
66	4.0084	4.622	98.01	71.22	.999	.989	-.024	25.239	20.199	7388.130

Table B10

RUN NO. 3. POINT 3.

BOUNDARY LAYER PROPERTIES

	LINEAR INTERPOLATION TO WALL	STANDARD SUBLAYER FUNCTION FROM WALL TO Y+=35
FREE STREAM VELOCITY =	98.101	98.101
FREE STREAM TEMPERATURE =	70.960	
WALL TEMPERATURE =	94.980	
WALL HEAT FLUX =	.07908	
FREE STREAM DENSITY =	.07541	
FREE STREAM KINEMATIC VISCOSITY =	.0001623	
DENSITY OF FLUID AT WALL =	.07214	
KINEMATIC VISCOSITY OF FLUID AT WALL =	.0001756	
WALL/FREE STREAM DENSITY RATIO =	.95669	
LOCATION REYNOLDS NUMBER (REX) =	2618495.47	
INPUT VALUE OF VELOCITY DELTA =	1.00000	
INPUT VALUE OF TEMPERATURE DELTA =	1.00000	
CALCULATED DELTA =		.86723
DELTA 99.5% INPUT =	.00000	
DISPLACEMENT THICKNESS (DELSTAR) =	.12408	.12411
MOMENTUM THICKNESS (THETA) =	.08716	.08756
ENERGY-DISSIPATION THICKNESS =	.15548	.15561
ENTHALPY THICKNESS =	.00436	.00437
SHAPE FACTOR 12 (DELSTAR/THETA) =	1.42349	1.41709
SHAPE FACTOR 32 (ENERGY/THETA) =	1.78378	1.77907
MOMENTUM THICKNESS REYNOLDS NUMBER =	4389.16	4410.12
DISPLACEMENT THICKNESS REYNOLDS NUMBER =	6247.94	6249.55
SKIN FRICTION COEFFICIENT =	.002998	
FRICTION VELOCITY =	3.88308	
LAW OF THE WALL CONSTANT (K) =	.41000	
LAW OF THE WALL CONSTANT (C) =	5.00000	
WAKE STRENGTH =		.46566
CLAUSERS 'DELTA' INTEGRAL =	-2.81396	-3.02501
CLAUSERS 'G' INTEGRAL =	20.20020	19.93822
DISPLACEMENT THICKNESS - CONSTANT DENSITY =	.11555	.11974
MOMENTUM THICKNESS - CONSTANT DENSITY =	.08806	.08850
SHAPE FACTOR 12 - CONSTANT DENSITY =	1.31209	1.35299

LOCATION -X- 52.00000

Te = 1.8%

Table B11

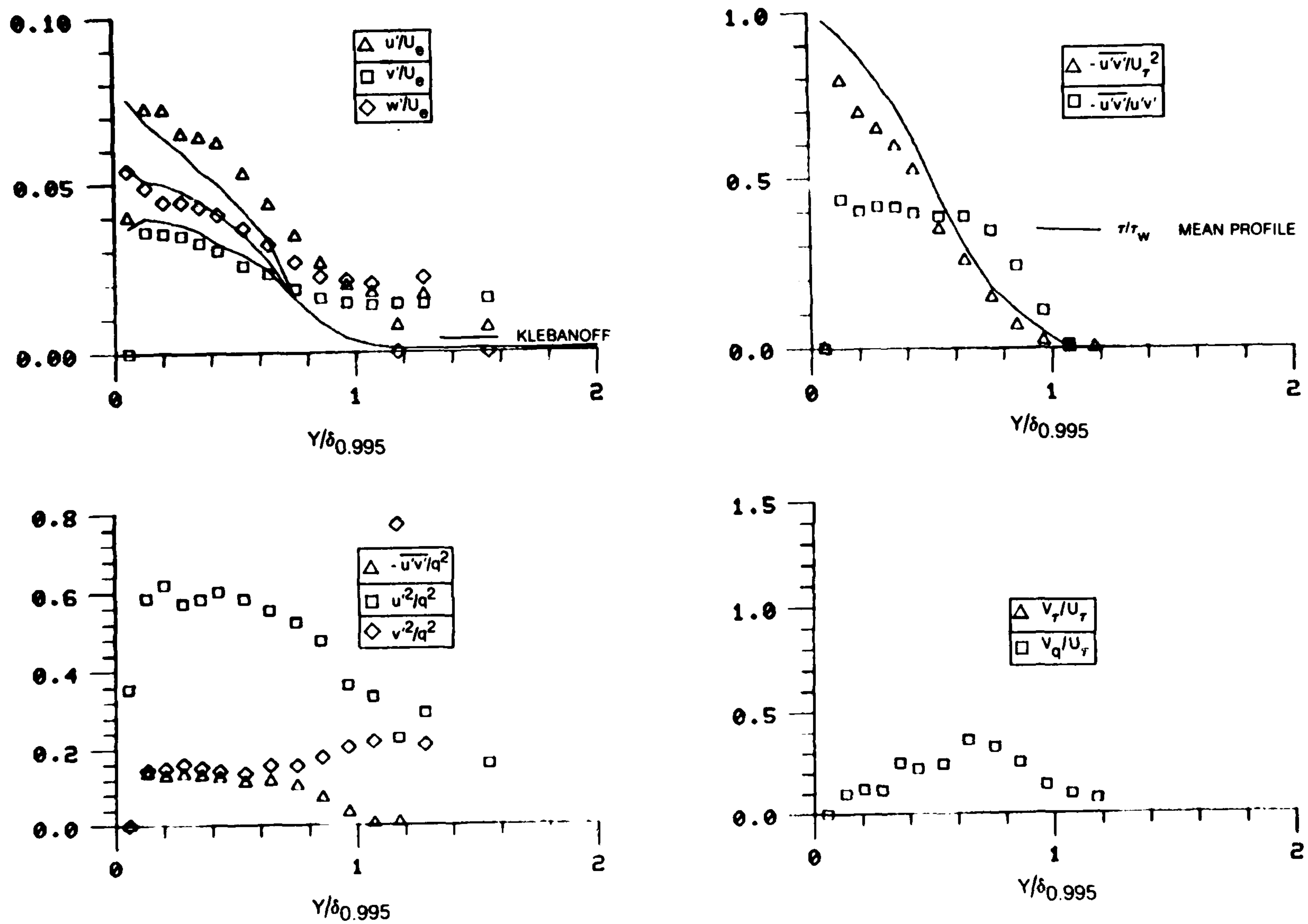

Figure B8A. Boundary Layer Turbulence Quantities $x = 52$ in, $T_e = 1.8\%$

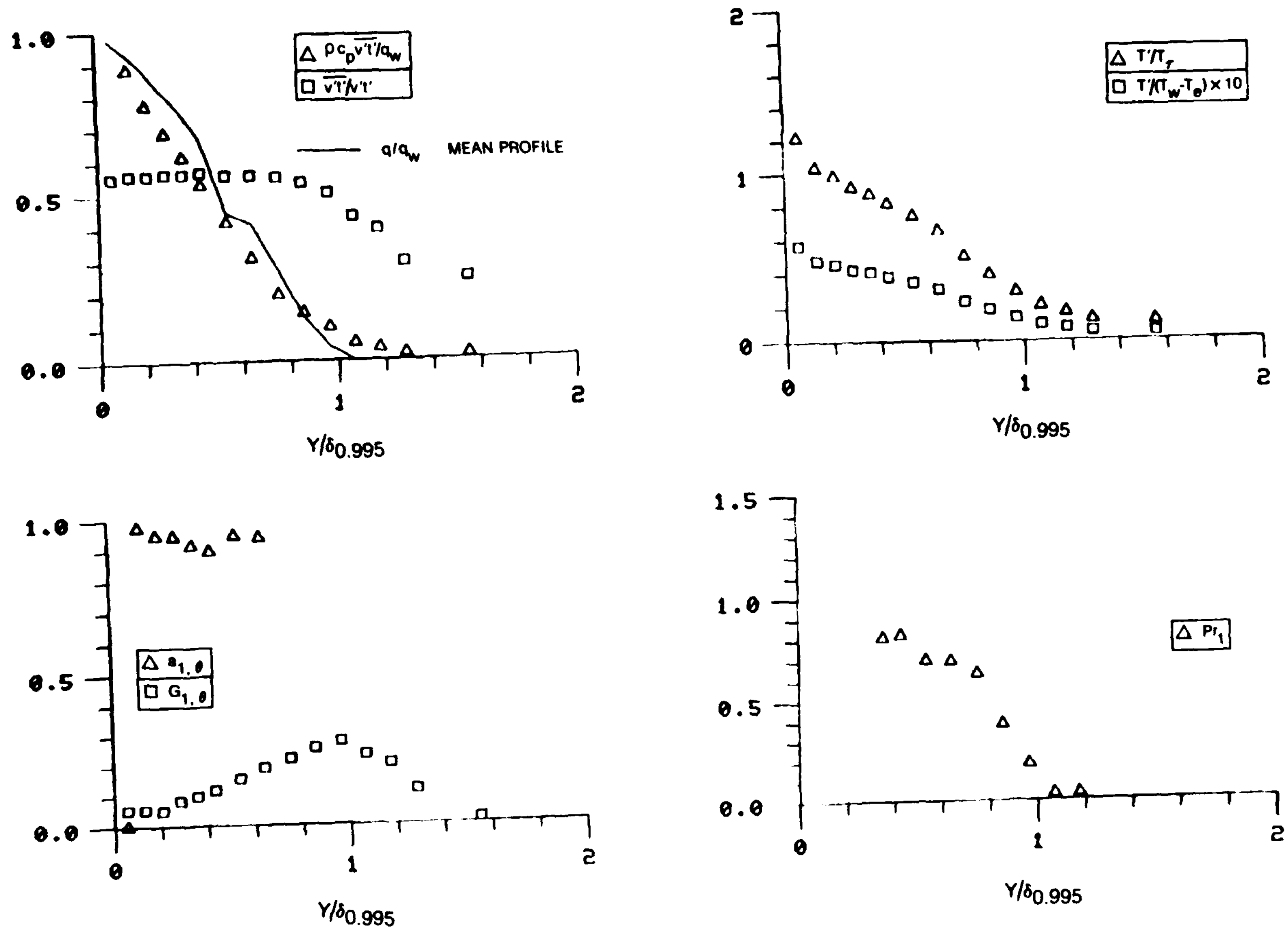

Figure B8B. Boundary Layer Turbulence Quantities x = 52 in, T_e = 1.8%

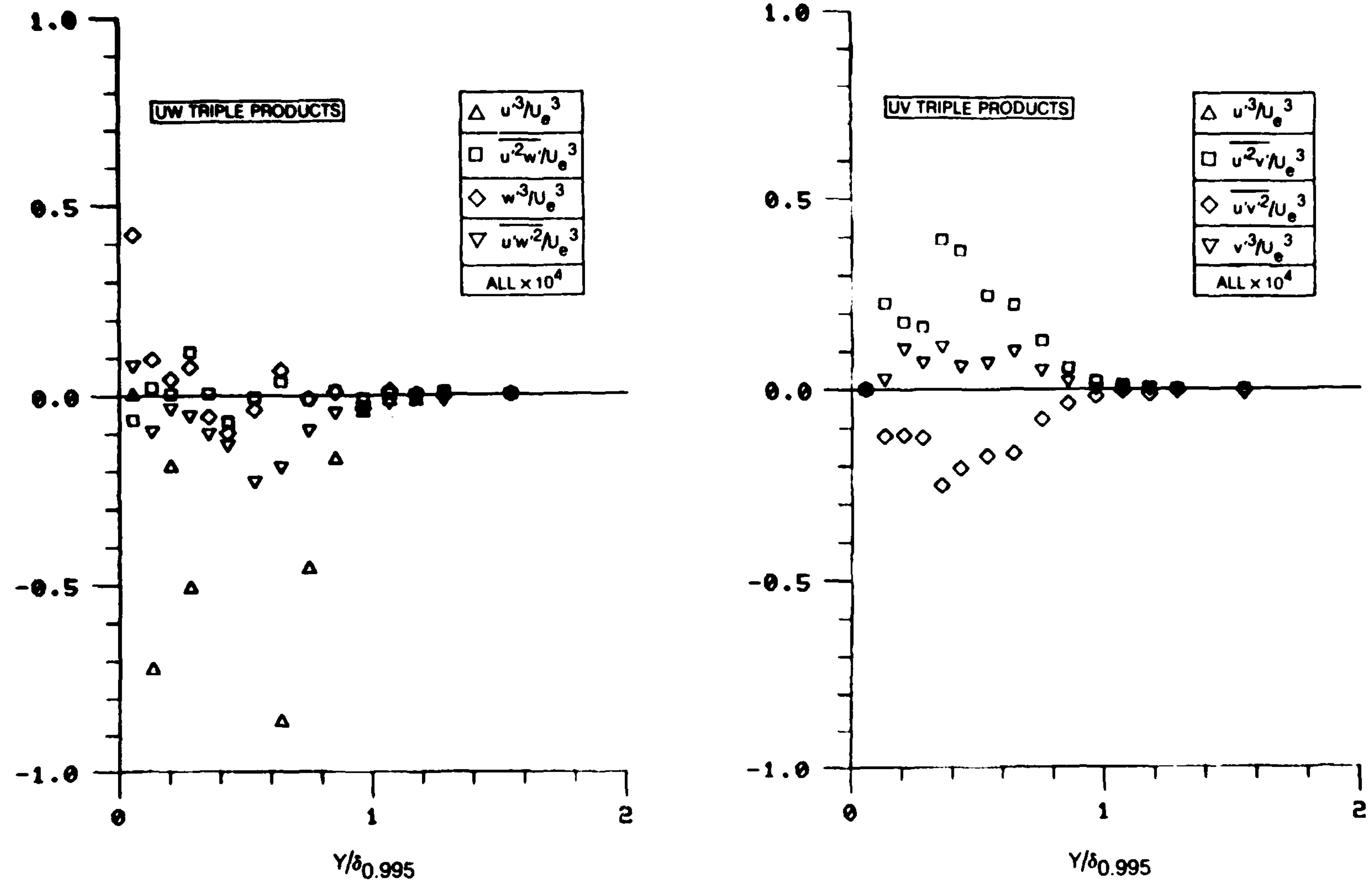

Figure B8C. Boundary Layer Triple Product Distributions $x = 52$ in, $T_e = 1.8\%$

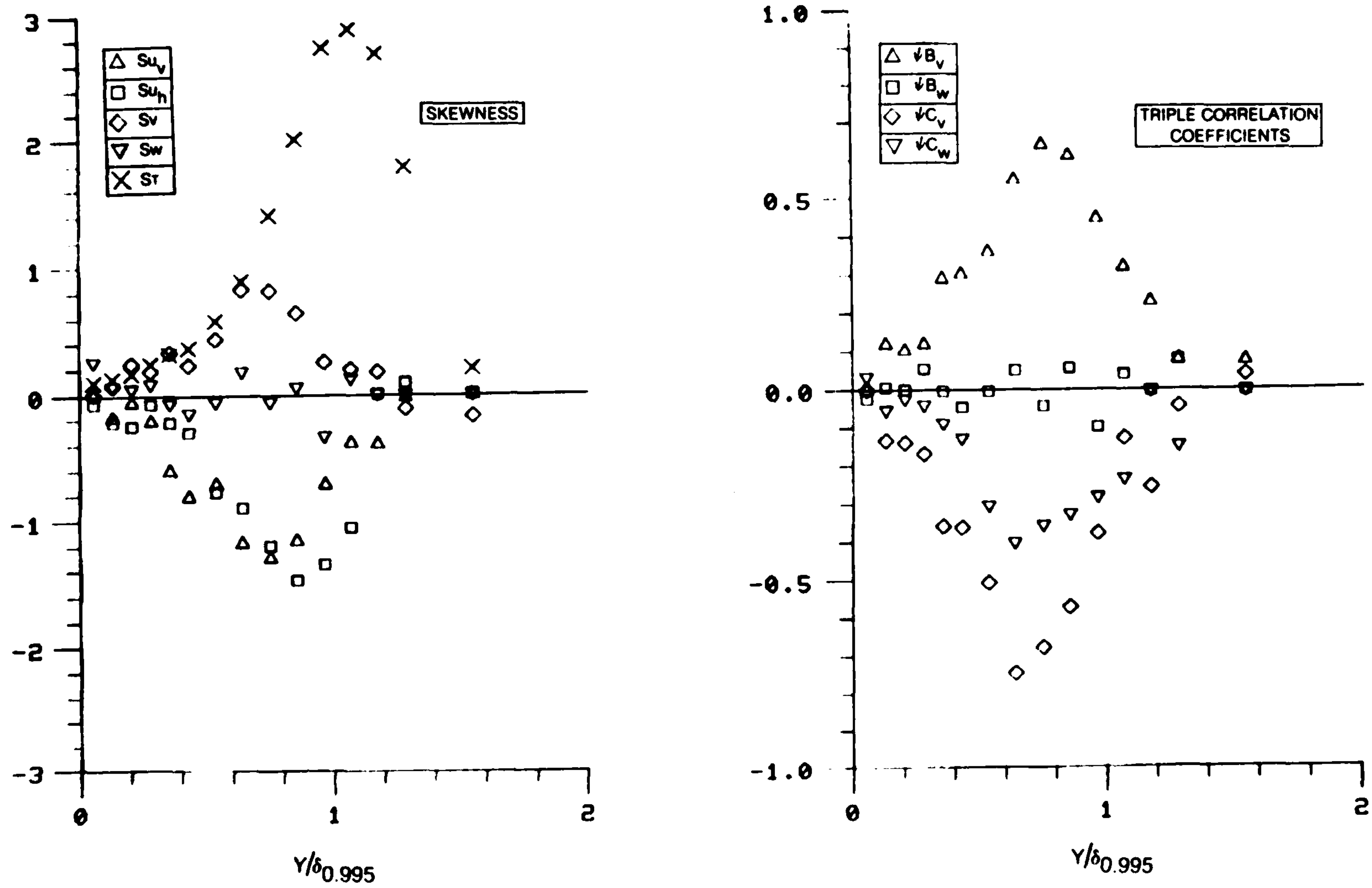

Figure B8D. Boundary Layer Skewness and Triple Product Correlation Coefficient Distributions $x = 52$ in, $T_e = 1.8\%$

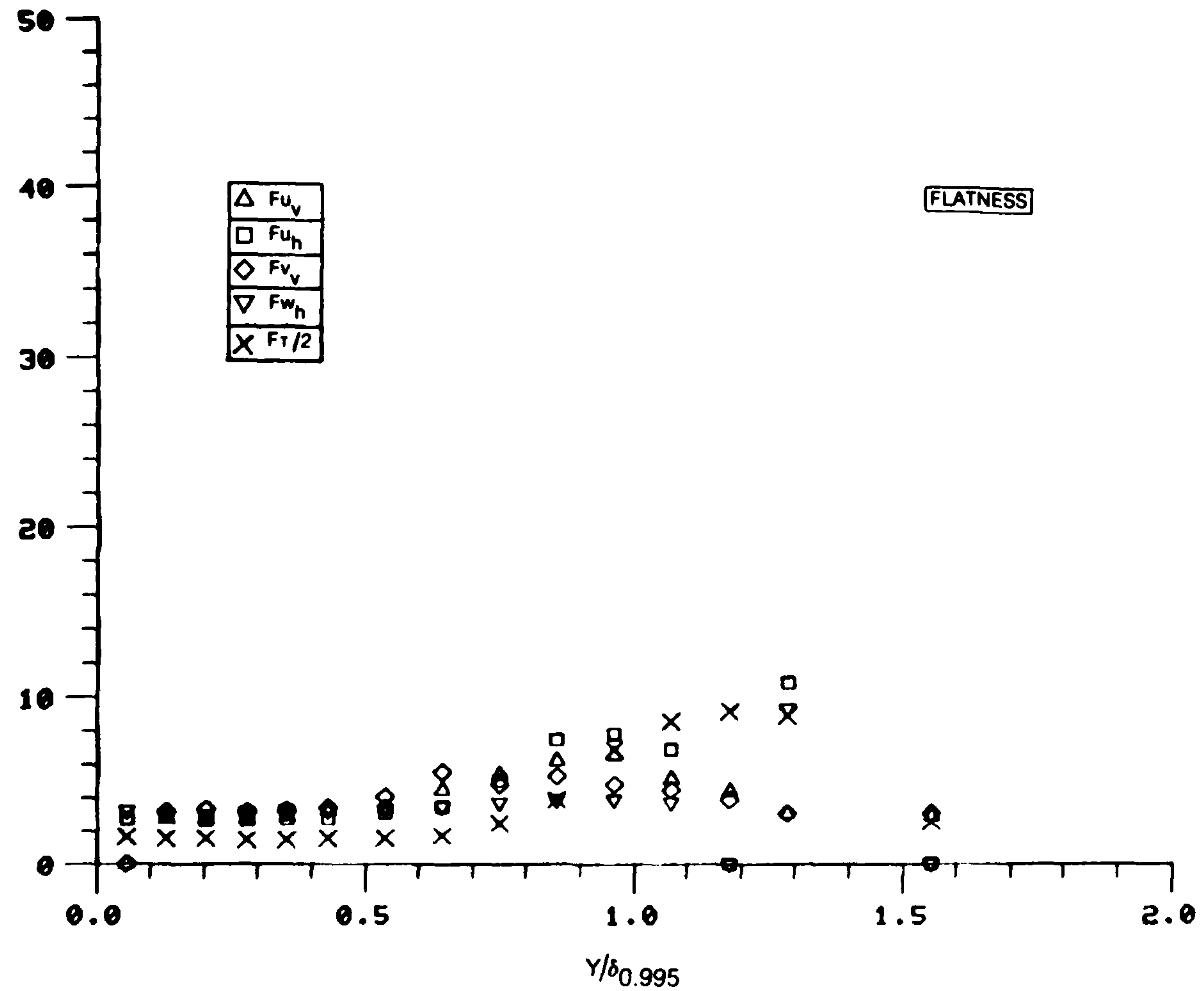

Figure B8E. Boundary Layer Flatness Distributions x =52 in, T_e = 1.8%

Fluctuating Profile Data

x = 52 in., Te = 1.8%

N	Y: INCHES	Y/DELTA	U'/UE	V'/UE	W'/UE	$\sqrt{\overline{U'V'}}$/UE	$\overline{U'V'}$/UTAU	$\overline{U'V'}$/U'V'	[illegible]/UE
1	4.000	4.278	.0075	.0000	.0173	.0000	[illegible]	[illegible]	[illegible]
[illegible]	[illegible]	[illegible]	[illegible]	[illegible]	[illegible]	[illegible]	[illegible]	[illegible]	[illegible]
[illegible]	.000	.000	.0000	.0000	.0000	.0000	[illegible]	[illegible]	[illegible]

N	Y: INCHES	Y/DELTA	$\overline{V'T'}$/[illegible]	[illegible]/C2	V'2/C[illegible]	W'2/C2	VTAU/UTAU	[illegible]/UTAU	$\overline{V'T'}$[illegible]WALL
1	4.000	4.278	[illegible]	[illegible]	[illegible]	.6761	[illegible]	[illegible]	[illegible]
[illegible]	[illegible]	[illegible]	[illegible]	[illegible]	[illegible]	[illegible]	[illegible]	[illegible]	[illegible]
[illegible]	.000	.000	[illegible]	.0000	[illegible]	.0000	[illegible]	[illegible]	[illegible]

N	Y: INCHES	Y/DELTA	$\overline{V'T'}$/V'T'	T'/TTAU	T'/(TW-TE)	A1E	G1E	[illegible]
1	4.000	4.278	.1004	.1040	.0049	.0000	-.0141	.0000
[illegible]	[illegible]	[illegible]	[illegible]	[illegible]	[illegible]	[illegible]	[illegible]	[illegible]
[illegible]	.000	.000	.0000	.0000	[illegible]	.0000	[illegible]	.0000

Table B12A

Fluctuating Profile Data

x = 52 in., Te = 1.8%

N	Y: INCHES	Y/ DELTA	U'3/UE3 x 10000	U'2W'/UE3 x 10000	W'3/UE3 x 10000	U'W'2/UE3 x 10000	U'2V'/UE3 x 10000	U'V'2/UE3 x 10000	V'3/UE3 x 10000
1	4.000	4.278	.0000	-.0046	-.0031	-.0065	.0000	.0000	.0000
2	.050	.053	.0000	-.0655	.4217	.0806	[illegible]	.0000	[illegible]
3	.120	.128	-.7268	.0155	.0923	-.0927	.2273	-.12[illegible]	[illegible]
4	.190	.203	-.19[illegible]	[illegible]	[illegible]	-.0327	.1759	-.1[illegible]	[illegible]
5	.260	.278	-.5[illegible]94	.1124	.0738	-.0[illegible]9	.16[illegible]	-.1[illegible]	[illegible]
6	.330	.353	-1.65[illegible]	[illegible]	-.0576	-.1006	.3[illegible]	-.2[illegible]	[illegible]
7	.400	.428	-2.0466	-.0695	-.0097	-.1277	.3631	-.2[illegible]	[illegible]
8	.500	.535	-1.04[illegible]4	-.0080	-.0[illegible]	-.1256	.2496	-.1[illegible]	[illegible]
9	.600	.642	-.6649	[illegible]52	.0635	-.1866	[illegible]	-.1677	[illegible]
10	.700	.749	-.4579	-.0138	-.0054	-.0917	.1[illegible]	-.0[illegible]	[illegible]
11	.800	.856	-.17[illegible]9	.0102	.0006	-.0437	.0570	-.0[illegible]	[illegible]
12	.900	.963	-.0441	-.0100	-.0034	-.0276	[illegible]	-.016[illegible]	[illegible]
13	1.000	1.070	-.0156	.0031	.0059	-.0183	.0117	-.00[illegible]7	[illegible]
14	1.100	1.176	-.0174	.0000	.0000	.0001	[illegible]	[illegible]	[illegible]
15	1.200	1.283	-.0010	.0056	-.0004	-.0116	[illegible]	-.0[illegible]	-.0[illegible]
16	1.450	1.551	-.0005	.0000	[illegible]	.0000	[illegible]	[illegible]	[illegible]
17	4.000	4.278	-.00[illegible]	.0018	-.0016	.0013	.0013	[illegible]	-.0[illegible]
18	.000	.000	.0000	.0000	.0000	.0000	.0000	.0000	.0000

N	Y: INCHES	Y/ DELTA	SU V	SU H	SV	SW	ST	PSIEV	PSIEW
1	4.000	4.278	.0000	-.6455	.0000	-.0677	.00[illegible]7	.0000	-.1[illegible]
2	.050	.053	.0000	-.0[illegible]32	.0000	.2655	.095[illegible]	[illegible]	[illegible]
3	.120	.128	-.1871	-.2199	.064[illegible]	.0707	.127[illegible]	.11[illegible]	[illegible]
4	.190	.203	-.07[illegible]	-.2[illegible]62	[illegible]	.047[illegible]	.263[illegible]	.20[illegible]	[illegible]
5	.260	.278	-.4097	-.0792	.1[illegible]	.0627	.24[illegible]	.1[illegible]	[illegible]
6	.330	.353	-.6141	-.2211	.328[illegible]	-.0711	.3[illegible]	.2857	[illegible]
7	.400	.428	-.60[illegible]	-.3003	.2[illegible]96	-.1467	.37[illegible]	.2[illegible]7	[illegible]
8	.500	.535	-.7174	-.7771	.4387	-.0554	.578[illegible]	.3[illegible]3	[illegible]
9	.600	.642	-1.1796	-.6958	.824[illegible]	.18[illegible]	.65[illegible]	.5[illegible]	[illegible]
10	.700	.749	-1.2939	-1.2[illegible]	.812[illegible]	-.0567	1.4[illegible]	.64[illegible]	[illegible]
11	.800	.856	-1.1565	-1.4[illegible]15	.640[illegible]	.0560	1.9997	.61[illegible]	[illegible]
12	.900	.963	-.7205	-1.7421	.25[illegible]	-.329[illegible]	2.7387	.44[illegible]	[illegible]
13	1.000	1.070	-.3850	-1.[illegible]	.169[illegible]	.1226	2.881[illegible]	.32[illegible]	[illegible]
14	1.100	1.176	-.3952	.0000	.1703	.0000	2.6917	.2[illegible]2	[illegible]
15	1.200	1.283	-.0264	.0050	-.1184	.0037	1.7[illegible]	.0[illegible]	[illegible]
16	1.450	1.551	-.00[illegible]	.0000	-.1697	.0000	.2034	.0786	[illegible]
17	4.000	4.278	-.154[illegible]	-.1659	-.1113	-.0414	-.[illegible]	.0[illegible]	[illegible]
18	.000	.000	.0000	.0000	.0000	.0000	.0000	.0000	.0000

N	Y: INCHES	Y/ DELTA	PSICV	PSICW	FU V	FU H	FL V	FU H	FT
1	4.000	4.278	.0000	-.1510	.0000	3.3682	.0000	3.226[illegible]	[illegible]
2	.050	.053	.00[illegible]	.0749	.0000	2.7567	.0000	3.2643	[illegible]
3	.120	.128	-.1323	-.0502	2.7903	2.6161	3.1661	3.0[illegible]4	[illegible]
4	.190	.203	-.1797	-.0[illegible]1	2.72[illegible]	2.6401	3.30[illegible]	3.0[illegible]4	[illegible]
5	.260	.278	-.1667	-.0795	2.7260	2.6966	3.1944	3.1915	[illegible]
6	.330	.353	-.3574	-.0[illegible]67	2.95[illegible]	2.77[illegible]	3.247[illegible]	3.3460	[illegible]
7	.400	.428	-.3556	-.1254	3.2401	2.7816	3.4520	3.2541	[illegible]
8	.500	.535	-.5072	-.3039	3.4[illegible]65	3.0943	4.0[illegible]	3.37[illegible]	[illegible]
9	.600	.642	-.7446	-.4010	4.4[illegible]5[illegible]	3.4685	5.5627	3.5[illegible]93	[illegible]
10	.700	.749	-.6766	-.3562	5.4118	5.101[illegible]	4.861[illegible]	3.7856	[illegible]
11	.800	.856	-.57[illegible]	-.3260	6.2421	7.529[illegible]	5.313[illegible]	3.94[illegible]	[illegible]
12	.900	.963	-.377[illegible]	-.2[illegible]	6.56[illegible]	7.8[illegible]71	4.873[illegible]	3.9196	13.76[illegible]
13	1.000	1.070	-.1261	-.2[illegible]38	5.140[illegible]	6.9500	4.476[illegible]	3.7640	17.[illegible]
14	1.100	1.176	-.2542	.0000	4.4199	.0000	3.92[illegible]	.0[illegible]	16.287[illegible]
15	1.200	1.283	-.0425	-.1450	3.0561	10.6572	3.109[illegible]	9.3[illegible]	17.7[illegible]
16	1.450	1.551	.0415	.0000	2.922[illegible]	.0000	3.17[illegible]	.0000	[illegible]
17	4.000	4.278	.0691	.0359	3.072[illegible]	2.9846	3.0557	2.9946	3.9716
18	.000	.000	.0000	.0000	.0000	.0000	.0000	.0000	.0000

Table B12B.

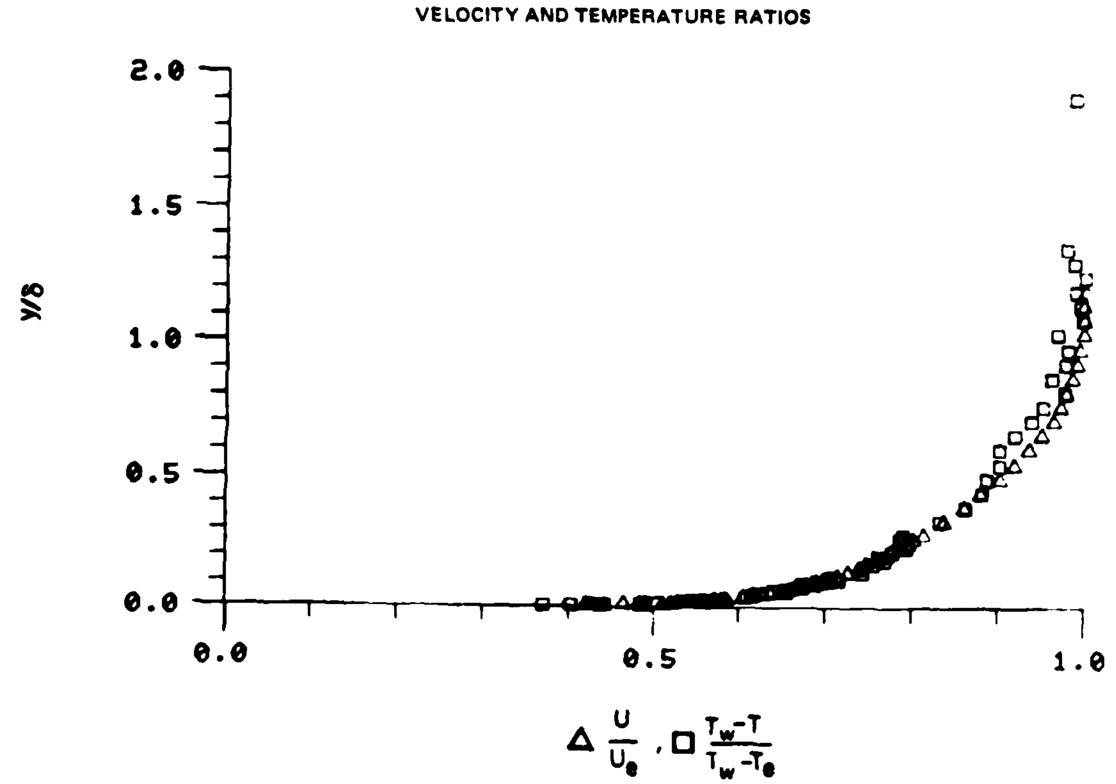

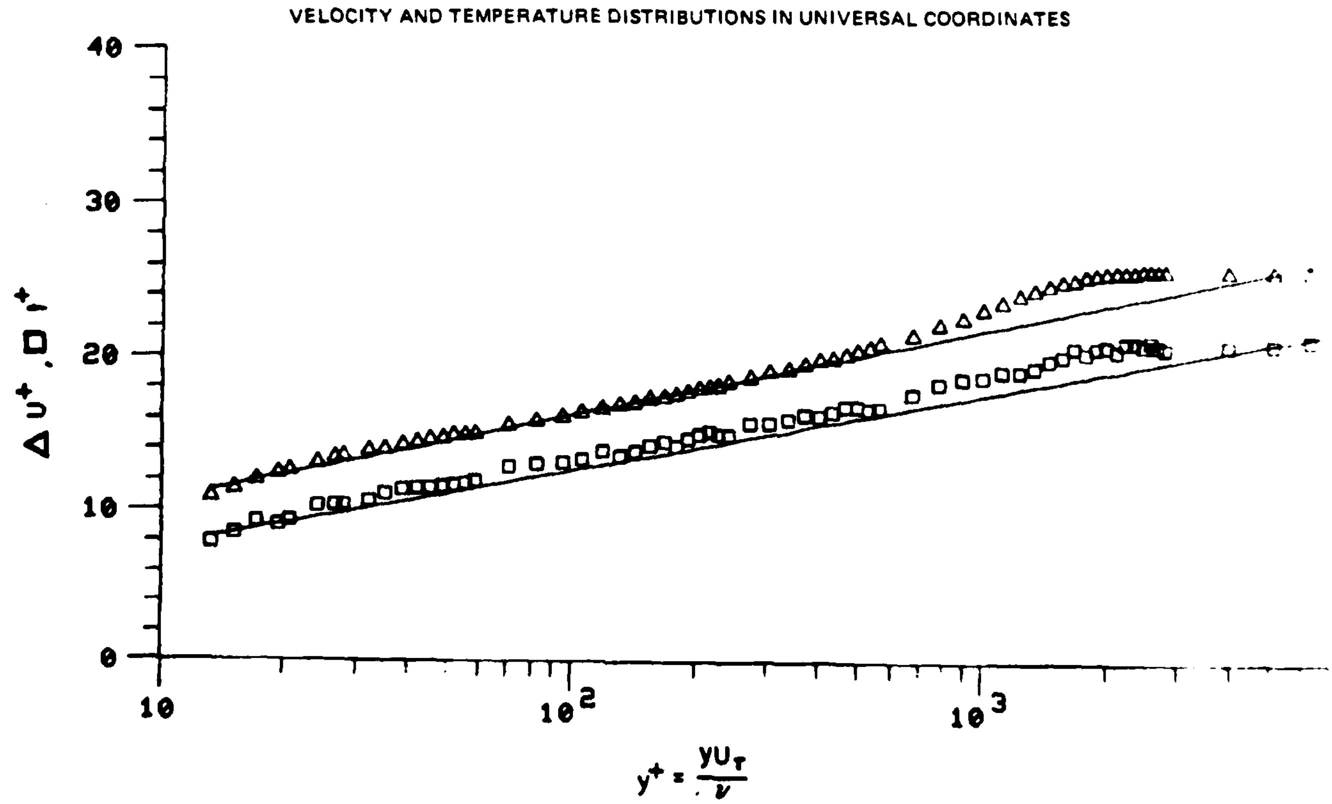

Figure B9. Mean Velocity and Temperature Profiles x = 68 in., Te = 1.6%

78-12-100-1

Mean Profile Data

x = 68 in., Te = 1.6%

N	Y INCHES	Y/ DELTA	U FT/SEC	T DEG.F	U/UE	THETA	U-UE UTAU	U(+)	T(+)	Y(+)
1	.0073	.007	41.30	86.26	.421	.371	-14.698	10.616	7.672	13.250
2	.0083	.007	43.36	85.45	.442	.403	-14.352	11.364	8.544	15.057
3	.0094	.008	45.51	84.60	.464	.436	-13.794	11.922	9.256	17.046
4	.0106	.009	47.35	84.65	.482	.426	-13.313	12.403	9.047	19.215
5	.0113	.010	48.06	84.44	.490	.442	-13.123	12.593	9.387	20.480
6	.0132	.012	50.00	83.36	.509	.485	-12.617	13.099	10.281	23.914
7	.0146	.013	51.08	83.24	.520	.489	-12.334	13.382	10.380	26.445
8	.0153	.014	51.66	83.27	.526	.488	-12.179	13.537	10.356	27.730
9	.0176	.016	52.95	82.87	.539	.504	-11.845	13.871	10.685	31.868
10	.0194	.017	53.42	82.37	.544	.523	-11.722	13.994	11.103	35.121
11	.0214	.019	54.41	82.04	.554	.536	-11.462	14.254	11.380	38.736
12	.0232	.021	55.16	81.92	.562	.541	-11.266	14.450	11.477	41.990
13	.0249	.022	55.70	81.91	.567	.541	-11.124	14.592	11.485	45.063
14	.0268	.024	56.15	81.83	.572	.544	-11.007	14.709	11.553	48.497
15	.0285	.025	56.82	81.71	.579	.549	-10.832	14.884	11.652	51.570
16	.0304	.027	57.06	81.54	.581	.556	-10.769	14.947	11.793	55.005
17	.0322	.029	57.40	81.34	.585	.564	-10.680	15.036	11.957	58.258
18	.0366	.035	59.29	80.24	.604	.607	-10.184	15.532	12.874	70.188
19	.0454	.041	60.37	80.03	.615	.615	-9.901	15.815	13.045	82.115
20	.0524	.047	61.65	79.94	.628	.618	-9.568	16.148	13.117	94.772
21	.0586	.052	62.44	79.73	.636	.626	-9.361	16.355	13.293	105.979
22	.0657	.059	63.60	79.02	.648	.654	-9.056	16.660	13.880	118.912
23	.0725	.065	64.57	79.39	.658	.640	-8.803	16.913	13.580	131.104
24	.0787	.070	65.19	78.99	.664	.656	-8.640	17.076	13.911	142.311
25	.0854	.076	66.02	78.53	.673	.673	-8.422	17.294	14.287	154.422
26	.0925	.083	66.60	78.18	.678	.687	-8.270	17.446	14.579	167.256
27	.0986	.086	67.23	78.53	.685	.673	-8.104	17.612	14.286	178.282
28	.1053	.094	67.83	77.97	.691	.695	-7.948	17.768	14.756	190.393
29	.1124	.100	68.49	77.70	.698	.706	-7.776	17.940	14.979	203.227
30	.1186	.106	68.98	77.44	.703	.716	-7.645	18.071	15.192	214.434
31	.1255	.112	69.24	77.70	.705	.706	-7.579	18.137	14.983	226.906
32	.1327	.118	70.17	77.71	.715	.706	-7.335	18.381	14.971	239.920
33	.1494	.133	71.33	76.75	.727	.743	-7.032	18.684	15.769	270.107
34	.1672	.149	72.67	76.74	.740	.743	-6.679	19.037	15.773	302.262
35	.1845	.165	73.35	76.45	.747	.755	-6.501	19.215	16.016	333.553
36	.2026	.181	74.45	76.11	.758	.768	-6.213	19.503	16.302	366.270
37	.2194	.196	75.70	76.25	.771	.762	-5.886	19.830	16.178	396.638
38	.2377	.212	76.13	75.89	.775	.777	-5.773	19.943	16.479	429.717
39	.2544	.227	77.18	75.43	.786	.795	-5.498	20.218	16.863	459.903
40	.2725	.243	78.20	75.43	.797	.795	-5.232	20.484	16.859	492.621
41	.2894	.258	78.68	75.67	.801	.785	-5.106	20.610	16.667	523.169
42	.3076	.275	79.86	75.59	.814	.789	-4.795	20.921	16.732	556.067
43	.3675	.328	82.08	74.49	.836	.831	-4.215	21.501	17.642	664.341
44	.4275	.382	84.49	73.71	.861	.862	-3.584	22.132	18.291	772.796
45	.4875	.435	86.40	73.22	.880	.881	-3.084	22.632	18.698	881.251
46	.5476	.489	88.40	73.09	.901	.886	-2.558	23.158	18.804	989.887
47	.6074	.542	90.14	72.70	.918	.901	-2.103	23.613	19.125	1097.980
48	.6675	.596	91.82	72.70	.935	.901	-1.664	24.052	19.126	1206.616
49	.7274	.649	93.24	72.28	.950	.918	-1.292	24.424	19.476	1314.690
50	.7876	.703	94.42	71.77	.962	.938	-.982	24.734	19.901	1423.706
51	.8474	.756	95.34	71.44	.971	.951	-.741	24.975	20.176	1531.800
52	.9073	.810	95.93	70.79	.977	.976	-.587	25.129	20.709	1640.074
53	.9676	.864	96.73	71.17	.985	.961	-.378	25.338	20.395	1749.071
54	1.0276	.917	97.21	70.78	.990	.976	-.251	25.465	20.719	1857.526
55	1.0876	.971	97.54	70.70	.994	.980	-.164	25.552	20.792	1965.981
56	1.1476	1.024	97.95	71.01	.998	.967	-.058	25.658	20.529	2074.436
57	1.2073	1.078	97.92	70.27	.997	.996	-.065	25.651	21.142	2182.349
58	1.2676	1.131	98.05	70.31	.999	.995	-.032	25.684	21.109	2291.346
59	1.3272	1.185	98.13	70.46	1.000	.988	-.011	25.705	20.967	2399.078
60	1.3874	1.238	98.20	70.16	1.000	1.000	.008	25.724	21.216	2507.894
61	1.4474	1.292	98.16	70.54	1.000	.986	.004	25.720	20.921	2616.349
62	1.5075	1.345	98.25	70.74	1.001	.978	.020	25.736	20.753	2724.985
63	2.1325	1.903	98.30	70.51	1.001	.987	.033	25.749	20.942	3854.724
64	2.7576	2.461	98.20	70.36	1.000	.992	.007	25.723	21.055	4984.644
65	3.3825	3.019	98.18	70.14	1.000	1.002	.003	25.719	21.252	6114.203
66	4.0074	3.577	98.27	70.59	1.001	.984	.026	25.742	20.878	7243.761

Table B13

RUN NO. 3. POINT 2.

BOUNDARY LAYER PROPERTIES

	LINEAR INTERPOLATION TO WALL	STANDARD SUBLAYER FUNCTION FROM WALL TO Y+=3[illegible]
FREE STREAM VELOCITY =	98.170	98.170
FREE STREAM TEMPERATURE =	70.180	
WALL TEMPERATURE =	95.750	
WALL HEAT FLUX =	.07954	
FREE STREAM DENSITY =	.07552	
FREE STREAM KINEMATIC VISCOSITY =	.0001619	
DENSITY OF FLUID AT WALL =	.07204	
KINEMATIC VISCOSITY OF FLUID AT WALL =	.0001760	
WALL/FREE STREAM DENSITY RATIO =	.95396	
LOCATION REYNOLDS NUMBER (REX) =	3435559.84	
INPUT VALUE OF VELOCITY DELTA =	1.30000	
INPUT VALUE OF TEMPERATURE DELTA =	1.30000	
CALCULATED DELTA =		1.12046
DELTA 99.5% INPUT =	.00000	
DISPLACEMENT THICKNESS (DELSTAR) =	.15429	.15443
MOMENTUM THICKNESS (THETA) =	.10938	.10967
ENERGY-DISSIPATION THICKNESS =	.19539	.19556
ENTHALPY THICKNESS =	.00597	.00598
SHAPE FACTOR 12 (DELSTAR/THETA) =	1.41057	1.40819
SHAPE FACTOR 32 (ENERGY/THETA) =	1.78634	1.78327
MOMENTUM THICKNESS REYNOLDS NUMBER =	5526.16	5540.66
DISPLACEMENT THICKNESS REYNOLDS NUMBER =	7795.01	7602.27
SKIN FRICTION COEFFICIENT =	.002865	
FRICTION VELOCITY =	3.81748	
LAW OF THE WALL CONSTANT (K) =	.41000	
LAW OF THE WALL CONSTANT (C) =	5.00000	
WAKE STRENGTH =		.44004
CLAUSERS 'DELTA' INTEGRAL =	-3.62559	-3.81767
CLAUSERS 'G' INTEGRAL =	24.97566	24.86643
DISPLACEMENT THICKNESS - CONSTANT DENSITY =	.14465	.14845
MOMENTUM THICKNESS - CONSTANT DENSITY =	.11055	.11085
SHAPE FACTOR 12 - CONSTANT DENSITY =	1.30848	1.33924

LOCATION -X- 68.00000

Te = 1.6%

Table B14

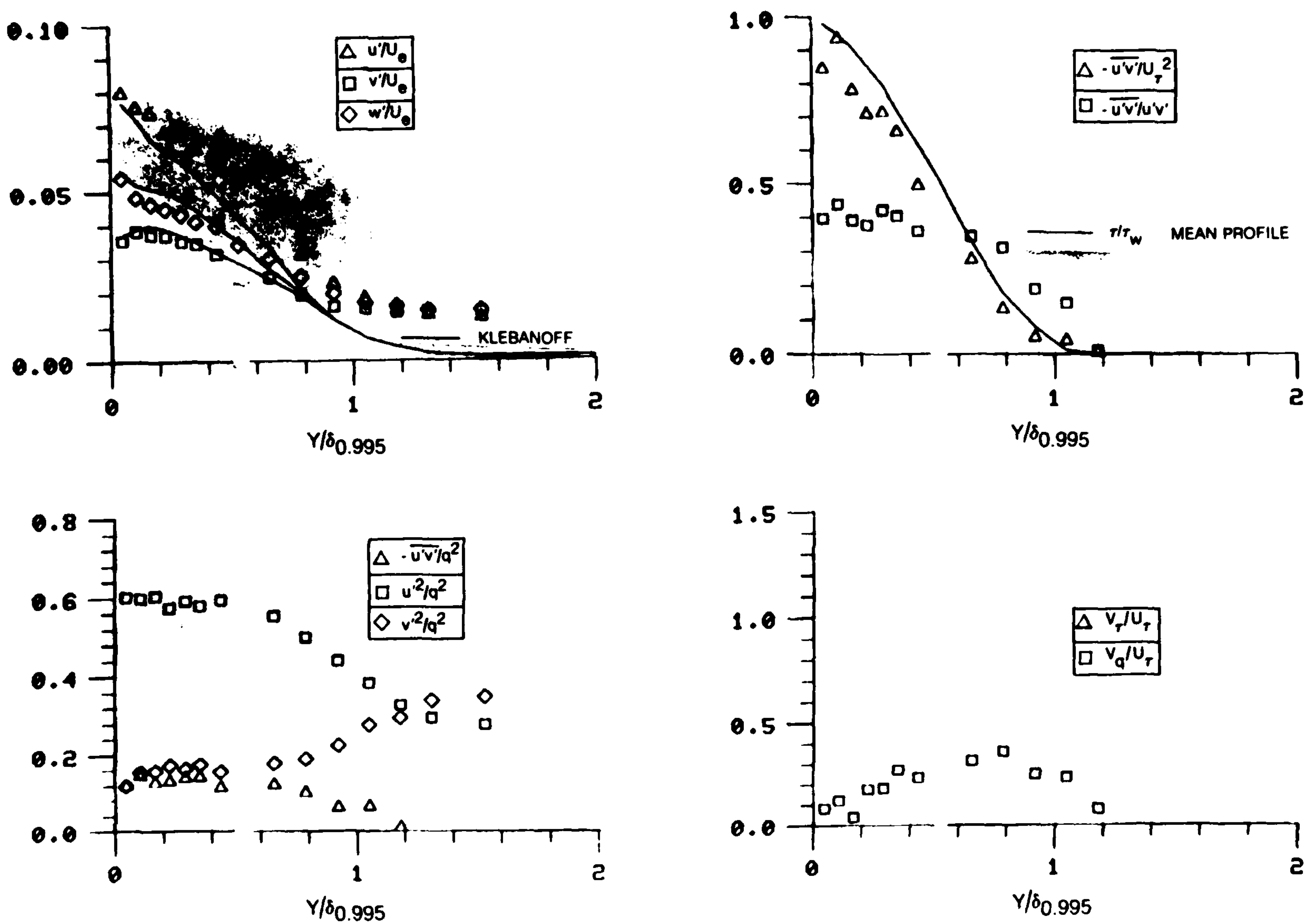

Figure B10A. Boundary Layer Turbulence Quantities $x = 68$ in, $T_e = 1.6\%$

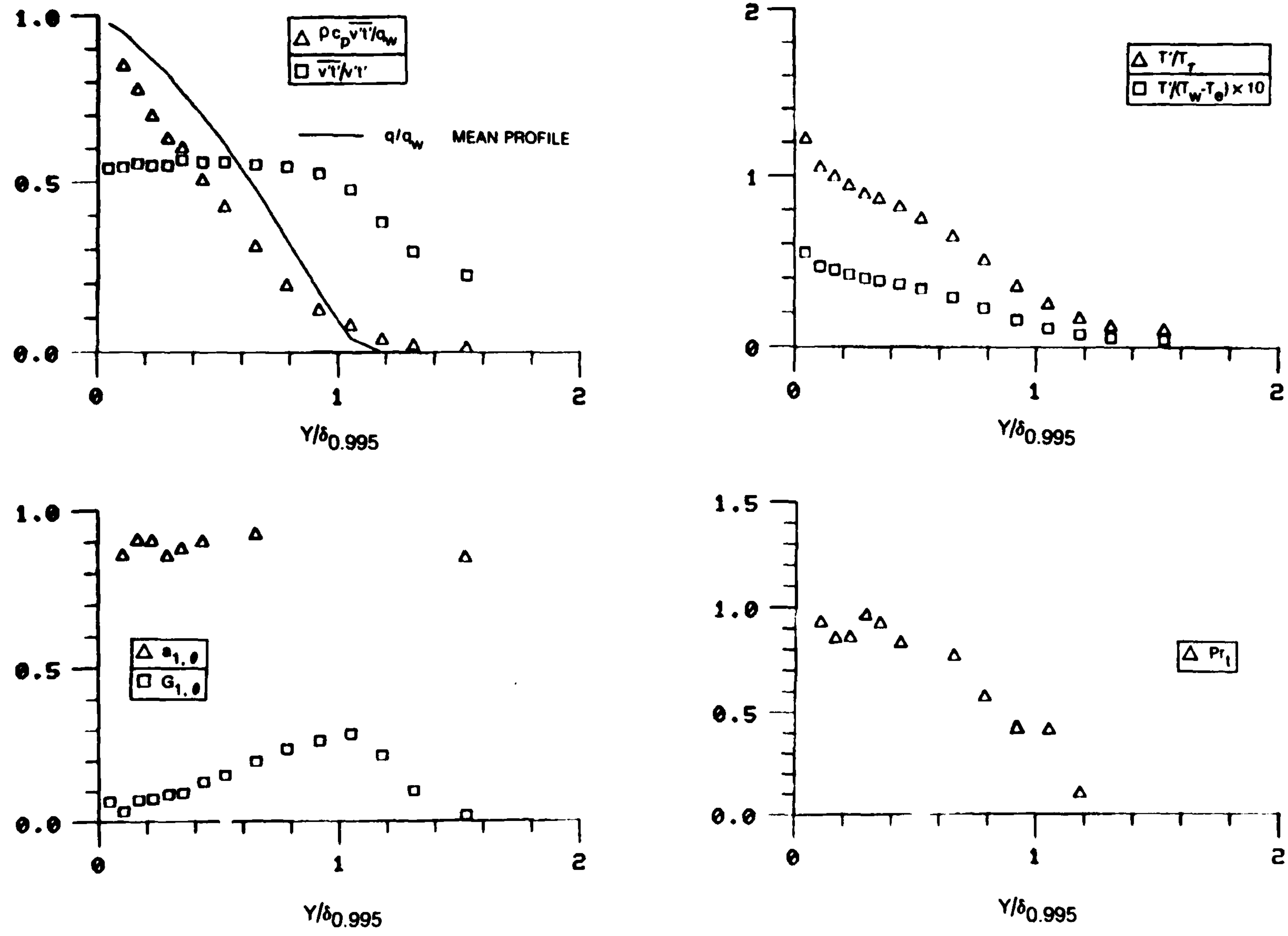

Figure B10B. Boundary Layer Turbulence Quantities $x = 68$ in, $T_e = 1.6\%$

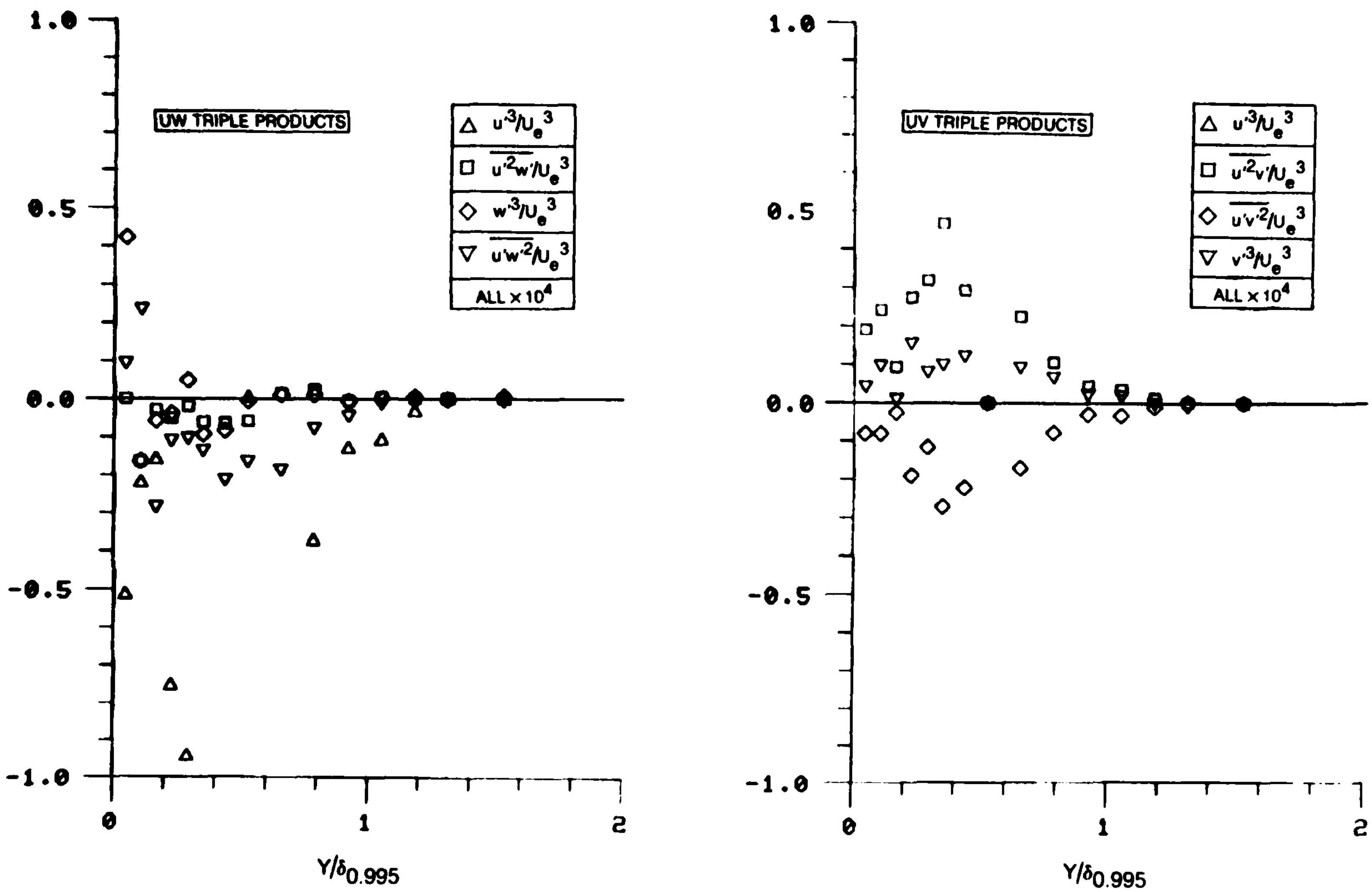

Figure B10C. Boundary Layer Triple Product Distributions $x = 68$ in, $T_e = 1.6\%$

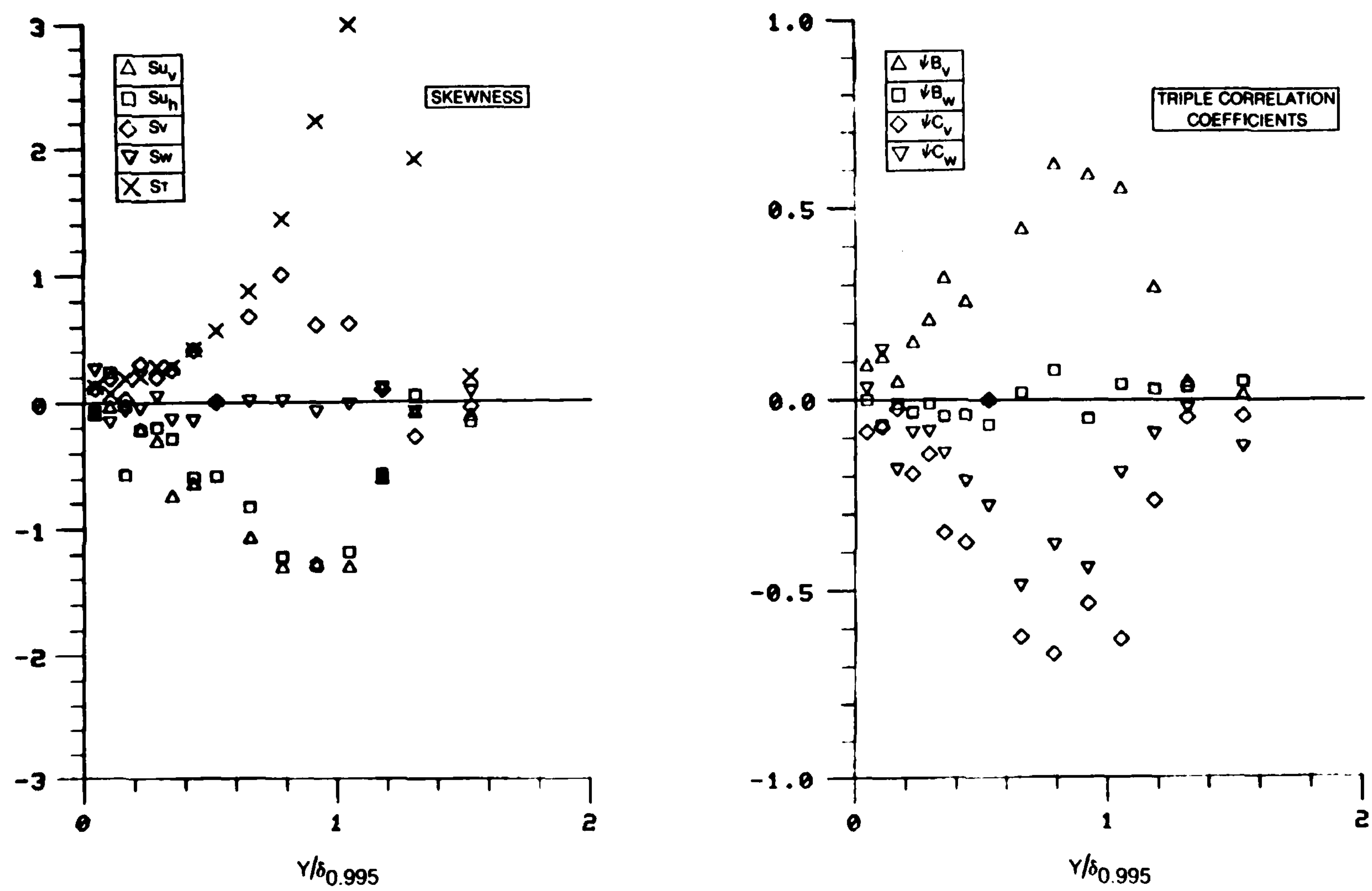

Figure B10D. Boundary Layer Skewness and Triple Product Correlation Coefficient Distributions $x = 68$ in, $T_e = 1.6\%$

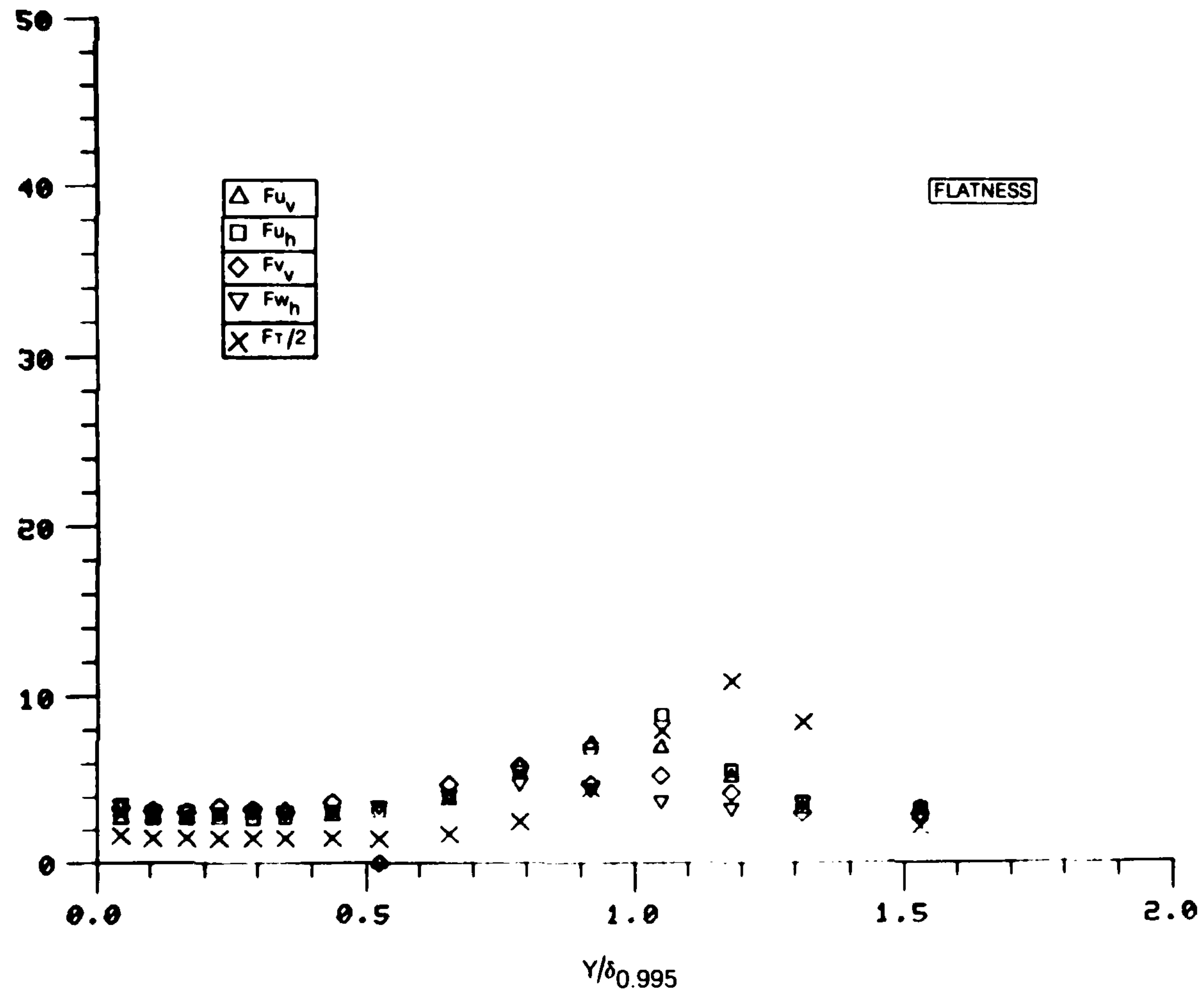

Figure B10E. Boundary Layer Flatness Distributions x =68 in, T_e = 1.6%

Fluctuating Profile Data

x = 68 in., Te = 1.6%

N	Y: INCHES	Y/ DELTA	U'/UE	V'/UE	W'/UE	√U'V'/UE	U'V'/ UTAU	U'V'/U'V'	[illegible]/UE
1	4.000	3.500	.0137	.0179	.0153	.0050	-.0169	-.0960	.0272
2	.050	.044	.0756	.0755	.0541	.0352	.6442	.3974	.1026
3	.120	.105	.0751	.0382	.0462	.0371	.9339	.4365	[illegible]
4	.190	.166	.0736	.0374	.0463	.0339	.7600	.3657	[illegible]
5	.260	.227	.0677	.0371	.0448	.0323	.7068	.3762	[illegible]
6	.330	.289	.0675	.0351	.0433	.0324	.7127	.4104	[illegible]
7	.400	.350	.0627	.0344	.0403	.0311	.6565	.4433	[illegible]
8	.500	.437	.0612	.0314	.0396	.0269	.4927	.36[illegible]	[illegible]
9	.600	.525	.0254	.0000	.0340	.0000	.0000	.0000	.0425
10	.750	.656	.0432	.0245	.0230	.0202	.2770	.3447	[illegible]
11	.900	.787	.0312	.0192	.0240	.0139	.1315	.3105	[illegible]
12	1.050	.919	.0225	.0160	.0195	.0085	.0490	.1910	[illegible]
13	1.200	1.050	.0180	.0153	.0169	.0074	.0360	.1476	[illegible]
14	1.350	1.181	.0147	.0140	.0155	.0024	.0040	.0191	[illegible]
15	1.500	1.312	.0131	.0141	.0145	.0036	-.0060	-.0677	[illegible]
16	1.750	1.531	.0125	.0140	.0144	.0048	-.0155	-.1257	[illegible]
17	4.000	3.500	.0125	.0163	.0141	.0046	-.0145	-.0954	[illegible]
18	.000	.000	.0000	.0000	.0000	.0000	.0000	.0000	[illegible]

N	Y: INCHES	Y/ DELTA	V'U'/C2	U'2/C2	V'2/C2	W'2/C2	VTAU/ UTAU	VC/ UTAU	[illegible]
1	4.000	3.500	-.0336	.2537	.4316	.3146	.0000	.0345	.0029
2	.050	.044	.1162	.6016	.1193	.2785	.0000	[illegible]	[illegible]
3	.120	.105	.1459	.5967	.1551	.2467	.0000	[illegible]	.0446
4	.190	.166	.1262	.6042	.1562	.2395	.0000	.0413	[illegible]
5	.260	.227	.1326	.5753	.1722	.2525	.0000	[illegible]	[illegible]
6	.330	.289	.1356	.5826	.1620	.2445	.0000	[illegible]	[illegible]
7	.400	.350	.1427	.5794	.1746	.2460	.0000	[illegible]	[illegible]
8	.500	.437	.1151	.5945	.1567	.2487	.0000	[illegible]	[illegible]
9	.600	.525	.0000	.3583	.0000	.6417	.0000	[illegible]	[illegible]
10	.750	.656	.1210	.5549	.1777	.2674	.0000	.3166	[illegible]
11	.900	.787	.0957	.5014	.1904	.3083	.0000	.3411	[illegible]
12	1.050	.919	.0637	.4404	.2241	.3355	.0000	[illegible]	[illegible]
13	1.200	1.050	.0639	.3841	.2772	.3367	.0000	[illegible]	[illegible]
14	1.350	1.181	.0089	.3284	.2964	.3752	.0000	.2779	[illegible]
15	1.500	1.312	-.0224	.2974	.3464	.3622	.0000	[illegible]	[illegible]
16	1.750	1.531	-.0405	.2793	.3505	.3699	.0000	[illegible]	[illegible]
17	4.000	3.500	-.0342	.2513	.4291	.3196	.0000	-.0306	.0045
18	.000	.000	.0000	.0000	.0000	.0000	.0000	.0000	[illegible]

N	INCHES	DELTA	V'T'/V'T'	T'/TTAU	T'/(TW-TE)	A10	G16	PRT
1	4.000	3.500	.0550	.0965	.0043	.2247	-.0075	-5.1615
2	.050	.044	.5414	1.2204	.0549	1.1025	.0654	
3	.120	.105	.5466	1.0489	.0472	.6541	.0330	.9272
4	.190	.166	.5554	.9900	.0445	.5045	.0693	.8479
5	.260	.227	.5466	.9364	.0423	.9303	.0741	[illegible]
6	.330	.289	.5466	.8876	.0399	.8513	.0860	.9656
7	.400	.350	.5646	.8614	.0387	.8756	.0930	.9233
8	.500	.437	.5572	.6139	.0366	.8967	.1234	.8266
9	.600	.525	.5564	.7446	.0335	.0000	.1582	.0000
10	.750	.656	.5524	.6429	.0269	.9193	.1661	.7657
11	.900	.787	.5440	.5022	.0226	1.0803	.2350	.5912
12	1.050	.919	.5234	.3509	.0153	1.5697	.2643	.8120
13	1.200	1.050	.4757	.2464	.0111	1.6204	.2856	.4130
14	1.350	1.181	.3827	.1647	.0074	3.3804	.2161	.0976
15	1.500	1.312	.2939	.4165	.0053	1.5145	.1516	-.4[illegible]
16	1.750	1.531	.6256	.3979	.0044	.8422	[illegible]	-1.24[illegible]
17	4.000	3.500	.0961	.1649	.0043	.4061	-.0110	-2.65[illegible]
18	.000	.000	.0000	.0000	.0000	.0000	.0000	.0000

Table B15A

Fluctuating Profile Data

x = 68 in., Te = 1.6%

N	Y: INCHES	Y/DELTA	U'3/UE3 X 10000	U'2W'/UE3 X 10000	W'3/UE3 X 10000	U'W'2/UE3 X 10000	[illegible]/UE3 X 10000	U'V'2/[illegible] X 10000	V'2/[illegible] X 10000
1	4.000	3.500	.0064	.0019	.0055	-.0726	.00[illegible]	.0[illegible]	.0[illegible]
2	.050	.044	-.5168	.0013	.4242	.0955	.19[illegible]	-.[illegible]	.[illegible]
3	.120	.105	-.2241	-.1647	-.165[illegible]	.24[illegible]	.2467	-.[illegible]	.[illegible]
4	.190	.166	-.1606	-.[illegible]95	-.056[illegible]	-.4797	.0929	-.[illegible]	.[illegible]
5	.260	.227	-.7562	-.[illegible]26	-.079[illegible]	-.1069	.27[illegible]	-.1[illegible]7	.[illegible]
6	.330	.289	-.9461	-.[illegible]55	.0047	-.0093	.32[illegible]	-.[illegible]	.[illegible]
7	.400	.350	-2.1945	-.[illegible]617	-.0092	-.1325	.46[illegible]	-.[illegible]	.[illegible]
8	.500	.437	-1.49[illegible]	-.[illegible]632	-.0849	-.2[illegible]57	.2[illegible]	-.[illegible]	.[illegible]
9	.600	.525	.0000	-.0576	-.0059	-.1622	.0[illegible]	.[illegible]	.0[illegible]
10	.750	.656	-1.[illegible]	.0119	.00[illegible]	-.1851	.2[illegible]	-.1[illegible]	.[illegible]
11	.900	.787	-.37[illegible]	.[illegible]14	.009[illegible]	-.0728	.1[illegible]	-.[illegible]	.[illegible]
12	1.050	.919	-.13[illegible]	-.0052	-.006[illegible]	-.041[illegible]	.044[illegible]	-.[illegible]	.[illegible]
13	1.200	1.050	-.1[illegible]	.[illegible]	.0[illegible]	-.0090	.07[illegible]	-.[illegible]	.[illegible]
14	1.350	1.181	-.[illegible]4	.[illegible]7	.0[illegible]	-.0029	.01[illegible]7	-.[illegible]	.[illegible]
15	1.500	1.312	-.002[illegible]	.0011	-.0017	-.0005	.0[illegible]	-.[illegible]	-.[illegible]
16	1.750	1.531	-.0025	.0011	.0[illegible]7	-.0033	.0[illegible]	-.[illegible]	-.[illegible]
17	4.000	3.500	.003[illegible]	.00[illegible]	-.005[illegible]	-.0023	.0[illegible]	-.[illegible]	-.[illegible]
18	.000	.000	.0[illegible]	.0000	.0000	.0000	.0[illegible]	.[illegible]	.[illegible]

N	Y: INCHES	Y/DELTA	SU V	SU W	SV	SW	ST	PSI[illegible] V	[illegible]
1	4.000	3.500	.29[illegible]7	-.[illegible]14	.0684	.15[illegible]	.0[illegible]	.[illegible]	.[illegible]
2	.050	.044	-.1028	-.0639	.1051	.2665	.1[illegible]	.0[illegible]	-.[illegible]
3	.120	.105	-.0[illegible]	.[illegible]39	.1816	-.1420	.06[illegible]	.10[illegible]	-.[illegible]
4	.190	.166	-.0[illegible]	-.[illegible]797	.[illegible]	-.0619	.15[illegible]	.0[illegible]	-.[illegible]
5	.260	.227	-.223[illegible]	-.[illegible]166	.2069	-.0421	.2[illegible]17	.1[illegible]	-.[illegible]
6	.330	.289	-.3175	-.2061	.1567	.0566	.249[illegible]	.2[illegible]	-.[illegible]
7	.400	.350	-.753[illegible]	-.2033	.2508	-.126[illegible]	.2[illegible]	.2[illegible]	-.[illegible]
8	.500	.437	-.6546	-.[illegible]4[illegible]	.404[illegible]	-.1339	.412[illegible]	.2[illegible]	-.[illegible]
9	.600	.525	.0000	-.[illegible]6[illegible]	.0[illegible]	-.0124	.557[illegible]	.0[illegible]	-.0[illegible]
10	.750	.656	-1.0854	-.[illegible]39	.6655	.019[illegible]	.6747	.4[illegible]	.[illegible]
11	.900	.787	-1.3156	-1.[illegible]330	.9953	.0218	1.4367	.613[illegible]	.[illegible]
12	1.050	.919	-1.2870	-1.3[illegible]	.[illegible]9	-.0647	2.2[illegible]	.5861	-.[illegible]
13	1.200	1.050	-1.3151	-1.1852	.6100	-.096[illegible]	2.975[illegible]	.5[illegible]7	.[illegible]
14	1.350	1.181	-.617[illegible]	-.5830	.0918	.1199	3.0840	.294[illegible]	.[illegible]
15	1.500	1.312	-.096[illegible]	.[illegible]	-.2775	-.069[illegible]	1.9[illegible]	.034[illegible]	.[illegible]
16	1.750	1.531	-.13[illegible]1	-.1690	-.044[illegible]	.0016	.153[illegible]	.01[illegible]	.[illegible]
17	4.000	3.500	.167[illegible]	-.357[illegible]	-.0331	-.1922	-.[illegible]	.0[illegible]	.[illegible]
18	.000	.000	.0000	.0000	.0000	.0000	.0[illegible]	.0[illegible]	.[illegible]

N	Y: INCHES	Y/DELTA	PSICV	PSICW	FU V	FU W	FL V	FU W	FT
1	4.000	3.500	.0909	-.0819	3.0503	3.0553	2.693[illegible]	2.72[illegible]8	3.[illegible]
2	.050	.044	-.084[illegible]	.[illegible]75[illegible]	2.666[illegible]	[illegible].7409	3.31[illegible]	3.[illegible]67[illegible]	[illegible]
3	.120	.105	-.0701	.1770	2.7296	2.6472	3.147[illegible]	3.155[illegible]	[illegible].969[illegible]
4	.190	.166	-.0240	-.1772	2.7025	2.6810	3.093[illegible]	3.128[illegible]	[illegible]
5	.260	.227	-.194[illegible]	-.0799	2.7011	2.7413	3.414[illegible]	3.074[illegible]	[illegible].927[illegible]
6	.330	.289	-.142[illegible]	-.[illegible]787	3.020[illegible]	2.668[illegible]	3.24[illegible]	3.10[illegible]	[illegible]
7	.400	.350	-.3469	-.1341	3.1547	2.7872	3.0947	3.1476	[illegible].99[illegible]
8	.500	.437	-.3731	-.2113	2.8791	2.9526	3.70[illegible]	3.1611	[illegible]
9	.600	.525	.0000	-.2741	.0000	3.1734	.0[illegible]	3.461[illegible]	[illegible]
10	.750	.656	-.6238	-.4836	3.8277	3.9672	4.7199	4.1736	[illegible]
11	.900	.787	-.6677	-.3769	[illegible].845[illegible]	5.5360	5.7597	4.8634	[illegible]
12	1.050	.919	-.5341	-.4766	7.1766	6.9262	4.75[illegible]	4.5[illegible]	[illegible]
13	1.200	1.050	-.6261	-.1867	6.8997	8.6146	5.2870	3.7[illegible]	[illegible]
14	1.350	1.181	-.2651	-.0826	5.1601	[illegible].6062	4.2719	3.3[illegible]	[illegible]
15	1.500	1.312	-.0440	-.[illegible]157	3.2720	3.6776	2.982[illegible]	3.6577	[illegible]
16	1.750	1.531	-.[illegible]	-.[illegible]152	3.279[illegible]	[illegible].2444	2.9744	[illegible].6316	[illegible]
17	4.000	3.500	-.037[illegible]	-.0936	2.937[illegible]	3.0763	2.6797	3.023[illegible]	3.6[illegible]
18	.000	.000	.0000	.0000	.0000	.0000	.0[illegible]	.0000	.0[illegible]

Table B15B

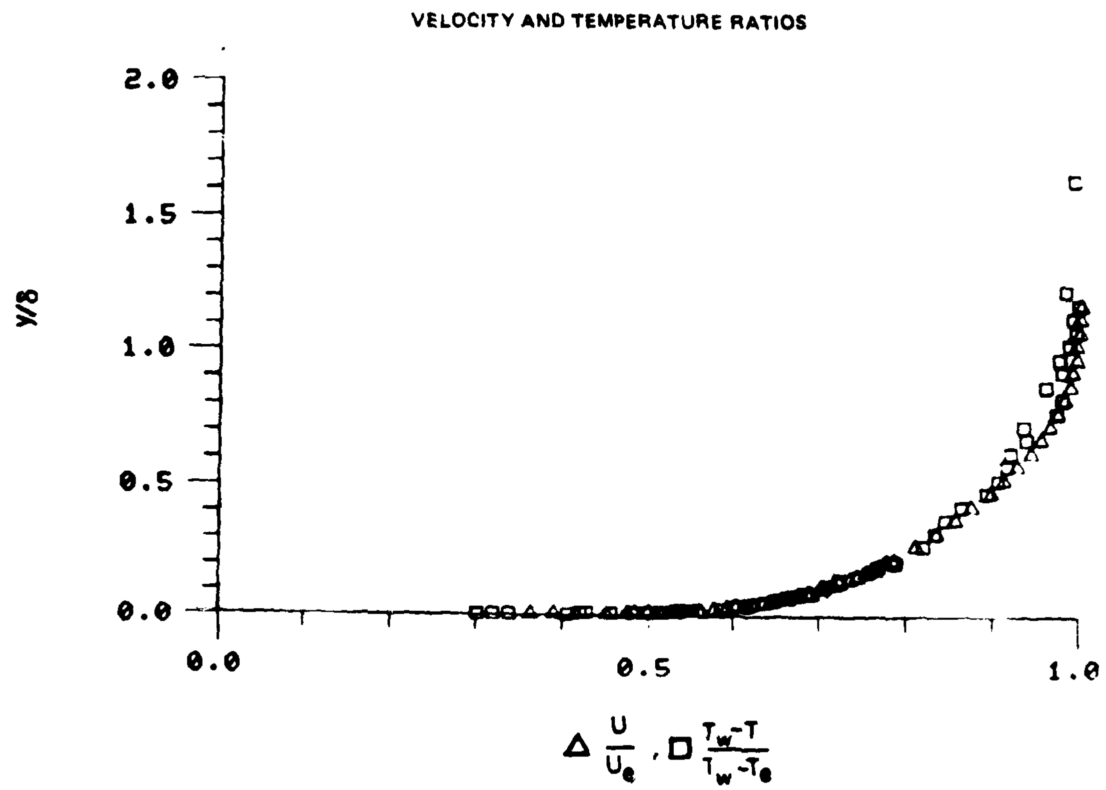

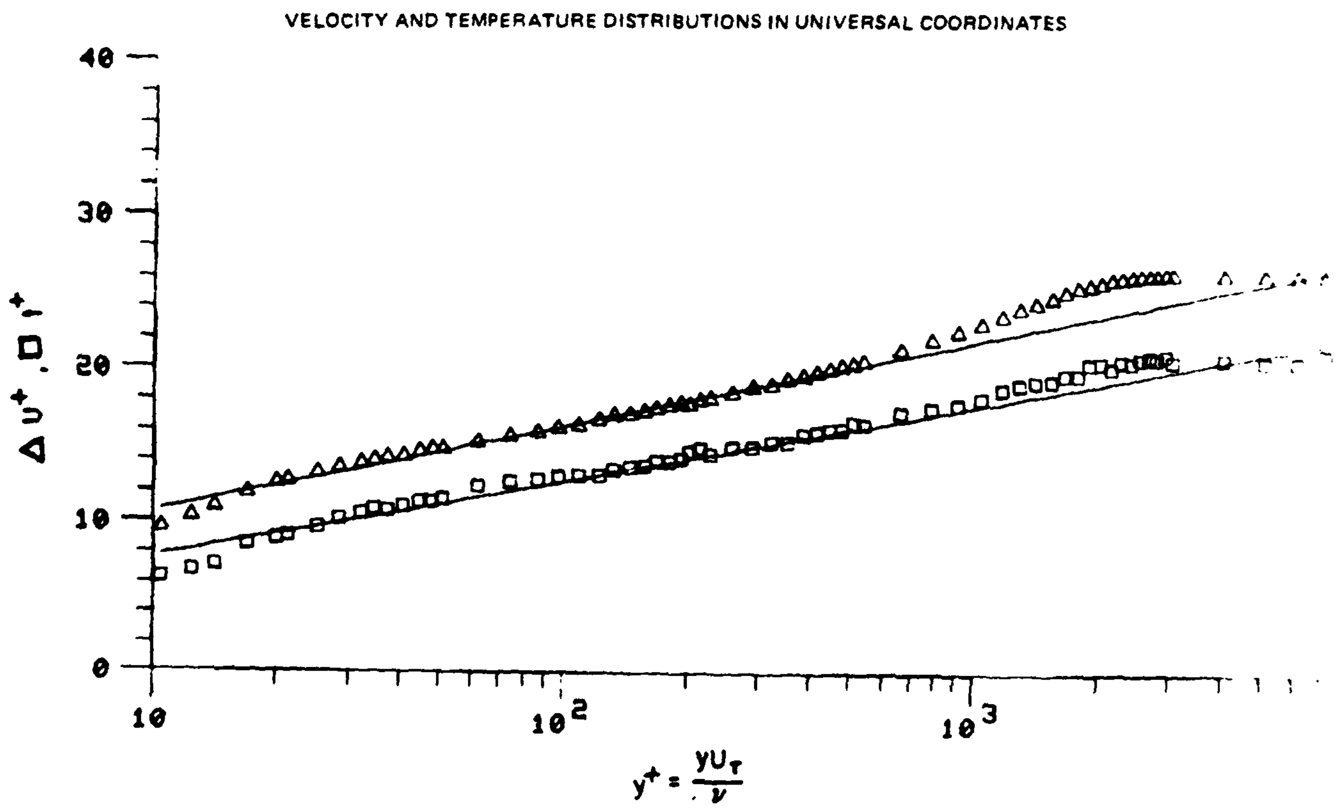

Figure B11. Mean Velocity and Temperature Profiles x = 84 in., Te = 1.4%

78-12-100-1

Mean Profile Data

x = 84 in., Te = 1.4%

N	Y INCHES	Y/ DELTA	U FT/SEC	T DEG.F	U/UE	THETA	U-UE UTAU	U(+)	T(+)	Y(+)
1	.0059	.004	35.41	87.49	.364	.301	-16.722	9.554	6.339	10.421
2	.0070	.005	38.09	86.99	.391	.320	-15.999	10.277	6.749	12.355
3	.0060	.006	40.60	86.53	.417	.338	-15.320	10.956	7.123	14.112
4	.0096	.007	44.01	84.77	.452	.406	-14.399	11.677	8.552	16.924
5	.0113	.008	46.34	84.35	.476	.422	-13.772	12.504	8.898	19.912
6	.0121	.009	47.12	84.17	.484	.429	-13.562	12.714	9.046	21.317
7	.0142	.010	48.68	83.44	.500	.457	-13.140	13.136	9.639	25.008
8	.0161	.012	50.16	82.75	.515	.484	-12.741	13.535	10.200	28.347
9	.0182	.013	51.13	82.36	.525	.499	-12.479	13.797	10.519	32.038
10	.0196	.014	51.89	81.93	.533	.516	-12.274	14.002	10.669	34.496
11	.0211	.015	52.35	82.04	.538	.511	-12.151	14.125	10.774	37.134
12	.0230	.017	52.81	81.78	.542	.521	-12.027	14.249	10.988	40.473
13	.0252	.018	53.86	81.39	.553	.536	-11.744	14.532	11.307	44.347
14	.0272	.020	54.42	81.39	.559	.536	-11.591	14.685	11.305	47.855
15	.0287	.021	54.72	81.22	.562	.543	-11.510	14.766	11.445	50.491
16	.0350	.025	56.17	80.13	.577	.585	-11.120	15.156	12.331	61.562
17	.0419	.030	57.66	79.75	.592	.599	-10.719	15.557	12.637	73.689
18	.0489	.035	58.68	79.63	.603	.604	-10.442	15.834	12.742	85.990
19	.0548	.039	59.82	79.39	.614	.613	-10.136	16.140	12.931	96.359
20	.0618	.044	60.53	79.24	.622	.619	-9.942	16.333	13.054	108.661
21	.0693	.050	61.70	79.24	.634	.619	-9.626	16.650	13.054	121.842
22	.0749	.054	62.65	78.81	.643	.636	-9.370	16.906	13.407	131.683
23	.0818	.059	63.08	78.51	.648	.648	-9.254	17.022	13.654	143.810
24	.0889	.064	63.75	78.46	.655	.649	-9.074	17.202	13.677	156.287
25	.0948	.068	64.65	78.11	.664	.663	-8.831	17.445	13.974	166.656
26	.1020	.073	65.21	78.05	.670	.665	-8.680	17.596	14.024	179.309
27	.1088	.078	65.87	77.83	.676	.674	-8.502	17.774	14.203	191.260
28	.1149	.082	65.69	77.36	.675	.692	-8.551	17.725	14.586	201.980
29	.1218	.087	66.71	77.09	.685	.702	-8.276	18.000	14.807	214.106
30	.1288	.092	67.02	77.50	.688	.687	-8.190	18.085	14.476	226.408
31	.1460	.105	68.29	77.02	.701	.705	-7.850	18.426	14.862	256.636
32	.1637	.117	69.69	76.94	.716	.708	-7.471	18.805	14.927	287.742
33	.1809	.130	70.44	76.55	.723	.723	-7.268	19.008	15.243	317.970
34	.1988	.143	71.55	76.57	.735	.723	-6.969	19.307	15.232	349.427
35	.2163	.155	72.31	75.98	.743	.745	-6.764	19.512	15.707	380.182
36	.2339	.166	73.30	75.67	.753	.757	-6.498	19.778	15.959	411.113
37	.2512	.180	74.01	75.46	.760	.765	-6.306	19.969	16.135	441.516
38	.2690	.193	74.77	75.44	.768	.766	-6.100	20.175	16.147	472.798
39	.2859	.205	75.43	74.90	.775	.787	-5.924	20.352	16.587	502.499
40	.3039	.218	76.35	75.01	.784	.782	-5.675	20.600	16.498	534.132
41	.3739	.268	78.81	74.10	.809	.818	-5.010	21.266	17.237	657.151
42	.4438	.318	81.16	73.74	.833	.832	-4.376	21.900	17.531	779.995
43	.5139	.368	83.37	73.45	.856	.843	-3.781	22.495	17.767	903.190
44	.5839	.419	85.07	72.96	.874	.862	-3.321	22.955	18.167	1026.209
45	.6540	.469	87.23	72.15	.896	.892	-2.740	23.536	18.801	1149.404
46	.7238	.519	88.79	71.86	.912	.904	-2.318	23.958	19.066	1272.072
47	.7938	.569	90.30	71.56	.927	.915	-1.909	24.367	19.292	1395.091
48	.8640	.619	91.71	71.51	.942	.918	-1.530	24.745	19.346	1518.462
49	.9339	.669	92.96	71.03	.955	.936	-1.191	25.085	19.739	1641.306
50	1.0038	.719	93.93	71.09	.965	.934	-.932	25.344	19.693	1764.149
51	1.0739	.770	94.79	70.13	.973	.971	-.698	25.578	20.470	1887.344
52	1.1439	.820	95.49	69.97	.981	.977	-.510	25.765	20.602	2010.364
53	1.2138	.870	96.24	70.44	.988	.959	-.307	25.969	20.218	2133.207
54	1.2838	.920	96.40	69.94	.990	.978	-.264	26.012	20.622	2256.226
55	1.3539	.970	96.92	70.05	.995	.974	-.123	26.152	20.535	2379.421
56	1.4240	1.021	96.96	69.73	.996	.986	-.112	26.164	20.796	2502.616
57	1.4937	1.071	97.20	69.55	.998	.993	-.048	26.226	20.940	2625.108
58	1.5637	1.121	97.28	69.66	.999	.989	-.028	26.248	20.654	2748.128
59	1.6337	1.171	97.34	69.47	1.000	.997	-.011	26.265	21.011	2871.147
60	1.7043	1.222	97.54	69.87	1.001	.981	.039	26.315	20.682	2995.221
61	2.2767	1.633	97.58	69.64	1.002	.990	.053	26.329	20.872	4004.662
62	2.8539	2.045	97.34	69.87	1.000	.981	-.009	26.266	20.685	5015.549
63	3.4269	2.458	97.41	69.86	1.000	.981	.008	26.284	20.691	6026.065
64	4.0043	2.870	97.41	69.21	1.000	1.006	.009	26.285	21.216	7037.283

Table B16

RUN NO. 3. POINT 1.

BOUNDARY LAYER PROPERTIES

		LINEAR INTERPOLATION TO WALL	STANDARD SUBLAYER FUNCTION FROM WALL TO Y+=35
FREE STREAM VELOCITY	=	97.379	97.379
FREE STREAM TEMPERATURE	=	69.380	
WALL TEMPERATURE	=	95.280	
WALL HEAT FLUX	=	.07879	
FREE STREAM DENSITY	=	.07563	
FREE STREAM KINEMATIC VISCOSITY	=	.0001615	
DENSITY OF FLUID AT WALL	=	.07210	
KINEMATIC VISCOSITY OF FLUID AT WALL	=	.0001757	
WALL/FREE STREAM DENSITY RATIO	=	.95333	
LOCATION REYNOLDS NUMBER (REX)	=	4220991.87	
INPUT VALUE OF VELOCITY DELTA	=	1.50000	
INPUT VALUE OF TEMPERATURE DELTA	=	1.80000	
CALCULATED DELTA	=		1.39524
DELTA 99.5% INPUT	=	.00000	
DISPLACEMENT THICKNESS (DELSTAR)	=	.19014	.19039
MOMENTUM THICKNESS (THETA)	=	.13559	.13572
ENERGY-DISSIPATION THICKNESS	=	.24207	.24207
ENTHALPY THICKNESS	=	.00739	.00739
SHAPE FACTOR 12 (DELSTAR/THETA)	=	1.40237	1.40265
SHAPE FACTOR 32 (ENERGY/THETA)	=	1.78534	1.78363
MOMENTUM THICKNESS REYNOLDS NUMBER	=	6813.21	6819.91
DISPLACEMENT THICKNESS REYNOLDS NUMBER	=	9554.62	9567.30
SKIN FRICTION COEFFICIENT	=	.002762	
FRICTION VELOCITY	=	3.70600	
LAW OF THE WALL CONSTANT (K)	=	.41000	
LAW OF THE WALL CONSTANT (C)	=	5.00000	
WAKE STRENGTH	=		.45923
CLAUSERS 'DELTA' INTEGRAL	=	-4.64864	-4.81114
CLAUSERS 'G' INTEGRAL	=	31.61966	31.69734
DISPLACEMENT THICKNESS - CONSTANT DENSITY	=	.17988	.18310
MOMENTUM THICKNESS - CONSTANT DENSITY	=	.13705	.13719
SHAPE FACTOR 12 - CONSTANT DENSITY	=	1.31253	1.33464

LOCATION -X- 64.00000

Te = 1.4%

Table B17

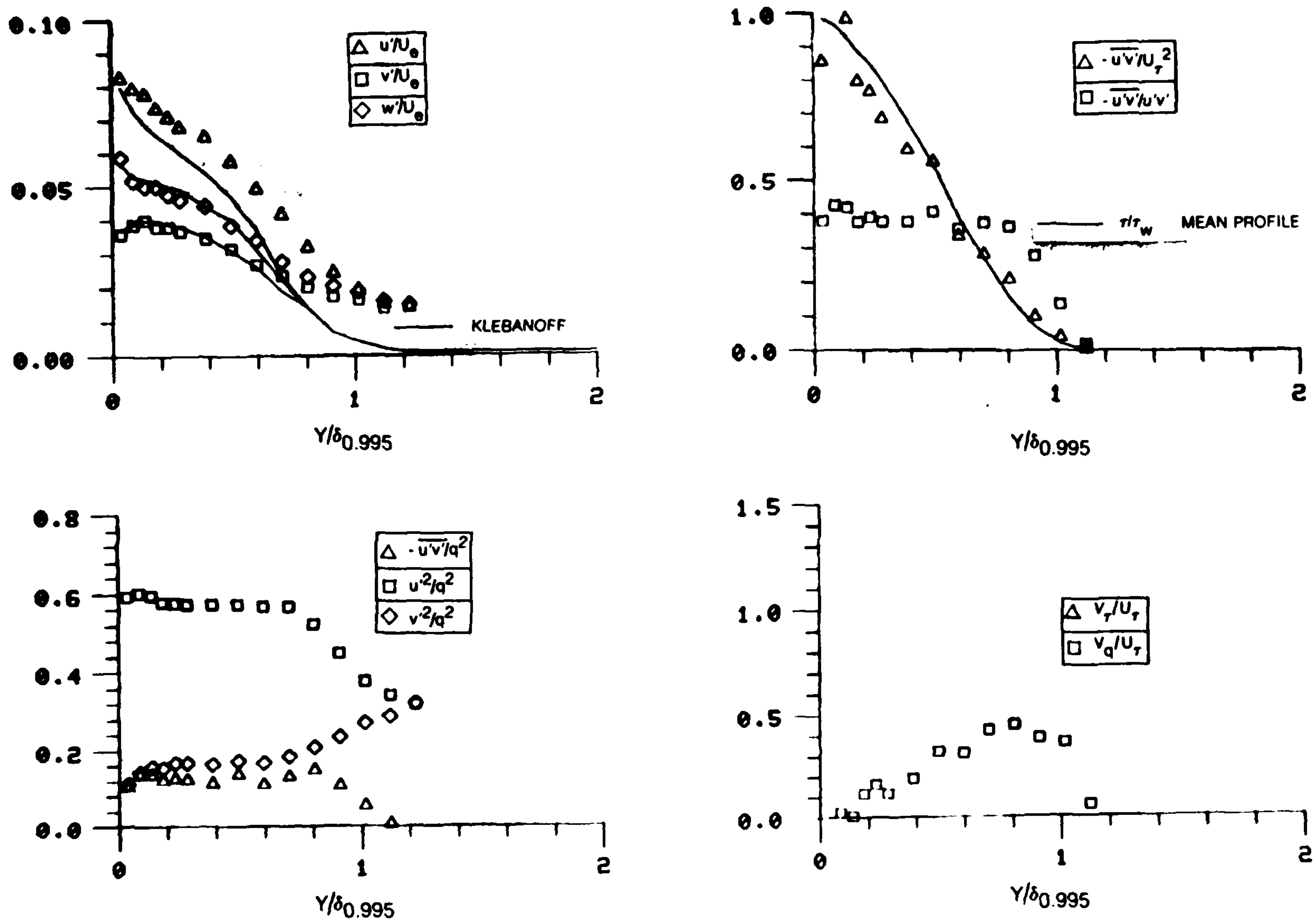

Figure B12A. Boundary Layer Turbulence Quantities $x = 84$ in, $T_e = 1.4\%$

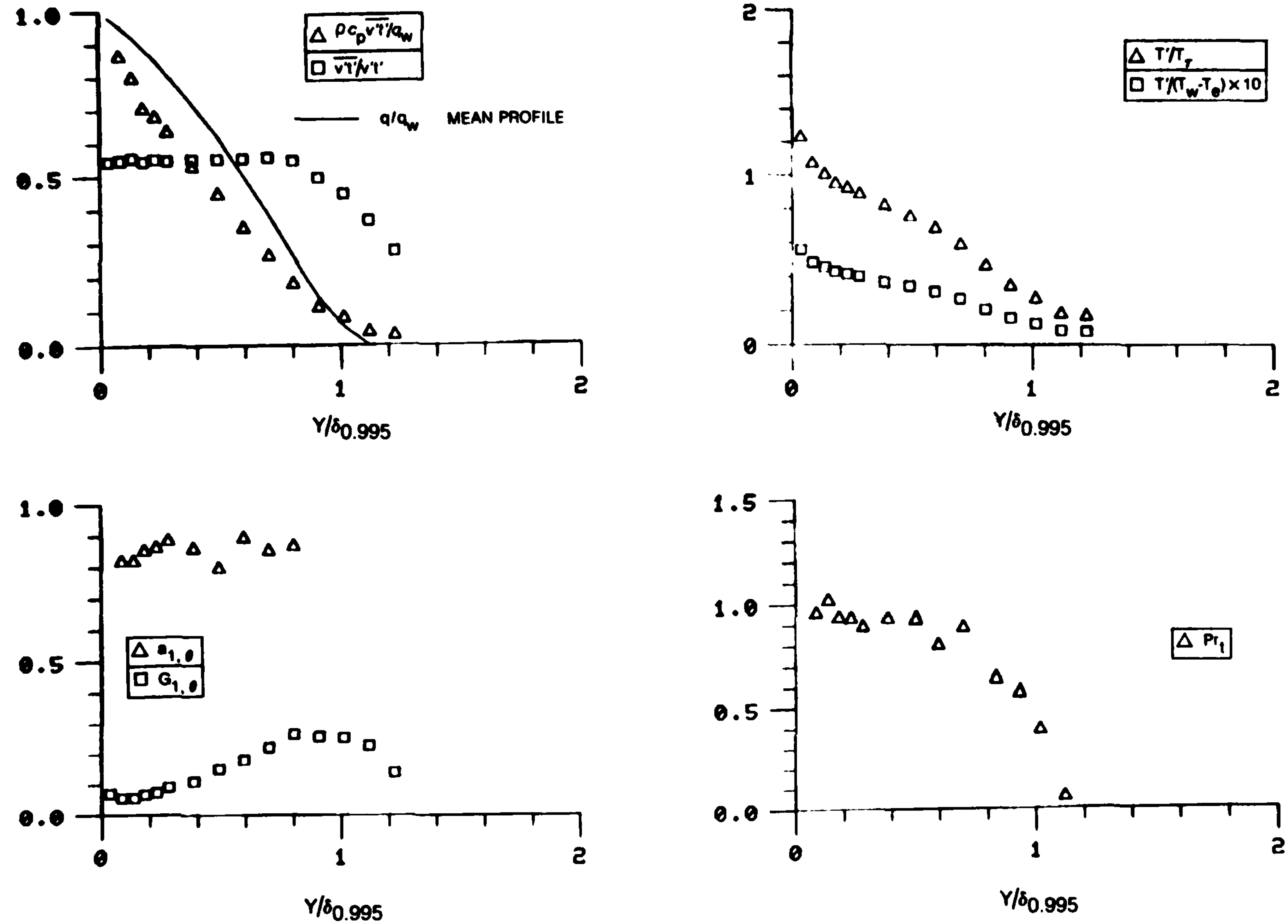

Figure B12B. Boundary Layer Turbulence Quantities $x = 84$ in, $T_e = 1.4\%$

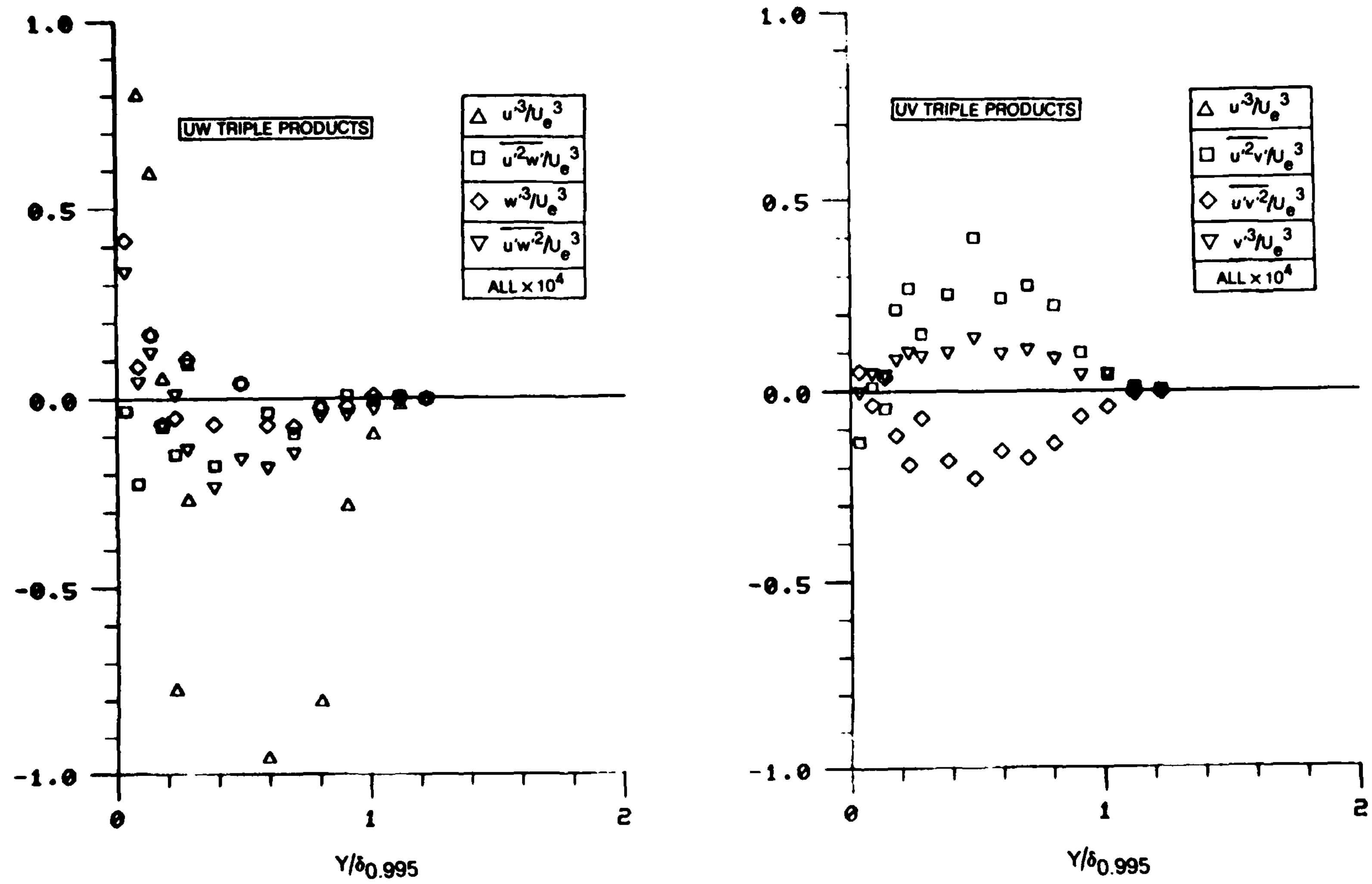

Figure B12C. Boundary Layer Triple Product Distributions $x = 84$ in, $T_e = 1.4\%$

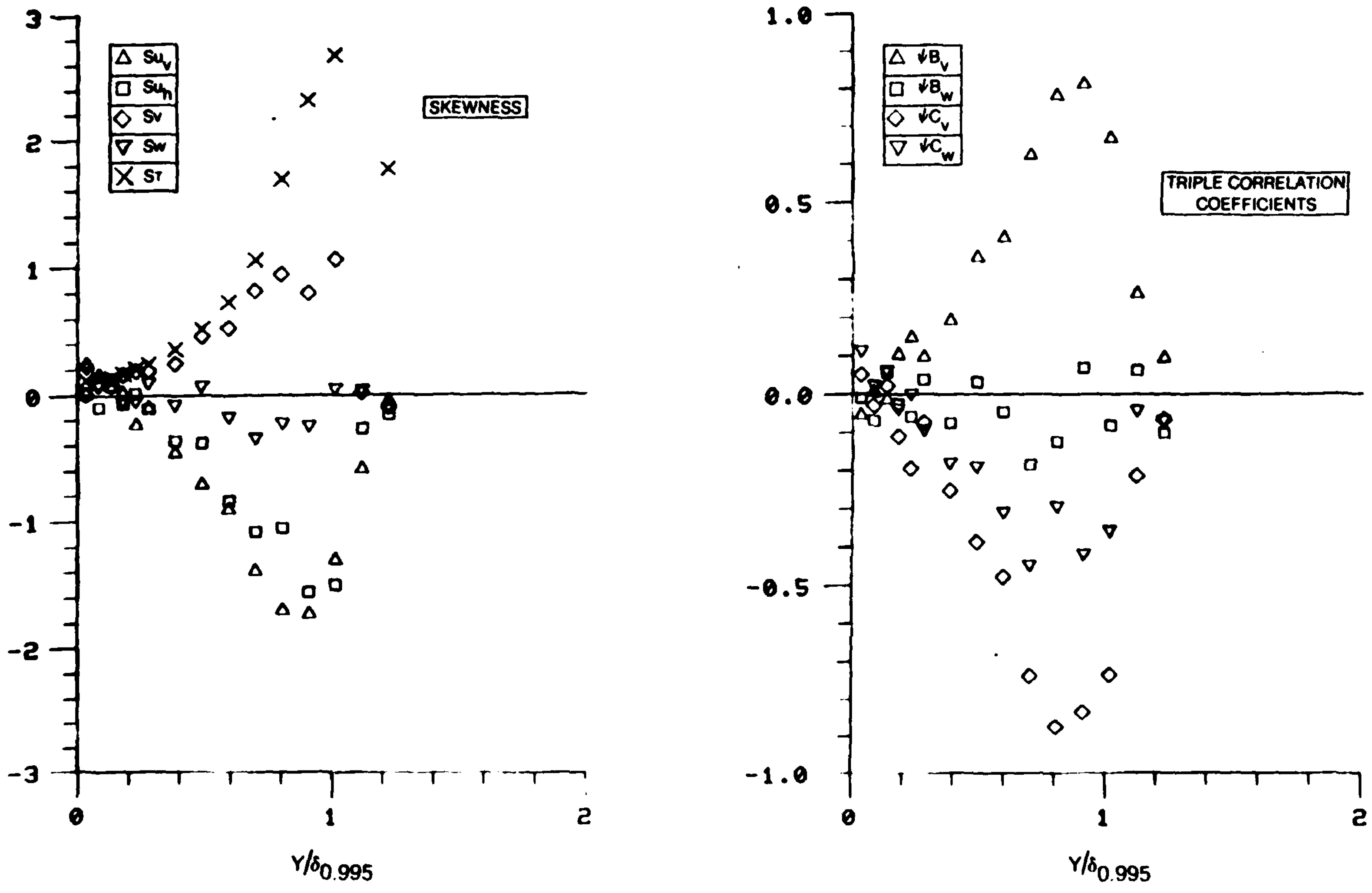

Figure B12D. Boundary Layer Skewness and Triple Product Correlation Coefficient Distributions $x = 84$ in, $T_e = 1.4\%$

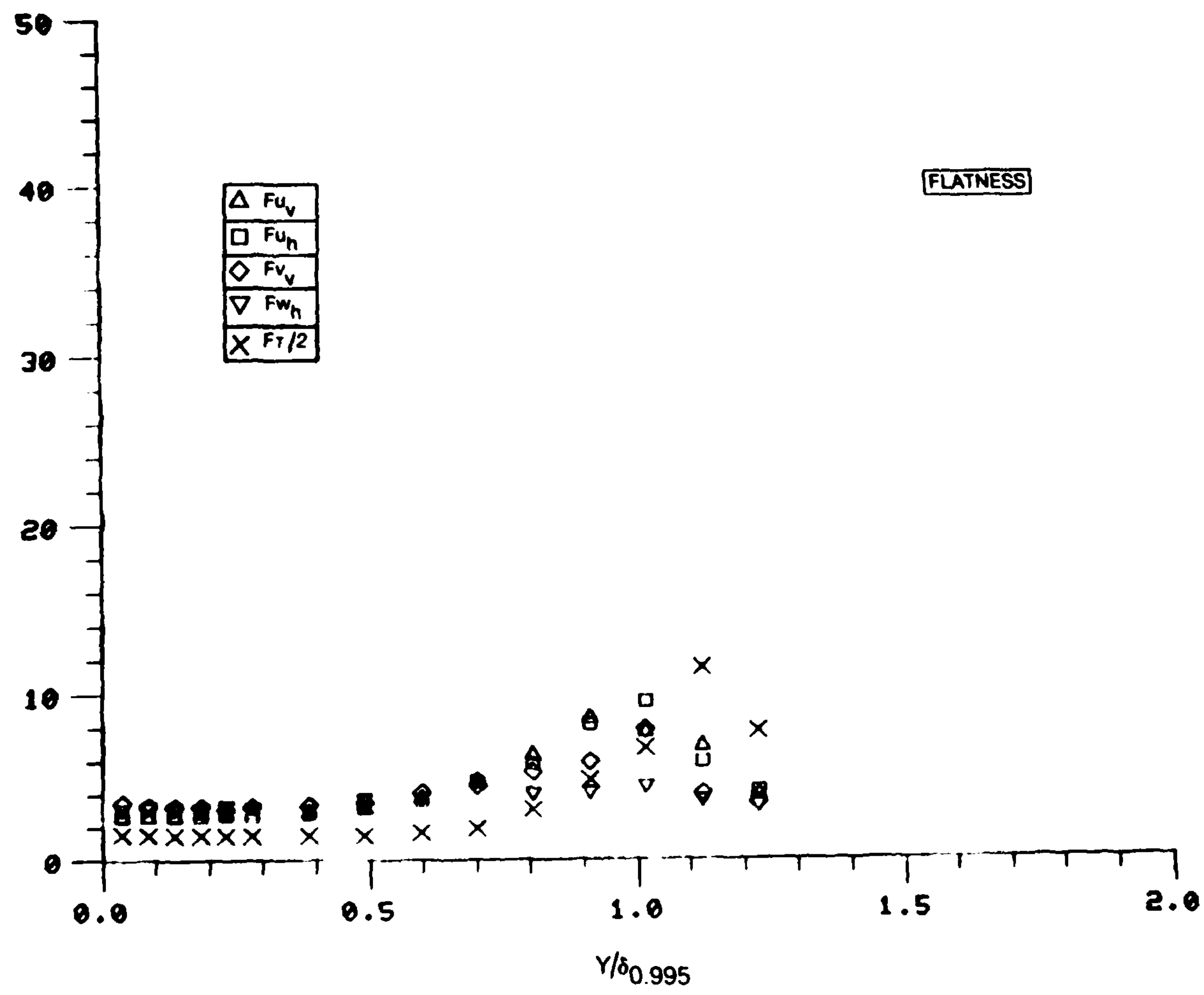

Figure B12E. Boundary Layer Flatness Distributions $x = 84$ in, $T_e = 1.4\%$

Fluctuating Profile Data

x = 84 in., Te = 1.4%

N	Y: INCHES	Y/DELTA	U'/UE	V'/UE	W'/UE	$\sqrt{\overline{U'V'}}$/UE	$\overline{U'V'}$/UTAU²	$\overline{U'V'}$/U'V'	C/UE
1	4.000	2.757	.0131	.0153	.0141	.0035	[illegible]	[illegible]	[illegible]
[illegible]	[illegible]	[illegible]	[illegible]	[illegible]	[illegible]	[illegible]	[illegible]	[illegible]	[illegible]
[illegible]	.120	[illegible]	.0754	.0767	.0516	.0377	[illegible]	[illegible]	[illegible]
[illegible]	.190	.133	.0777	.0759	.0499	.0373	[illegible]	.3775	[illegible]
[illegible]	[illegible]	[illegible]	.0738	.0762	.0501	.0336	.7955	[illegible]	[illegible]
[illegible]	.33	[illegible]	.0766	[illegible]	.0474	[illegible]	[illegible]	[illegible]	[illegible]
[illegible]	[illegible]	[illegible]	.0677	.0766	[illegible]	.0311	[illegible]	.3772	[illegible]
[illegible]	.55	.365	.0647	.0745	[illegible]	.0289	[illegible]	.374	[illegible]
[illegible]	.70	.49	.0573	.0714	.0364	.0281	[illegible]	[illegible]	[illegible]
[illegible]	[illegible]	[illegible]	.0490	.0266	[illegible]	.0217	[illegible]	[illegible]	[illegible]
11	1.[illegible]	[illegible]	[illegible]	.0235	.0276	.0198	.27	[illegible]	[illegible]
[illegible]	1.1	[illegible]	.0219	.0221	[illegible]	.0171	[illegible]	[illegible]	[illegible]
[illegible]	[illegible]	[illegible]	[illegible]	.0174	[illegible]	.0117	.097	[illegible]	[illegible]
[illegible]	1.45	[illegible]	[illegible]	.0161	[illegible]	.0072	[illegible]	.016	[illegible]
[illegible]	1.60	1.[illegible]	.0151	.0159	.015	.0019	[illegible]	[illegible]	[illegible]
[illegible]	1.75	1.2	.0140	.0141	.015	.0021	[illegible]	-.119	[illegible]
[illegible]	4.00	2.757	[illegible]	.0161	.015	.0052	[illegible]	[illegible]	[illegible]
[illegible]	.00	[illegible]	.0000	.0000	.000	.0000	[illegible]	[illegible]	[illegible]

N	Y: INCHES	Y/DELTA	$\overline{T'U'}$/C2	U'2/C2	V'2/C2	W'2/C2	VTAU/UTAU	VC/UTAU	$\overline{V'T'}$ RHOCP/QWALL
1	4.[illegible]	2.757	[illegible]	.2648	.3855	.3297	[illegible]	-.03	-.000
[illegible]	.05	.035	[illegible]	[illegible]	.1117	.2966	[illegible]	[illegible]	.661
[illegible]	[illegible]	[illegible]	.1358	.6624	.1437	[illegible]	[illegible]	[illegible]	.75
[illegible]	[illegible]	.133	[illegible]	.5967	.1571	[illegible]	[illegible]	[illegible]	[illegible]
[illegible]	.26	.162	[illegible]	.5762	.154	.2678	[illegible]	.166	[illegible]
[illegible]	[illegible]	.231	[illegible]	[illegible]	.166	.2592	[illegible]	.116	[illegible]
[illegible]	[illegible]	[illegible]	[illegible]	.5711	.1673	.2619	[illegible]	[illegible]	[illegible]
[illegible]	.55	.36	.1138	.5714	.1626	.2660	[illegible]	[illegible]	[illegible]
[illegible]	.7	[illegible]	[illegible]	[illegible]	.171	[illegible]	[illegible]	.31	[illegible]
[illegible]	[illegible]	.594	.1111	.5651	.1665	.2684	[illegible]	[illegible]	[illegible]
11	1.00	.659	.1257	.5665	.182	.2512	[illegible]	[illegible]	[illegible]
[illegible]	[illegible]	[illegible]	.1456	.5214	[illegible]	.2703	[illegible]	[illegible]	[illegible]
[illegible]	1.30	.909	.1067	.4477	.274	.3175	[illegible]	[illegible]	[illegible]
[illegible]	1.4	[illegible]	[illegible]	.3769	.266	.3549	[illegible]	[illegible]	[illegible]
[illegible]	1.6	1.11	[illegible]	.3793	.28	.3726	[illegible]	[illegible]	[illegible]
[illegible]	1.75	1.26	-.0069	.3178	.3	.362	[illegible]	[illegible]	[illegible]
[illegible]	4.00	2.75	-.04	[illegible]	.397	.346	[illegible]	[illegible]	[illegible]
[illegible]	.00	.000	.0000	.0000	.0000	.0000	.00	[illegible]	[illegible]

N	Y: INCHES	Y/DELTA	$\overline{V'T'}$/V'T'	T'/TTAU	T'/(TW-TE)	A10	G16	PRT
1	4.000	2.757	-.0161	.0879	.004	-.0849	-.022	10.4532
[illegible]	[illegible]	[illegible]	.5461	1.0281	.05	1.1194	.07	.9575
[illegible]	.12	[illegible]	.5497	1.0914	.046	.6197	[illegible]	1.0165
[illegible]	.190	.133	[illegible]	[illegible]	[illegible]	.6167	.0571	.9133
[illegible]	.26	.162	[illegible]	.9448	.0427	.6517	.0664	.9
6	.33	.231	.552	.9188	.0416	.6613	[illegible]	.8911
7	[illegible]	[illegible]	[illegible]	[illegible]	[illegible]	.6834	.091	.926
[illegible]	[illegible]	[illegible]	[illegible]	[illegible]	.036	.6583	.11	.8876
[illegible]	.7	.49	[illegible]	.7649	[illegible]	.7970	.1511	.795
[illegible]	[illegible]	.594	[illegible]	.6799	[illegible]	.6916	[illegible]	.6816
11	1.00	.659	[illegible]	.5895	[illegible]	.6527	.22	.6380
[illegible]	1.15	[illegible]	.5444	.4599	.0156	.6676	.266	.565
[illegible]	1.30	.909	.4927	.3444	.012	1.0252	[illegible]	.3655
[illegible]	1.4	1.034	.44	.2691	.006	1.5365	.25	[illegible]
[illegible]	1.6	1.1	.36	.1768	[illegible]	4.2649	.2297	-.0985
[illegible]	1.75	1.264	.2766	[illegible]	[illegible]	2.5271	.14	-.0967
[illegible]	4.00	2.7	.0590	.1746	[illegible]	[illegible]	.0857	[illegible]
[illegible]	[illegible]	[illegible]	[illegible]	[illegible]	[illegible]	[illegible]	[illegible]	[illegible]

Table B18A

Fluctuating Profile Data

x = 84 in., Te = 1.4%

N	Y: INCHES	Y/DELTA	U'3/UE3 x 10000	U'2W'/UE3 x 10000	W'3/UE3 x 10000	U'W'2/UE3 x 10000	U'2V'/UE3 x 10000	U'V'2/UE3 x 10000	V'3/UE3 x 10000
1	4.000	2.797	-.0069	.0010	-.0030	.0007	-.0021	-.0044	-.0028
2	.050	.035	1.2649	-.0318	.4159	.3750	-.1320	-.0510	[illegible]
3	.120	.084	.8[illegible]	-.2267	.0924	.0451	-.0103	[illegible]	[illegible]
4	.190	.133	.59[illegible]	.1664	.1684	.1242	-.0459	-.0341	[illegible]
5	.260	.182	.0514	-.0745	-.0664	-.0663	.2133	-.1165	.0525
6	.330	.231	-.7747	-.1498	-.0505	-.0125	.2685	-.1527	[illegible]
7	.400	.280	-.2708	.0914	.1020	-.1315	.1494	-.0724	[illegible]
8	.550	.385	-1.1150	-.1771	-.0693	-.2326	.2500	-.1848	.1015
9	.700	.490	-1.5284	.0789	.0395	-.1574	.4000	-.2297	.14[illegible]
10	.850	.594	-.9574	-.0463	-.0696	-.1791	.2431	-.1590	[illegible]
11	1.000	.699	-1.1239	-.0931	-.0731	-.1425	.2734	-.1780	[illegible]
12	1.150	.804	-.8027	-.0232	-.0271	-.0450	.2230	-.1730	[illegible]
13	1.300	.909	-.2864	.0075	-.0222	-.0415	.0997	-.0676	[illegible]
14	1.450	1.014	-.0977	-.0064	.0050	-.0268	.0424	-.0425	[illegible]
15	1.600	1.119	-.0203	.0027	.0010	-.0017	.0000	[illegible]	[illegible]
16	1.750	1.224	-.0022	-.0030	-.0035	-.0019	.0031	-.0030	[illegible]
17	4.000	2.797	.0124	-.0010	.0062	-.0015	.0009	.0054	-.0065
18	.000	.000	.0010	.0000	.0000	.0000	.0000	.0000	.0000

N	Y: INCHES	Y/DELTA	SU V	SU H	SV	SW	ST	PSI V	PSI W
1	4.000	2.797	-.4056	.1711	-.0784	-.1085	.0607	-.0796	.0794
2	.050	.035	.2730	.0774	-.0151	.2067	.1110	-.0[illegible]	[illegible]
3	.120	.084	.1466	-.1096	.0834	.0638	.1060	.0050	-.0693
4	.190	.133	.1110	[illegible]	.0714	.1379	.0976	-.0114	[illegible]
5	.260	.182	.0000	-.0743	.1546	-.0480	.16[illegible]	[illegible]	[illegible]
6	.330	.231	-.2378	.0099	.1577	-.0456	.2730	.145[illegible]	[illegible]
7	.400	.280	-.1100	-.1173	.1831	.0974	.2419	.096[illegible]	[illegible]
8	.550	.385	-.4654	-.3677	.2467	-.0774	.35[illegible]	.199[illegible]	[illegible]
9	.700	.490	-.7196	-.3833	.4528	.0718	.51[illegible]	.357[illegible]	[illegible]
10	.850	.594	-.9061	-.6435	.5353	-.1741	.7[illegible]	.47[illegible]	[illegible]
11	1.000	.699	-1.3929	-1.0865	.8090	-.3430	1.0569	.62[illegible]	[illegible]
12	1.150	.804	-1.7077	-1.0529	.9399	-.2238	1.6797	.7943	[illegible]
13	1.300	.909	-1.7304	-1.5577	.7954	-.2444	2.3054	.616[illegible]	[illegible]
14	1.450	1.014	-1.3060	-1.4953	1.0515	.0517	2.6660	.6[illegible]	[illegible]
15	1.600	1.119	-.5888	-.2671	.0141	.0378	3.3869	.265[illegible]	.063[illegible]
16	1.750	1.224	-.0606	-.1666	-.1[illegible]	-.1[illegible]6	1.7640	[illegible]	[illegible]
17	4.000	2.797	.4945	-.0625	-.1573	.1847	-.2610	[illegible]	[illegible]
18	.000	.000	.0000	.0005	.0000	.0000	.0000	.0000	.0000

N	Y: INCHES	Y/DELTA	PSICV	PSICW	FU V	FU H	FL V	FL H	FT
1	4.000	2.797	-.1454	.0250	3.0165	3.2165	3.0553	3.2464	[illegible]
2	.050	.035	.0510	.1162	2.6921	2.6388	3.4889	3.1443	[illegible]
3	.120	.084	-.0292	.0268	2.6133	2.6692	3.2884	[illegible]	[illegible]
4	.190	.133	.0216	.0642	2.6263	2.6329	3.2650	3.1367	[illegible]
5	.260	.182	-.1062	-.0366	2.8435	2.6999	3.24[illegible]	3.1[illegible]6	[illegible]
6	.330	.231	-.1949	.0048	2.8571	2.7399	3.0840	3.3435	[illegible]
7	.400	.280	-.0754	-.0900	2.6367	2.6862	3.2640	[illegible]	[illegible]
8	.550	.365	-.2527	-.1779	2.9258	2.6166	3.3744	3.0914	[illegible]
9	.700	.490	-.3851	-.1685	3.1917	3.1295	3.4544	3.7461	[illegible]
10	.850	.594	-.4761	-.3073	3.7186	3.5462	4.1243	3.7637	[illegible]
11	1.000	.699	-.7355	-.4449	4.7151	4.7311	4.5187	4.4556	[illegible]
12	1.150	.804	-.8755	-.2915	6.3139	5.6185	5.3567	4.0906	[illegible]
13	1.300	.909	-.6357	-.4173	6.5332	6.1341	5.6997	4.14[illegible]	[illegible]
14	1.450	1.014	-.7358	-.3561	7.7005	9.5199	7.8505	4.4661	13.[illegible]
15	1.600	1.119	-.2125	-.0379	6.8574	5.9104	4.0055	3.6293	[illegible]
16	1.750	1.224	-.0637	-.0642	3.9464	4.1988	3.3933	3.3233	15.54[illegible]
17	4.000	2.797	.1538	-.0541	3.4617	3.0999	2.8500	3.0649	[illegible]
18	.000	.000	.0000	.0000	.0000	.0000	.0000	.0000	.0000

Table B18B

VELOCITY AND TEMPERATURE RATIOS

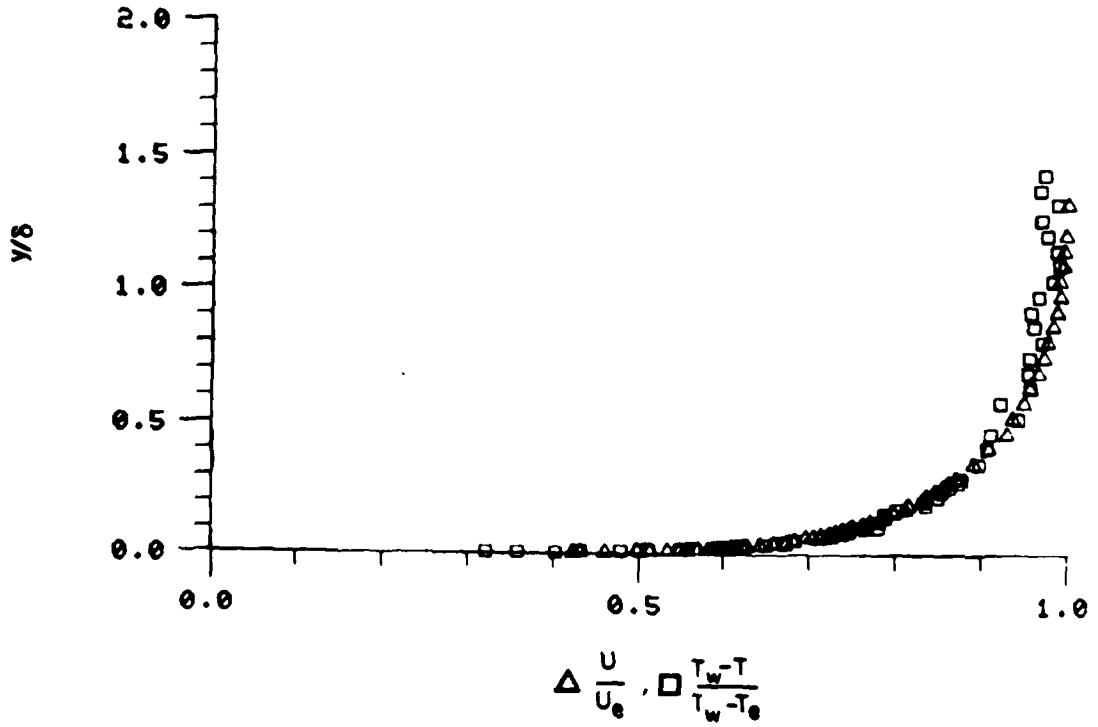

VELOCITY AND TEMPERATURE DISTRIBUTIONS IN UNIVERSAL COORDINATES

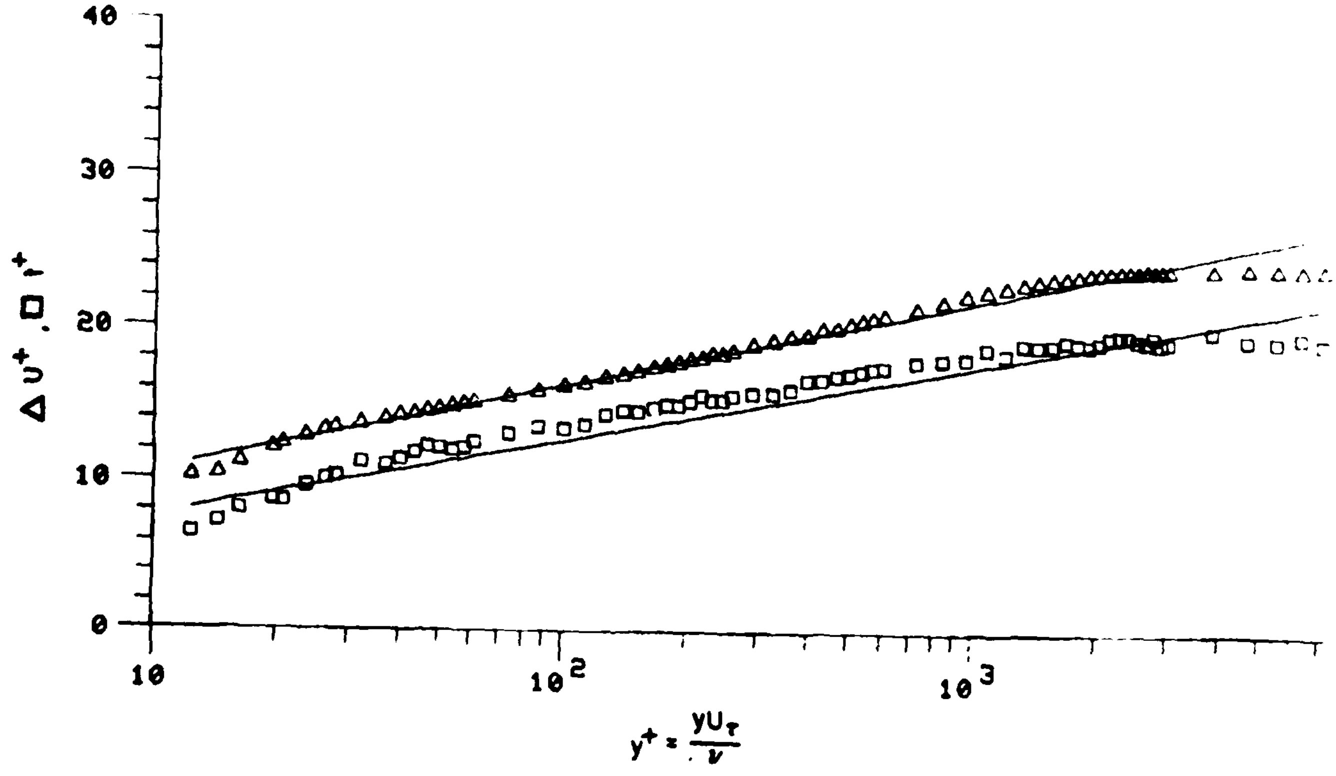

Figure B13. Mean Velocity and Temperature Profiles x = 52 in., Te - 4.7%

78-12-100-1

Mean Profile Data

x = 52 in., Te = 4.7%

N	Y INCHES	Y/ DELTA	U FT/SEC	T DEG.F	U/UE	THETA	U-UE UTAU	U(+)	T(+)	Y(+)
1	.0063	.006	42.10	87.64	.424	.321	-13.870	10.223	6.451	12.332
2	.0073	.007	42.87	86.79	.432	.359	-13.682	10.410	7.214	14.282
3	.0063	.006	45.70	85.92	.461	.403	-12.994	11.097	8.066	16.228
4	.0100	.010	49.46	85.17	.499	.432	-12.083	12.010	8.675	19.540
5	.0106	.010	50.89	85.25	.513	.426	-11.736	12.357	8.602	20.709
6	.0121	.012	52.96	84.10	.534	.480	-11.229	12.864	9.635	23.631
7	.0134	.013	54.41	83.62	.548	.501	-10.862	13.211	10.069	26.164
8	.0143	.014	55.25	83.38	.557	.512	-10.676	13.417	10.286	27.917
9	.0164	.016	56.59	82.36	.570	.558	-10.353	13.740	11.204	32.008
10	.0188	.018	57.75	82.57	.582	.549	-10.071	14.022	11.017	36.684
11	.0205	.019	58.77	82.16	.592	.567	-9.822	14.271	11.386	39.996
12	.0222	.021	59.21	81.68	.597	.588	-9.715	14.376	11.816	43.308
13	.0236	.023	59.77	81.25	.602	.606	-9.579	14.514	12.205	46.425
14	.0254	.024	60.40	81.38	.609	.602	-9.427	14.666	12.084	49.542
15	.0274	.026	60.93	81.56	.614	.594	-9.298	14.795	11.919	53.439
16	.0293	.028	61.74	81.34	.622	.604	-9.101	14.992	12.120	57.140
17	.0311	.030	62.34	80.91	.628	.623	-8.956	15.137	12.508	60.647
18	.0378	.036	63.72	80.32	.642	.649	-8.622	15.471	13.041	73.699
19	.0446	.042	65.38	79.78	.659	.673	-8.217	15.876	13.521	86.947
20	.0516	.049	66.81	79.85	.673	.670	-7.871	16.222	13.461	100.584
21	.0578	.055	67.61	79.57	.681	.683	-7.676	16.417	13.716	112.663
22	.0647	.061	69.00	79.91	.695	.713	-7.338	16.755	14.309	126.105
23	.0716	.068	69.90	79.60	.704	.726	-7.120	16.973	14.564	139.547
24	.0777	.074	70.64	78.65	.712	.724	-6.941	17.152	14.547	151.431
25	.0848	.081	71.76	78.33	.723	.738	-6.670	17.423	14.829	165.263
26	.0913	.087	72.37	78.16	.729	.746	-6.520	17.573	14.984	177.926
27	.0977	.093	73.23	78.19	.738	.745	-6.311	17.782	14.955	190.395
28	.1046	.099	74.03	77.79	.746	.763	-6.117	17.976	15.319	203.837
29	.1113	.106	74.43	77.44	.750	.779	-6.019	18.074	15.635	216.890
30	.1176	.112	75.40	77.72	.760	.766	-5.785	18.307	15.380	229.163
31	.1244	.118	75.58	77.74	.762	.765	-5.741	18.352	15.366	242.411
32	.1318	.125	76.42	77.40	.770	.780	-5.536	18.555	15.668	256.827
33	.1486	.141	78.00	77.22	.786	.788	-5.154	18.939	15.626	289.556
34	.1661	.158	79.14	77.24	.796	.788	-4.876	19.217	15.616	323.649
35	.1837	.174	80.44	76.95	.811	.800	-4.560	19.533	16.071	357.937
36	.2015	.191	80.77	76.19	.814	.834	-4.481	19.612	16.754	392.615
37	.2185	.207	82.27	76.16	.829	.836	-4.118	19.975	16.783	425.733
38	.2367	.225	82.91	75.88	.836	.849	-3.960	20.133	17.039	461.190
39	.2537	.241	83.85	75.78	.845	.853	-3.733	20.360	17.129	494.309
40	.2716	.258	84.67	75.56	.853	.863	-3.534	20.559	17.325	529.181
41	.2888	.274	85.36	75.33	.860	.873	-3.367	20.726	17.531	562.690
42	.3063	.291	86.21	75.28	.869	.875	-3.160	20.933	17.579	596.783
43	.3668	.348	88.25	74.81	.889	.896	-2.665	21.428	17.998	714.647
44	.4266	.405	90.07	74.60	.908	.906	-2.222	21.871	18.192	831.147
45	.4868	.462	92.05	74.52	.928	.909	-1.741	22.352	18.257	948.427
46	.5466	.519	92.86	73.78	.936	.943	-1.546	22.547	18.929	1064.928
47	.6066	.576	94.16	74.24	.949	.922	-1.229	22.864	18.509	1181.818
48	.6667	.633	94.92	73.48	.957	.956	-1.046	23.047	19.202	1298.903
49	.7267	.690	95.67	73.58	.964	.952	-.862	23.231	19.112	1415.793
50	.7866	.747	96.40	73.52	.972	.954	-.686	23.406	19.166	1532.488
51	.8464	.803	96.90	73.18	.977	.969	-.565	23.528	19.466	1648.969
52	.9066	.861	97.31	73.41	.981	.959	-.464	23.629	19.257	1766.268
53	.9665	.917	97.84	73.48	.986	.956	-.336	23.757	19.195	1882.964
54	1.0266	.975	98.22	73.31	.990	.964	-.245	23.848	19.353	2000.049
55	1.0866	1.032	98.23	72.90	.990	.982	-.241	23.852	19.716	2117.328
56	1.1465	1.088	98.60	72.75	.994	.989	-.151	23.942	19.657	2233.634
57	1.2063	1.145	98.76	72.60	.996	.987	-.107	23.986	19.811	2350.135
58	1.2665	1.202	98.86	73.06	.996	.975	-.087	24.006	19.577	2467.414
59	1.3262	1.259	99.30	73.21	1.001	.968	.019	24.112	19.441	2583.720
60	1.3865	1.316	99.10	72.81	.999	.986	-.029	24.064	19.805	2701.195
61	1.4463	1.373	99.26	73.26	1.000	.966	.009	24.102	19.395	2817.695
62	1.5066	1.430	99.31	73.16	1.001	.970	.020	24.113	19.486	2935.170
63	1.9226	1.825	99.43	72.36	1.002	1.006	.050	24.143	20.208	3745.608
64	2.3396	2.221	99.73	73.00	1.005	.977	.123	24.216	19.628	4557.995
65	2.7566	2.617	99.76	73.14	1.005	.971	.131	24.224	19.503	5370.381
66	3.1726	3.012	99.64	72.79	1.004	.987	.102	24.195	19.615	6181.209
67	3.5896	3.407	99.92	73.19	1.007	.969	.170	24.263	19.468	6993.206
68	4.0066	3.803	99.53	72.77	1.003	.988	.073	24.166	19.637	7805.592

Table B19

RUN NO. 1. POINT 4.

BOUNDARY LAYER PROPERTIES

		LINEAR INTERPOLATION TO WALL	STANDARD SUBLAYER FUNCTION FROM WALL TO Y+=35
FREE STREAM VELOCITY	=	99.223	99.223
FREE STREAM TEMPERATURE	=	72.500	
WALL TEMPERATURE	=	94.800	
WALL HEAT FLUX	=	.07890	
FREE STREAM DENSITY	=	.07489	
FREE STREAM KINEMATIC VISCOSITY	=	.0001638	
DENSITY OF FLUID AT WALL	=	.07188	
KINEMATIC VISCOSITY OF FLUID AT WALL	=	.0001762	
WALL/FREE STREAM DENSITY RATIO	=	.95978	
LOCATION REYNOLDS NUMBER (REX)	=	2624417.81	
INPUT VALUE OF VELOCITY DELTA	=	1.35000	
INPUT VALUE OF TEMPERATURE DELTA	=	1.45000	
CALCULATED DELTA	=		1.05346
DELTA 99.5% INPUT	=	.00000	
DISPLACEMENT THICKNESS (DELSTAR)	=	.11874	.11877
MOMENTUM THICKNESS (THETA)	=	.08814	.08841
ENERGY-DISSIPATION THICKNESS	=	.16040	.16061
ENTHALPY THICKNESS	=	.00427	.00428
SHAPE FACTOR 12 (DELSTAR/THETA)	=	1.34716	1.34342
SHAPE FACTOR 32 (ENERGY/THETA)	=	1.81990	1.81669
MOMENTUM THICKNESS REYNOLDS NUMBER	=	4448.29	4461.89
DISPLACEMENT THICKNESS REYNOLDS NUMBER	=	5992.57	5994.21
SKIN FRICTION COEFFICIENT	=	.003307	
FRICTION VELOCITY	=	4.11836	
LAW OF THE WALL CONSTANT (K)	=	.41000	
LAW OF THE WALL CONSTANT (C)	=	5.00000	
WAKE STRENGTH	=		.10069
CLAUSERS 'DELTA' INTEGRAL	=	-2.60818	-2.76130
CLAUSERS 'G' INTEGRAL	=	14.96252	14.81376
DISPLACEMENT THICKNESS - CONSTANT DENSITY	=	.11142	.11461
MOMENTUM THICKNESS - CONSTANT DENSITY	=	.08881	.08909
SHAPE FACTOR 12 - CONSTANT DENSITY	=	1.25461	1.28645

LOCATION -X- 52.00000

Te = 4.7%

Table B20

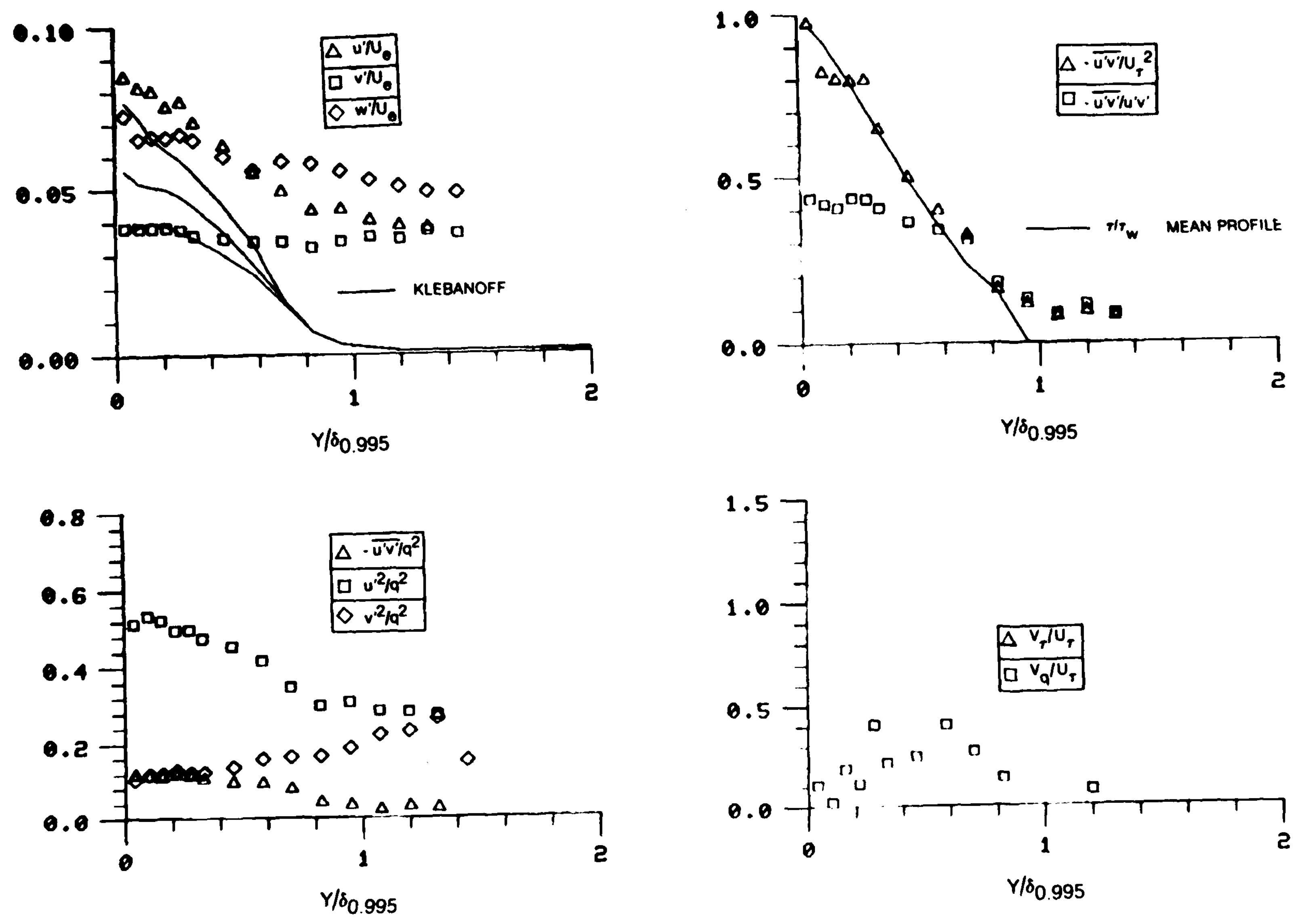

Figure B14A. Boundary Layer Turbulence Quantities, x = 52 in, T_e = 4.7%

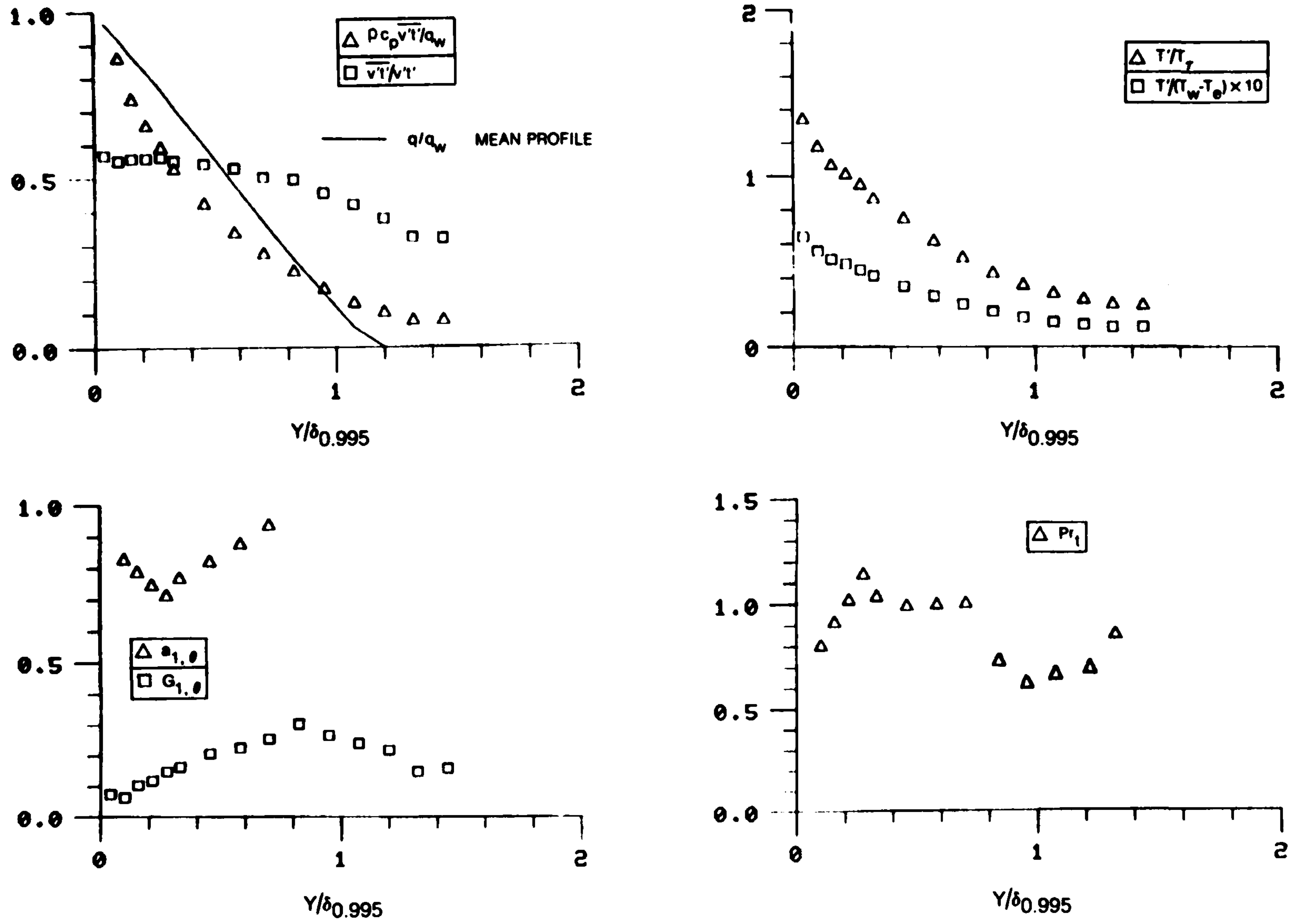

Figure B14B. Boundary Layer Turbulence Quantities, x = 52 in, T_e = 4.7%

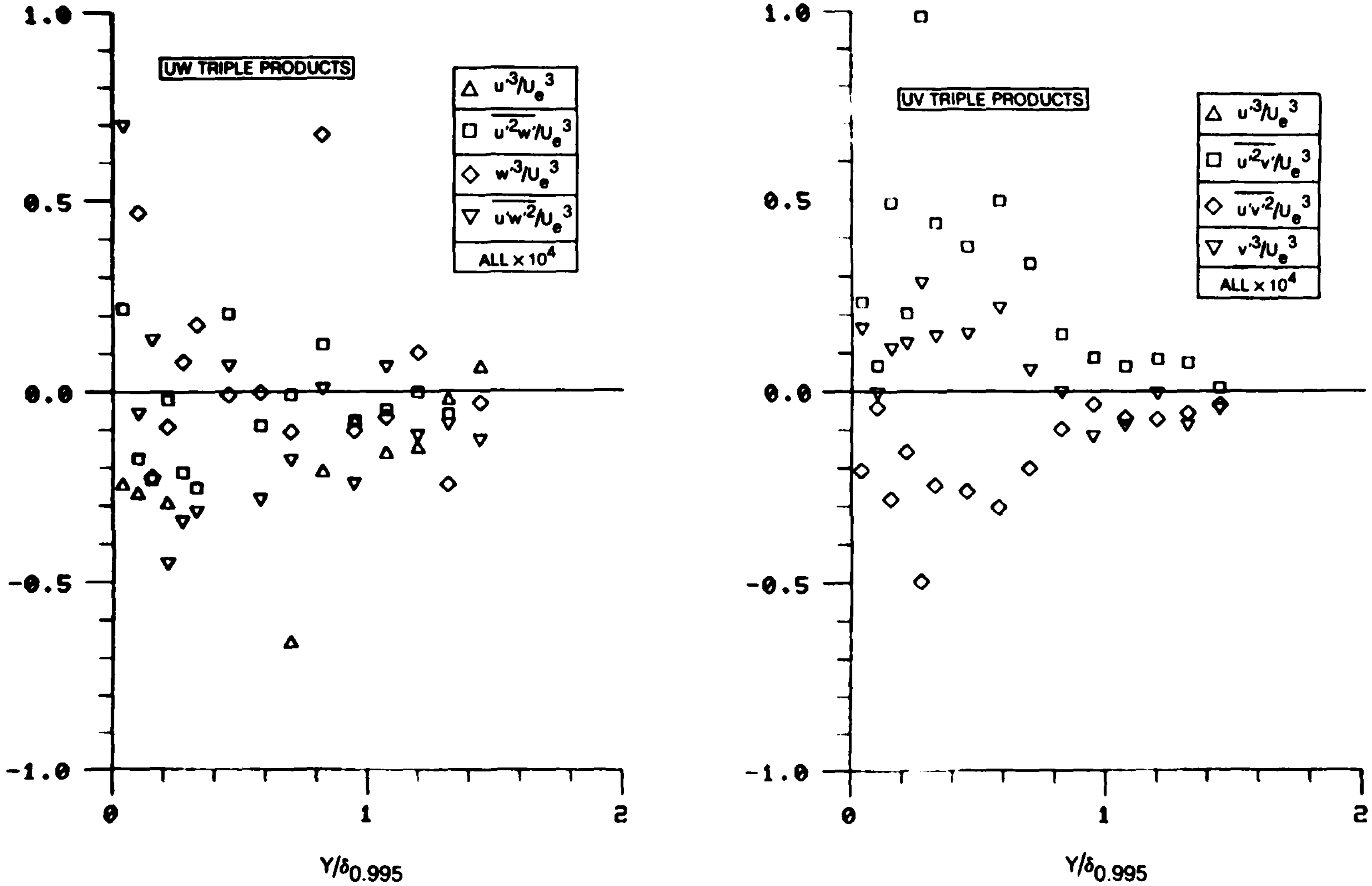

Figure B14C. Boundary Layer Triple Product Distributions $x = 52$ in, $T_e = 4.7\%$

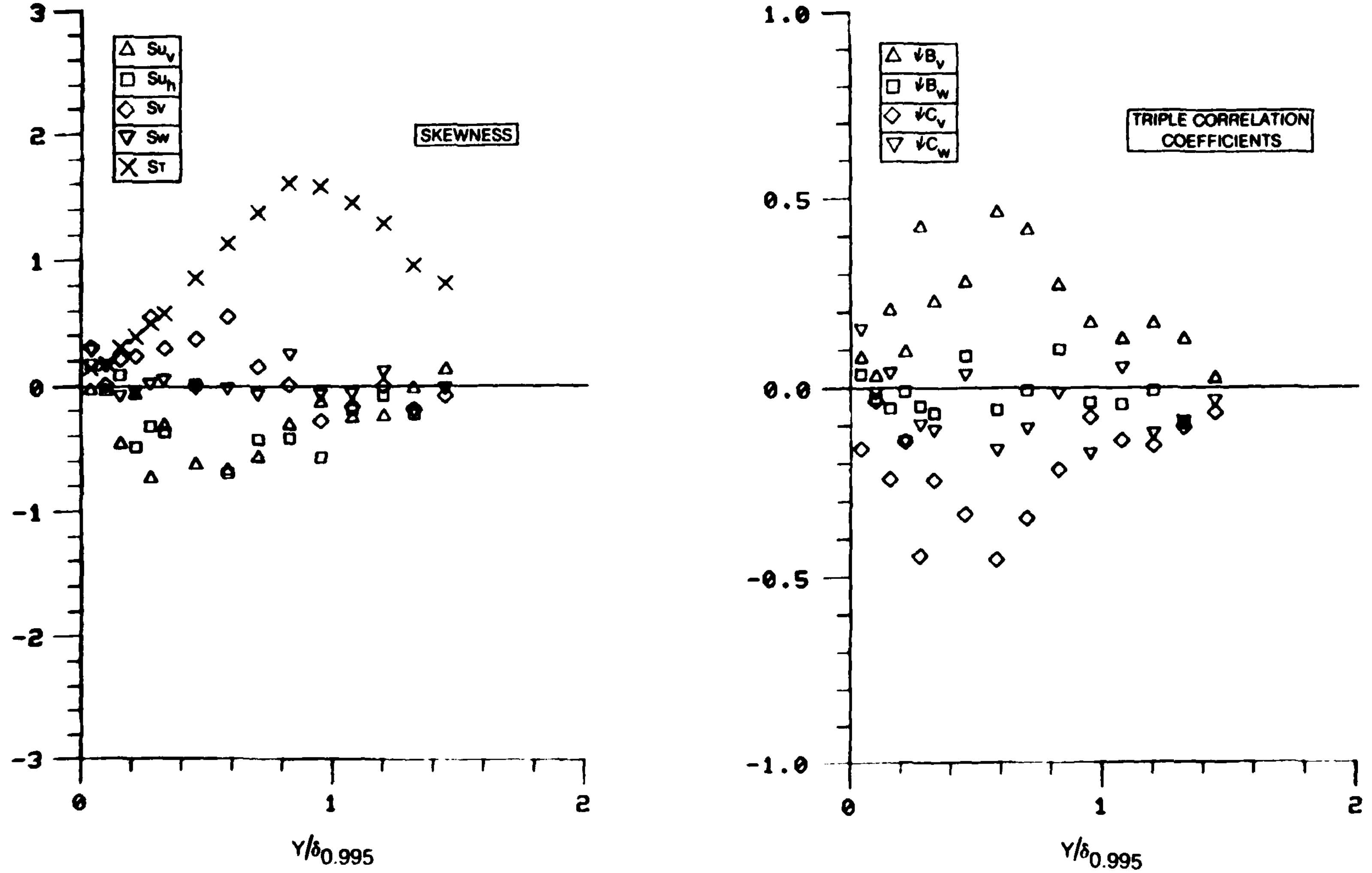

Figure B14D. Boundary Layer Skewness and Triple Product Correlation Coefficient Distributions $x = 52$ in, $T_e = 4.7\%$

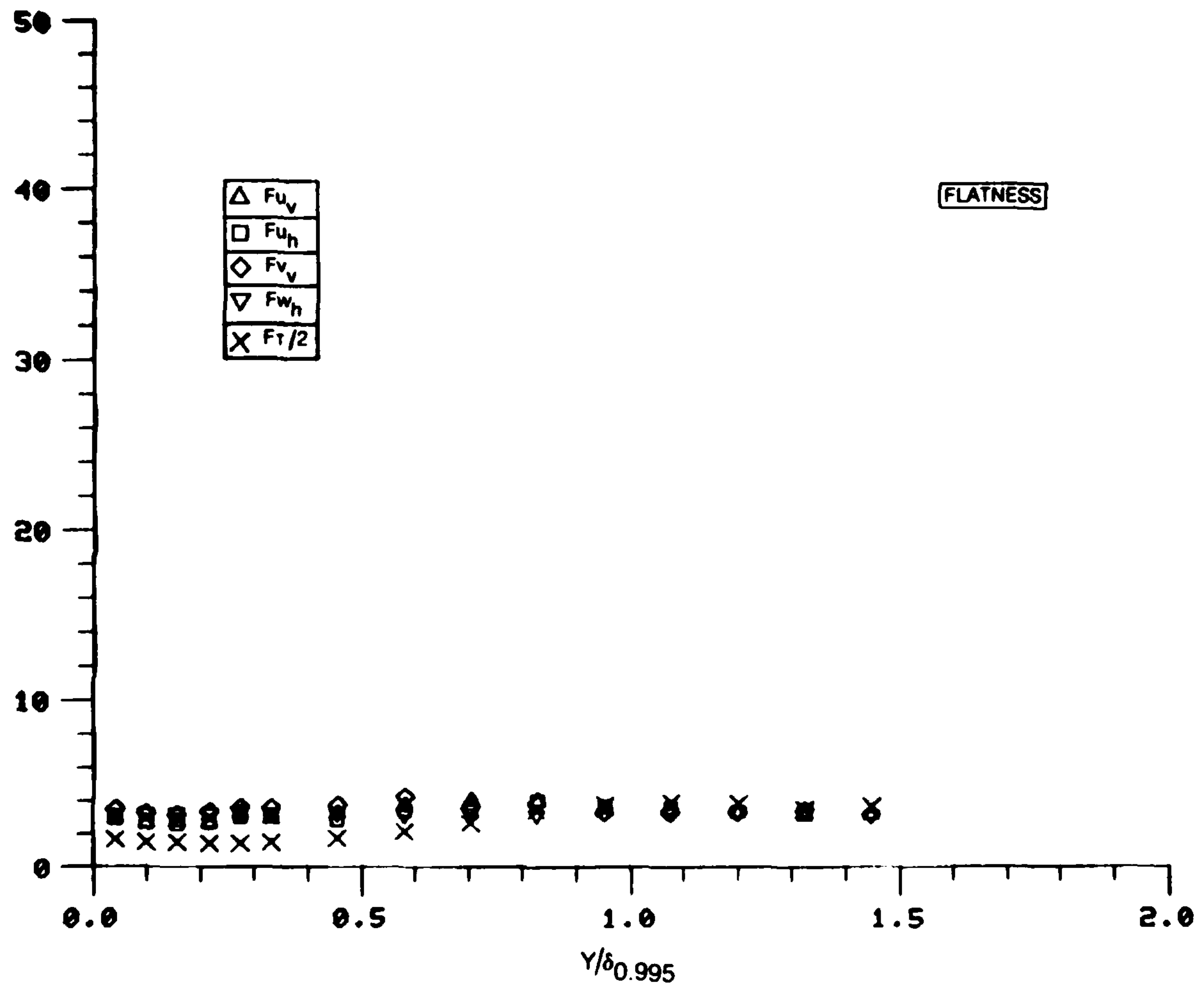

Figure B14E. Boundary Layer Flatness Distributions $x = 52$ in, $T_e = 4.7\%$

Fluctuating Profile Data

x = 52 in., Te = 4.7%

N	Y: INCHES	Y/DELTA	U'/UE	V'/UE	W'/UE	$\sqrt{\overline{U'V'}}$/UE	$\overline{U'V'}$/UTAU²	$\overline{U'V'}$/U'V'	[illegible]/UE
1	4.000	3.306	.0368	.0418	.044[illegible]	.0025	[illegible]	[illegible]	[illegible]
[illegible]	[illegible]	.041	.0646	.076[illegible]	.0729	.0403	.972[illegible]	.47[illegible]	.216[illegible]
[illegible]	.12[illegible]	.099	[illegible]	.0762	.065[illegible]	.0371	[illegible]	.417[illegible]	[illegible]
4	.19[illegible]	.157	[illegible]	.0762	.066[illegible]	.0365	.795[illegible]	.47[illegible]	[illegible]
[illegible]	.26[illegible]	.215	[illegible]	.0762	.0659	.0364	.793[illegible]	.47[illegible]	[illegible]
6	.330	.273	.0766	.0776	.0669	.0365	.796[illegible]	.47[illegible]	[illegible]
[illegible]	.400	.331	.070[illegible]	.0357	.065[illegible]	.0328	.6454	.4[illegible]	[illegible]
[illegible]	.55[illegible]	.455	.0601	.0347	.060[illegible]	.0288	.496[illegible]	.3[illegible]	[illegible]
[illegible]	.7[illegible]	.579	.0546	.0337	.0556	.0257	.395[illegible]	.37[illegible]	[illegible]
[illegible]	.85[illegible]	.702	.0490	.0337	.0561	.027[illegible]	.3[illegible]	.3[illegible]	[illegible]
11	1.000	.826	.0432	.0321	.0576	.0169	.1[illegible]	.1[illegible]	[illegible]
[illegible]	1.150	.950	.04[illegible]	.029[illegible]	.055[illegible]	.013[illegible]	.11[illegible]	.1[illegible]	[illegible]
[illegible]	1.300	1.074	.04[illegible]	.0[illegible]	.052[illegible]	.0111	[illegible]	[illegible]	[illegible]
14	1.450	1.198	.03[illegible]	.0346	.0504	.0125	.093[illegible]	.1127	[illegible]
15	1.600	1.322	.03[illegible]	.0[illegible]68	.0487	.0117	.0766	.0[illegible]	[illegible]
[illegible]	1.750	1.446	.0369	.0358	.048[illegible]	.006[illegible]	-.0[illegible]	-.0[illegible]	[illegible]
[illegible]	4.000	3.306	[illegible]	[illegible]	.044[illegible]	.005[illegible]	-.0[illegible]	-.0[illegible]	[illegible]
[illegible]	.000	.000	.0000	.0000	.0000	.0000	.0000	.0000	[illegible]

N	Y: INCHES	Y/DELTA	$\overline{V'U'}$/C2	U'2/C2	V'2/C2	W'2/C2	VTAU/UTAU	V/UTAU	$\overline{V'T'}$[illegible]
1	4.000	3.306	.0017	.2966	.3724	.381[illegible]	.0000	-.1[illegible]	[illegible]
[illegible]	.050	.041	.116[illegible]	.5137	.1[illegible]	.3817	[illegible]	.1[illegible]	
[illegible]	.120	.099	.111[illegible]	.5336	.117[illegible]	.3484	.0000	.02[illegible]	.5[illegible]
4	.190	.157	.109[illegible]	.52[illegible]	.119[illegible]	.3564	.0000	.1[illegible]	.7[illegible]
[illegible]	.26[illegible]	.215	.1156	.4[illegible]	.127[illegible]	.3765	.0000	.11[illegible]	.6[illegible]
6	.330	.273	.11[illegible]	.499[illegible]	.1[illegible]	.3807	.0000	.4[illegible]	[illegible]
[illegible]	.40[illegible]	.331	.1[illegible]	.4[illegible]	.1[illegible]	.4[illegible]	[illegible]	[illegible]	[illegible]
[illegible]	.55[illegible]	.455	.094[illegible]	.4534	.177[illegible]	.4[illegible]94	[illegible]	[illegible]	[illegible]
9	.700	.579	.0916	.4137	.1574	.4269	.0000	[illegible]	[illegible]
[illegible]	.85[illegible]	.702	.0778	.3469	.164[illegible]	.48[illegible]	.0000	.2[illegible]	[illegible]
11	1.000	.826	.0466	.3002	.1657	.5341	.0000	.13[illegible]	[illegible]
[illegible]	1.150	.950	.031[illegible]	.3090	.18[illegible]	.5030	.0000	-.0[illegible]7	[illegible]
[illegible]	1.300	1.074	.022[illegible]	.2854	.2213	.4933	.0000	-.0[illegible]	[illegible]
[illegible]	1.450	1.198	.0299	.2603	.2301	.4896	.0000	[illegible]	[illegible]
[illegible]	1.600	1.322	.024[illegible]	[illegible]36	.264[illegible]	.4621	.0000	-.0[illegible]	[illegible]
[illegible]	1.750	1.446	-.0045	.5738	.1519	.2743	.0000	-.0256	.[illegible]76[illegible]
[illegible]	4.000	3.306	-.006[illegible]	.2550	.3346	.4104	.0000	-.065[illegible]	[illegible]
[illegible]	.000	.000	.0000	.0000	.0000	.0000	.0000	[illegible]	[illegible]

N	Y: INCHES	Y/DELTA	$\overline{V'T'}$/V'T'	T'/TTAU	T'/(TW-TE)	A10	G16	PRT
1	4.000	3.306	.0866	.2098	.010[illegible]	1.49[illegible]9	-.0[illegible]	.169[illegible]
[illegible]	.050	.041	.5666	1.3407	.0641	1.0191	.0[illegible]	
[illegible]	.12[illegible]	.099	.55[illegible]9	1.17[illegible]1	.056[illegible]	.6249	.0[illegible]	.8[illegible]
4	.19[illegible]	.157	.5569	1.0643	.050[illegible]	.7866	.103[illegible]	.911[illegible]
[illegible]	.260	.215	.5578	1.0050	.048[illegible]	.7449	.1166	1.01[illegible]
[illegible]	.33[illegible]	.273	.561[illegible]	.9442	.0451	.7[illegible]98	.14[illegible]	1.1[illegible]
[illegible]	.400	.331	.55[illegible]6	.6635	.0413	.7663	.164[illegible]	1.0[illegible]57
[illegible]	.55[illegible]	.455	.54[illegible]	.7414	.0[illegible]54	.6168	.2[illegible]	.9[illegible]96
[illegible]	.7[illegible]	.579	.52[illegible]	.6166	.0295	.6725	.2263	.9967
[illegible]	.85[illegible]	.702	.49[illegible]	.519[illegible]	.024[illegible]	.9326	.254[illegible]	.9996
11	1.000	.826	.493[illegible]	.4[illegible]69	.0[illegible]04	1.3255	.30[illegible]	.7240
[illegible]	1.150	.950	.4510	.3618	.0173	1.3914	.2659	.8160
[illegible]	1.300	1.074	.417[illegible]	.30[illegible]1	.014[illegible]	1.5[illegible]	.24[illegible]1	.6290
[illegible]	1.450	1.198	.376[illegible]	.274[illegible]	.0131	1.2109	.216[illegible]	.8800
[illegible]	1.60[illegible]	1.322	.3214	.2465	.011[illegible]	1.1215	.148[illegible]	.847[illegible]
[illegible]	1.75[illegible]	1.446	.316[illegible]	.2439	.011[illegible]	2.0989	.157[illegible]	-.2516
[illegible]	4.000	3.306	.1330	.216[illegible]	.0104	1.0533	-.022[illegible]	-.5[illegible]
[illegible]	.000	.000	.0000	.0000	.0000	.0000	.0000	.0000

Table B21A

Fluctuating Profile Data

x = 52 in., Te = 4.7%

N	Y, INCHES	Y/DELTA	U'3/UE3 X 10000	U'2V'/UE3 X 10000	V'3/UE3 X 10000	U'W'2/UE3 X 10000	U'2V'/UE3 X 10000	U'V'2/UE3 X 10000	[illegible]
1	4.000	3.306	.1565	-.0531	-.1293	-.1269	-.0547	-.0217	-.1828
2	.050	.041	-.2476	.2151	1.1627	.7015	.2723	-.2765	[illegible]
3	.125	.079	-.2707	-.1784	.4693	-.0555	.0656	-.0415	[illegible]
4	.190	.157	-2.4750	-.2224	-.2263	.1365	.4657	-.0155	[illegible]
5	.260	.215	-.2969	-.0211	-.0938	-.4499	.2042	-.1500	[illegible]
6	.330	.273	-3.7532	-.2137	.0764	-.3399	.9684	-.4576	[illegible]
7	.400	.331	-1.3157	-.2546	.1749	-.3140	.4781	-.2457	[illegible]
8	.550	.455	-1.6777	.2028	-.0061	.0707	.3774	-.2616	[illegible]
9	.700	.579	-1.2736	-.0513	-.0024	-.2815	.4559	-.3741	[illegible]
10	.850	.702	-.6626	-.0095	-.1073	-.1774	.3766	-.1697	[illegible]
11	1.000	.826	-.2115	.1219	.6702	-.0108	.1513	-.0555	[illegible]
12	1.150	.950	-.0794	-.0781	-.1047	-.0355	.1837	-.0743	[illegible]
13	1.300	1.074	-.1644	-.0488	-.0693	.0668	.0697	-.0567	[illegible]
14	1.450	1.198	-.1526	-.0034	.0986	-.1138	.0562	-.0625	[illegible]
15	1.600	1.322	-.0249	-.0618	-.2460	-.0834	.0773	-.0739	[illegible]
16	1.750	1.446	.0578	-3.3740	-.0336	-.1247	.0313	-.0712	[illegible]
17	4.000	3.306	.0720	-.0729	-.0855	.0748	-.0212	.0655	[illegible]
18	.000	.000	.0000	.0000	.0000	.0000	.0000	.0000	[illegible]

N	Y, INCHES	Y/DELTA	SU V	SU H	SV	SW	ST	PSIEV	FSIEW
1	4.000	3.306	.2491	-.7072	-.2221	-.1438	.0567	-.0517	[illegible]
2	.050	.041	-.0251	.1618	.3017	.2915	.1376	.0772	[illegible]
3	.125	.079	-.0466	-.0759	.0009	.1604	.1696	.0268	[illegible]
4	.190	.157	-.4777	.0868	.2771	-.0763	.3043	[illegible]	[illegible]
5	.260	.215	-.0729	-.4916	.2331	-.0372	.3500	.0936	[illegible]
6	.330	.273	-.7468	-.3725	.5462	.0191	.4597	[illegible]	[illegible]
7	.400	.331	-.3296	-.3743	.2272	.0463	.5746	.2356	[illegible]
8	.550	.455	-.6356	.0043	.3644	-.0167	.8547	.2776	[illegible]
9	.700	.579	-.6867	-.7734	.5357	-.0163	1.1249	.4599	[illegible]
10	.850	.702	-.5766	-.4355	.1444	-.0445	1.3627	.4165	[illegible]
11	1.000	.826	-.3216	-.4254	-.0003	.2522	1.5947	[illegible]	[illegible]
12	1.150	.950	-.1464	-.5769	-.2934	-.0665	1.5700	.1724	[illegible]
13	1.300	1.074	-.2661	-.1916	-.1746	-.0573	1.4426	.1763	[illegible]
14	1.450	1.198	-.2467	-.0844	-.0074	.1172	1.2797	.1721	[illegible]
15	1.600	1.322	-.0257	-.4925	-.1867	-.2014	.9511	.1285	[illegible]
16	1.750	1.446	.1171	-1.6812	-.0914	-.0219	.7989	.0265	[illegible]
17	4.000	3.306	.1667	.2723	-.1087	-.0914	.0854	-.0117	-.1727
18	.000	.000	.0000	.0000	.0000	.0000	.0000	.0000	[illegible]

N	Y, INCHES	Y/DELTA	PSICV	PSICW	FU V	FU H	FL V	FU H	F?
1	4.000	3.306	-.0039	-.1695	2.9124	2.9409	2.9460	3.2754	[illegible]
2	.050	.041	-.1601	.1572	2.8955	2.8976	3.5226	3.1651	[illegible]
3	.125	.079	-.0356	-.0107	2.6859	2.7030	3.2446	3.2554	[illegible]
4	.190	.157	-.2422	.0412	2.7314	2.6139	3.1619	3.2565	[illegible]
5	.260	.215	-.1426	-.1396	2.6463	2.6724	3.3726	[illegible]	[illegible]
6	.330	.273	-.4440	-.0629	3.2471	3.0366	[illegible]	3.2699	[illegible]
7	.400	.331	-.2457	-.1094	2.9103	3.1521	3.5624	[illegible]	[illegible]
8	.550	.455	-.3339	.0771	3.2906	2.6744	3.7496	3.2616	[illegible]
9	.700	.579	-.4555	-.1626	3.7909	3.4418	4.2417	3.1454	[illegible]
10	.850	.702	-.3467	-.1041	3.9810	3.5552	3.5517	[illegible]	[illegible]
11	1.000	.826	-.2163	-.0685	3.9584	4.0207	3.6156	3.1452	[illegible]
12	1.150	.950	-.0761	-.1704	3.5416	3.6262	3.2466	3.2855	[illegible]
13	1.300	1.074	-.1364	.0576	3.4261	3.6037	3.2714	3.2519	[illegible]
14	1.450	1.198	-.1517	-.1159	3.2225	3.3704	3.2269	3.3519	[illegible]
15	1.600	1.322	-.1040	-.0838	3.0863	3.4304	3.3786	3.3291	[illegible]
16	1.750	1.446	-.0647	-.0277	3.1523	13.0504	3.1851	3.0452	[illegible]
17	4.000	3.306	.0753	.0002	2.8806	3.2753	2.9699	3.1715	[illegible]
18	.000	.000	.0000	.0000	.0000	.0000	.0000	.0000	.0000

Table B12B

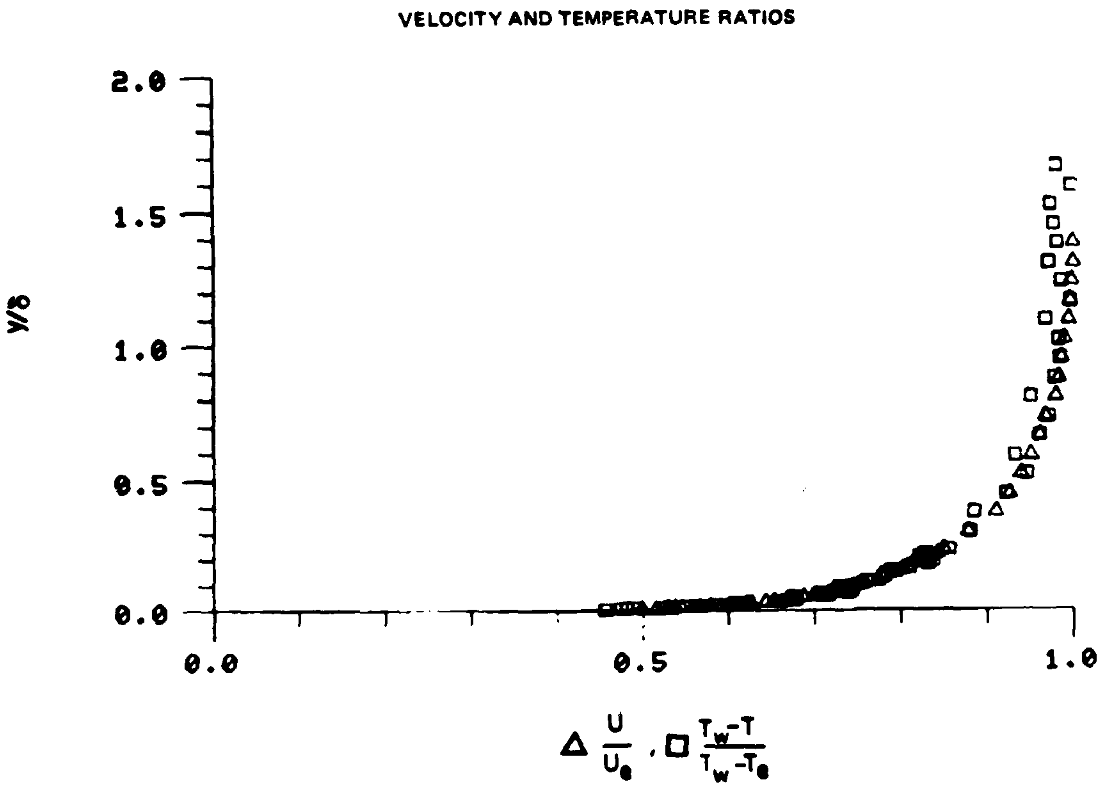

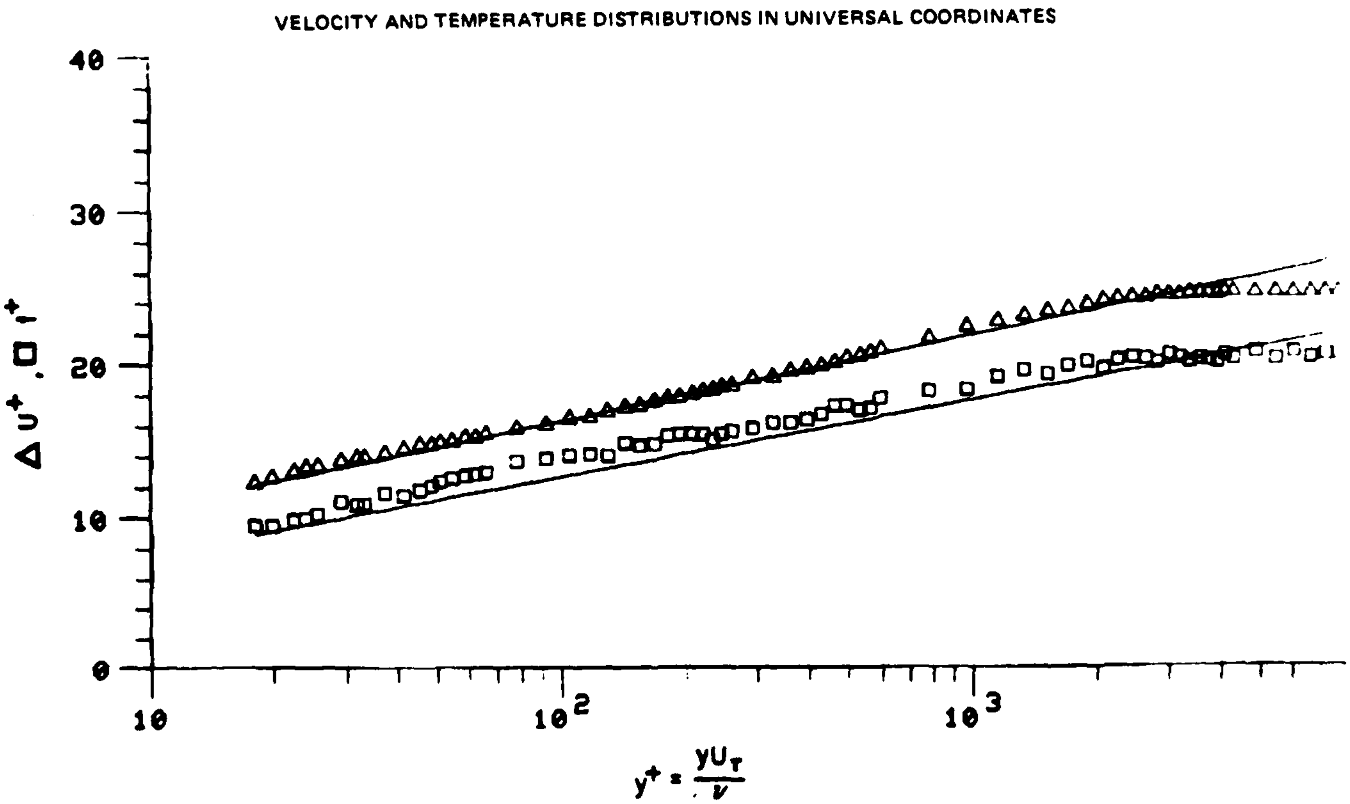

Figure B15. Mean Velocity and Temperature Profiles x = 68 in., Te = 4.2%

78-12-100-1

Mean Profile Data

x = 68 in., Te = 4.2%

N	Y INCHES	Y/ DELTA	U FT/SEC	T DEG.F	U/UE	THETA	U-UE UTAU	U(+)	T(+)	Y(+)
1	.0093	.007	49.56	84.94	.499	.456	-12.300	12.240	9.427	17.824
2	.0103	.008	51.13	84.91	.515	.457	-11.911	12.626	9.448	19.735
3	.0116	.009	52.54	84.52	.529	.474	-11.563	12.976	9.792	22.218
4	.0124	.009	53.44	84.34	.536	.482	-11.342	13.197	9.953	23.747
5	.0133	.010	54.00	84.07	.543	.493	-11.205	13.335	10.189	25.466
6	.0152	.011	55.51	83.15	.559	.533	-10.831	13.709	10.999	29.096
7	.0166	.012	56.13	83.34	.565	.525	-10.678	13.862	10.833	31.770
8	.0173	.013	56.30	83.34	.567	.525	-10.636	13.903	10.836	33.108
9	.0193	.015	57.44	82.48	.578	.561	-10.354	14.185	11.593	36.929
10	.0216	.016	58.56	82.76	.590	.549	-10.071	14.468	11.345	41.323
11	.0235	.018	59.55	82.25	.599	.571	-9.833	14.706	11.793	44.952
12	.0252	.019	59.71	81.94	.601	.584	-9.794	14.746	12.065	48.200
13	.0265	.020	60.12	81.66	.605	.596	-9.693	14.846	12.311	50.664
14	.0283	.021	60.43	81.45	.608	.605	-9.614	14.925	12.496	54.122
15	.0305	.023	61.57	81.27	.620	.613	-9.334	15.205	12.657	58.325
16	.0323	.024	61.67	81.16	.621	.618	-9.309	15.231	12.754	61.764
17	.0341	.026	62.13	81.05	.625	.622	-9.197	15.343	12.850	65.203
18	.0406	.031	63.87	80.15	.643	.661	-8.765	15.774	13.644	77.621
19	.0475	.036	64.81	80.01	.652	.667	-8.534	16.005	13.766	90.803
20	.0545	.041	66.41	79.77	.668	.677	-8.139	16.401	13.982	104.176
21	.0609	.046	66.91	79.71	.673	.679	-8.015	16.524	14.030	116.402
22	.0675	.051	68.22	79.74	.687	.678	-7.692	16.847	14.009	129.011
23	.0744	.056	69.45	78.87	.699	.715	-7.388	17.151	14.772	142.193
24	.0805	.060	69.79	79.04	.702	.708	-7.305	17.235	14.625	153.847
25	.0874	.066	70.91	78.92	.714	.713	-7.028	17.511	14.732	167.029
26	.0944	.071	71.53	78.33	.720	.738	-6.874	17.665	15.248	180.402
27	.1007	.076	72.15	78.20	.726	.744	-6.722	17.817	15.361	192.437
28	.1077	.081	72.82	78.21	.733	.744	-6.555	17.984	15.359	205.810
29	.1147	.086	73.50	78.24	.740	.742	-6.387	18.152	15.327	219.183
30	.1206	.091	73.84	78.57	.743	.728	-6.303	18.236	15.036	230.837
31	.1273	.096	74.61	78.22	.751	.743	-6.114	18.426	15.345	243.255
32	.1345	.101	75.01	77.99	.755	.753	-6.014	18.525	15.549	257.010
33	.1513	.114	76.76	77.81	.773	.760	-5.582	18.958	15.706	289.105
34	.1691	.127	77.38	77.38	.779	.779	-5.429	19.111	16.083	323.110
35	.1868	.140	78.72	77.31	.792	.782	-5.099	19.441	16.152	356.925
36	.2043	.153	79.62	77.16	.801	.788	-4.876	19.662	16.282	390.357
37	.2215	.166	80.32	76.60	.808	.809	-4.704	19.835	16.704	423.217
38	.2396	.180	80.99	76.14	.815	.832	-4.539	20.001	17.179	457.795
39	.2563	.192	81.99	76.04	.825	.836	-4.292	20.247	17.265	489.700
40	.2746	.206	82.93	76.40	.835	.821	-4.059	20.480	16.952	524.667
41	.2913	.219	83.65	76.26	.842	.827	-3.881	20.658	17.072	556.564
42	.3093	.232	84.26	75.56	.848	.856	-3.731	20.808	17.673	590.952
43	.4044	.304	87.26	75.05	.878	.878	-2.990	21.550	18.142	772.634
44	.4996	.375	90.36	74.90	.910	.885	-2.218	22.321	18.273	954.506
45	.5949	.447	91.88	74.04	.925	.922	-1.849	22.690	19.034	1136.570
46	.6896	.518	93.25	73.49	.938	.945	-1.509	23.030	19.515	1317.467
47	.7847	.589	94.40	73.79	.950	.932	-1.227	23.312	19.249	1499.169
48	.8794	.660	95.40	73.13	.960	.960	-.980	23.559	19.829	1680.266
49	.9748	.732	96.18	72.86	.968	.971	-.788	23.752	20.054	1862.341
50	1.0697	.803	97.34	73.34	.980	.951	-.501	24.036	19.650	2043.640
51	1.1643	.874	97.66	72.70	.983	.979	-.416	24.123	20.211	2224.366
52	1.2593	.946	98.06	72.54	.987	.985	-.324	24.216	20.349	2405.857
53	1.3541	1.017	98.37	72.61	.990	.982	-.246	24.293	20.290	2586.965
54	1.4491	1.088	98.80	72.97	.994	.967	-.140	24.399	19.969	2768.456
55	1.5446	1.160	98.99	72.29	.996	.996	-.092	24.447	20.572	2950.922
56	1.6392	1.231	99.16	72.50	.996	.987	-.050	24.489	20.385	3131.628
57	1.7343	1.302	99.32	72.88	1.000	.971	-.011	24.528	20.049	3313.309
58	1.8292	1.374	99.34	72.63	1.000	.981	-.006	24.533	20.270	3494.609
59	1.9241	1.445	99.39	72.73	1.000	.977	.005	24.544	20.183	3675.908
60	2.0193	1.516	99.37	72.79	1.000	.975	.001	24.540	20.137	3857.761
61	2.1142	1.588	99.56	72.26	1.002	.997	.048	24.587	20.601	4039.080
62	2.2094	1.659	99.75	72.63	1.004	.981	.096	24.635	20.270	4220.953
63	2.5091	1.884	99.71	72.13	1.003	1.003	.084	24.623	20.716	4793.508
64	2.8091	2.109	99.78	72.61	1.004	.983	.101	24.641	20.294	5366.635
65	3.1092	2.335	99.65	72.14	1.003	1.002	.069	24.608	20.704	5939.954
66	3.4092	2.560	99.62	72.48	1.003	.988	.063	24.602	20.402	6513.062
67	3.7095	2.785	99.71	72.35	1.004	.993	.086	24.626	20.518	7086.763
68	4.0093	3.010	99.85	72.36	1.005	.993	.120	24.659	20.510	7659.529

Table B22

RUN NO. 1. POINT 3.

BOUNDARY LAYER PROPERTIES

		LINEAR INTERPOLATION TO WALL	STANDARD SUBLAYER FUNCTION FROM WALL TO Y+=35
FREE STREAM VELOCITY	=	99.365	99.365
FREE STREAM TEMPERATURE	=	72.200	
WALL TEMPERATURE	=	95.630	
WALL HEAT FLUX	=	.07913	
FREE STREAM DENSITY	=	.07493	
FREE STREAM KINEMATIC VISCOSITY	=	.0001637	
DENSITY OF FLUID AT WALL	=	.07177	
KINEMATIC VISCOSITY OF FLUID AT WALL	=	.0001766	
WALL/FREE STREAM DENSITY RATIO	=	.95781	
LOCATION REYNOLDS NUMBER (REX)	=	3440281.97	
INPUT VALUE OF VELOCITY DELTA	=	1.80000	
INPUT VALUE OF TEMPERATURE DELTA	=	2.15000	
CALCULATED DELTA	=		1.33179
DELTA 99.5% INPUT	=	.00000	
DISPLACEMENT THICKNESS (DELSTAR)	=	.14511	.14498
MOMENTUM THICKNESS (THETA)	=	.10836	.10894
ENERGY-DISSIPATION THICKNESS	=	.19802	.19856
ENTHALPY THICKNESS	=	.00565	.00567
SHAPE FACTOR 12 (DELSTAR/THETA)	=	1.33910	1.33073
SHAPE FACTOR 32 (ENERGY/THETA)	=	1.82738	1.82262
MOMENTUM THICKNESS REYNOLDS NUMBER	=	5482.28	5511.75
DISPLACEMENT THICKNESS REYNOLDS NUMBER	=	7341.33	7334.64
SKIN FRICTION COEFFICIENT	=	.003181	
FRICTION VELOCITY	=	4.04924	
LAW OF THE WALL CONSTANT (K)	=	.41000	
LAW OF THE WALL CONSTANT (C)	=	5.00000	
WAKE STRENGTH	=		.08475
CLAUSERS 'DELTA' INTEGRAL	=	-3.20155	-3.42664
CLAUSERS 'G' INTEGRAL	=	16.42084	17.96570
DISPLACEMENT THICKNESS - CONSTANT DENSITY	=	.13513	.13965
MOMENTUM THICKNESS - CONSTANT DENSITY	=	.10921	.10961
SHAPE FACTOR 12 - CONSTANT DENSITY	=	1.23740	1.27169

LOCATION -X- 68.00000

Te = 4.2%

Table B23

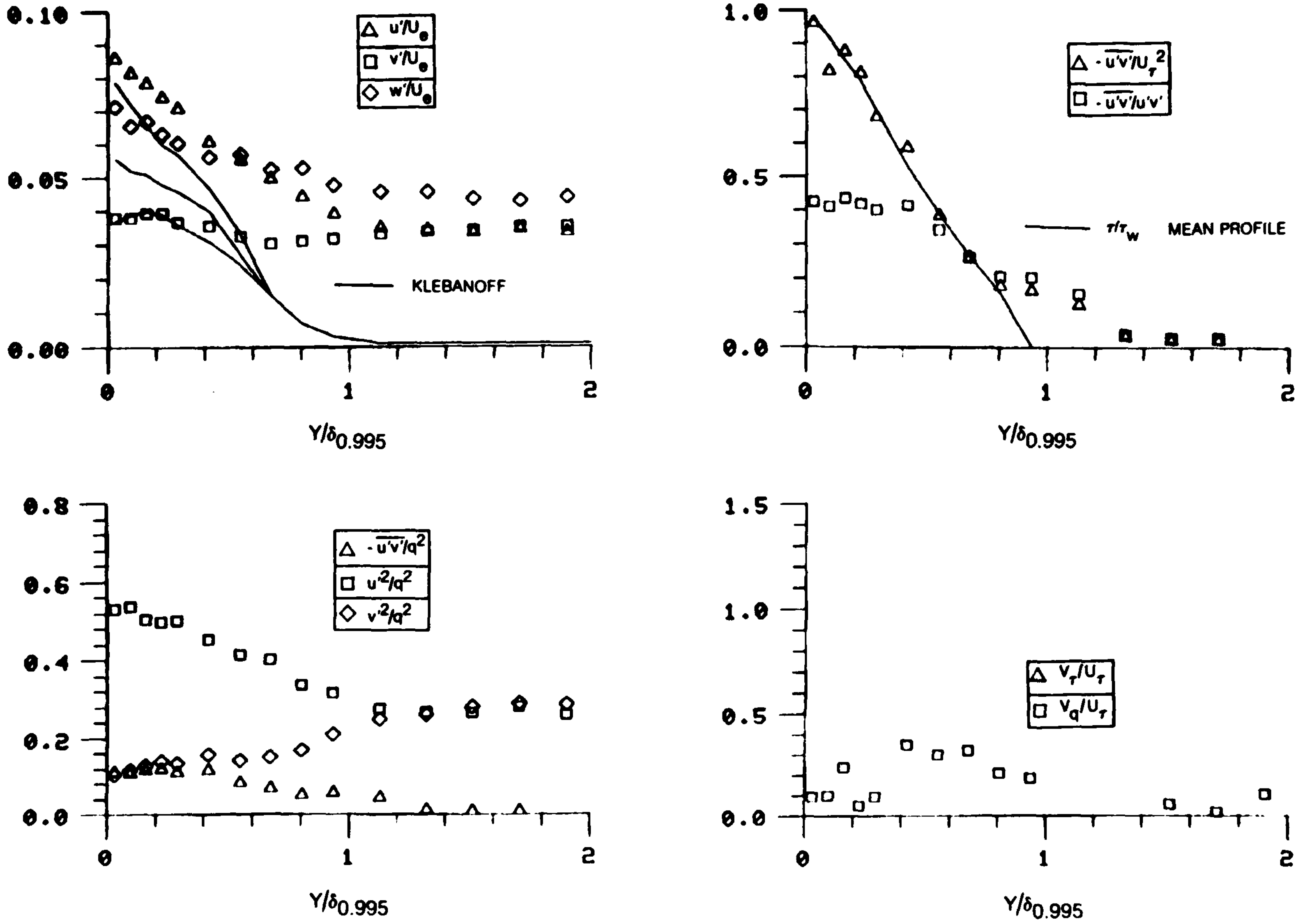

Figure B16A. Boundary Layer Turbulence Quantities, x = 68 in, T_e = 4.2%

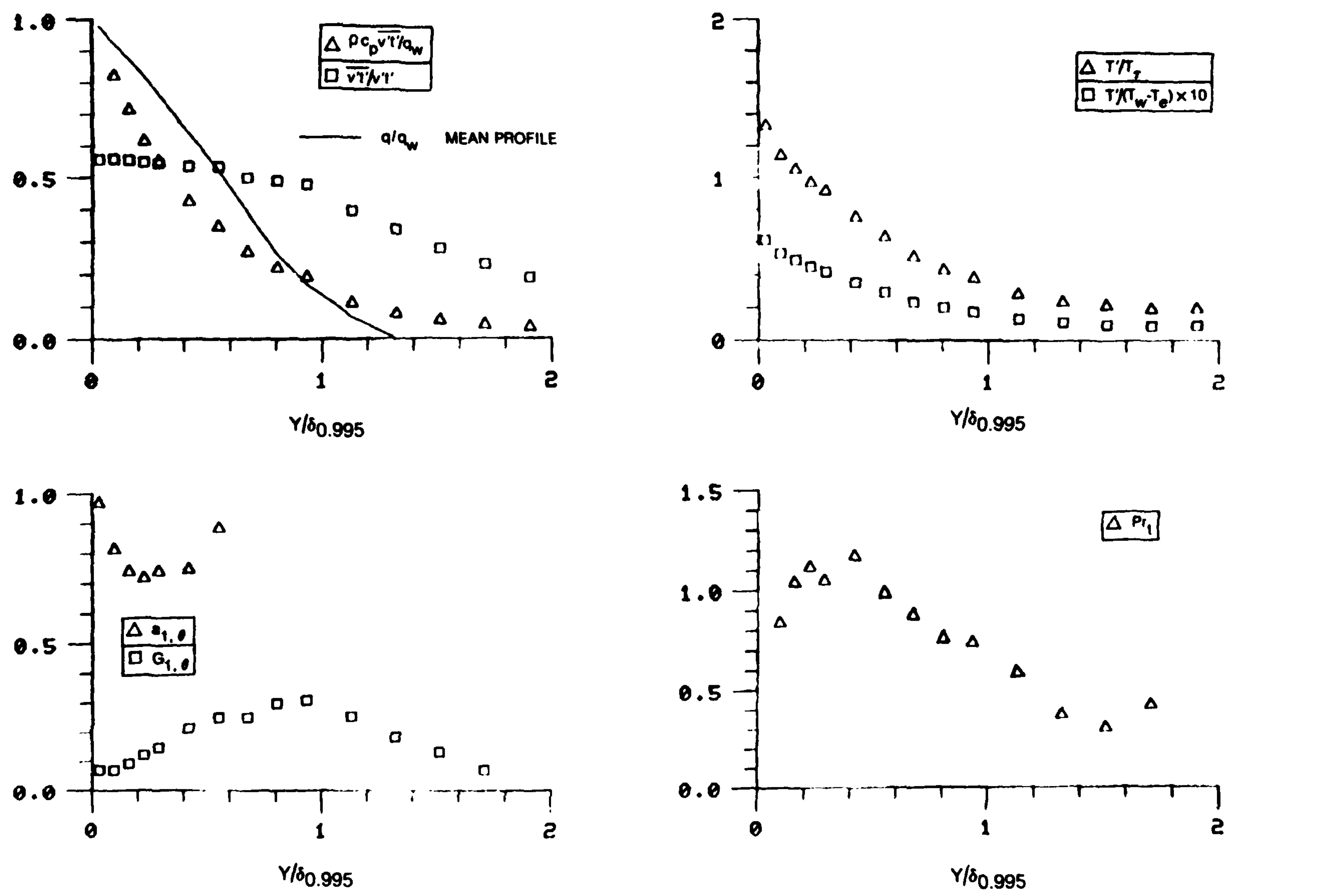

Figure B16B. Boundary Layer Turbulence Quantities, x = 68 in, T_e = 4.2%

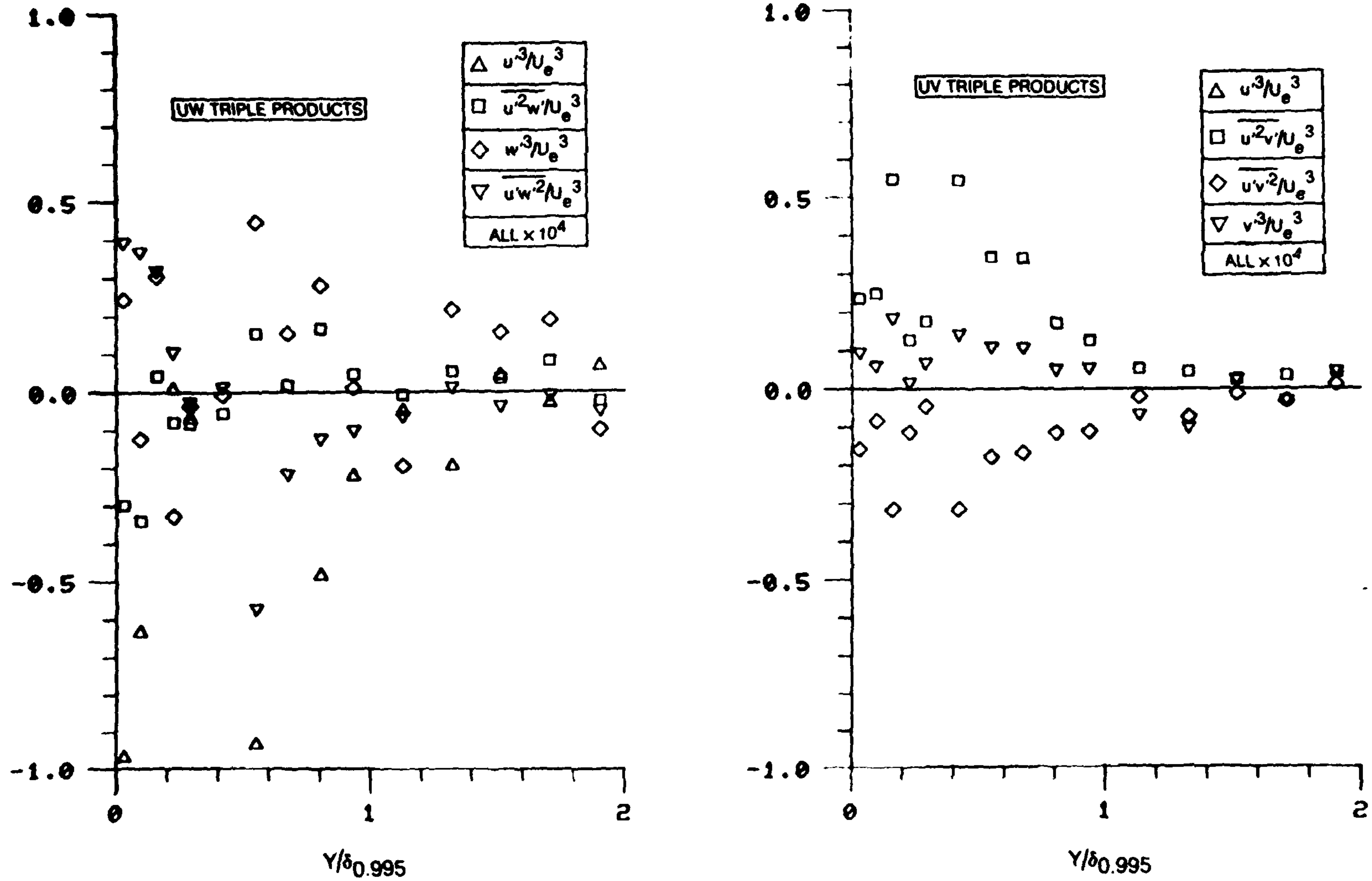

Figure B16C. Boundary Layer Triple Product Distributions $x = 68$ in, $T_e = 4.2\%$

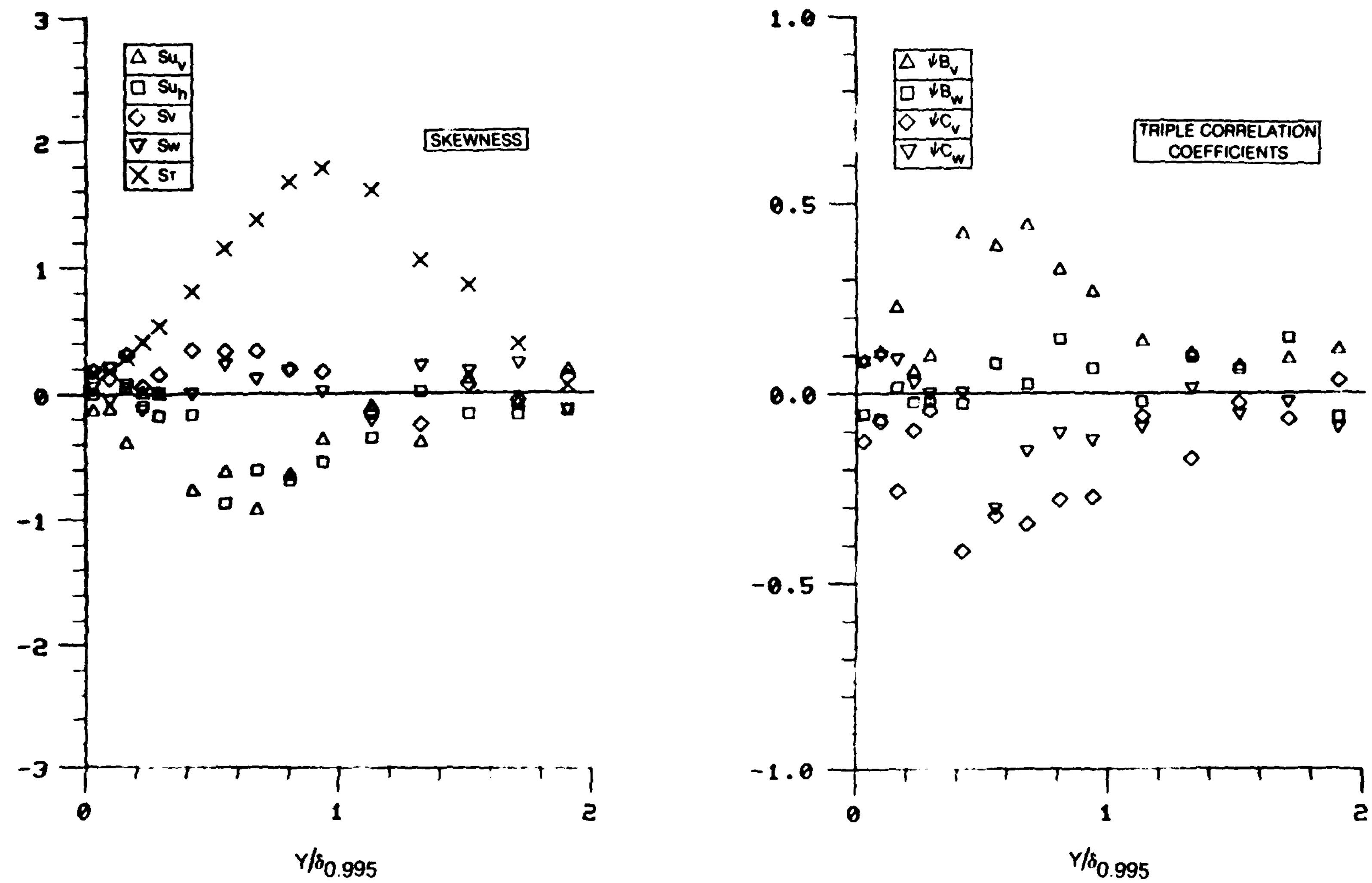

Figure B16D. Boundary Layer Skewness and Triple Product Correlation Coefficient Distributions $x = 68$ in, $T_e = 4.2\%$

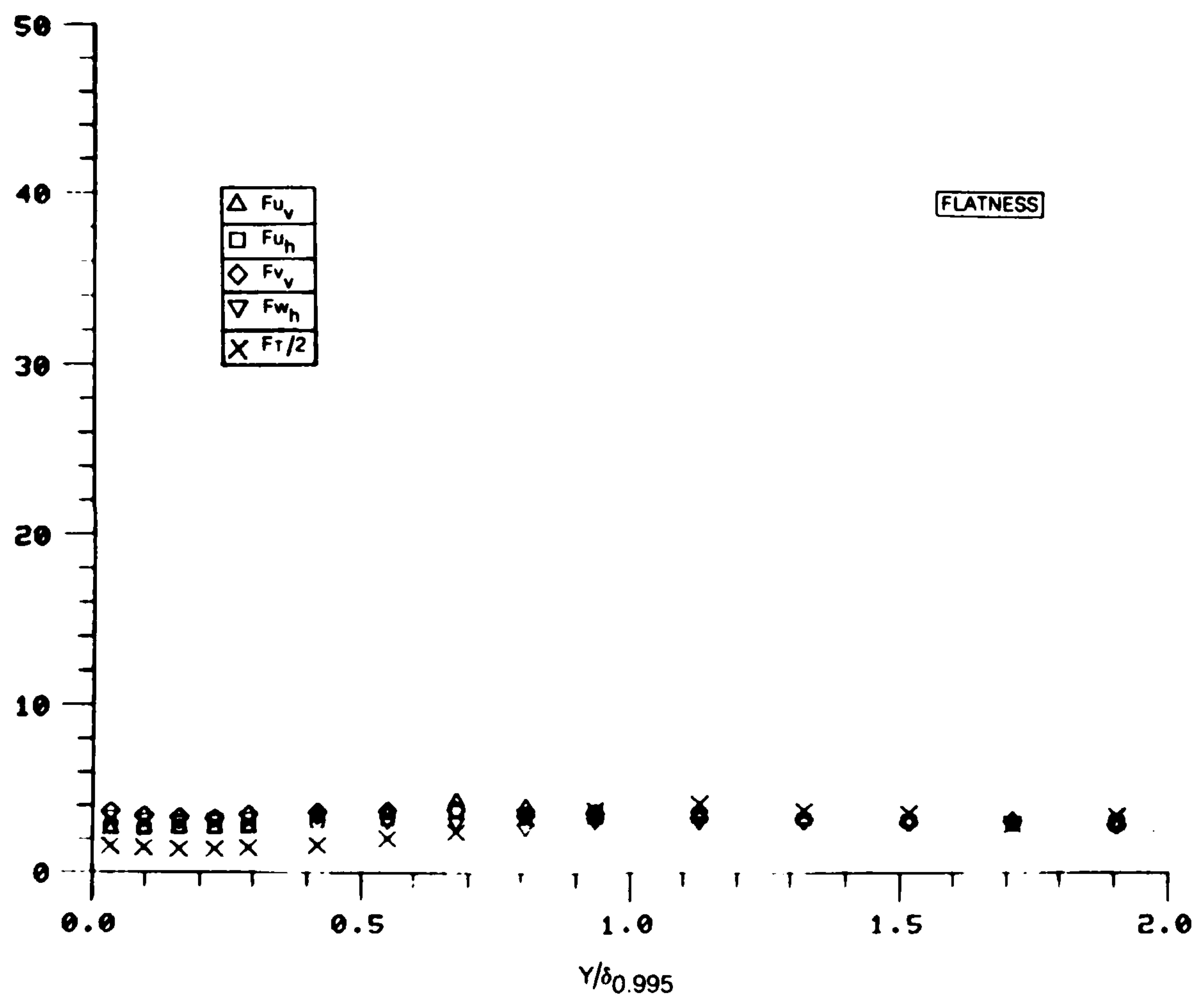

Figure B16E. Boundary Layer FLatness Distributions $x = 68$ in, $T_e = 4.2\%$

Fluctuating Profile Data

x = 68 in., Te = 4.2%

N	Y: INCHES	Y/ DELTA	U'/UE	V'/UE	W'/UE	√U'V'/UE	U'V'/ UTAU2	U'V'/U'V'	[illegible]
1	4.000	2.561	.0325	.0792	.0467	.0337	-.0069	-.0063	[illegible]
2	.050	.032	.0659	.0760	.0715	.0393	.9613	.4254	[illegible]
3	.150	.097	.0617	.0779	.0655	.0363	.8179	[illegible]	[illegible]
4	.250	.161	.0782	.0794	.0669	.0375	.6767	[illegible]	[illegible]
5	.350	.226	.0741	.0792	.0631	.0361	.6111	[illegible]	[illegible]
6	.450	.290	.0707	.0766	.0607	.0333	.6790	[illegible]	[illegible]
7	.650	.419	.0606	.0755	.0567	.0307	.5860	[illegible]	[illegible]
8	.850	.548	[illegible]	.0737	.0577	.0248	.3834	.3446	[illegible]
9	1.050	.677	.0498	.0704	.0525	.0206	.2637	.2627	[illegible]
10	1.250	.806	.0440	.0711	.0525	.0169	.1724	[illegible]	[illegible]
11	1.450	.935	.0369	.0717	.0477	.0167	.1650	[illegible]	[illegible]
12	1.750	1.129	.0348	.0731	.0455	.0141	.1220	.1587	[illegible]
13	2.050	1.323	.0344	.0738	.0454	.0072	.0320	.0387	[illegible]
14	2.350	1.516	.0334	.0741	.0434	.0057	[illegible]	.0294	[illegible]
15	2.650	1.710	.0346	.0752	.0442	.0057	[illegible]	[illegible]	[illegible]
16	2.950	1.903	.0335	.0752	.0439	.0069	-.0273	-.0370	[illegible]
17	4.000	2.561	.0333	.0770	.0441	.0087	-.0460	-.0570	[illegible]
18	.000	.000	.0000	.0000	.0000	.0000	.0000	.0000	[illegible]

N	Y: INCHES	Y/ DELTA	V'C'/C2	U'2/C2	V'2/C2	W'2/C2	VTAU/ UTAU	VC/ UTAU	V'T' [illegible]
1	4.000	2.561	-.0022	.0201	.3219	.4587	.0000	-.1163	.0195
2	.050	.032	.1110	.5295	.1037	.3670	.0000	.0919	
3	.150	.097	.1065	.5750	.1162	.3478	.0000	[illegible]	[illegible]
4	.250	.161	.1164	.5037	.1361	.3652	.0000	.2779	[illegible]
5	.350	.226	.1162	.4988	.1359	.3614	.0000	.0528	[illegible]
6	.450	.290	.1096	.5013	.1343	.3644	.0000	.0966	[illegible]
7	.650	.419	.1166	.4539	.1559	.3902	.0000	[illegible]	[illegible]
8	.850	.548	.0640	.4154	.1421	.4424	.0000	.2095	[illegible]
9	1.050	.677	.0669	.4025	.1497	.4478	.0000	[illegible]	[illegible]
10	1.250	.806	.0557	.3792	.1703	.4907	.0000	[illegible]	[illegible]
11	1.450	.935	.0556	.3158	.2097	.4746	.0000	.1915	[illegible]
12	1.750	1.129	.0452	.2772	.2507	.4731	.0000	[illegible]	[illegible]
13	2.050	1.323	.0149	.2675	.2665	.4720	.0000	[illegible]	[illegible]
14	2.350	1.516	.0078	.2679	[illegible]	.4523	.0000	[illegible]	[illegible]
15	2.650	1.710	.0077	.2812	.2915	.4275	.0000	[illegible]	[illegible]
16	2.950	1.903	-.0110	.2615	.2869	.4496	.0000	[illegible]	[illegible]
17	4.000	2.561	-.0170	.2505	.3097	.4398	.0000	-.1339	[illegible]
18	.000	.000	.0000	.0000	.0000	.0000	.0000	.0000	[illegible]

N	Y: INCHES	Y/ DELTA	V'T'/V'T'	T'/TTAU	T'/(TW-TE)	A10	G10	PRT
1	4.000	2.561	.1038	.1566	.0067	1.4711	-.0715	-.2965
2	.050	.032	.5567	1.3254	.0615	.9661	.0691	
3	.150	.097	.5557	1.1384	.0528	.6160	.0733	.8794
4	.250	.161	.5567	1.0511	.0488	.7405	.0934	1.0373
5	.350	.226	.5490	.9686	.0449	.7177	.1234	1.1163
6	.450	.290	.5429	.9138	.0424	.7413	.1467	1.0456
7	.650	.419	.5341	.7520	.0347	.7490	.2162	1.1721
8	.850	.548	.5316	.6775	.0296	.6955	[illegible]	.9580
9	1.050	.677	.4966	.5121	.0237	1.0222	[illegible]	.6668
10	1.250	.806	.4864	.4297	.0199	1.2159	.2956	[illegible]
11	1.450	.935	.4757	.3777	.0175	1.2572	.3116	.7363
12	1.750	1.129	.3926	.2816	.0131	1.1251	.2745	.5900
13	2.050	1.323	.3351	.2731	[illegible]	1.7960	.1605	[illegible]
14	2.350	1.516	.2759	.2136	.0059	1.6700	.1330	.3270
15	2.650	1.710	.2261	.1948	.0059	1.4973	[illegible]	[illegible]
16	2.950	1.903	.1861	.1699	.0068	1.0540	-.0079	-.7370
17	4.000	2.561	.1391	.1813	.0064	.6146	-.0111	-1.6765
18	.000	.000	.0000	.0000	.0000	.0000	.0000	.0000

Table B24A

Fluctuating Profile Data

x = 68 in., Te = 4.2%

N	Y: INCHES	Y/DELTA	U'3/UE3 x 10000	U'[illegible]W'/UE[illegible] x 10000	W'3/UE3 x 10000	U'[illegible]/UE3 x 10000	U'[illegible]/UE3 x 10000	U'[illegible]/UE[illegible] x 10000	V'[illegible] x [illegible]
1	4.000	2.561	-.620[illegible]	.0216	.010[illegible]	-.0517	-.0229	-.[illegible]	-.1[illegible]
2	.050	.032	-.9724	-.2989	.2414	.3937	.23[illegible]	-.[illegible]7[illegible]	.[illegible]
3	.150	.097	-.6367	-.3420	-.12[illegible]	.3682	.24[illegible]	-.[illegible]	.[illegible]
4	.250	.161	-1.9795	.0435	.303[illegible]	.3208	.54[illegible]	-.[illegible]	.[illegible]
5	.350	.226	.0060	-.[illegible]	-.3259	.1067	.127[illegible]	-.1117	.[illegible]
6	.450	.290	-.0716	-.1026	-.0395	-.0256	.17[illegible]	-.[illegible]	.[illegible]
7	.650	.419	-1.7746	-.[illegible]579	-.0111	.0115	.54[illegible]	-.[illegible]	.[illegible]
8	.850	.548	-.9355	.1532	.4422	-.5705	.3457	-.17[illegible]	.1[illegible]
9	1.050	.677	-1.1516	.0159	.150[illegible]	-.2152	.34[illegible]	-.1[illegible]	.[illegible]
10	1.250	.806	-.4[illegible]	.1652	.2763	-.1211	.17[illegible]	-.11[illegible]	.[illegible]
11	1.450	.935	-.2211	.[illegible]	.0391	-.099[illegible]	.12[illegible]	-.1[illegible]	.[illegible]
12	1.750	1.129	-.0551	-.[illegible]91	-.1971	-.0646	.0495	-.[illegible]	-.[illegible]
13	2.050	1.323	-.1950	.[illegible]01	.2114	.0122	.039[illegible]	-.[illegible]	-.[illegible]
14	2.350	1.516	.0426	.[illegible]344	.155[illegible]	-.0764	.039[illegible]	-.[illegible]	.[illegible]
15	2.650	1.710	-.0726	.[illegible]64	.1540	-.0067	.047[illegible]	.[illegible]	-.[illegible]
16	2.950	1.903	.0645	-.[illegible]69	-.0990	-.0475	-.04[illegible]	-.[illegible]	.[illegible]
17	4.[illegible]	2.561	-.0071	.[illegible]66	.235[illegible]	.1330	.0[illegible]	.[illegible]	-.[illegible]
18	.000	.000	.0000	.0000	.0000	.0000	.0000	.[illegible]	.[illegible]

N	Y: INCHES	Y/DELTA	SU V	SU H	SV	SW	ST	PSIE V	[illegible]
1	4.000	2.561	-.1661	-.0528	-.1699	.0297	.166[illegible]	-.[illegible]7	.[illegible]
2	.050	.032	-.1457	-.[illegible]1	.1754	.0610	.15[illegible]	.[illegible]	-.[illegible]
3	.150	.097	-.1[illegible]	.[illegible]4	.1121	-.0524	.1[illegible]	.1[illegible]	-.[illegible]
4	.250	.161	-.4173	.0410	.2977	.0810	.2[illegible]	.2[illegible]	.[illegible]
5	.350	.226	-.[illegible]	-.1109	.0451	-.1245	.4[illegible]	.[illegible]4	-.[illegible]
6	.450	.290	-.[illegible]	-.1642	.1441	.0107	.5297	.[illegible]	-.[illegible]
7	.650	.419	-.7866	-.1724	.3345	.0014	.7597	.41[illegible]7	-.[illegible]
8	.850	.548	-.6[illegible]	-.6854	.3[illegible]	.2362	1.1309	.[illegible]	.[illegible]
9	1.050	.677	-.5365	-.6616	.161[illegible]	.1170	1.3624	.44[illegible]	.[illegible]24
10	1.250	.806	-.6646	-.6026	.165[illegible]	.1816	1.6667	.[illegible]	.[illegible]
11	1.450	.935	-.3750	-.5478	[illegible]	.0164	1.7676	.[illegible]	.[illegible]
12	1.750	1.129	-.4122	-.3614	-.1550	-.2109	1.5944	.1[illegible]	-.[illegible]
13	2.050	1.323	-.3920	.0121	-.25[illegible]	.2220	1.0[illegible]	.1[illegible]	.[illegible]
14	2.350	1.516	.1049	-.1697	.065[illegible]	.1944	.6530	.[illegible]	.[illegible]
15	2.650	1.710	-.0857	-.1769	-.062[illegible]	.2386	.3830	.[illegible]4	.[illegible]
16	2.950	1.903	.1698	-.1451	.118[illegible]	-.1273	.0[illegible]	.1[illegible]7	-.[illegible]
17	4.[illegible]	2.561	-.0173	.3654	-.179[illegible]	.2743	.0[illegible]	-.[illegible]	.[illegible]
18	.000	.000	.0000	.0000	.0000	.0000	.0000	.[illegible]	.[illegible]

N	Y: INCHES	Y/DELTA	PSICV	PSICH	FU V	FU H	FL V	FL H	F[illegible]
1	4.000	2.561	-.0146	-.0744	3.1126	3.3276	3.1245	3.[illegible]	[illegible]
2	.050	.032	-.1261	.0867	2.5906	2.7692	3.6767	3.4[illegible]6	[illegible]
3	.150	.097	-.0758	.1031	2.6771	2.5760	3.4[illegible]	3.[illegible]	[illegible]
4	.250	.161	-.0570	.0937	2.6749	2.6800	3.2953	3.10[illegible]6	[illegible]
5	.350	.226	-.0966	.[illegible]9	2.6426	2.665[illegible]	3.[illegible]7	3.24[illegible]	[illegible]
6	.450	.290	-.04[illegible]	.0017	2.6555	2.7990	3.5167	3.3[illegible]2	[illegible]
7	.650	.419	-.4151	.0049	3.4[illegible]	3.0430	3.6[illegible]	3.[illegible]	[illegible]
8	.850	.548	-.32[illegible]	-.2968	3.611[illegible]	3.2590	3.7799	3.1063	[illegible]
9	1.050	.677	-.3436	-.1496	4.3056	3.7764	3.8155	3.[illegible]4	[illegible]
10	1.250	.806	-.[illegible]	-.[illegible]	3.9666	3.6111	3.4955	4.7748	[illegible]
11	1.450	.935	-.2744	-.1191	3.367[illegible]	3.6605	3.70[illegible]	3.2[illegible]5	[illegible]
12	1.750	1.129	-.0595	-.0841	3.336[illegible]	3.5[illegible]	3.3[illegible]	3.0[illegible]	[illegible]
13	2.050	1.323	-.1[illegible]	.[illegible]179	3.216[illegible]	3.2762	3.2[illegible]	3.[illegible]	[illegible]
14	2.350	1.516	-.0220	-.[illegible]00	3.0725	3.4061	3.0[illegible]	3.[illegible]	[illegible]
15	2.650	1.710	-.0659	-.[illegible]57	3.1274	2.9320	3.0594	3.1137	[illegible]
16	2.950	1.903	.0356	-.[illegible]8	2.8021	3.0652	2.814[illegible]	3.0[illegible]9	[illegible]
17	4.[illegible]	2.561	-.1[illegible]	.[illegible]7	3.0[illegible]	2.7[illegible]	2.[illegible]	4.6666	[illegible]
18	.000	.000	.0000	.0000	.0000	.0000	.0000	.0000	.[illegible]

Table B24B

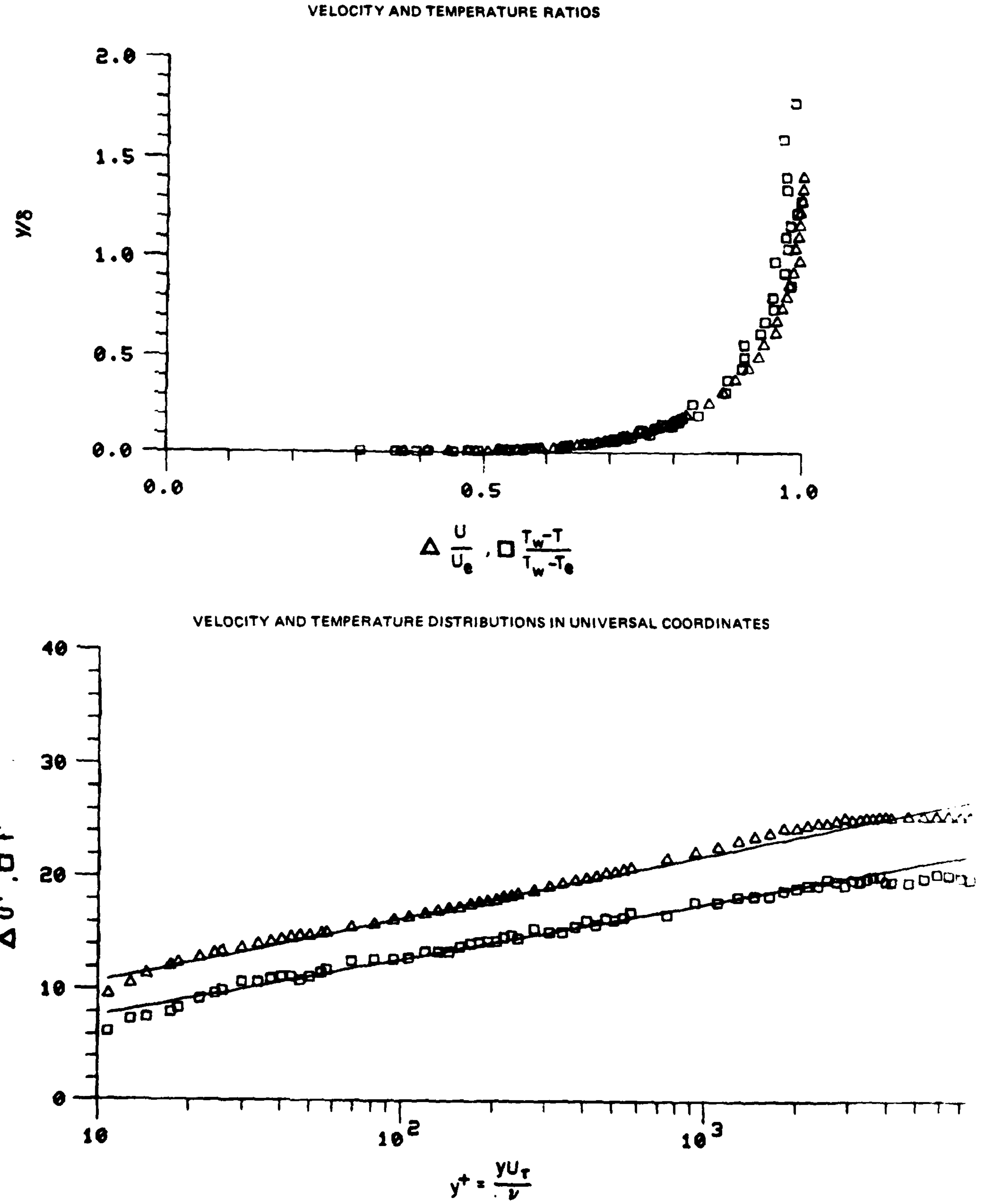

Figure B17. Mean Velocity and Temperature Profiles x = 84 in., Te = 3.9%

78-12-100-1

Mean Profile Data

x = 85 in., Te = 3.9%

N	Y INCHES	Y/ DELTA	U FT/SEC	T DEG.F	U/UE	THETA	U-UE / UTAU	U(+)	T(+)	Y(+)
1	.0056	.004	37.25	87.96	.376	.307	-15.784	9.523	6.192	10.771
2	.0069	.004	40.81	86.62	.412	.363	-14.873	10.434	7.326	12.803
3	.0078	.005	44.11	86.39	.446	.373	-14.029	11.278	7.528	14.466
4	.0093	.006	47.12	85.87	.476	.394	-13.261	12.046	7.963	17.238
5	.0099	.006	48.24	85.41	.487	.414	-12.973	12.334	8.353	18.346
6	.0117	.007	50.10	84.47	.506	.453	-12.498	12.809	9.146	21.672
7	.0131	.008	51.60	83.93	.521	.476	-12.114	13.193	9.612	24.558
8	.0138	.009	51.99	83.57	.525	.491	-12.015	13.292	9.912	25.552
9	.0160	.010	53.22	82.69	.538	.528	-11.702	13.605	10.663	29.616
10	.0181	.011	54.76	82.73	.553	.527	-11.301	14.006	10.628	33.496
11	.0201	.013	55.57	82.42	.561	.540	-11.100	14.206	10.893	37.191
12	.0217	.014	56.15	82.13	.567	.552	-10.952	14.355	11.133	40.147
13	.0233	.015	56.81	82.16	.574	.550	-10.783	14.524	11.108	43.103
14	.0250	.016	57.67	82.46	.583	.538	-10.564	14.743	10.854	46.344
15	.0269	.017	57.72	82.18	.583	.550	-10.551	14.756	11.094	49.754
16	.0294	.019	58.18	81.69	.586	.570	-10.433	14.874	11.510	54.373
17	.0307	.019	58.55	81.41	.592	.582	-10.338	14.969	11.748	56.775
18	.0371	.023	60.43	80.47	.610	.621	-9.859	15.448	12.543	68.599
19	.0440	.026	61.60	80.29	.622	.629	-9.558	15.749	12.695	81.347
20	.0509	.032	62.91	80.34	.636	.627	-9.222	16.084	12.654	94.055
21	.0571	.036	64.14	80.18	.646	.633	-8.909	16.398	12.784	105.550
22	.0644	.041	65.14	79.49	.658	.663	-8.655	16.652	13.374	119.037
23	.0710	.045	66.27	79.56	.669	.660	-8.364	16.942	13.317	131.231
24	.0772	.049	66.97	79.55	.677	.660	-8.185	17.121	13.322	142.666
25	.0842	.053	67.39	79.04	.681	.681	-8.077	17.229	13.756	155.619
26	.0911	.058	68.27	78.70	.690	.696	-7.853	17.454	14.046	168.367
27	.0971	.061	69.21	78.58	.699	.701	-7.613	17.694	14.146	179.452
28	.1039	.066	69.64	78.39	.703	.709	-7.504	17.803	14.303	192.015
29	.1112	.070	70.03	78.42	.708	.707	-7.402	17.905	14.280	205.687
30	.1170	.074	71.16	78.01	.719	.725	-7.114	18.193	14.630	216.218
31	.1240	.078	71.26	77.79	.720	.734	-7.089	18.218	14.809	229.151
32	.1309	.083	71.91	78.12	.726	.720	-6.924	18.383	14.530	241.899
33	.1478	.094	73.27	77.11	.740	.762	-6.574	18.733	15.388	273.122
34	.1657	.105	74.74	77.43	.755	.749	-6.200	19.107	15.117	306.193
35	.1832	.116	75.55	77.49	.763	.747	-5.991	19.316	15.069	338.525
36	.2012	.127	76.83	76.90	.776	.771	-5.664	19.642	15.567	371.781
37	.2182	.138	77.68	76.28	.785	.797	-5.448	19.859	16.094	403.189
38	.2364	.150	78.39	76.69	.792	.780	-5.267	20.040	15.748	436.814
39	.2531	.160	79.35	76.07	.802	.806	-5.022	20.285	16.270	467.669
40	.2714	.172	79.74	76.16	.806	.802	-4.920	20.387	16.197	501.478
41	.2876	.182	80.29	75.93	.811	.812	-4.780	20.526	16.387	531.778
42	.3063	.194	80.98	75.36	.818	.836	-4.605	20.702	16.676	565.958
43	.4008	.254	84.49	75.56	.854	.827	-3.707	21.600	16.703	740.550
44	.4963	.314	86.73	74.28	.876	.881	-3.134	22.173	17.784	916.991
45	.5913	.374	88.52	74.25	.894	.883	-2.677	22.630	17.816	1092.507
46	.6861	.434	90.50	73.71	.914	.905	-2.170	23.137	18.274	1267.654
47	.7811	.494	92.16	73.65	.931	.908	-1.746	23.561	18.319	1443.171
48	.8759	.554	92.99	73.64	.939	.908	-1.534	23.773	18.330	1618.318
49	.9708	.614	94.84	73.04	.958	.933	-1.060	24.247	18.836	1793.650
50	1.0663	.675	94.94	72.85	.959	.941	-1.034	24.273	18.996	1970.099
51	1.1611	.735	95.82	72.53	.968	.955	-.810	24.496	19.268	2145.237
52	1.2560	.795	96.52	72.59	.975	.952	-.630	24.677	19.219	2320.569
53	1.3506	.854	96.77	71.91	.978	.981	-.567	24.740	19.800	2495.346
54	1.4457	.915	97.42	72.14	.984	.971	-.400	24.907	19.600	2671.048
55	1.5411	.975	98.56	72.49	.996	.956	-.110	25.196	19.305	2847.303
56	1.6357	1.035	97.74	72.03	.987	.976	-.320	24.987	19.694	3022.081
57	1.7306	1.095	98.29	72.11	.993	.972	-.177	25.129	19.624	3197.782
58	1.8257	1.155	98.41	71.93	.994	.980	-.147	25.160	19.775	3373.114
59	1.9207	1.215	98.41	71.71	.994	.989	-.147	25.159	19.964	3548.630
60	2.0162	1.275	98.80	71.53	.998	.997	-.049	25.256	20.119	3725.071
61	2.1107	1.335	98.93	72.06	.999	.974	-.014	25.293	19.670	3899.663
62	2.2059	1.395	98.93	72.10	.999	.973	-.014	25.293	19.638	4075.549
63	2.5057	1.585	99.10	72.20	1.001	.968	.028	25.335	19.548	4629.443
64	2.8056	1.775	99.20	71.78	1.002	.986	.054	25.361	19.905	5183.521
65	3.1057	1.965	99.20	71.37	1.002	1.003	.055	25.362	20.251	5737.969
66	3.4057	2.154	99.26	71.43	1.003	1.001	.070	25.377	20.201	6292.231
67	3.7064	2.345	99.41	71.65	1.004	.992	.109	25.416	20.015	6847.787
68	4.0062	2.534	99.22	71.87	1.002	.982	.059	25.366	19.627	7401.680

Table B25

RUN NO. 1. POINT 2.

BOUNDARY LAYER PROPERTIES

		LINEAR INTERPOLATION TO WALL	STANDARD SUBLAYER FUNCTION FROM WALL TO Y+=35
FREE STREAM VELOCITY	=	98.987	98.987
FREE STREAM TEMPERATURE	=	71.450	
WALL TEMPERATURE	=	95.270	
WALL HEAT FLUX	=	.07956	
FREE STREAM DENSITY	=	.07504	
FREE STREAM KINEMATIC VISCOSITY	=	.0001633	
DENSITY OF FLUID AT WALL	=	.07182	
KINEMATIC VISCOSITY OF FLUID AT WALL	=	.0001764	
WALL/FREE STREAM DENSITY RATIO	=	.95708	
LOCATION REYNOLDS NUMBER (REX)	=	4244178.31	
INPUT VALUE OF VELOCITY DELTA	=	2.05000	
INPUT VALUE OF TEMPERATURE DELTA	=	2.10000	
CALCULATED DELTA	=		1.58079
DELTA 99.5% INPUT	=	.00000	
DISPLACEMENT THICKNESS (DELSTAR)	=	.17966	.18012
MOMENTUM THICKNESS (THETA)	=	.13448	.13465
ENERGY-DISSIPATION THICKNESS	=	.24493	.24498
ENTHALPY THICKNESS	=	.00715	.00715
SHAPE FACTOR 12 (DELSTAR/THETA)	=	1.33749	1.33772
SHAPE FACTOR 32 (ENERGY/THETA)	=	1.82137	1.81943
MOMENTUM THICKNESS REYNOLDS NUMBER	=	6794.61	6803.22
DISPLACEMENT THICKNESS REYNOLDS NUMBER	=	9087.75	9100.78
SKIN FRICTION COEFFICIENT	=	.002989	
FRICTION VELOCITY	=	3.91148	
LAW OF THE WALL CONSTANT (K)	=	.41000	
LAW OF THE WALL CONSTANT (C)	=	5.00000	
WAKE STRENGTH	=		.17313
CLAUSERS 'DELTA' INTEGRAL	=	-4.22327	-4.37735
CLAUSERS 'G' INTEGRAL	=	23.76288	23.81295
DISPLACEMENT THICKNESS - CONSTANT DENSITY	=	.16980	.17297
MOMENTUM THICKNESS - CONSTANT DENSITY	=	.13561	.13579
SHAPE FACTOR 12 - CONSTANT DENSITY	=	1.25212	1.27363

LOCATION -X- 84.00000

Te = 3.9%

Table B26

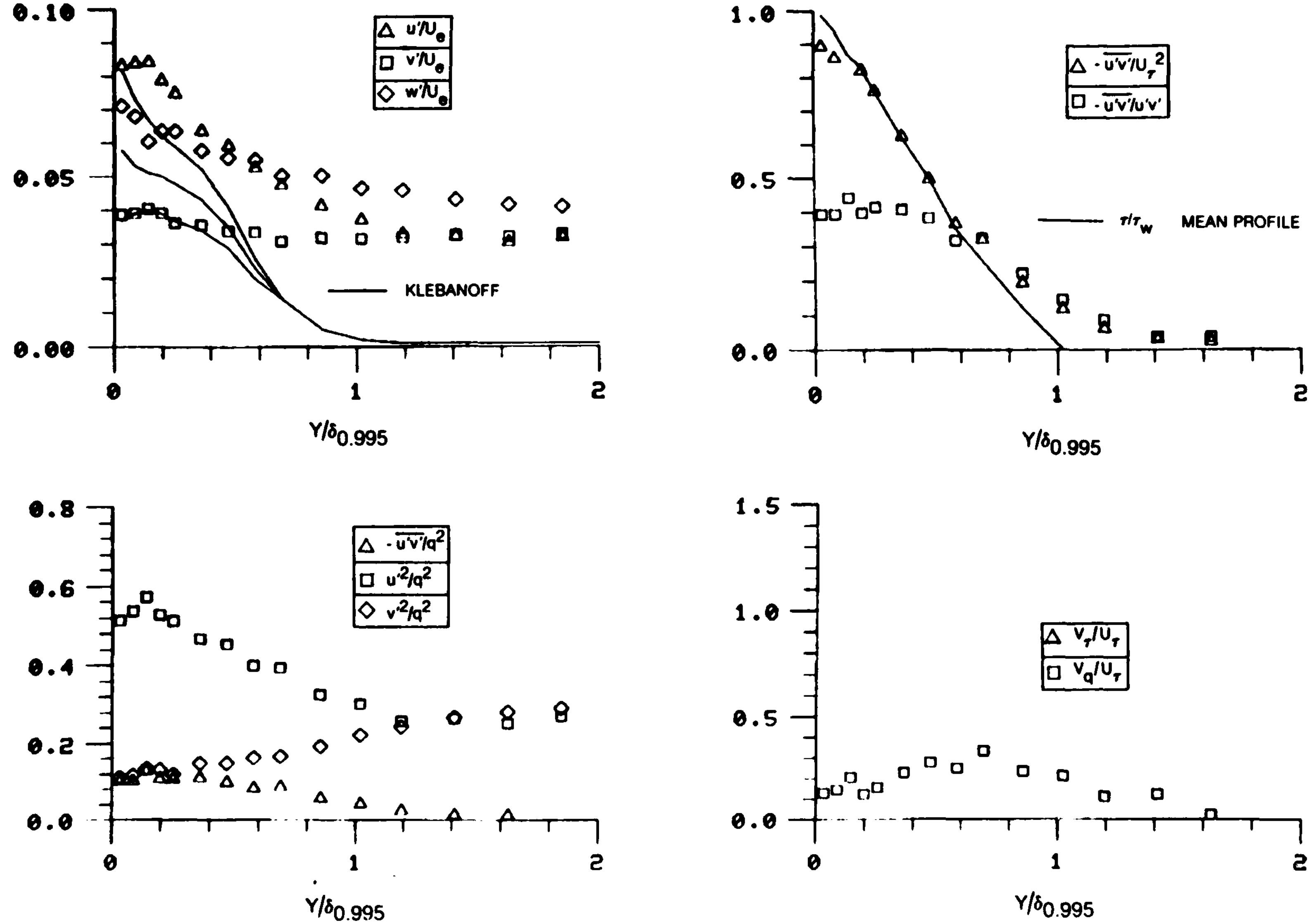

Figure B18A. Boundary Layer Turbulence Quantities, x = 84 in, T_e = 3.9%

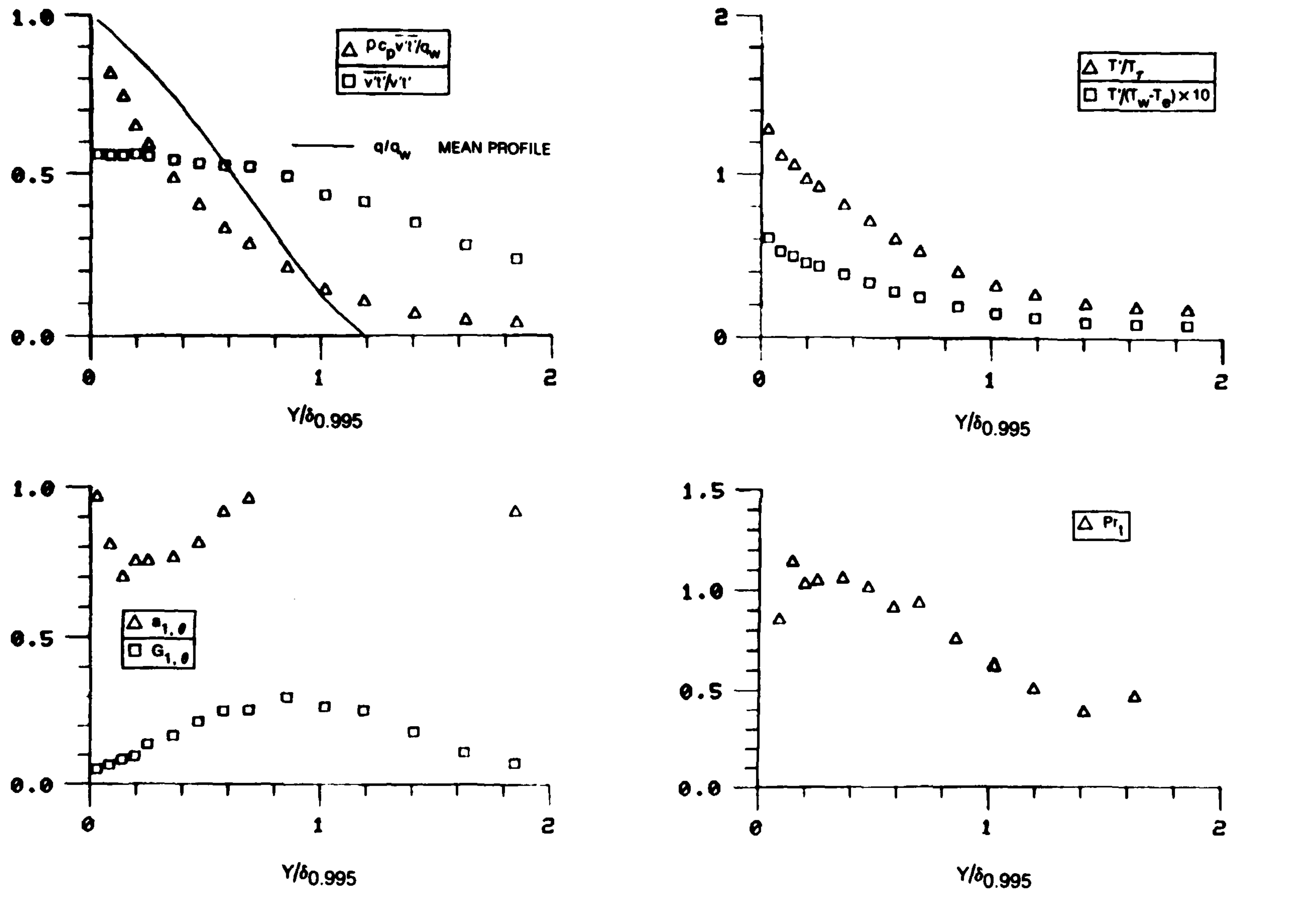

Figure B18B. Boundary Layer Turbulence Quantities $x = 84$ in, $T_e = 3.9\%$

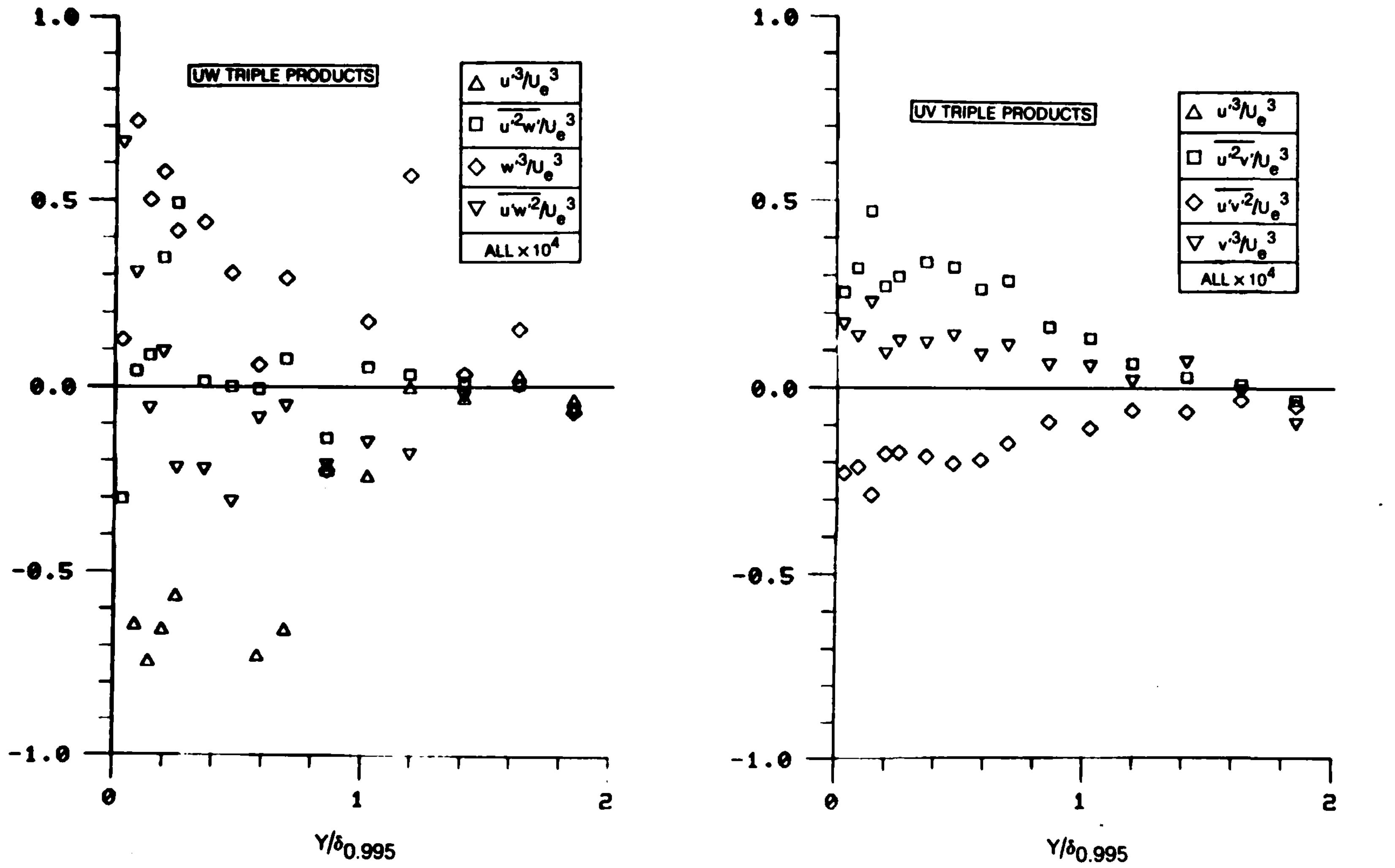

Figure B18C. Boundary Layer Triple Product Distributions x = 84 in, T_e = 3.9%

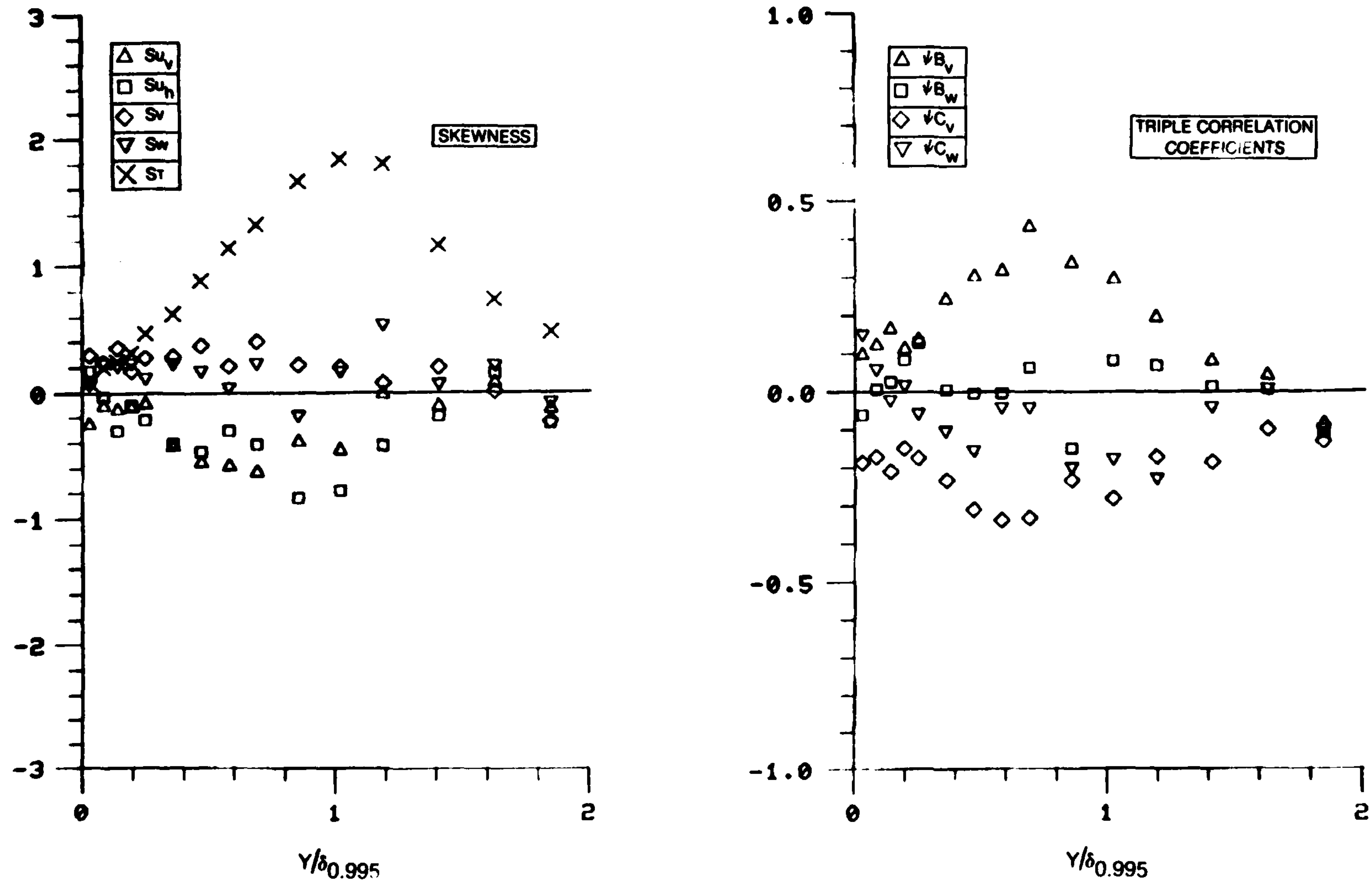

Figure B18D. Boundary Layer Skewness and Triple Product Correlation Coefficient Distributions $x = 84$ in, $T_e = 3.9\%$

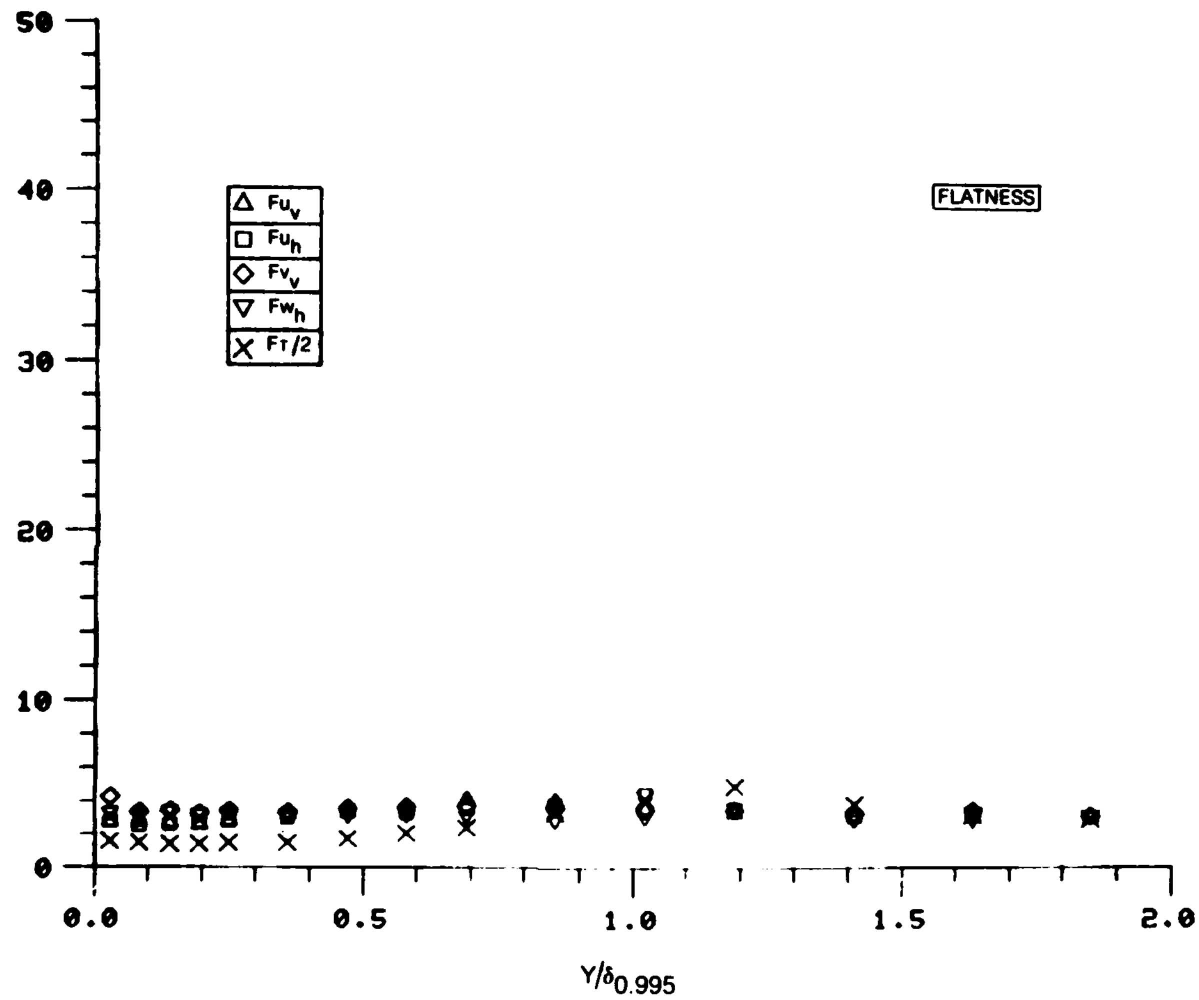

Figure B18E. Boundary Layer Flatness Distributions $x = 84$ in, $T_e = 3.9\%$

Fluctuating Profile Data

x = 84 in., Te = 3.9%

N	Y: INCHES	Y/DELTA	U'/UE	V'/UE	W'/UE	$\sqrt{\overline{U'V'}}$/UE	$\overline{U'V'}$/UTAU²	$\overline{U'V'}$/U'V'	E/UE
1	4.[illegible]	2.21[illegible]	.0322	.0?62	.0414	.0117	.0869	.1??2	[illegible]
2	.05[illegible]	[illegible]	.08??	.0366	.0711	.0371	.8543	.3???	.116?
3	.15[illegible]	[illegible]	.0846	.0365	.0673	.0363	.8577	.3???	[illegible]
4	.25[illegible]	.136	.0841	.0405	.0660	.0390	1.0376	.4???	[illegible]
5	.35[illegible]	.193	.0766	.0390	.0635	.0355	.8157	.3???	[illegible]
6	.45[illegible]	.2??	.0749	.0362	.0636	.0341	.7584	.4???	[illegible]
7	.65[illegible]	.3?9	.0636	.0356	.0575	.0309	.623?	.4???	[illegible]
8	.85[illegible]	[illegible]	.0590	.0338	.0554	.0276	.4596	.3???	[illegible]
9	1.05[illegible]	.560	.0522	.0335	.0547	.0237	.3654	.3???	[illegible]
10	1.25[illegible]	.651	.0474	.0308	.0501	.0222	.32?4	.32??	[illegible]
11	1.55[illegible]	[illegible]	.041?	.0316	.0500	.0172	.1???	.2???	[illegible]
12	1.85[illegible]	1.[illegible]	.036?	.0314	.0461	.013?	.11??	.1???	[illegible]
13	2.15[illegible]	1.16?	[illegible]	.0318	.0454	.0098	.0627	.0?7?	[illegible]
14	2.55[illegible]	1.4[illegible]	[illegible]	.032?	.042?	.0068	[illegible]	[illegible]	[illegible]
15	2.95[illegible]	1.6[illegible]	[illegible]	.0329	.041?	[illegible]	[illegible]	[illegible]	[illegible]
16	3.35[illegible]	1.8[illegible]	[illegible]	.0340	.040?	.0091	-.0???	-.0???	[illegible]
17	4.[illegible]	2.[illegible]	[illegible]	[illegible]	.036?	.013?	-.11??	-.1???	[illegible]
18	.[illegible]	.[illegible]	.0000	.0003	.0000	.000?	.0000	[illegible]	[illegible]

N	Y: INCHES	Y/DELTA	$\overline{V'U'}$/C2	U'²/C2	V'2/C2	W'2/C2	VTAU/UTAU	VC/UTAU	$\overline{V'T'}$[illegible]
1	4.[illegible]	2.21[illegible]	.0336	.2566	.3?2?	.4214	[illegible]	.3?63	.0???
2	.05[illegible]	[illegible]	.10??	.6141	.110?	.3753	[illegible]	.17??	[illegible]
3	.15[illegible]	[illegible]	.1???	.576?	.114?	.3491	[illegible]	[illegible]	[illegible]
4	.25[illegible]	.1[illegible]	.12??	.5718	.12??	.2956	[illegible]	[illegible]	[illegible]
5	.35[illegible]	.15[illegible]	.1?7?	.5264	.12?9	.3438	[illegible]	[illegible]	[illegible]
6	.45[illegible]	.24[illegible]	.10??	.5116	.1?9?	.369?	[illegible]	[illegible]	[illegible]
7	.65[illegible]	.47[illegible]	.11??	.4666	.147?	.3841	[illegible]	[illegible]	[illegible]
8	.85[illegible]	.5??	.096?	.4???	.1484	.3951	[illegible]	[illegible]	[illegible]
9	1.05[illegible]	.651	.0815	.3956	.1637	.4373	[illegible]	[illegible]	[illegible]
10	1.25[illegible]	.??6	.086?	.3???	.166?	.4396	[illegible]	[illegible]	[illegible]
11	1.55[illegible]	[illegible]	.056?	.325?	.1922	.4824	[illegible]	[illegible]	[illegible]
12	1.85[illegible]	1.[illegible]	[illegible]	.30??	.222?	.4763	[illegible]	[illegible]	[illegible]
13	2.15[illegible]	1.16?	.023?	.2587	.2435	.4978	[illegible]	[illegible]	[illegible]
14	2.55[illegible]	1.4[illegible]	.01??	.2648	.2669	.4686	[illegible]	[illegible]	[illegible]
15	2.95[illegible]	1.6[illegible]	.01??	.2818	.2817	.466?	[illegible]	-.1467	[illegible]
16	3.35[illegible]	1.8[illegible]	-.0???	.266?	.2894	.4421	[illegible]	-.???7	[illegible]
17	4.30[illegible]	2.2[illegible]	-.047?	.27??	.321?	.4080	[illegible]	[illegible]	[illegible]
18	.[illegible]	.[illegible]	.0000	.0000	.0000	.0000	.0000	[illegible]	[illegible]

N	Y: INCHES	Y/DELTA	$\overline{V'T'}$/V'T'	T'/TTAU	T'/(TW-TE)	A1B	G1E	PRT
1	4.[illegible]	2.2[illegible]	.2165	.1719	.0CE?	.6485	.0?85	2.??64
2	.05[illegible]	[illegible]	.56??	1.?756	.0605	.9674	.0?57	.8???
3	.15[illegible]	[illegible]	.5613	1.1076	.052?	.8089	.0669	1.17??
4	.25[illegible]	.1??	.5564	1.??5	.049?	.7016	.0E6?	1.????
5	.35[illegible]	.15?	.5614	.9668	.0455	.7506	.0949	1.0???
6	.45[illegible]	.2??	.5541	.9160	.0434	.7512	.1756	1.0???
7	.65[illegible]	.3?0	.5430	.6090	.03?4	.7639	.1674	1.???7
8	.85[illegible]	.47?	.5306	.7084	.03??	.8096	.21??	.91??
9	1.05[illegible]	.5??	.5???	.5966	.02??	.9145	.2??1	.97??
10	1.25[illegible]	.651	.5210	.5211	.0247	.957?	.2537	.758?
11	1.55[illegible]	.856	.4930	.4030	.0151	1.1825	.2594	.8060
12	1.65[illegible]	1.0??	.4300	.3176	.0151	1.2664	.2669	.409?
13	2.15[illegible]	1.1??	.4051	.2627	.012?	1.5744	.2?5?	.39??
14	2.55[illegible]	1.4??	.3436	.2051	.0097	1.6168	.1E1?	.4???
15	2.95[illegible]	1.65?	.275?	.1830	.0067	1.5529	.11??	-1.2???
16	3.35[illegible]	1.8??	.23??	.172?	.00??	.9136	.0731	-3.61??
17	4.30[illegible]	2.21?	.1654	.166?	.0074	.4557	-.0???	.0???
18	.00[illegible]	.0??	.0000	.0000	.0?0?	.0000	.0???	[illegible]

Table B27A

Fluctuating Profile Data

x = 84 in., Te = 3.9%

N	Y: INCHES	Y/DELTA	U'3/UE3 x 10000	U'2W'/UE3 x 10000	W'3/UE3 x 10000	U'W'2/UE3 x 10000	U'2V'/UE3 x 10000	U'V'2/UE3 x 10000	V'3/UE3 x 10000
1	4.000	2.210	-.0762	-.0233	.1963	-.0001	.0817	[illegible]	[illegible]
2	.050	.028	-1.6041	-.3042	.1255	.6561	[illegible]	[illegible]	[illegible]
3	.150	.083	-.6456	.0416	.7131	.3096	[illegible]	[illegible]	[illegible]
4	.250	.138	-.7448	.0822	.5009	-.0564	[illegible]	[illegible]	[illegible]
5	.350	.193	-.6576	.3440	.574[illegible]	.096[illegible]	.2715	-.1775	[illegible]
6	.450	.249	-.5661	.4908	.4163	-.2152	[illegible]	[illegible]	[illegible]
7	.650	.359	-1.08[illegible]	.0131	.4375	-.019[illegible]	[illegible]	[illegible]	[illegible]
8	.850	.470	-1.04[illegible]	-.0002	.3024	-.3073	[illegible]	[illegible]	[illegible]
9	1.050	.580	-.7265	-.0080	.0573	-.0821	[illegible]	[illegible]	[illegible]
10	1.250	.691	-.6574	.0047	.2890	-.0478	[illegible]	[illegible]	[illegible]
11	1.550	.856	-.2266	-.1771	-.2256	-.0265	[illegible]	[illegible]	[illegible]
12	1.850	1.022	-.2450	.0515	.1739	-.1463	[illegible]	[illegible]	[illegible]
13	2.150	1.168	-.0067	.0734	.5613	-.1766	.067[illegible]	[illegible]	[illegible]
14	2.550	1.409	-.0361	.0088	.0317	-.0199	[illegible]	[illegible]	[illegible]
15	2.950	1.630	.0216	.0048	.1511	.0060	.0134	[illegible]	[illegible]
16	3.350	1.851	-.0415	-.0062	-.0697	-.0603	-.0275	[illegible]	[illegible]
17	4.000	2.210	-.1961	-.0219	-.0758	-.0597	[illegible]	[illegible]	[illegible]
18	.000	.000	.0000	.0000	.0000	.0000	.0000	.0000	[illegible]

N	Y: INCHES	Y/DELTA	SU V	SU W	SV	SW	ST	PSIUV	PSIUW
1	4.000	2.210	-.2091	-.0118	.5853	.2770	.1295	[illegible]	[illegible]
2	.050	.028	-.2634	.1605	.2953	.0666	.0798	[illegible]	[illegible]
3	.150	.083	-.1156	-.2742	.2351	.2316	.1936	[illegible]	[illegible]
4	.250	.138	-.1411	-.3139	.3454	.2095	[illegible]	.1447	[illegible]
5	.350	.193	-.1241	-.1054	.1637	.2329	[illegible]	[illegible]	[illegible]
6	.450	.249	-.0936	-.2204	.2671	.1196	.4666	[illegible]	[illegible]
7	.650	.359	-.4335	-.4072	.2776	.2739	[illegible]	[illegible]	[illegible]
8	.850	.470	-.5597	-.4763	.3691	.1779	[illegible]	[illegible]	[illegible]
9	1.050	.580	-.5873	-.3767	.2013	.0390	1.1323	[illegible]	[illegible]
10	1.250	.691	-.64[illegible]	-.4158	.3977	.2215	[illegible]	[illegible]	[illegible]
11	1.550	.856	-.3972	-.6408	.2161	-.1831	[illegible]	[illegible]	[illegible]
12	1.850	1.022	-.4688	-.7877	.1975	.1659	[illegible]	[illegible]	[illegible]
13	2.150	1.188	-.0200	-.4265	[illegible]	.5294	[illegible]	[illegible]	[illegible]
14	2.550	1.409	-.1164	-.1698	.1934	.0703	1.1536	[illegible]	[illegible]
15	2.950	1.630	.0632	.1451	.0044	.2159	.7296	.0439	[illegible]
16	3.350	1.851	-.1360	-.2469	-.2355	-.0799	[illegible]	[illegible]	[illegible]
17	4.000	2.210	-.5664	-.2674	-.3861	-.1344	[illegible]	[illegible]	[illegible]
18	.000	.000	.0000	.0000	.0000	.0000	.0000	[illegible]	[illegible]

N	Y: INCHES	Y/DELTA	PSICV	PSICW	FU V	FU W	FL V	FL W	F[illegible]
1	4.000	2.210	-.2367	-.0002	2.7394	3.0851	[illegible]	[illegible]	[illegible]
2	.050	.028	-.1867	.1518	[illegible]	2.7445	[illegible]	[illegible]	[illegible]
3	.150	.063	-.1697	.0599	2.7186	2.5057	[illegible]	[illegible]	[illegible]
4	.250	.138	[illegible]	-.0187	2.6765	2.6059	3.4113	3.3967	[illegible]
5	.350	.193	-.1492	.0199	2.5561	2.7580	[illegible]	3.2462	[illegible]
6	.450	.249	-.1717	[illegible]	2.6267	2.7102	[illegible]	3.3152	[illegible]
7	.650	.359	-.2338	-.1002	3.2239	2.9647	[illegible]	[illegible]	[illegible]
8	.850	.470	-.3106	-.1524	3.3519	3.3706	3.6147	3.1272	[illegible]
9	1.050	.580	-.3366	-.0401	3.4655	3.2795	[illegible]	[illegible]	[illegible]
10	1.250	.691	[illegible]	-.0396	4.0932	3.5996	3.7623	3.1572	[illegible]
11	1.550	.856	-.2338	-.1961	3.9936	3.6201	[illegible]	2.9355	[illegible]
12	1.850	[illegible]	[illegible]	[illegible]	[illegible]	[illegible]	[illegible]	[illegible]	[illegible]
13	2.150	1.168	-.1727	-.2251	3.3777	[illegible]	3.5667	[illegible]	[illegible]
14	2.550	1.409	-.1634	-.0743	3.1615	3.0708	3.2989	2.6594	[illegible]
15	2.950	1.630	-.0973	.0126	3.0755	3.2128	[illegible]	[illegible]	[illegible]
16	3.350	1.851	-.1297	[illegible]	[illegible]	2.9785	[illegible]	3.0719	[illegible]
17	4.000	2.210	-.1828	-.1359	[illegible]	3.0218	[illegible]	[illegible]	[illegible]
18	.000	.000	.0000	.0000	.0000	.0000	[illegible]	.0000	[illegible]

Table B27B

DATE
ILME